Technical Comparative Analysis of "Best of Breed: Turnkey Si-based Processes and Equipment, to be Used to Produce a Combined Multi-Entity Research and Development Technology Roadmap for Thick and Thin Silicon PV

Funded by the United States Department of Energy
Through Grant:

DE-EE0000282

Participants

Harold J. Hovel
Kevin Prettyman
IBM, as sub recipient to TSEC (The Solar Energy Consortium)

Table of Contents:

1. Figures and Tables.

2. Scope of Work

European and Asian Photovoltaic (PV) implementation is roughly a decade ahead of that in the US, despite much of the technology being developed here. This gap can be quickly eliminated by starting with the most promising turnkey processes and equipment globally available today and aggressively combining technology roadmaps to decrease cost and increase solar efficiencies. A full cost and technology comparison of what is currently available in crystalline (mono, multi, poly) Si PV production was done , along with providing a technology road map to drive toward being able to compete on a cost basis, with traditional methods for generating electricity. Thick and thin Si was included in the evaluation. Without a full and complete understanding of what is the most effective Si based PV methodology globally available today, the risk of "starting in the hole" exists, thereby wasting effort and funding needed to move forward. Once technology, with all its nuances and options, is understood, a qualified, multi-entity team (national labs, academia, industry,etc.) can move forward in achieving the necessary cost reduction and efficieny gains to compete with traditional power generation techniques (coal fired, gas turbine, etc.) in follow on work.

The purpose of this project was to make a comprehensive assessment of the state of solar photovoltaic manufacture world-wide and the possibility of suggesting advances to bring the United States PV industry "up to speed" and competitive where possible. The environment at the start was multifaceted. Solar manufacture in Europe and Asia was developing rapidly while interest in the technology was declining in the United States, and as years were going by, the US industry was falling increasingly farther behind. In much of the world, equipment manufacturers had sprung-up producing what became known as turn-key Si solar cell manufacturing lines where customers could purchase entire manufacturing lines ready to produce Si solar cells of 5 to 6 inch square variety at a rate of 2000-3000 cells per hour, accumulating to 30-60 Megawatt capacity per year for each line. Little attention was paid to the starting material quality or the nuances of the device physics; emphasis was on throughput and reproducibility at an acceptable efficiency and reliance on the academic community plus some internal efforts by a few companies to raise the performance and yield. At one point the cost of the raw Si starting material was very high and interest arose in possibly using lower quality, lower cost Si wafers such as UMG – Upgraded Metallurgical Grade – which was several orders of magnitude lower in quality as measured by impurity content. It was for this reason that when this project began, emphasis was placed on cells made from UMG on industrial turn-key lines. As the project continued, the price of Si dropped and interest in UMG waned, while the industry mostly moved away from the turn-key line manufacturing model. Therefore, mid-way through, the effort focused more on other means of possibly enhancing US manufacturing: material quality control, forensic analysis of the "good" and "bad" factors influencing Si solar cell efficiency, understanding ways to enhance cell performance, and considering alternatives that could be used to advantage.

An economic and engineering "side-by-side" analysis was done on then currently available technology, along with the roadmaps needed to push each particular option forward. Variations in turnkey line processes and procedures can and do result in finished solar cell device performance. Together with variations in starting material quality, the result is a distribution of efficiencies. Reducing this distribution variation as well as moving the entire distribution upward is a major goal of solar cell manufacturing and turnkey line production. Forensic analysis and characterization of each crystalline Si based technology will determine the most promising approach with respect to cost, efficiency and reliability. Forensic analysis will also shed light on the causes of binning variations and suggest possibilities for improving the distribution. The use of a commonest of starting material will

reduce the material-related variations and increase learning from the turnkey processes and procedures. A valid, achievable roadmap will be established for future work on both thick and thin crystalline silicon.

A report showing the advantages and disadvantages of what is currently available in Si PV, along with a technical roadmap for moving forward was generated, and already submitted to the DOE. Comparisons of the various currently available techniques and materials was used as a starting point for moving the technology forward.

Engineering analysis of the (4-5) most promising turnkey crystalline providers commercially available lines was completed. Each turnkey process utilizes multiple key steps, which include defect etching, texturizing, emitter diffusion, glass etch, nitride deposition by PECVD, bottom and top contact screen printing, metal firing and edge isolation. Each of these steps can add to the final variability and lower the average efficiency. The engineering analysis included careful examination and comparison of each step to determine its efficacy and contribution. Turnkey line producers generally have their own ideas and intentions of how to improve their processes and enhance the distribution, and these potential improvements and technology roadmaps will also be compared.

Visitation and Assessment of Turnkey Facilities where available, visits and analyses were made on site for the various turnkey lines. Such visits and analyses are highly valuable in detecting details of key process steps that aren't apparent in "paper descriptions". A useful evaluation was done to determine where benefits would accrue for metrology measurements of layer thickness, surface properties and other parameters in the manufacturing process. Such measurements are valuable in quality control and are known to increase yield and decrease costs of the finished product.

Si Solar cells were forensically analyzed from each turnkey supplier available using a host of techniques. Differences in basic designs and manufacturing processes used by different turnkey suppliers lead to differences in device behavior. Cells were available from turnkey suppliers using different quality of starting material as well as monocrystalline and multicrystalline starting material. An amount of starting material supplied to the turnkey manufacturers was available at IBM and some laboratory cells were fabricated in IBM's facility using this or similar starting material for comparison purposes, especially after determining efficiency limiting properties of the turnkey cells and developing ideas for enhancements that would benefit the US industry and Si photovoltaics in general.

As the project evolved, the basic intended tasks were carried out and the scope was expanded to include new learning. Visits were made to multiple turn-key manufacturers in Europe and the United States under the project and visits were also made at about the same time to Asian manufacturers under other projects. UMG material was investigated thoroughly including cells made on a manufacturing line at Schmid in Germany. Gettering was investigated extensively as a technique for improving starting material quality. Forensic measurements were carried out on multiple solar cell lots made by 10 different manufacturers, and both monocrystalline and multicrystalline cells were studied. The forensic measurements revealed the factors limiting the performance in these manufactured cells. Finally, full solar panels from 10 different manufacturers were compared under "real world" conditions.

3. Organization of this Report.

This final report is an extended summary of the project carried out by IBM personnel over the life of the grant. It only covers those portions for which IBM was responsible (other tasks were also carried out under the Grant by other organizations). After an Executive Summary, a description of the highlights of each quarterly report is given; much more detail can be found in the quarterly reports themselves. The methods used for forensic analysis

are described followed by detailed analysis of the 18 Si cell lots that were extensively analyzed. Suggested enhancements for improved device performance are presented in several locations illustrated by cell measurements on devices fabricated at IBM. The report concludes with a synopsis and comments.

4. Executive Summary.

4.1 Turn-key Lines. Visits were made to the following manufacturers: Schmid, Roth & Rau, Manz, OTB, Spire, Linuo, and DelSolar, and discussions / meetings were held with Centrotherm, Jusung, Oerlikon, Spectrawatt, and GT Solar. This group included US-based companies, 4 from Germany, one from the Netherlands, one from Korea, and several from Taiwan or China. At the time of these contacts, most of these manufacturers were offering turn-key lines ranging from 30 to 60 Mwatts/year, both mono and multicrystalline. Some manufacturers specialized in specific equipment such as Centrotherm for furnaces and OTB for PECVD deposition. Spire specialized in module assembly lines rather than cell lines.

The technologies used in these lines were very similar: $POCL_3$ or H_3PO_4 for the emitter diffusion, acid texturing for multi material and base texturing for mono, PECVD SiN_x for the upper AR coating, screen-printed grid, and Al back side contact. Most used laser edge isolation. Efficiencies were typically in the 15.5-16.5% range for multicrystalline material with 93-96% line yield. Characterization was almost exclusively by pulsed simulator efficiency measurement of cells exiting the line followed by binning in 0.1-0.2% sections. Little if any quality control on starting material was used other than thickness, cracks, and resistivity. All the manufacturers had multi-year roadmaps for increasing efficiency, mostly consisting of selective emitter, improved BSF, and better passivation. A few were considering Cu plating for the upper grid and busbar.

IBM discussed joint research and development with most of these contacts, and began a joint development project with a Chinese company, Linuo, unrelated to this DOE/TSEC project. The downturn in interest in solar technology that took place in the 2010+ time frame terminated the joint project and the other outside contacts.

4.2 Gettering. Gettering is the process of removing impurities from a substrate or rendering them internally inactive. For solar cells, gettering is usually carried out by phosphorus diffusion, Al alloying, or both. In this project, gettering was studied extensively due to the encouraging benefits to lifetime in both UMG and non-UMG material and the surprising large benefit to the shunt resistance. Gettering was carried out by P diffusion at 850-950^{O}C for periods of 20 minutes to 4 hours. The heavily-doped surface region was then etched off before cell fabrication. It was found beneficial to leave the saw damage in place during the gettering, though saw damage by itself had no beneficial effect. A 600^{O}C 1 hour “plateau” while cooling down the wafer after the high temperature step was also found useful, believed due to an internal chemistry where lifetime-damaging impurities are rendered neutral by oxygen bonding or some other impurity complexing.

With a few exceptions, gettering improved the lifetime of all starting material, but it improved the worst material the most (except for 100% UMG where the impurity density was so high that gettering could not significantly reduce it). Commercial material from SUMCO, REC, and MEMC were used in the gettering studies and were then made into cells. UMG wafers from Apollon (France) and new UMG material from MEMC were also included. Several alternatives to standard POCL3 furnace diffusions were tested: high temperature thermal annealing at 1325^{O}C for 10 hours in TCA/ Ar +Oxygen gas, and phosphorus diffusion from P-doped spin-on glass at 900^{O}C for 30 minutes plus a 5 hour plateau at 600^{O}C. It’s was clear that in some cases gettering improved lifetimes by factors of 6-8, while

in others it actually degraded it. The low temperature spin-on glass method resulted in better lifetimes than the very high temperature TCA diffusion.

It became apparent that gettering efficacy is very wafer dependent, possibly due to the different types of impurities governing the lifetime, the oxygen content, and the grain boundary / dislocation structure. What is particularly relevant is that gettering can take some unusable raw starting material and raise it into the realm of acceptable quality. However, even though gettering can raise the lifetime substantially in some material and benefit the efficiency of cells made from those wafers, the price to be paid is the extra processing and its associated time, cost, and reduced throughput, which are contrary to manufacturing practice. The benefits of gettering may not be worth this added price for manufacturing.

Gettering was shown to significantly improve the efficiency distribution (binning) of a multicrystalline lot fabricated on a turn-key line.

4.3. Thin Film Si Solar Cells. The words “thin film Si solar cells” cover a wide range of possibilities. It could include bulk cells where the substrate is made ever thinner compared to the 200-220 microns of today. More often it means a film of Si less than 100 microns thick deposited on a foreign substrate: glass, graphite, metal, or plastic. For this project, films of Si from 5 to 40 microns thick were grown on P+ Si substrates. Such substrates could easily be low cost UMG or solar grade material; the substrate only serves to support the film and act as the back contact, and otherwise doesn’t participate in solar cell activity. Depositing on Si, however, obviates the problems with foreign substrates such as lattice mismatch and interface interaction, and allows a real assessment of thin film potential.

Voc, Isc, efficiency, and quantum efficiency measurements were made on the thin film cells as a function of Si film thickness. As expected, long wavelength response and Isc were reduced in the thinner films, though Voc increased as theoretically predicted and FF was excellent due to the high conductivity substrate which minimized series resistance. Efficiencies of greater the 12% for the 40 micron film and 10% for the 20 micron film were obtained using simple, conventional processing, values which were at or above simulated values. The use of enhanced device designs such as selective emitter and light trapping could raise these numbers significantly. This result establishes the potential usefulness of thin film Si cells on low cost P+ Si substrates.

4.4. Forensic Measurements. In the extension to the contract for 2014, the focus of the project centered on forensic analysis as a means to analyze and improve upon conventional manufactured cells. To accomplish this, Si cells from 18 separate multi and mono cell lots were obtained and subjected to extensive analysis. For a few of these lots, starting material characterization was employed as well as finished cell characterization. Ten cell lots were purchased from 10 different commercial manufacturers and added to the 8 lots already available in-house. Analysis included Voc, Isc, FF, and efficiency under a solar simulator, series and shunt resistance, diode properties J0 and n (quality factor), lifetime maps, LBIC maps, photoluminescence, quantum efficiency, temperature dependence, trap density, resistivity, and reflectance.

It was found that no single factor correlated with performance in all the cells, not even Voc or Isc. Instead, FF was the dominant factor in some, Voc in others, series resistance in still others. Substrate quality was highly important for many in terms of lifetime and lifetime distribution, but as the substrates are made thinner, lifetime and diffusion length become less significant. Shunt resistance was of almost no importance in any of the lots unless drastically low, which precludes one of the benefits of gettering (reducing leakage).

The lack of one or two dominant controlling factors makes it difficult to identify the underlying physics limiting the efficiencies of the cells in these particular lots. The likely meaning is that multiple of factors taken together determine the performance. Some of the

analyses were more straight-forward. For example, many of the lots showed a minimum of reflectance around 700 nm wavelength and were light blue in color when 600 nm and dark blue or black are optimum. This caused a loss of 0.1-0.2% in efficiency. Mono cells had considerably higher reflectance at short wavelengths than multi cells due to the nature of the texturing. Mono cells also showed higher dependence on angle of incidence than multi cells due to the nature of the texturing. LBIC and lifetime maps of multi wafers showed many high defect, low lifetime areas which reduced the photocurrent by 5-10% and are the main cause of the lower efficiencies of multi cells compared to mono. Quantum efficiency scans showed problems in passivation in some lots and lifetime / BSF problems in others. In some lots, the series resistance was nearly the same for all the cells in the lot, while in others variations in Rs correlated with variations in efficiency within that lot.

Some factors which would benefit performance and binning for future manufacturers were easily identified. Grid size could be reduced by a factor of 2 compared to the 90 – 100 micron widths seen in most of the lots. AR coatings, whether a SLARC such as SiNx of a DLARC with multiple layers, could also be optimized. Better quality control of the substrate in terms of lifetime, resistivity, and impurity content would also be beneficial, leading into another purpose of the project, to suggest enhancements.

4.5. Enhancements. Several enhancements that could boost cell performance by several % absolute have been known for years, while others are less well known. Starting with the conventional design, wafer quality control with a goal of quality improvement (reduced impurity and oxygen content, lower dislocation densities, higher lifetime) would be beneficial. This could also reduce light-induced degradation and improve the energy output of the cell as measured over long time periods. As a characterization tool, defect band photoluminescence imaging would be highly valuable in selecting out unacceptably low quality starting material. Selective emitters with reduced doping over most of it and high doping only under the contacts would raise the emitter diffusion length by 5-10x without increasing series resistance, and improve emitter passivation while increasing Voc. Local BSF, perhaps created with the help of laser processing, also boosts Voc while improving long wave response. Thinner grid fingers can reduce shadowing without resistance penalty and TiO_2/SiN_x AR coatings can reduce reflectance. Processing such as ion implantation to replace diffusion and EWT(emitter wrap-through) to eliminate the front grid altogether would also have benefits.

Going away from the conventional design, the use of n-type substrates would have several advantages. The lifetimes are considerably higher than for p-type material, the resistivity is lower for the same doping, and there is little or no light-induced degradation (LID). Two manufactured cell designs make use of n-type substrates: HIT cells manufactured by Panasonic / Sanyo, and IBC (Interdigitated Back Contact) cells made by Sunpower. Both these devices have efficiencies well above 20% with module efficiencies themselves nearing or at 20%. Their drawbacks include higher cost, the need for high quality monocrystalline material, and the lower supply of n-type material in the solar industry.

All of these alternatives have been explored at IBM Research (though not necessarily under this project): selective emitter, ion implantation, local BSF, thin grids, high performance DLSARCs, HIT cells, and IBC cells. The expected enhancements were verified by the nearly perfect quantum efficiency, the boost in V_{OC}, and Jsc values in outdoor sunlight above 41 mA/cm^2. The results obtained are validations that the enhancements are beneficial for cell performance. Decisions about cost effectiveness would be those of the manufacturers, but It is clear that some or many of these cell performance enhancements could be beneficial to US manufacturing and it is likely that the few US Si cell manufacturers and many manufacturers in other countries are already considering or already making use of some of these concepts.

4.6. Panel Measurements. As an addition to comparing Si cells from different manufacturers, ten solar panels were purchased from 9 different manufacturers and mounted on the rooftop at IBM, all facing due south and tilted at the local latitude. The output from each panel was recorded at 30-40 times during the day with all the panels measured by I-V curve within 2 minutes of each other. Most measurements were made on cloudless days in September with several also made on totally overcast days with no direct sunlight at all. The motivation for this was the expectation that differences in temperature and intensity dependence, series resistance, and optical effects such as reflectance at high angles would show up as differences when panels were measured over long periods of time. Ideally this measurement would be carried out over months with automatic recording, or even several years to assess LID.

Measurements made from early morning until sunset showed that most of the panels had significant series resistance losses (though panels mounted on domestic rooftops would have shorter cables and therefore less resistance). Since the panels were a mixture of mono and multicrystalline types, with obvious differences in reflectivity (some were light blue, some dark blue, and some black), interesting optical effects were noted such as panels with the lowest photocurrents in the morning having nearly the highest in the afternoon. Many of the panels showed this effect. It would likely be absent in panels which tracked the sun or even for panels mounted in a different configuration (tilt and azimuth). During totally overcast days, almost 15% as much power was developed as during cloudless days. The panel V_{OC} values were strong functions of the outside temperature as expected from the temperature coefficients. The HIT and IBC panels were considerably better in performance than the conventional cell panels.

4.7. Remarks. The purposes of the contract were to visit and analyze turn-key suppliers, to assess the potential of UMG, to determine the value of gettering for material improvement, to use detailed forensic techniques to analyze commercial cell strengths and weaknesses and recommend enhancements while proving the value of those enhancements where possible, to assess the potential of thin film Si cells in at least one of their many forms, and to recommend where US manufacturing could be jump-started if it so chose. As past paragraphs have outlined, these goals and purposes have been accomplished, with the beginnings of the interesting full panel assessments as "icing on the cake."

5. Detailed Description.

5.1 Forensic Techniques. As the forensic analysis played such a large role in parts of this project, a description of these techniques and what can be learned from them is given here.

5.1a Material Quality.

Lifetime. The most important parameter in assessing material quality has been the minority carrier lifetime. The lifetime is controlled by defects, recombination centers, and is usually related to impurity densities of fast recombination centers such as iron, and sometimes to complexes such as the boron-oxygen couple. Lifetime is difficult to separate from surface recombination.

"Sinton" lifetime, named after Ron Sinton who developed it, is an eddy current response to an intense light pulse, usually between 30 and 50 "suns" intensity, or 3 – 5 watts of optical power per cm^2. This is sometimes called high injection lifetime because the photogenerated carrier density may exceed the background doping carrier density. This measurement also allow the estimate of trap densities in multicrystalline material. The spot size resolution is of the order of several centimeters.

Photoconductivity decay (PCD) is a response measured by microwave detection to the increased conductivity created by a light pulse. The light intensity is less than 1 "sun" and the resolution can be as low as several hundred microns, allowing detailed maps to be obtained. Maps can be made for raw starting material (although dominated by surface recombination) or finished cells which include the busbar and grids. Raw wafers can be passivated to reduce SRV with an alcohol-iodine solution.

Resistivity is an important control parameter that can be measured by 4-point probe or eddy current. Manufacturers usually have a resistivity specification for incoming wafers.

Photoluminescence is related to lifetime. Band-to-band PL measures the number of carriers recombining across the energy bandgap. Recombination through impurities subtracts from band-to-band PL; high PL areas correspond to high lifetime and low PL corresponds to low lifetime where defects are likely located. Defect-band PL is the output of long wavelength light when photocarriers recombine through impurities. The higher the defect band PL is, the higher the recombination rate is and the lower the lifetime is in the material. In one sense, B-to-B PL and defect band PL are mirror images; the higher the defect band PL is the higher the defect density is and the lower the B-to-B PL is likely to be. Electroluminescence is very similar to PL and can reveal series resistance problems.

5.1b. Electrical Quality

Diode quality. A solar cell is basically a photogenerator in parallel with a diode. The higher the quality of the diode, the less it will rob the photogenerator of power. (More accurate equivalent circuits include 2 diodes in parallel, where the 2nd diode becomes significant at low voltages.) Diode quality is measured by shunt resistance, series resistance, and the diode terms J0 and "n" which are contained in the equation $J_{diode} = J0 \cdot (e^{qV/nkT} - 1)$. J0 is determined by the doping levels, the lifetime, the diffusion constant, and the surface recombination velocity. The J0 term can vary over 3 orders of magnitude between good and bad cells. Together, J0 and n largely determine the Voc and have influence on the FF as well. The better the quality of the material and the processing, the lower J0 and n will be and the better Voc and FF will be (FF is also influenced by Rs and Rsh).

Voc-Isc is a very convenient way to determine the diode parameters. At very low voltages, the I-V slope is linear and the shunt resistance is given by the slope. At higher voltages, the diode "dark current" is affected strongly by the series resistance while the corresponding Voc-Isc curve is not. Comparing Voc and Vdark for Idark = Isc directly determines the series resistance (as long as the temperature can be kept constant). The slope of the log Isc – Voc curve directly yields J0 and n. The same technique at low light intensities can be used to obtain the second diode parameters. The 2nd diode only becomes important at low light levels unless the material quality is very poor.

Temperature coefficients for Voc, Isc, FF, and efficiency can be easily obtained using a solar simulator and temperature-controlled chuck. A thermocouple is bonded directly to the surface of the cell to read the temperature accurately. Mono- and multi-crystalline cells have the same coefficients, though HIT cells with amorphous Si junctions may have somewhat different ones.

LBIC (Light Beam Induced Current) is a map of photocurrent obtained when a laser beam is scanned across the finished cell surface. Since the photocurrent is dependent on lifetime and any losses due to defects, it is basically a map of the effective lifetime as determined by defects and surface (front or back) losses. With long wavelength lasers, almost all the signal comes from the cell base region, and with short wavelengths, the signal is derived only from the emitter. Short and long wavelength measurements therefore can separate out problems in the base from those in the emitter.

DLIT (Dark Lok-in Thermography) is a method for finding local defects where current non-uniformities occur, and is highly useful for finding shunt leakage locations and in some cases series resistance problems. Heat generated in the higher current regions generates a temperature difference which can be detected in the infrared wavelength region. Temperature differences of 0.1 degree are easily detected. A comparison of forward and reverse bias DLIT allows discrimination between ohmic shunts such as "pipes" and pinholes and rectifying shunts such as junction leakage or contact problems.

5.1c Optical Quality.

Reflection is determined by the surface texturing and the optical coating. A more accurate optical quality is transmission, which includes both reflection and absorption in the optical coating, but nearly all such coatings are transparent down to the ultraviolet so that simple reflection measurements suffice. Another property of interest is the angle of incidence dependence of reflection which is different for mono compared to multi cells due to the nature of the texturing.

Spectral Response is the single most important forensic measurement. It is defined as the quantum efficiency versus wavelength, where the quantum efficiency is the # of photocharge carriers collected by the junction divided by the # of incident photons. At long wavelengths the quantum efficiency is a measure of the collection probability from the base, determined by the diffusion length in the base and the effect of the BSF. At short wavelengths it is a measure of the emitter quality and the front surface passivation quality. The EQE is the external quantum efficiency which includes the reflection loss; the IQE is the internal quantum efficiency - the EQE corrected for reflection.

5.1d Panel Forensics Limited forensic measurements can be made on full panels as well as individual cells. The full I-V curve yields the sum of the individual Voc's, the average of the cell photocurrents, the power out, and the panel fill factor, which in turn is determined by the cell fill factors and the connection and cable resistances. In the dark, the panel I-V curve can be obtained and used to estimate the series and shunt resistances by comparison with the Isc-Voc of the panel as done for individual cells, though the problem with this method for panels is that the temperature is also a variable. An alternate technique which reduces the temperature problem is to plot panel FF versus Isc or Jsc and compare against simulations.

6. Turnkey Supplier Evaluation (2010-2012)

Comparisons of the various currently available techniques and materials could be used as a starting point for moving the technology forward at a much faster pace. ***The information provided in this report, with special emphasis on conclusions and recommendations, represents only the opinion of IBM's researchers involved in this study. There could be disagreements from others that may wish to repeat the study, and certainly disagreements from representatives of the companies studied in this report. The only information that was used in this analysis was that provided by the companies themselves in the form of non-proprietary information verbally given, through written documentation, or through the company's website. The authors of this study have no intention to promote one turnkey company or its technology over another and have nothing to gain by doing so. What was attempted was an impartial analysis of what was available in the industry, and is accurate to the best of our knowledge and unbiased to the best of our ability.***

In determining which turnkey providers to evaluate, experience, stability, and technology roadmap were critical in culling down the list. Seven turnkey manufacturing equipment suppliers were evaluated for multi-crystalline solar cell production. These

included two US based companies (Spire Corporation and GT Solar), three from Germany (Centrotherm Photovoltaics AG, Roth & Rau AG, Schmid Group GmbH), one from the Netherlands (OTB Solar, which has since been acquired by Roth & Rau), and one from Korea (Jusung Engineering Co. LTD). The companies are all capable of delivering a turnkey line according the requirements listed below. Requirements

Manufacturing size:	100MWp production per year, with smaller lines using processes directly scaleable to a 100MWp facility.
Technology:	The equipment should be capable to manufacture poly-crystalline silicon wafers with a size of 156 x 156 mm² and wafer thickness down to 180µm. Monocrystalline capabilities were also assessed where appropriate.
Location:	The turnkey companies could be from anywhere in the world in order to evaluate the best providers, but their offering had to meet any requirements that might be unique to the US
Line concept:	Keep flexibility at maximum utilization and production volume
Yield:	Supplier to guarantee minimum yield (>95%)
Utilization:	Supplier to guarantee minimum utilization (~90%)
Volume:	Supplier to guarantee projected volume of ≥100MWp per year
References:	Supplier should provide references on installed facilities and have a good reputation in the market
Experience:	Supplier should have sufficient expertise on the overall process as well as all individual steps.
Risk Assessment:	Based on technical and business capabilities of suppliers

Turnkey Suppliers

6.1 Centrotherm

Company profile

Headquarter: Blaubeuren, Germany, state of Baden-Württemberg
Centrotherm Photovoltaics has been in existance for 6 years
Began with furnace, diffusion and deposition equipment for semiconductor industry
IPO 2007, listed at TecDAX
Head count: 1,200
85% of revenue from PV
Subsidiaries:
- ISC (Konstanz, Germany): Process development and R&D, connected with University of Konstanz
- GP Solar (metrology equipment)b
- FHR: Si deposition equipment
- SolMic: Poly Si production

Outlook: Doubling build capacity by Jan 09
References: 20 turnkey lines in operation, 20 lines on order

Contact: Josef Haase (*Senior Director of Technology and Marketing*), Martin Meyer

Production line

Manufacturing runs in a 2 shift model, each shift has ~150 operators

Actual capacity is at 20 furnaces and 20 PECVD per month
Furnaces are manufactured in-house, due to criticality and expertise:

- PECVD (direct plasma) uses thin wire heating (max 500°C)
- Furnaces use 6mm and 8mm wire heating, considered very powerful and efficient
- (~900°C) process temperature
- Drying uses infrared and ceramic heating (~250°C)
- Firing uses lamp heating (~900°C)

Quality control management system and control mechanisms are in place.
Besides heating systems, all other assembly parts come from supply base either as a component or already pre-assembled.
Centrotherm has the capability to assemble furnaces or PECVD with internally built parts only, which is practiced for prototype equipment.
The other equipment, besides furnaces and PECVD, are purchased externally from suppliers which work with Centrotherm in close collaboration.
Manufacturing equipment can be provided in a 5 lane or 8 lane arrangement.
Expertise seems to be available for all thermal processes, including PECVD.
Technology roadmaps are developed to match the solar industry requirements.

Technology Supported

Efficiency: 15.6 % (16% expected next year with new emitter design)
Yield: 96 %
Breakage rate: 1-2% for 180-200 um thick multi crystalline wafers
Turnkey facility contract guarantees:

- line throughput
- efficiency
- production yield
- project schedule

Texturing: Acid vs. none for multi-crystalline
Acid vs. KOH/IPA for single crystalline
Single crystalline: 125 mm vs. 156 mm (currently only 125 mm due to crystal availability and cost of pullers in China)
N-type diffusion: POCl3 vs. Spray on- +0.2 % efficiency (due to better gettering with POCl3)
Flexline: has higher overall performance/yield - + 0.4 %
Inline can be provided as well with all process steps tightly linked through automation.
Dielectric layer deposition: direct (better efficiency) plasma vs. REPCVD (deposition on walls) with typical thickness at 70 – 100 nm
Efficiency: lower cut off defined at 13.5 – 14.0 %
Incoming inspection: using GT Solar inspection station (optional)
Wafer ID: possible but concerns about maintaining readability
Post diffusion measurement: sheet resistance for 1/5 wafers

Technology roadmap in place to improve processes and efficiency according to solar industry requirements. The new emitter design supports 16% average efficiency for multi-crystalline silicon wafer technology.

Operational Requirements
For 60 MWp line:
Floor space: 60 m x 25 m (two identical lines)

Operations: 14 headcount (10 operators, 2 maintenance, 2 engineers)/shift and 4 shifts
Power requirements: 900 kWh

Production cost: 1.74 Euro/Wp (at 2.2 Euro/Wp sale price)
Wafer cost: 75% (wafer cost: 4.0-5.5 Euro/wafer)
Electrical power: 1.2%
Profit: 15.6% (full utilization)

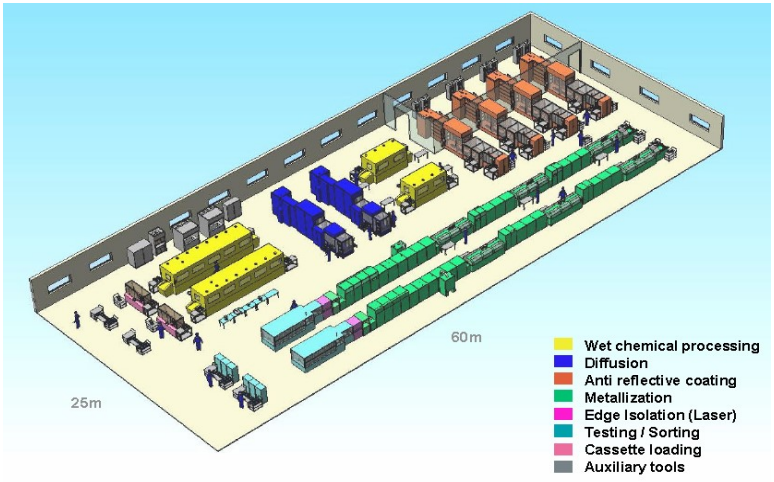

Figure 1: Centrotherm line setup (60 MWp):

Cost Structure

Line options:

1. Single line @ 30 MW: 14M Euro
2. Double line @ 60 MW: 28 M Euro
3. Single Line @ 50 MW: 19 M Euro

Centrotherm Photovoltaic visit at Valencia booth

cell lead time analysis			MWp/year	clock rate is at 1 wafer per second
acid / text.	1900	wafers/h	51,04	
diffusion	1900	wafers/h	51,04	
etching	1900	wafers/h	51,04	
PECVD	1900	wafers/h	51,04	not bottle neck, 4 tubes
screen print/firing	1900	wafers/h	51,04	
LIP	0	wafers/h	0,00	
test	1900	wafers/h	51,04	
maintenance	?	h per week and tube - PECVD has 4 tubes, 3 run while one is in maintenance (e.g.)		
efficiency	16,0%	new emitter and change to 3 busbars		
utilization	90,0%			
yield	96,0%			
facility	NON	specific requirements		
shift model	21,6	h per day		
delivery	7,0	months after PO	(and another 2 months for installation, automation etc.)	
ramp time	3,0	months		
& installation				
floor space	70	X	10 M²	700 M²
energy consumption	1000	kWh		
operators required	60		15 per shift	4 shifts
material cost (Wp)	1	€		
raw silicon cost (Wp)	1	€		
price	17	M€ for fully installed line with 60MWp production capacity		
+ metrology	17		50MW:	17 M€
distribution capability		± %	(see presentation from Milan 2007)	

comments
centrotherm comes from thermal equipment
large reference base, including Qcells, Advent, Helios, Schott (> 25 lies are installed and running)
tools are not linked (not in-line) - automation can slow down ??
no automation is recommended

Table 1: Business data for cost estimate calculations- Centrotherm Summary

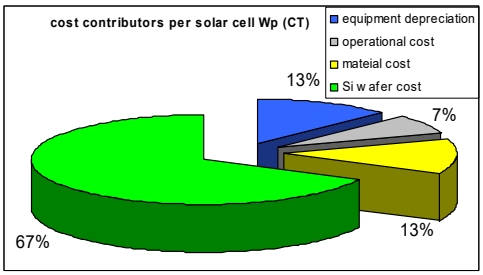

Figure 2: Cost Contribution Chart -Centrotherm

6.2 Schmid Group

Company Profile

Tech center in Germany (Freudenstadt), manufacturing site for Wet Bench equipment (PSG Etch and Edge Isolation)
ISO 9001 certified
Company is family owned and operated.
Schmid has supplied wets tools for IBM PCB fab at Endicott
In PV business since 2000, currently have 1800+ employees
References: 8 lines installed, around same number on order
Revenue: 2007 - 300 M Euro , 2008 - 400 M Euro
Contact: Steve Paufve (*Director of Solar Cell Project Mgt*) and Mike Wageli (*Sales Manager PV)*

Production Line

Manufacturing runs in a 1 shift model, having ~160 operators working.
Actual capacity is at 2,5 wet benches per week, ending up at ~10 per month.
Thermal process equipment:
Purchased from Sierra Therm
Inline type
Cleaning equipment: built by Schmid at Freudenstadt
Inline type
Acquiring Sierra Therm (current furnace supplier)

Technology Supported
Laser marking of wafers is possible, but not yet included in offerings. Schmid very interested in including this as feature of the line. Marking the edge of the wafers is considered possible.
Thickness measurement of incoming wafers is not standard practice for current customers. Can be achieved using a two camera technique (additional information is proprietary).
Fully automated line where wafers are handled by operators at beginning and end points of manufacturing line only. Minimizes wafer breakage.
Product data can be captured using Schmids Overall Factory Control (OFC) system. This system does not control the process. It can only collect data as often as every 30 sec. at specified locations within the production line. Wet Benches are designed for minimal chemical usage and minimal waste generation. (Not tank-type tools).
Effective throughputs are 1 kwph, 1.65 kwph, and 2.2 kwph (Standard configurationss only). This method of describing line capacity is preferred by Schmid over MW out due to uncertainties with how line will be run vs. theoretical.
Fully automated line – Inline type manufacturing
*Recently developed (not fully marketed) handler that allows customer to load/unload wafers at key places in the manufacturing line. Wafers are placed in “bister boxes” that protect them from breakage.
Note: Could be used for buffering if needed, but not designed for this.

Roadmap
Efficiency improvement:
- + selective emitter
- + backside contact (1 ½ years development time, beginning Dec. 08)

BASF (joint development): contact free printing process

Operational Requirements
Capacity: 56 MW, can increase to 80 MW
Floor space: 100 m x 20 m (100 m x 30 m with capacity increase)
7 months lead time for equipment delivery
3 months installation
3 months ramp up
PECVD longest lead time item
Capacity bottle neck: P diffusion
Factory monitoring software – OFC

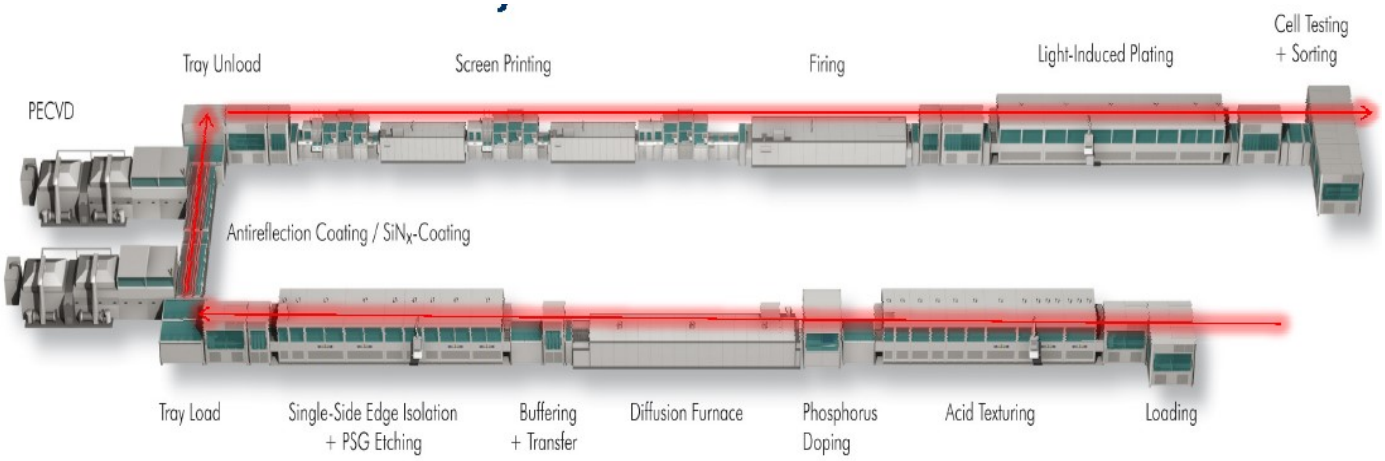

Figure3: Schmid Group line setup (60 MWp):

Cost Structure

Cost: around 25 M Euro (for a 60 MWp line set up)

Table 2: Schmid Business Data For Cost Estimate

Schmid GmbH visit at Valencia booth

cell lead time analysis			MWp/year		
acid / text.	2260	wafers/h	58,45		
diffusion	2260	wafers/h	58,45		
etching	2260	wafers/h	58,45		
PECVD (2x)	2260	wafers/h	58,45	bottle neck	
screen print/firing	2260	wafers/h	58,45		
LIP	2260	wafers/h	58,45		
test	2260	wafers/h	58,45		
maintenance	10	h per week on PECVD (bottle neck)			
efficiency	15,9%				
utilization	90,0%				
yield	93,0%				
facility	NON	specific requirements			
shift model	21,6	h per day			
delivery	7	months after PO			
ramp time & installation	3	months			
floor space	91	X	24 M²	2184 M²	
energy consumption	1300	kWh			
operators required	48		15 per shift	4 shifts	
material cost (Wp)	1	€			
raw silicon cost (Wp)	1	€			
price	25,8	M€ for fully installed line with 56MWp production capacity			
+ metrology	25,8				
distribution capability		± %			

comments
furnace, PECVD and screen printing equipment are from partners
8 turn key fabs had been installed and are fully working
2 total and 8 partial mfg lines are waiting for installation

Table Business data for cost estimate calculations- Schmid Summary

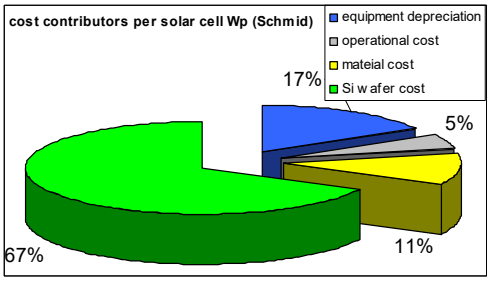

Figure4: Cost Contribution Chart -Schmid

6.3 OTB Solar

Company Profile

Company headquarter is in the Netherlands (Eindhoven).
PECVD development and equipment assembly in Eindhoven.
Actual growth rate is in the range of 75%, significant above industry average.
In February, 2010, OTB Solar was acquired by Roth & Rau, although company integration from both a technical and business viewpoint still required much work at the time of our last visit in 2010.
Contact: Don Veri

Production Line

Eindhoven manufacturing line visited as well as a customer (Arise) in Germany.
Leadtime: 7-9 months
Installation and ramp : 3 months
References: 4 lines installed and operating [Germany (Dresden), Korea, India, China], 4 lines on order
The PECVD tools are the only tools assembled at OTB. All other equipment comes from the external supply base directly to the customer. This indicates high supply base dependency but also good and structured supply chain management.
10 PECVD tools can be assembled in parallel. Assembly and test time is 4 weeks.
Screen printing (Metx), small footprint (paternoster approach), are in development. Process time will be at around 90sec per print step.

Technology Supported

Yield 93 %
Uptime 90%
Efficiency: 15.5- 15.8% average (15.8% with POCl3) (50-55% of wafers above)- RENA cleaning equipment
Doping: batch POCl3, inline P mist
Front side metal contact: Ag (screen printing)
Options:
Inline: all current installations
Hybrid inline/batch
Batch
Strong points:
Line integration
Fewer operators
High level of automation
Around 40 engineers work in OTB engineering.
New PECVD in development to achieve a deposition rate of 10nm/sec, the future will beat 20nm/sec, at thicknesses of 70 – 100nm. Today's capability is at 4nm/sec.

Actual PECVD equipment performs at 4 wafers/ chamber. New development will be able to process 3 x 4 wafers/chamber.

The PECVD technology used at OTB is shown in Figure 5. The plasma is applied above the solar cell surface. This is a homogenous approach. Remote plasma is used, with lower energy. It is only low energy necessary to achieve fairly homogenous dielectric layer deposition.

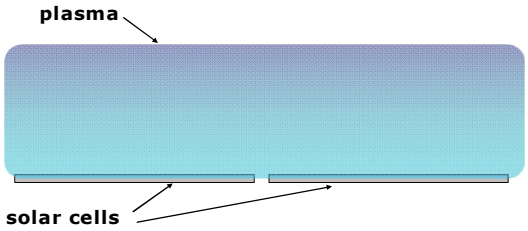

Figure 5: PECVD Technology Used at OTB

The low energy used for the plasma ensures that the silicon is not damaged. This helps to prevent degradation and pinholes. The plasma is jetted to the target which prevents re-deposition on the source.

An alternative PECVD method is shown Figure 6. The plasma has to fill the gap's between the wafers. The required energy is much higher and could cause damage on the silicon. Deposition is less homogenous across the carrier and causes larger thickness distribution of the dielectric layer. The inhomogeneity as well as the defects could cause pinholes in the deposited layer.

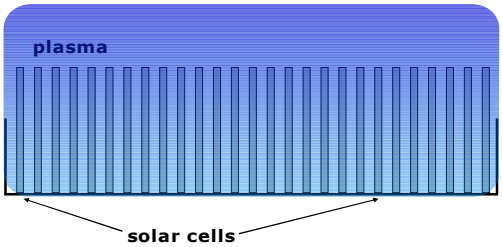

Figure 6: Alternate PECVD Method

The OTB PECVD technology thus has a significant advantage in cell production. This is especially important for future products where backside passivation will be required with pinhole free layers.
Here, three plasma sources are used to achieve maximum homogeneity. The pre-heating chamber is at a temperature of 550 – 600°C. The actual process temperature in the deposition chamber is at ~450°C.

Screen printing:

Year	Line width
2008	120µm
2009	100µm
2011	50µm

Table 3: Screen Printing Line Width

The actual line height printed is at 20 – 40µm. The lower line width reduces shadowing of the front contact grid significantly.

Operational Requirements

Floor space: 12 m x 75m (50MWp)
Operations: 4 shifts /5 operators/shift + 1-2 maintenance per shift

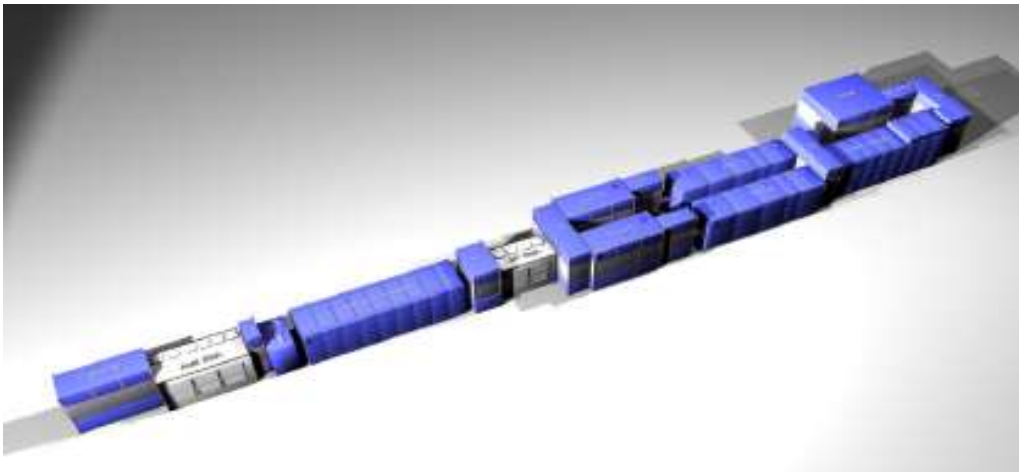

Figure 7: OTB solar line setup (60 MWp)

Cost Structure

Line configuration: 50 MW at 18M Euro (22M Euro for 60 MW)

6.4 GT Solar (now GT Advanced Technologies)

Company Profile

Company located in New Hampshire.
Contact: Vikram Singh
Turnkey business unit 2 years old

Production line

No company visit could be performed, no specific process and equipment details are available compared to the information gathered from European based companies. CDA/NDA's could not be established. Information was obtained through available literature and phone conversations.

Technology Supported

Besides inspection/characterization equipment, GT did not appear to produce their own manufacturing equipment for cell production.
Efficiency: 15.5 %
Line Yield 96 %
MES software: developed by Siemens: Smart Solar.
All components purchased from other suppliers, as GT is an integrator only
No installed lines, although five had been ordered by 2009.

Operational Requirements

No details known or supplied because of low experience and exposure in the PV solar industry.

Cost Structure

Information provided indicated that price would probably “on high end” and would be difficult to compete with the larger European Turnkey manufacturers.

Table 4: OTB Solar Business Data For Cost Estimate

OTB Solar visit at Valencia booth

cell lead time analysis			MWp/year	
acid / text.	2575	wafers/h	67.60	
diffusion	2575	wafers/h	67.60	
etching	2575	wafers/h	67.60	
PECVD (2x)	2575	wafers/h	67.60	bottle neck
screen print/firing (2x)	2575	wafers/h	67.60	
test (2x)	2575	wafers/h	67.60	
maintenance	3	h every 3 to 4 days on PECVD (bottle neck) --> feed into buffer during		
efficiency	15.8%	higher with batch (15,8%)		maintenance
utilization	90.0%			
yield	95.0%	(could be also 96%, due to OTB)		
facility	NON	specific requirements		
shift model	21.6	h per day		
delivery	9	months after PO (dependent on equipment suppliers)		
ramp time	4	months		
& installation				
floor space	80	X	8 M²	640 M²
energy consumption	1500	kWh		
operators required	40		15 per shift	4 shifts
material cost (Wp)	1	€		
raw silicon cost (Wp)	1	€		
price	17.35	M€ for fully installed line with 56MWp production capacity		
+ metrology	17.35			
distribution capability		± %		

comments
automation is included, can be run also run separate
texturig from Ryder, as well as all chemical processes, all other equipment is from OTB

Cost contribution chart:

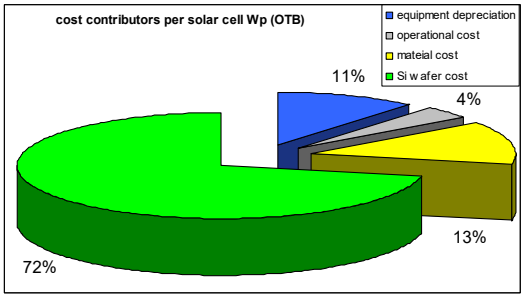

Figure 8: Cost Contribution -OTB

6.5 JUSUNG

Company Profile

Company located in Korea.

Contact:

Turnkey business unit recently, based on existing semiconductor equipment business.

Production Line

No company visit performed, no detailed information available.

Requested CDA/NDA for detailed discussions/next steps
Demonstration line was small (much less than 30MW, probably closer to 10MW, in a prototype arrangement.

Technology Supported

Besides semiconductor based equipment, did not produce their own solar equipment.
Efficiency: 15.5 %
Line Yield 95 %
All components purchased from other suppliers, integrator only
No installed units known.

Operational Requirements

No details known because of low experience and exposure in the PV solar industry.

Cost Structure

Cost should be competitive to the others included in this report.

Table 5: Jusung Business Data For Cost Estimate

JUSUNG Photovoltaic no visit

cell lead time analysis			MWp/year		
acid / text.	1400	wafers/h	34,32		
diffusion	1100	wafers/h	26,96		
etching	1400	wafers/h	34,32		
PECVD	1100	wafers/h	26,96	bottle neck	
screen print/	1400	wafers/h	34,32		
		wafers/h	0,00		
test	1400	wafers/h	34,32		
maintenance		h per week on PECVD (bottle neck)			
efficiency	15,5%				
utilization	90,0%				
yield	93,0%				
facility	NON	specific requirements			
shift model	21,0	h per day			
delivery	10,0	months after PO			
set up time	3,0	months			
ramp time	3	months			
& installation					
floor space	60	X	50 m	3000 m	
energy consu	1000	kWh			
operators rec	60				
material cost	1	€			
raw silicon cc	1	€			
price	25	M$ for fully installed line with 56MWp production capacity			
+ metrology	30				
distribution capability		± %			

comments
comes from semiconductor equipment manufacturing - limited to batch process line concept
first steps are on the way to establish in the solar turn key business
no real references are really available

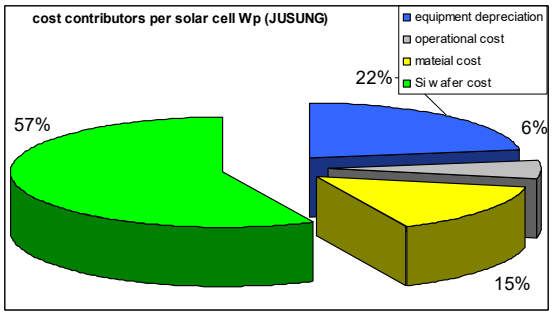

Figure 9: Cost Comparison –Jusung

JUSUNG so far would be ranking in fourth place based on the listed data in above matrices.

Table 6: Wafer cost comparison:

company	cost/Wp
Centrotherm	1,566
Schmid Group	1,6
OTB Solar	1,495
JUSUNG	1,922

*100MW production per anno

6.6 Roth & Rau

Company Profile

Company located in Germany (Saxony).
Contact: Charles Hagopian, President and CEO, R&R USA
Turnkey business unit is based on in-house metallization and automation, all other required technologies are supplied externally.

Production Line

Company may be over committed, based on solar internal industry information.
Site visit in Germany performed and technology and production facilities explored. A typical 30 MW installed production line was observed and toured at one of their customers, Spectrawatt in Hopewell Junction, NY.
Assessments of their current SINA systems and technologies were made, and their new MAiA systems potential were discussed.
Furnace suppliers in their turnkey line included those produced by Tecnofimes (for firing, drying, doping, and diffusion) as well as from Siemens.

Technology Supported

Other than metallization and automation equipment, other equipment in the turnkey line was obtained through external suppliers.
Efficiency: ~15 %
Line Yield: ~95 %
An optimized emitter produced through inline diffusion with > 80 ohm square resistivity.
Screen back surface field with Al screenprint covering entire surface.

Roadmap work included selective emitter work with SiN/SiO stack with high passivation, and contacts made with laserfiring, laser ablated holes, or etched holes. Process definition was very preliminary.
Roadmap also included high ohmic emitter and laser doping producing local n++ regions, with top surface contacts produced with either the traditional Ag screen printing technique or with NiCu plating. Again, results were very preliminary at the time of our visit.

Future concepts included a heterojunction cell, with anticipated efficiencies of >19% although there was no data to support this claim at the time.

6.7 Spire

Company Profile

Company located in Bedford, Massachussetts
Contact: Roger Little, CEO
Turnkey business is based on designing a production line consisting of equipment purchased externally from multiple suppliers.
There appears to be more expertise and experience in assembling module lines and equipment rather than cell lines, although they are very willing to put together a cell line as well, depending on the needs of the customer.

Production line

Site visit in Mass. performed and technology and production facilities explored. No prototype or production line was observed.
Individual module production and solar simulator were observed. No cell production equipment was seen.

Technology Supported

Equipment in the turnkey line was obtained through external suppliers.
Efficiency: ~15.5-16.5 % for P type multicrystalline and 17.5% for P type monocrystalline, depending on quality of incoming wafers
Utilization: ~90%
Line Yield: ~95 %
Typical line size: 30 MW/yr on 156mm2 wafers
Line specifications include 156 mm2 wafers with thickness of 200 +/- 20 um
Gross wafer throughput: 1025 wafers/hr
Uses POCL3 bath diffusion.
Can design a line for either alkaline or acid texturing.
Specifies wafers of 40-100 ohm square sheet resistivity.
Single and double AR coating
2 or 3 busbars
Roadmap for multi includes selective emitter, fine line printing, improved surface passivation, metal wrap through, laser ablation and plating, laser fired BSF and light induced plating.
Roadmap for mono includes plating, fine line printing, and ion implantation.

Operational Requirements and Cost structure not available

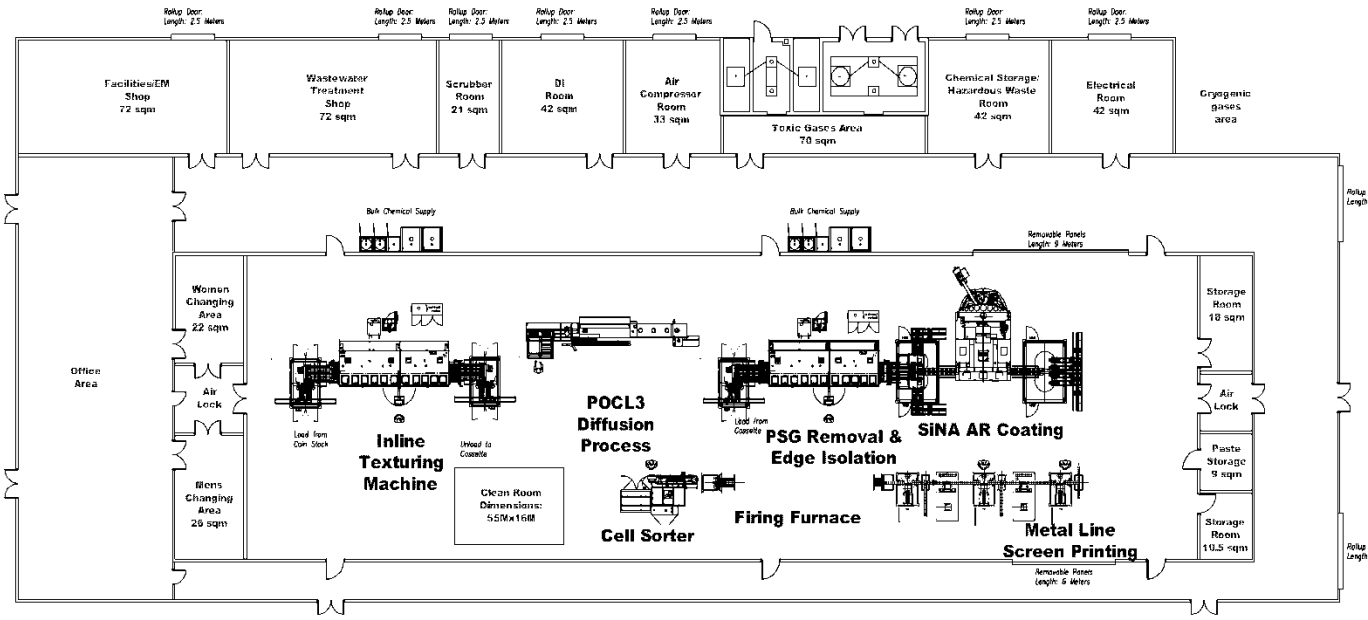

Figure10: Spire Line Setup 30 MW

6.8 Comparison

Technical comparison matrices are listed below. The tables summarize the process equipment used for the solar manufacturing process. With this the table shows the related expertise of the supplier as well as the level of criticality.

. Table 7: Summary comparing the data from subset of suppliers:

	OTB	Schmid	CT
Price	17.35 M Euro	25.8 M Euro	17 M Euro
Size:	80 m x 8 m	91 m x 24m	70 m x10m
Capacity (wafers/hr)	2400	2200	1650
Annual capcaity (MW) (multi cryst, 156 mm)	67,8	58,6	51,1
Efficiency (%)	15,8	15,9	16
Yield	95	93	96
Utilization			
	Supplier		
Unstacker	OTB	Schmid	CT
Acid Etch	RENA	Schmid	RENA
Phos doper	--	Schmid	--
Phos diffusion	Tempress	Sierratherm	CT
Edge isolation (wet)	(optional, RENA)	Schmid	--
Oxide etch	RENA	Schmid	RENA
ARC PECVD	OTB	Shimadzu	CT
Metallization	OTB	Schmid	CT
Firing	Despatch	Sierratherm	CT
Plating	--	(optional, Schmid)	--
Laser edge isolation	OTB	--	CT
Test	OTB	Schmid	CT
Sort	OTB	Schmid	CT
RPT	1hr	2.5 hrs	6 -8 hrs
Wafer thickness (min.)	180	160	180
UMG compatiblity automated wafer transfer	Experiments at Fraunhofer?	1 customer has used, 0.5 % lower efficiency	Efficiency degrade 0.8- 1.0 %
Roadmap			
R&D Facility	Fraunhofer ISE	Fraunhofer ISE	ISC
Staffing	10/shift	12/shift	15/shift
No. of lines installed	4	6	20

	Centrotherm				Schmid Group			
	Supplier	Type	Risk	criticality	Supplier	Type	Risk	criticality
Inspection	GTS	inline	expertise external	low	Schmid/external	inline	some internal exp.	low
Wet Etch	RENA	inline	expertise external	medium	Schmid	inline	internal expertise	medium
Phos Diffusion	Centrotherm	batch	internal expertise	high	Sierratherm*	inline	external expertise	high
Oxide Etch	RENA	batch or inline	external expertise	low	Schmid	inline	internal expertise	low
Edge Isolation	external	laser	external expertise	medium	Schmid	inline (wet etch)	internal expertise	medium
Dielectric Layer Dep.	Centrotherm	batch (direct plasma)	internal expertise	high	Shimitsu (Japan)	inline	external expertise	high
Metallization	external	inline	external expertise	high	Schmid/external	inline	some internal exp.	high
Firing	Centrotherm	inline	internal expertise	medium	external	inline	external expertise	medium
Testing	external	inline	external expertise	low	Schmid/external	inline	some internal exp.	low
Automation	external	inline	external expertise	low	Schmid	inline	internal expertise	low

**Schmid will aquire Sierratherm*

	OTB Solar				GT Solar			
	Supplier	Type	Risk	criticality	Supplier	Type	Risk	criticality
Inspection	RENA	inline	external expertise	low	GTS	inline	internal expertise	low
Wet Etch	RENA	inline	external expertise	medium	external	inline	external expertise	medium
Phos Diffusion	Tempress	batch ($POCL^3$)	external expertise	high	external	inline	external expertise	high
Oxide Etch	RENA	inline	external expertise	low	external	inline	external expertise	low
Edge Isolation	RENA[1]	inline	external expertise	medium	external	inline	external expertise	medium
Dielectric Layer Dep.	OTB	inline	internal expertise	high	external	inline	external expertise	high
Metallization	OTB[2]	inline	internal expertise	high	external	inline	external expertise	high
Firing	Despatch	inline	external expertise	medium	external	inline	external expertise	medium
Testing	OTB	inline	internal expertise	low	external	inline	external expertise	low
Automation	OTB	inline	internal expertise	low	external	inline	external expertise	low

1Edge isolation: wet etch; alternative: laser integrated with Tester (OTB solution)
2Can be replaced by Baccini unit upon request

	JUSUNG				Roth & Rau			
	Supplier	Type	Risk	criticality	Supplier	Type	Risk	criticality
Inspection	Jusung	inline	internal expertise	low	R & R	inline	internal expertise	low
Wet Etch	Jusung	inline	internal expertise	medium	external ?	inline	external expertise	medium
Phos Diffusion	external ?	inline	external expertise	high	external ?	inline	external expertise	high
Oxide Etch	Jusung	inline	internal expertise	low	external ?	inline	external expertise	low
Edge Isolation	external ?	inline	external expertise	medium	external ?	inline	external expertise	medium
Dielectric Layer Dep.	Jusung	inline	internal expertise	high	external ?	inline	external expertise	high
Metallization	external ?	inline	external expertise	high	R & R	inline	internal expertise	high
Firing	external ?	inline	external expertise	medium	external ?	inline	external expertise	medium
Testing	external ?	inline	external expertise	low	R & R	inline	internal expertise	low
Automation	Jusung	inline	internal expertise	low	R & R	inline	internal expertise	low

.

Table 8: Summary Tables of Technical Expertise Comparison

Centrotherm / Schmid				
	Supplier	Type	Risk	criticality
Inspection	Schmid	inline	some internal exp.	low
Wet Etch	Schmid	inline	internal expertise	medium
Phos Diffusion	Centrotherm	batch	internal expertise	high
Oxide Etch	Schmid	batch or inline	internal expertise	low
Edge Isolation	Schmid	etch	internal expertise	medium
Dielectric Layer Dep.	Centrotherm	batch (direct plasma)	internal expertise	high
Metallization	Schmid	inline	some internal exp.	high
Firing	Centrotherm	inline	internal expertise	medium
Testing	Schmid	inline	some internal exp.	low
Automation	Schmid	inline	internal expertise	low

OTB Solar / Schmid				
	Supplier	Type	Risk	criticality
Inspection	Schmid	inline	some internal exp.	low
Wet Etch	Schmid	inline	internal expertise	medium
Phos Diffusion	Tempress	batch	internal expertise	high
Oxide Etch	Schmid	batch or inline	internal expertise	low
Edge Isolation	Schmid	etch	internal expertise	medium
Dielectric Layer Dep.	OTB Solar	batch (direct plasma)	internal expertise	high
Metallization	OTB Solar	inline	internal expertise	high
Firing	Tempress	inline	internal expertise	medium
Testing	OTB Solar	inline	internal expertise	low
Automation	OTB Solar	inline	internal expertise	low

OTB Solar / Centrotherm				
	Supplier	Type	Risk	criticality
Inspection	RENA	inline	external expertise	low
Wet Etch	RENA	inline	external expertise	medium
Phos Diffusion	Centrotherm	batch	internal expertise	high
Oxide Etch	RENA	inline	external expertise	low
Edge Isolation	RENA[1]	inline	external expertise	medium
Dielectric Layer Dep.	OTB	inline	internal expertise	high
Metallization	OTB[2]	inline	internal expertise	high
Firing	Centrotherm	inline	internal expertise	medium
Testing	OTB	inline	internal expertise	low
Automation	OTB	inline	internal expertise	low

The comparison is based on the questionnaire we used to interview the suppliers as well as the visit It is very obvious, that Centrotherm, Schmid and OTB Solar all have excellent expertise in the solar manufacturing related processes. Interesting is the fact that the combination of both works extremely complementary. OTB, on the other

hand, produces only the dielectric layer deposition and metallization equipment internally (all other process steps are obtained from external suppliers). While the external suppliers for the critical process steps (RENA for cleaning, Tempress for POCl3 diffusion and Despatch for firing) are well established players in their respective area, it is not clear how much expertise OTB has built up in these critical areas internally. For GT Solar, all process equipment is obtained from external suppliers and only the metrology part is developed internally. GT Solar is assuming solely the role of the equipment integrator without strong internal expertise on critical process steps.

6.9 Risk Assessment

The summarized risk assessment for the companies investigated is listed below (other companies' entries to be included in final report).

Table 9: Risk assessment table listing arguments based on data above

ranking/criteria	business risk	technical risk
Centrotherm	turn key line delivers good business numbers, this in terms of equipment cost as well as volume, yield and efficiency capability	all critical process steps are covered with internal skill and expertise, technical roadmap in place to go at least in line with solar device producing industry, very excellent references are available
Schmid Group	turn key line delivers good business numbers, this in terms of equipment cost as well as for the volume capability, yield and efficiency capability could be better	critical process steps are not covered with internal skill and expertise, all wet processes are supported with excellent expertise and related technical support and roadmap, number of references are OK
OTB Solar	turn key lines delivers reasonable business numbers, the equipment cost is OK as well as volume and yield capability, the efficiency could be better	dielectric layer deposition is a specific expertise and unique resolved with state of the art technology to secure pinhole free deposition, good collaboration with the supply base to secure good tecnical roadmap, low number of references in place
GT Solar	not suffiecient numbers available to validate the turn key line capabilities, price for equipment seems to be highest compared to others, volume and yield outlook looks reasonable, but not the secured efficiency	non of the critical process steps are supported through internal expertise, technical improvement and roadmap is dependent on the supply base, pretty much no references shown
JUSUNG	Jusung comes from semiconductor equipment side, but has no strong references within the solar business, seems that they want to get established (new in the business)	good semiconductor equipment background, but seem to have quite some defizite in solar specific requirements, like diffusiona nd metallization
Roth & Rau	after decent market search we got the impression, that R&R is quite over commited and shows fairly high lack of flexibility	R&R has excelent skill and experience in metallization and pretty much buys all other necessary equipment, therefore we see quite some deficite in sufficient technical support

Table 10: Risk Assessment by Criteria

assessment criteria	Centrotherm	Schmid	OTB Solar	GT Solar	JUSUNG	Roth & Rau
efficiency	16%	15,7%	15,5%	15,5%	15,5%	~15%
yield	96%	95%	95%	96%	95%	95%
utilization	90%	90%	90%	90%	90%	90%
60MW cost (M€)	28,00	25,00		NA	NA	NA
mfg cost* (€)	1,32	1,37	1,39	NA	NA	NA
60MW revenue forecast** (M€)	246,4	245,4	242,3	NA	NA	NA
total cost for 60MW production* (M€)	147,4	152,3	152,5	NA	NA	NA
delta between revenue and cost (M€)	99,0	93,1	89,8	NA	NA	NA

** doesn't include overhead and profit*

*** based on 2,2€ price per Wp*

Table 11: Summation of Advantages and Disadvantages (partial list)

ranking/criteria	advantages	disadvantages
Centrotherm	Good POCL furnace technology Most references High effeciency guarantied Good R&D support and roadmap Good finished cell cost Line layout ha	Inline furnace to big, high energy consumption No inline support and automation Too much operation required Too much handling required No internal wet pr
Schmid Group	Excellent wet process capabilities Excellent R&D support and roadmap Owns wet edge isolation technology Owns condensation chamber doping technology Light induced plating capability Hig	Inline technology favored Line layout pretty rigid No internal PECVD expertise No internal furnace expertise Largest footprint required Highest turn key line cost
OTB Solar	Excellent PECVD technology (pinhole free) Highly automated layout Lowest operational effort Highest throughput Best finished cell cost	Smallest reference list Inline technology favorized No internal furnace expertise No internal metalization expertise No internal wet process expertise

Table 12 compares POCL vs inline diffusion capabilities to process UMG type of wafer substrates. Details to the table above must be further investigated to understand the impact of temperature and duration UMG wafers on UMG wafers. This in consideration of bulk defects / contaminations.

	inline diffusion and wet doping	**POCL diffusion and gaseous doping**
pro's	good monitoring possible high phosphor concentration possible short process time	gaseous doping industry trend efficiency advantage ? higher flexibility
con's	backside has contact to teflon belt less flexibility	uniformity is questionable long process time required

Table 12 Comparing POCL vs inline diffusion for UMG usage.

7. Forensic Analysis

7.1 Project Highlights

After a pause in carrying out the work statement in the project, work was resumed in January, 2014. The emphasis in the project shifted to forensic measurements of solar cells made on turn-key lines from different manufacturers. As much as possible and when available, analysis would be made on starting material as well as finished cells. Forensic measurement techniques have already been described earlier in this report.

Gettering was studied extensively in previous years and it was decided to finish this study in order to come to a conclusion. While there is no doubt about the benefits coming from gettering: lifetime increase, shunt leakage decrease, higher Voc's and better standard deviations, these advantages come at the price of slower throughput, increased complexity, and higher cost.

For the forensic measurements of turn-key fabricated devices, solar cells were purchased from 10 different suppliers to add to the lots already in hand, resulting in 18 different solar cell lots from 11 different manufacturers available for comparison and learning. Lot sizes ranged from 10 cells to 50, with 20 being the median number. All cells in all lots were measured by a host of techniques in order to obtain reasonable statistics, although it was found that 10 cells in a lot weren't always sufficient for high confidence levels. The purpose of the project was to determine what factors could be identified that controlled device performance and therefore what improvements could be made to enhance efficiency. Some thin film Si solar cell experiments were described and full solar cell panel performance was measured for panels from 9 different solar cell manufacturers.

∗ Gettering has been studied at many facilities using many types of material and many gettering protocols. Most processes involve phosphorus diffusion with subsequent removal of the defective impurity-containing zones at the surfaces. Al alloy gettering has also been used, and a combination of Al alloying and phos, diffusion. Results on "poor quality" starting material as evidenced from these studies are compiled in Table 13. Lifetimes can be improved by 2-10x by several time/temperature protocols and for both p-type and n-type

Table 13. Literature Gettering Results. L = diffusion length = √(D*❶)

Getter	Temp. °C	Time, mins	Other	Start	After Getter	Year
Phos.	880		n-type, bad area	25 µs	200 µs	1991
Phos.	920		n-type, bad area	25 µs	300 µs	1991
Phos.	880		n-type, good area	69 µs	312 µs	1991
Phos.	920		n-type, good area	69 µs	590 µs	1991
Aluminum	800	30	Diffusion length	70 µm	160 µm	1993
Phos.	900	210	L / L(start)		0.7 - 1	1996
Aluminum	900	210	L / L(start)		1.0-1.5	1996
Phos. + Al	900		L / L(start)		0.7-1.3	1996
Phos.	850	30	p-type	40 µs	70 µs	1997
Phos.	850	180	p-type	40 µs	94 µs	1997
Phos.	900	180	p-type	40 µs	180 µs	1997
Phos.	1000	180	p-type	40 µs	40 – 60 µs	1997
Phos.	900	20	p-type	6 µs	8 µs	2000
Phos.	900	60	p-type	6 µs	45 µs	2000
Phos.	900	120	p-type	6 µs	50 µs	2000
Phos.	860	300	p-type	35 µs	135 µs	2006
Phos.	880	90	p-type	35 µs	105 µs	2006
Phos.	880	120	p-type	35 µs	110 µs	2006
Phos.	900	60	p-type	35 µs	110 µs	2006

Phos.	880	45	without plateau	78 μs	122 μs	2007
Phos.	880	45	with plateau	78 μs	164 μs	2007
Phos.	850	20	UMG Si	L = 40 μm	L = 50 μm	2008
Phos.	880	60	UMG Si	L = 40 μm	L = 70 μm	2008
Phos. + Al	880	60' + 30'	UMG Si	L = 40 μm	L = 100 μm	2008
Phos. + Al	880	60' + 120'	UMG Si	L = 40 μm	L = 150 μm	2008
Phos.	900	10	Fe contaminated	2 μs	22 μs	2009
Phos. + Al	900	10	Fe contaminated	2 μs	73 μs	2009

material. It is common that low starting lifetimes is generally improved more than better quality raw material, and that the degree of improvement is very material-dependent. This was seen and noted in earlier quarterly reports.

Gettering was studied extensively in earlier periods of this project, and reported on at length in previous quarterly reports. Generally, results at IBM are in total agreement with the outside literature results, but some of the IBM findings are new. The key features of gettering include:

1) the lifetime in poor initial lifetime UMG material could be improved by as much as 10X;
2) the biggest efficiency limiting factor in UMG cells was shunt leakage; however, gettering in turn-key manufactured cells was considerably improved by the gettering;
3) the saw damage present on both surfaces of starting wafers does not provide effective gettering in spite of high defect densities, but saw damage enhances gettering by phosphorus diffusion and is better left on during gettering;
4) the lifetime in high dislocation density regions does not improve significantly with gettering while in low DD regions the lifetime can improve substantially;
5) gettering efficacy is very substrate dependent, improving in some starting material, degrading in other material, or remaining the same. Differences in impurity content, oxygen content, and dislocation distributions can account for the differences.
6) spin-on phosphorus-doped glass can be used as an alternative to $POCl_3$ diffusion,
7) gettering is improved by adding a low ($600^{O}C$) "soak" step after the high temperature treatment, which adds an "internal" gettering effect that removes recombination centers from the material (even if they are not removed physically); the optimum times were not established;
8) ingots where gettering degrades rather than enhances lifetime are usually monocrystalline and exhibit very different lifetime maps indicative of radial oxygen distribution
9) the improvement in lifetime due to gettering is often accompanied by Jsc and Voc improvements as well as reduced shunt leakage.
10) gettering can improve device parameter standard deviations as a percentage of lifetime, increasing uniformity.

Figure 11a is a simulation of efficiency versus lifetime which illustrates the benefit of higher lifetime values (higher Voc, Jsc, and even FF). Figure 11b is a schematic of the benefit of gettering, based on the demonstrated lifetime improvements. Figure 12 is an experimental result comparing gettered and non-gettered turnkey cells from a Chinese turn-key

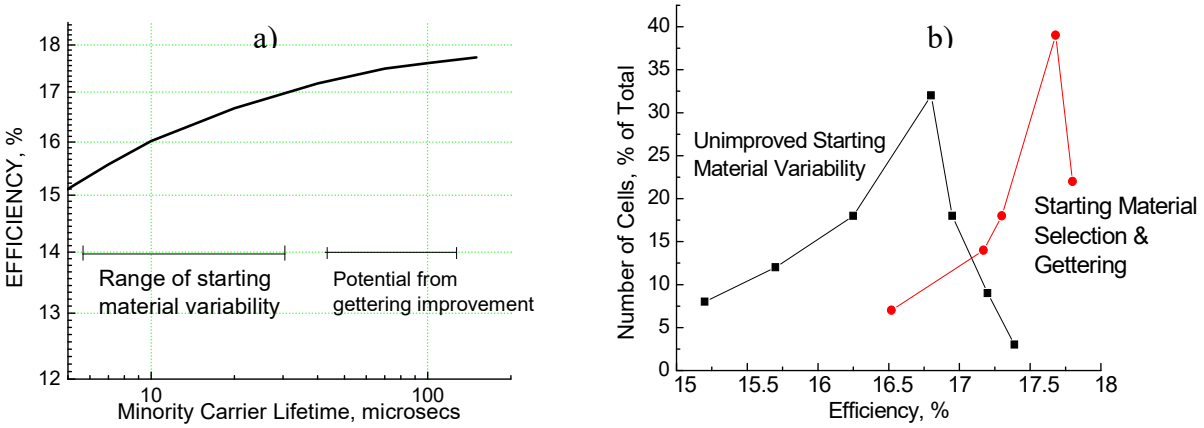

Figure 11a (left). Simulated efficiency versus base lifetime. b) (right) hypothesized distribution of cell frequency versus efficiency, indicating reduced binning.

manufacturer. The experimental result is consistent with the simulations of Figure 11. In addition to improved efficiencies and higher yields from gettering, the better distributions also improve cell "binning," leading to higher averages. However, the added cost of the procedure would have to be weighed against these benefits.

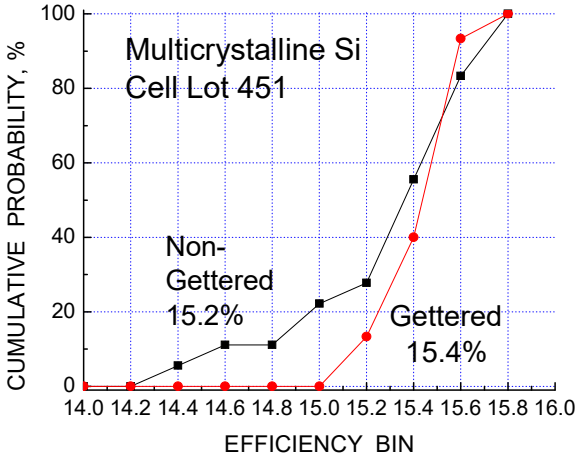

Figure 12. Experimental demonstration of gettering improvements made on a multicrystalline turn-key lot.

Other important device parameters are also enhanced by gettering. Figure 13 shows the effect of gettering on shunt resistance and fill factor. Slight improvements were also observed on the short circuit current, but there was no benefit to series resistance from gettering. The biggest effect, as seen in all cells including UMG devices and indicated in Figure 13 was in the shunt resistance, sometimes improved by a factor of 10 in leaky material.

Figure 13. Effect of gettering in a turn-key lot on Rsh and FF distribution

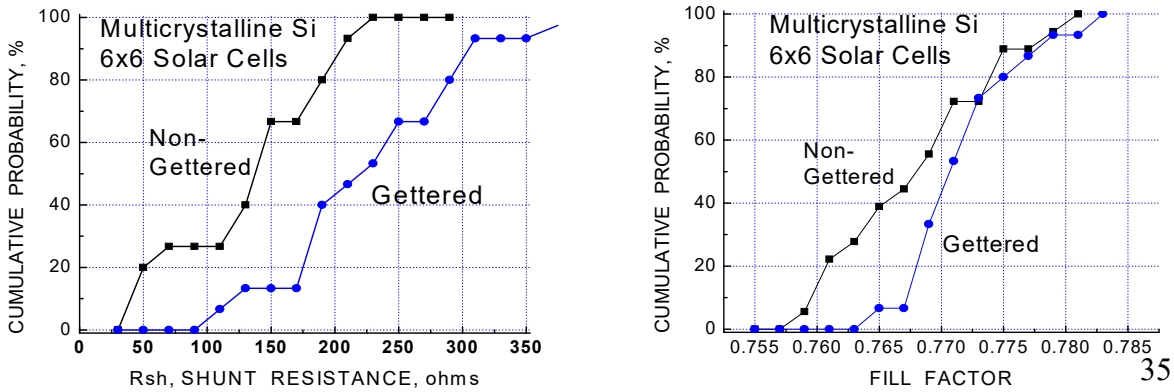

.* In this quarterly report, a detailed description was given of different forensic techniques that can be used to analyze devices, with the goal of determining what physical effects are limiting the efficiency. A brief description has already been given for these techniques. For convenience, they are listed again here.

Dark I-V analysis	- Rshunt, shunt leakage
Light I-V analysis	- Voc, Isc, Rseries, Efficiency, FF
Quantum Efficiency	- Lifetime, passivation, reflectance
Reflectance vs wavelength	- Optical performance
Reflectance vs angle	- IR Transmission
Pulse Eddy Current	- Lifetime, Trap density, Resistivity
Photoconductivity decay	- Lifetime, Diffusion Length, mapping, dislocations
Photoluminescence	- Lifetime, mapping
Lok-in Thermography	- Electroluminescence
Impedance Spectroscopy	- Series resistance, capacitance

* Electrical Analysis. In this quarter, the first highly detailed analysis of the 18 turn-key lots was begun. This entailed:

Solar Simulator : used to measure Efficiency, Voc, Jsc, FF, Vmp. Imp
Voc – Isc : used to obtain J0 and n, the key diode parameters under cell operation
Dark I-V : together with Voc/Isc, used to obtain Rseries and Rshunt
Correlation Plots : correlations of efficiency and other key parameters

The lots being investigated and the number of cells in each lot are given in Table 14. Correlation charts were made by plotting efficiency against Voc, FF, Rs, etc. to see what dominant factors emerged. Some examples of correlation plots for several turn-key lots are given in Figure 14. What emerged quickly was that different cell lots were dominated by different parameters. In some cases, efficiency correlated well with Voc or Jsc, in other cases they didn't correlate at all. J0 and n were important for a few lots while Rs or FF were key parameters for others. The implication is that the physics going on could be different for cells from different manufacturers due to different processes and different starting material.

Company/Ingot	Type	# Cells	<η>	Min - Max	Range	Std. Dev.
Linuo /111	5" Mono	70	17.87	17.11 – 18.04	0.93	0.17
Linuo /201	5" Mono	49	17.84	17.67 – 18.03	0.36	0.093
NNMN	5" Monos	31	17.12	13.05 – 17.68	4.63	1.10
TG Solar	6" Mono	10	17.74	15.18 – 17.9	2.72	0.82
Green Energy	5" Mono	20	15.60	3.8 – 15.63	11.8	5.51
Top Solar	5" Mono	20	16.34	2.57 – 17.29	14.7	5.25
PVL451	Multi	30	15.79	15.59 – 15.92	0.33	0.084
PVL161	Multi	30	15.55	15.23 – 15.75	0.52	0.13
NNML	Multi	16	15.38	14.25 – 15.69	1.44	0.40
GTML	Multi	15	15.40	15.13 – 15.7	0.57	0.15
Casting	Multi	39	15.49	14.51 – 16.2	1.69	0.36
Allpowers	Multi	16	16.31	15.45 – 16.82	1.37	0.37
GinTech	Multi	11	15.82	15.74 – 15.92	0.18	0.55

ML Solar	**Multi**	**18**	**15.37**	**14.57 – 16.23**	**1.66**	**0.47**
TG Solar	**Multi**	**10**	**15.74**	**14.32 – 16.21**	**1.89**	**0.59**
YYOO67890	**Multi**	**10**	**15.12**	**14.83 – 15.49**	**0.66**	**0.19**
Kyocera	**Multi**	**31**	**13.75**	**13.3 – 14.95**	**1.65**	**0.45**
Big Sun Solar	**Multi**	**11**	**15.59**	**15.55 – 15.84**	**0.29**	**0.109**
LED Solar	**Multi**	**20**	**16.09**	**15.82 – 16.23**	**0.94**	**0.28**

Table 14. Average efficiencies, ranges, and standard deviations for the turn-key lots.

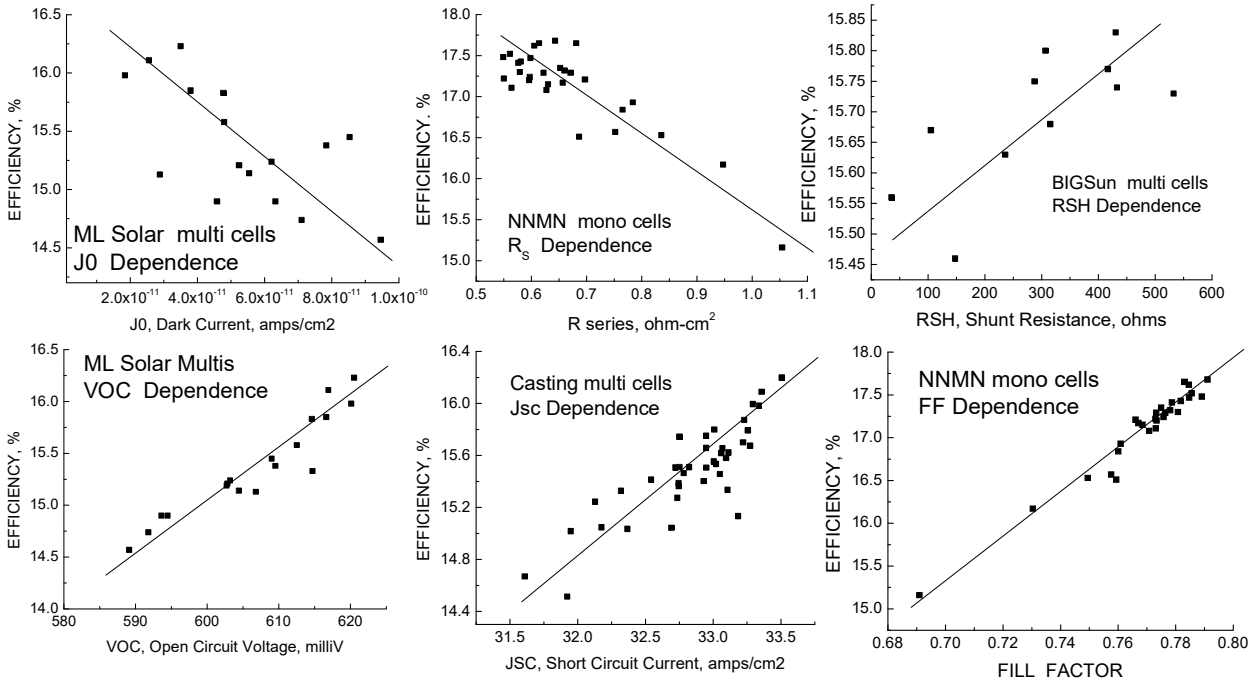

Figure 14. Examples of correlations between efficiency and cell parameters.

For the first segment of turn-key lots, correlations (or lack thereof) between major device parameters were tabulated to see what trends would become apparent. The correlations for all the lots were completed during the next quarter. A comparison of average values for the major solar cell parameters is also very important and is shown in Table 14. Table 14 accompanies Table 14which listed efficiencies and standard deviations for these lots.

Table 15. Average values for the cells in the turn-key lots.

Cell Lot	<Voc>	<Jsc>	<FF>	<J0>	<Rs>	<Rsh>	<η>
NNMN	620.4	35.85	0.770	1.5e-11	0.667	146	17.12
Green E.	618.7	32.71	0.771	7.1e-9	0.741	221	15.60
TOP Solar	623.8	33.55	0.781	1.4e-9	0.872	2570	16.34
111	625.9	36.22	0.788				17.87
201	624.1	36.22	0.791				17.84
TG Solar	638.8	35.39	0.785	4.6e-12	0.535	8.34	17.74
MLSolar	606.9	32.12	0.789	6.6e-11	0.588	373	15.37
PVL 451	617.4	32.34	0.791	2.2e-11	0.444	730	15.79
Casting	610.9	32.84	0.772	6.5e-11	0.598	222	15.49

PVL 161	614.1	32.21	0.786	3.7e-11	0.434	708	15.55
NNML	613.5	32.59	0.769	4.1e-11	0.619	146	15.38
GinTech	615.9	32.76	0.784	2.4e-11	0.514	389	15.82
AllPower	624.4	32.98	0.792	4.3e-11	0.431	13.3	16.31
BigSun	615.2	32.41	0.787	2.7e-11	0.618	295	15.69
Led Solar	619.3	32.82	0.790	7.4e-11	0.513	358	16.09
YYOO Sol.	607.9	32.17	0.773	3.7e-10	0.531	331	15.12
Kyocera	602.1	30.17	0.757	8.4e-9	0.209	210	13.75
GETML	613.4	32.53	0.772	4.0e-11	0.635	237	15.42

Cells in yellow are mono and cells in green are multis. Clear trends are evident between the two. Monos exhibit higher Voc, Jsc, and efficiency than multis, not surprising since lifetimes are generally higher and J0 usually lower, with no grain boundary effects and lower impurity levels. On the other hand, Rs, Rsh, and FF are comparable. These are determined mostly by design factors such as grid design, and base and emitter resistivities, and partly by process factors such as diffusion temperature and Al alloying and are much less affected by the material directly except in gross cases where microcracks can cause low shunt resistances. The shunt resistance is shown to be largely unimportant; one of the highest efficiency lots has the lowest value of Rsh. There is a weak trend of FF with series resistance - higher values of FF for lower Rs - but within individual lots this isn't always the case (as will be seen in correlation plots).

* Factors Which Influence Efficiency. Nearly all solar cell results are quoted as peak efficiency, usually under solar simulators which mimic the solar spectrum reasonably well but contain excess light in the infrared region. In the "real world," conditions outdoors are always changing during the day, week, or month, while measurements are complicated by clouds which block sunlight at some times but actually reflect sunlight onto cells at other times and increase the incoming optical power in periodic bursts compared to a cloudless day. Sunlight is also incident at oblique angles rather than normal to the cell or panel surface, which reduces the light intensity as the cosine of the angle of incidence. Temperature variations, Air Mass values (path of sunlight through the atmosphere) and possibly spectral effects can also lower the power output and efficiency. The effects of Air Mass and incidence angle are given by:

$$Pout_{direct} = SC * 0.7^{\cos(Z)^{-0.678}} * \cos(A) * Efficiency$$

where Z is the zenith angle and A the angle of incidence with respect to the wafer or panel normal., and SC is the solar constant: 1.35 kilowatts/m^2. Diffuse radiation reflected from clouds, buildings, etc. add to the incident intensity while cloud shadowing subtracts from it. Figure 15 shows the incidence angle as a function of time of day for a fixed panel facing south and tilted at the local latitude (Albany, NY) while Figure 16 shows the power incident on the panel through the day. Efficiency can vary as a result of temperature, intensity, and reflection versus angle, but the biggest losses in power output are due to the cosine loss and secondarily by the atmospheric absorption.

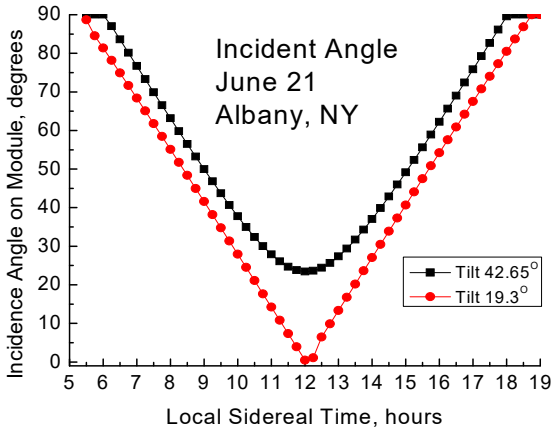

Figure 15. Angle of incidence of sunlight on a fixed solar panel or cell versus time of day. Black: tilt at local latitude; red: optimized at a fixed angle for summer.

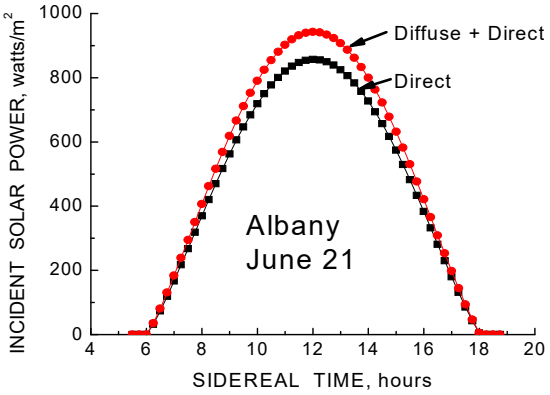

Figure 16.. Power incident on a solar panel or individual cell versus time of day. Panel facing south with tilt equal to the local latitude.

The incident solar spectrum changes slightly throughout a day and over the time of year due to the passage of sunlight through the atmosphere. Absorption and scattering are affected by the humidity, dust, aerosols, ozone, and other atmospheric conditions and therefore related to the path length and air mass. Since scattering is related to the 4th power of the wavelength, it might be expected that the solar *spectrum* incident on cells and modules would change with these atmospheric conditions, and since solar cells don't exhibit uniform quantum efficiency at all wavelengths, changes in incoming spectra could causes changes in efficiency. However, analysis of the spectrum under various conditions shows that while the total incident power changes with these atmospheric conditions, the spectrum itself on the panel is almost constant, so that the spectral effect of incoming sunlight coupled with the spectral response of typical cells is of minor importance (except near sunrise and sunset when the sun "turns red").

∗ Thin Film Si Solar Cells. The thickness of raw wafers used for Si solar cell fabrication has been dropping steadily and is now less than 200 microns due to advances in wafer handling. Light trapping and surface texturing minimize the loss of solar photons at long wavelengths. The reduced thickness results in lower cost without much (if any) loss in efficiency, making the cost per watt increasingly attractive.

An entirely different type of thin film Si device is obtained by thin Si films deposited on "low cost substrates." Devices have been made in the solar community with Si films on graphite, stainless steel, glass or quartz, and even plastic, but such devices have not demonstrated high efficiencies. A different approach is to use low cost P+ Si as the substrate, which can even be UMG material. The P+ Si substrate does not participate in the conversion efficiency but does provide a low resistance mounting and an excellent BSF, and it provides a substrate lattice-matched to the film which greatly lowers defect densities.

For this project, solar cells were made by conventional phos. diffusion on Si films of 5, 10, 20, and 40 microns thickness grown epitaxially upon P+ Si <100> oriented wafers with 1-4x10^{19} cm^{-3} doping. The substrate forms the back contact and the upper contact was a TiPdAg grid with additional Cu plating. Figure 21 shows the spectral responses of these thin film cells of different thicknesses. As expected, the long wave response suffers from light penetrating through the film without being absorbed, since these cells did not include any form of light trapping to gain some of these long wavelength photons back. (This can be remedied by using thinner P+ wafers and better back surface reflection.)

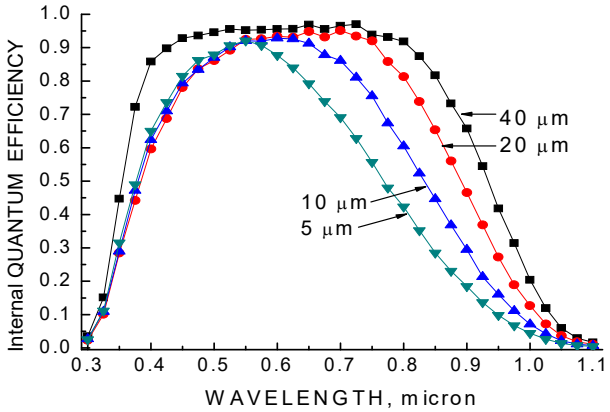

Figure 17. Internal quantum efficiencies of Si thin film cells on P+ substrates.

Table 15 and Figure 17 show the parameters for the cells versus Si thickness. The FF is very high as a result of the low series resistance associated with the P+ substrate. The Jsc decreases due to the lost photons. The Voc follows the theoretical prediction that it increases as the film is made thinner on devices with high quality BSF's; this result is due to the reduced recombination and reduced dark current in the diode for thinner layers. Figure 18 shows a comparison of a conventional cell design and an enhanced cell design, showing

Table 16. Device solar cell parameters for thin film Si cells

Thickness μm	Voc	Isc	FF	Effic.
40	.61	26.0	.808	12.6
20	.608	21.9	.81	10.7
10	.619	19.4	.81	9.25
5	.624	16	.82	7.64

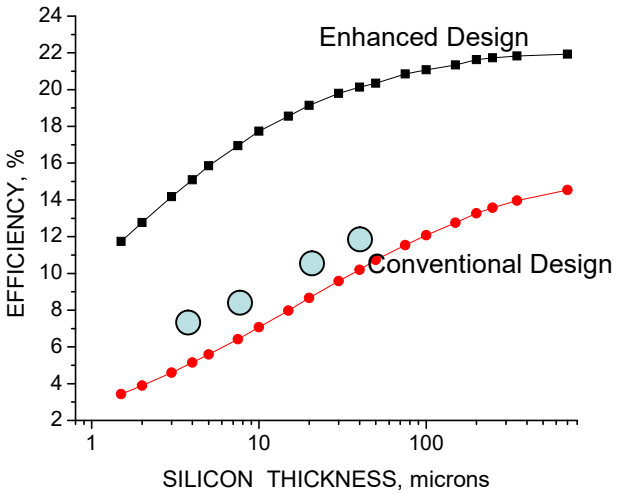

Figure 18. Measured efficiencies compared to simulations with conventional design and with enhanced design.

the potential of thin film Si devices made on low cost P+ Si substrates. The "conventional" design uses single emitter, single layer AR coating, no texturing, and no light trapping. Double layer ARCs, selective emitter, and light trapping can raise these efficiencies to near bulk values.

* Optical measurements as a function of incidence angle for the 18 lots discussed previously were carried out for angles from 15^{O} to 75^{O}. The motivation for doing this was the varying angle of sunlight on a fixed panel over the course of a day and the expected effect of incidence angle on the reflectance and quantum efficiency of AR-coated and surface textured Si cells and panels. It was already known that angles from 0 to 40^{O} make almost no difference on reflectance from ***flat*** surfaces, while higher angles produce higher reflectances and consequently lower quantum efficiencies. It was not known to what degree this would also occur with ***textured*** surfaces. In addition, mono cell surfaces receive a base (NaOH) chemical etching which results in a pyramidal surface with facets all oriented the same way, while multi cell surfaces receive an acid etch which leaves a randomly-oriented scalloped surface with multiple dimensions on the different grains. Monos and multis could therefore exhibit differences in their reflectance versus angle.

Figure 19 shows reflectance vs angle from 15 to 45^{O} for mono cells (left) and multis (right). There is virtually no difference with angle for the multicrystalline device and little

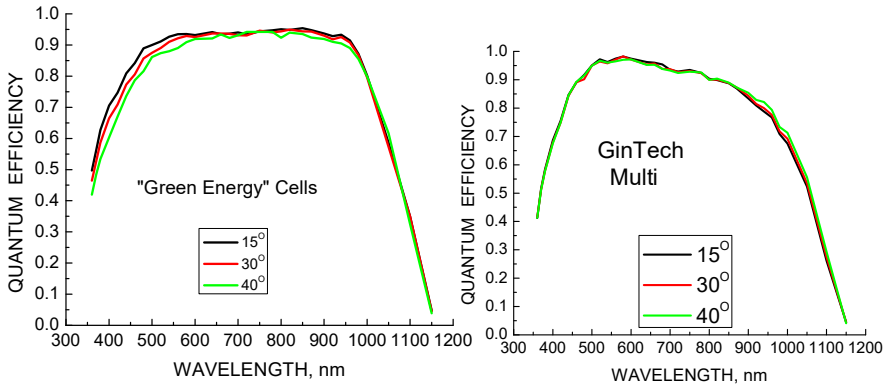

Figure 19. Spectral responses versus angle from 15 to 45O for mono cells (left) and multis (right).

difference for the monos except a slight decrease in the short wave region. Figure 20 compares responses over the whole wavelength range. The difference between monos

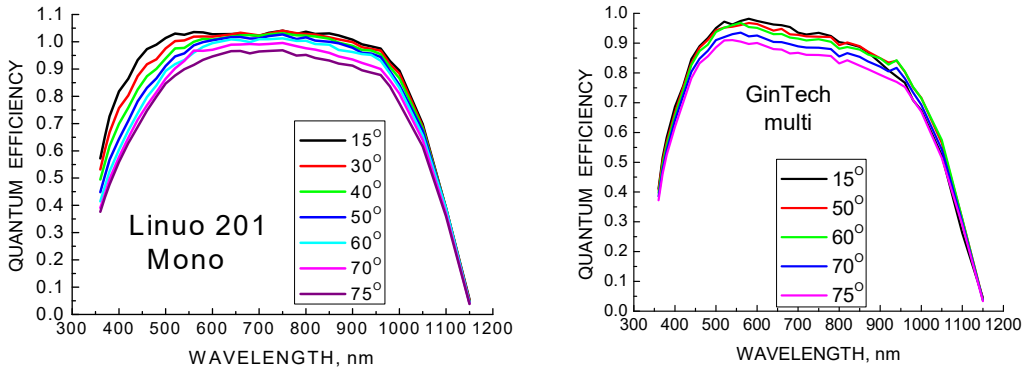

Figure 20. Spectral response versus wavelength for monos (left) and multis (right).

and multis is striking. Both show small dependence for long wavelengths and the expected decrease in QE in the visible range. The pyramidal textured surface of the mono cells, however, causes a considerably higher reflectance and lower QE at short wavelengths, while the scalloped surface of the multicrystalline cells results in a much smaller dependence. This dependence of reflection and QE on solar angle will likely show up in diurnal solar panel performance as well as for individual cells.

∗ Correlations. Some preliminary correlations of efficiency with forensic cell parameters were described in last quarter's report. Correlations or lack thereof have been completed for all 18 turnkey lots and are given in detail in the section of this report on individual cell lots. Table 17 summarizes these correlations using the high, medium, low, and "no" description.

Table 17. Correlations between efficiencies and forensic I-V parameters.

Cell Lot	≈ - Voc	≈- Jsc	≈ - FF	≈ - J0	≈ - n	≈ - Rs	≈ - Rsh
NNMN	M	N	H	N	L	N	N
NONMN	H	L	H	N	N	H	L
Green Energy	N	N	H	N	N	L	N
TOP Solar	N	N	H	N	N	N	N
111	H	M	H				
201	H	M	N	N			
TGSolar mono	M	L	M	N	N	M	N
MLSolar	H	H	N	L	L	N	N
PVL 451	N	L	M	N	N	N	L
Casting	H	H	M	N	N	N	N
PVL 161	N	N	M	N	H	N	N
NONML	H	H	N	L	N	L	N
NNML2	H	H	N	N	N	Anti	N
GinTech	N	N	M	L	N	N	N
AllPower	H	M	L	L	L	M	N
BigSun	L	N	H	M	M	N	M
LED Solar	L	L	N	L	N	N	N
TG Solar multi	N	L	H	L	N	N	N
Kyocera	H	H	N	M	M	N	N
YYOO Solar	L	M	N	N	N	N	N
GETML	N	H	N	N	N	N	N

The expectation was that efficiency would correlate strongly with Voc, Jsc, and FF, since efficiency is defined as (Voc∗Jsc∗FF) / P_{IN}. While this is apparent in many cases as seen in Table 16, there are also many cases where there is little or no dependence on one or more of these parameters. It is also true that the efficiency doesn't correlate well with Rs or Rsh, and in one case there was actually an anti-correlation where efficiency increased as Rs

became higher. What these results are saying is that there is no one parameter in general which dominates for all turn-key cells, but that each manufacturer has to investigate his starting material quality and his process to maximize good features and minimize bad ones,

and these may differ significantly between manufacturers. Forensic correlations such as Table 16 would be valuable in helping them identify problems. In addition, when a parameter such as FF dominates efficiency, the sub-correlations between FF and Rs, Rsh, J0, or n may lead toward problem solving and reduced binning. Many of these sub-correlations will be shown in the detailed summaries of individual lots in following sections.

∗ Lifetime and LBIC Maps. Both these kinds of maps can help in showing uniformity, hot spots, edge effects, and so forth. Lifetime maps on finished cells are not the same as on etched and passivated starting material, since the finished cells include the metal electrodes on front and back and the emitter region, as well as any effects of processing. LBIC maps however are direct and include the same factors: lifetime, BSF, non-uniformity, as affect the performance in full sunlight. LBIC maps are also valuable in that LBIC at long wavelength comes entirely from the base region while LBIC at short wavelength comes entirely from the emitter region. Spectral response measurements – quantum efficiency versus wavelength – provide similar information but only for one position on the wafer at a time. LBIC maps measure 20,000-30,000 points on the wafer in a time of several hours.

Figure 21 shows LBIC maps taken at 981 nm laser excitation where the maps show collection only from the base. The cell on the left yields an efficiency of 0.4% with poor

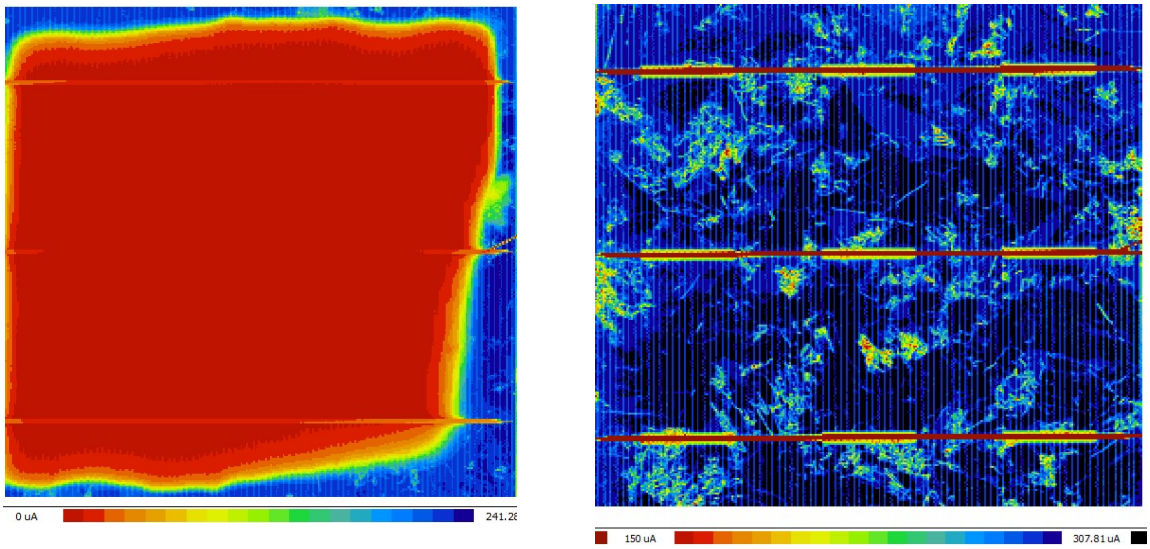

Figure 21. LBIC maps for cells from a turn-key supplier using long wavelength excitation. (AllPowers: Left – cell 16, 0.4%; Right – cell 6, 16.2%).

Jsc, while the cell on the right shows normal response for a multicrystalline cell and has an efficiency of 16.2%. At the same time, portions of the left cell show normal high response. An LBIC map such as this is a valuable forensic tool to illustrate uniformity issues. (It should be said also that an electroluminescence or photoluminescence map would also reveal such problems but are less direct and less quantitative, though faster.) Figure 22 shows these same two cells measured with 404 nm excitation where light is absorbed entirely in the emitter. Evidently the problems with the poor quality cell #16 extend into the surface as well as the base. The map of cell 6 on the right is more typical of LBIC maps of

multi wafers; the grain structure has disappeared since the lifetime is entirely dominated by Auger recombination with no significant contribution from grain boundaries. Nonuniformities in the emitter are easily seen in such maps.

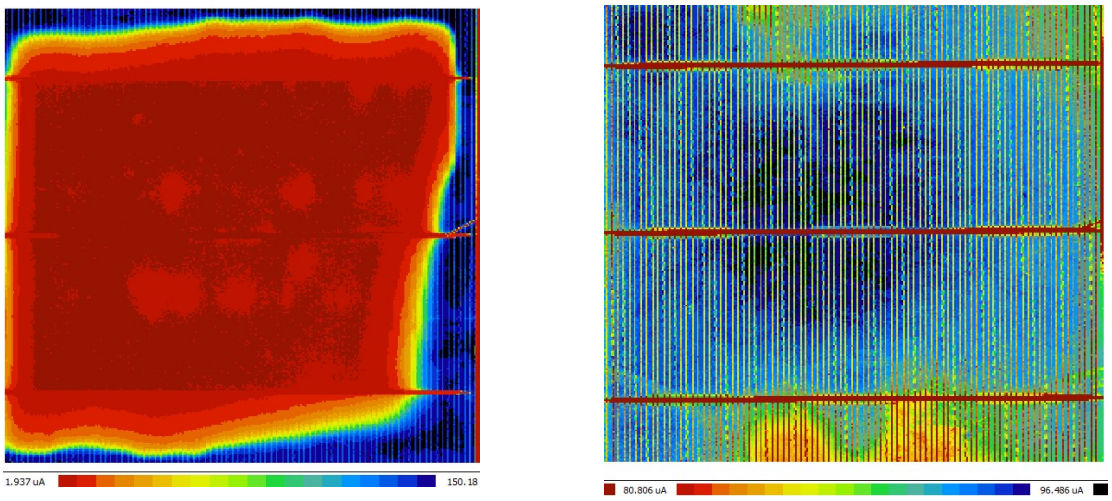

Figure 22. LBIC maps at short wavelength (404 nm) for the same cells as Figure 25..

.

Figure 23 is an excellent example of the correspondence between lifetime, photocurrent, and the effect of wavelength. The left picture shows the LBIC at long wavelength and the middle picture shows the corresponding lifetime map. The wafer has a large and wide distribution of dislocations covering much of the wafer which show 1:1 correspondence in both maps. The right picture is an LBIC map taken for 404 nm excitation where all the grain boundaries and dislocations have disappeared and the map shows quite uniform response for the emitter. This cell's performance is clearly determined by starting wafer quality and not by cell processing.

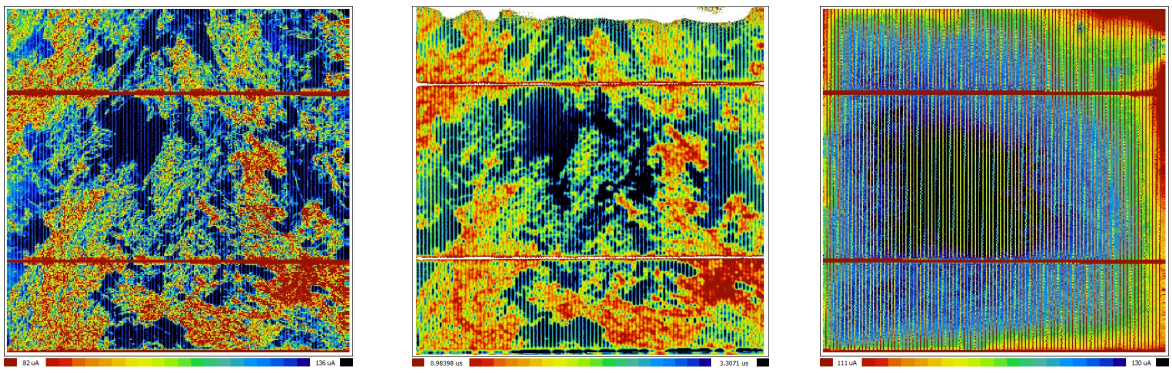

Figure 23. LBIC at long wavelength (left), lifetime (middle) and LBIC at short wavelength (right) for ML Solar, cell 12.

∗ Detailed forensic measurements on finished manufactured solar cells showed that in many cases the "quality" of the raw starting material was an important and sometimes dominant factor. It is highly desirable to separate out poor quality material before subjecting it to expensive processing only to reject the cells at the end or bin the cells in low efficiency categories. Photoluminescence in its several forms is particularly valuable as a diagnostic tool. There are several commercially-available tools that measure the

PL of either starting wafers or finished cells and use algorithms to convert the data to lifetime values. Such measurements are still affected by surface recombination and saw damage. For defect band luminescence, surface recombination is not as significant.

Band-to-band luminescence is the form of PL most often measured, determined by recombination in the body of the wafer and at the surfaces. In defect band PL, luminescence takes place in which carriers captured at defects can recombine with majority carriers and produce light at longer wavelengths. Both the Si body and the surfaces are transparent to this light which is why surface recombination doesn't much affect it and saw damage only affects it minimally (both only through a reduction in intensity). As can be expected, the intensity of the defect band emission is related to the defect density and type. The defect PL can be a significant fraction of the band to band PL since the latter has to obey selection rules involving phonons while recombination via the much lower density of defect states (relative to the CB or VB density of states) does not involve that restriction.

A number of the mono and multi substrates later made into cells in a turn-key line were measured with the generous help of Steve Johnston at NREL. Measurements included lifetime maps and LBIC at IBM and PL measurements made at NREL. The conclusion of these measurements was that the defect band PL was the most useful for assessing starting material quality. Figure 24 shows a defect band image (left) and finished cell LBIC (right). The defects revealed in the starting wafer PL predict the low lifetime, lower photocurrent

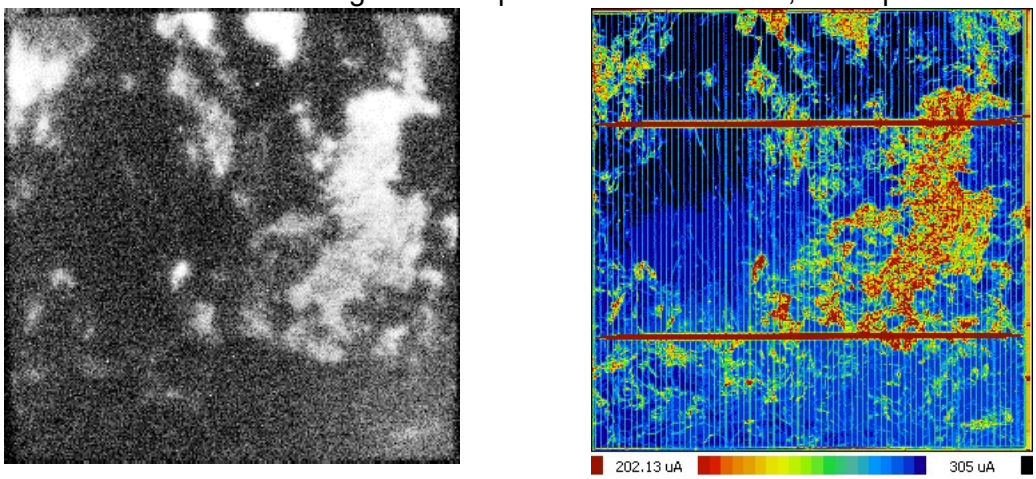

Figure 24. Defect band image (left) and finished cell LBIC (right, 981 nm) of cell B4A4. Bright areas correspond to higher defect densities.

regions of the finished cell. Band-to band PL images would be dominated by surface recombination, though they do have the advantage of showing the grain structure more visibly than other mapping techniques.

At NREL, algorithms were developed that allow quantitative PL measurements to be compared with final cell efficiencies. Basically, image brightness could be quantified across the wafer and the integrated brightness compared to cell performance. The analysis showed that the defect band PL correlates best with cell efficiency as being the least dependent on surface recombination and saw damage, which dominate in starting wafers but largely disappear in finished cells. Figure 26 shows NREL data where cell efficiency is plotted against defect band PL imaging analysis (fraction of image related to defects versus the entire wafer area). Although some scatter is apparent, a relatively good correlation is seen, and this correlation also holds true for V_{OC} and I_{SC}. Defect band imaging could therefore be a valuable wafer quality control measurement for raw starting wafers.

∗ Efficiency Enhancements. The forensic analysis, and particularly the efficiency-parameter correlations, the quantum efficiencies, and the reflectances, have identified performance-limiting issues with each of the 18 turn-key lots, but the main conclusion is that there is no one dominant factor for all of them. Some lots are limited by substrate quality, some by series or shunt resistance, and some by diode quality (J0 and n). It is possible to model

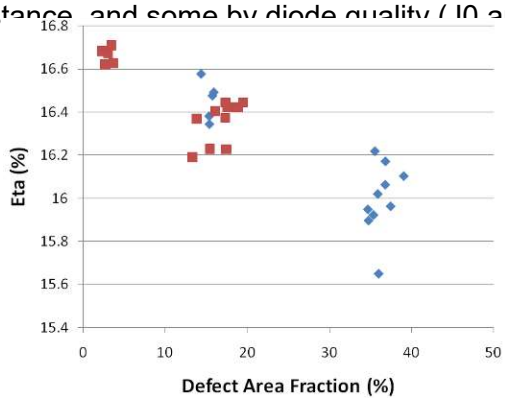

Figure 26. Correlation between defect band imaging in as-received starting material and efficiency of finished solar cells. (NREL data.)

each lot and apply various enhancements to estimate what efficiency the particular lot would have had if it had been fabricated differently. There are several performance enhancements well known in the industry that are often applied in the laboratory but not in manufactured cells (at least in the past). Several of these enhancements have been explored at IBM and implemented in various device lots. A list of these concepts and example benefits they bring is given in Figure 27.

Figure 27. Possible efficiency enhancements for Si solar cells.

Si Solar Cell Enhancements

Emitter
- Lower Doping Level – improved lifetime and passivation.
- Selective Emitter:
  - N++ under contacts, N+ elsewhere ε improved lifetime while maintaining low Rs

Deeper Junction ε lower N+ doping allows deeper junctions without a quantum efficiency loss Base
- Higher resistivity to increase lifetime, (but could raise Rs)
- Reduce base (wafer) thickness ε improves Ld /Thick. ratio, raises Voc but may lower Jsc

Back Surface Field
- Improved passivation ε Al_2O_3 for p-type, SiO_2 for n-type
- Local BSF (PERL structure) ε improves passivation, raises Voc
- Contact geometry to minimize series resistance.

Optical
- Better awareness of SiN thickness in fabrication
- Replacement of Si3N4 with optimum SLARC or DLARC

Material
- Quality control of starting substrates ε reduced binning, higher effic.
- Reduced light-induced degradation “LID” (reduced oxygen; n-type substrates)
- Reduced thickness.

Contacts
- Thinner grids ε reduce shadowing
- Design optimized based on current crowding concepts.

Processing
- Maintain optimum light trapping ε maintain Jsc for thinner substrates
- Gettering ε (improve lifetime and shunting, but could decrease throughput significantly)
- Laser Doping, particularly for the selective emitter and LBSF
- Laser–fired contacts ε reduced back contact resistance

Device Design
- HIT Cells (Heterojunction with Thin Intrinsic Layer)
- IBC (interdigitated Back Contact)
- EWT (Emitter Wrap Through)
- N-Type Substrates (higher lifetime, no LID, easier back surface passivation

The “selective emitter” in which the main part of the emitter has a much lower doping level than the regions beneath the contacts, significantly improves the short wavelength response and allows deeper emitter junctions for improvements in series resistance. It can also increase the V_{OC} by 10-20 millivolts. In an analogous way, a blanket or local back surface field improves the long wavelength response and can also raise the V_{OC} by tens of millivolts depending on the substrate resistivity. A local BSF where the main part of the back surface is passivated is the optimum configuration. Optically, better control of the Si3N4 AR coating thickness or replacing it with a higher index DLARC can result in reduced reflectance, though the gain is relatively small when the cells are encapsulated with glass or plastic.

Material quality is obviously important; the higher the starting material lifetime, lower defect density, and oxygen content, as well as the dislocation density in cast material, the better the cell is likely to be. Gettering has been shown to improve the lifetime considerably but at the expense of more complex processing and lower throughput. Thinner wafers can actually improve efficiency as long as the diffusion length exceeds the thickness and high quality passivation is present (selective emitter and local or blanket BSF). Texturing is always included to enhance light trapping to minimize or prevent loss of photocurrent with thickness.

Contacts can be narrowed to less than 60 micron width without loss of series resistance due to the phenomenon of current crowding which can render portions of the grid line ineffective for collecting current. Present trends in turn-key cells include narrower finger widths. Copper plating has also been of interest in manufacturing to replace the more expensive Ag fingers and gain a degree of finger conductivity.

Copper plating is one example of possible enhancements in processing. The use of lasers to process cells can also be of advantage. Lasers are often used for edge isolation. They can also be used to create the selective emitter and local BSF, and to create structures such as the Emitter Wrap-Through (EWT) where lasers drill holes through the entire substrate. Ion implantation is a radical departure in conventional cell processing which replaces the emitter diffusion with its unavoidably high surface concentration, and poor emitter lifetime. Ion implantation has the advantages of higher control of emitter doping level, doping profile, junction depth, and thermal budget.

Finally, alternate device designs are making their way into the market, including the HIT cell where the junction and BSF are replaced by p, n, and intrinsic regions of amorphous Si, and the IBC device which incorporates both the emitter and base contacts on the rear side. Both of these make use of n-type substrates which prevents LID and therefore results in more energy output over the life of the panel. Emitter wrap-through also places both contacts on the back side.

∗ Panel measurements. Ten solar panels from different manufacturers, both mono- and multi- crystalline, were mounted on the roof facing south and tilted at the local latitude. The power and energy output for these panels were compared over a number of days from early morning to sunset. One such plot is shown in Figure 28. Plots were made of power output density, short circuit current density, V_{OC}, and FF for each panel as a function of both total cell area and full module area. The IBC and HIT panels were the most efficient followed by the mono panels and then the multi panels. Forensic analysis of each panel was made, particularly the panel series resistance, by comparing the temperature-corrected Fill Factor with simulations as a function of incident sunlight intensity. Panels were compared on both bright cloudless days and totally overcast days. Interesting differences were observed where photocurrent and power output highest for some panels in the morning became lower or lowest in the afternoon, probably due to reflection differences. Future analysis would benefit greatly from additional measurements over longer periods of time.

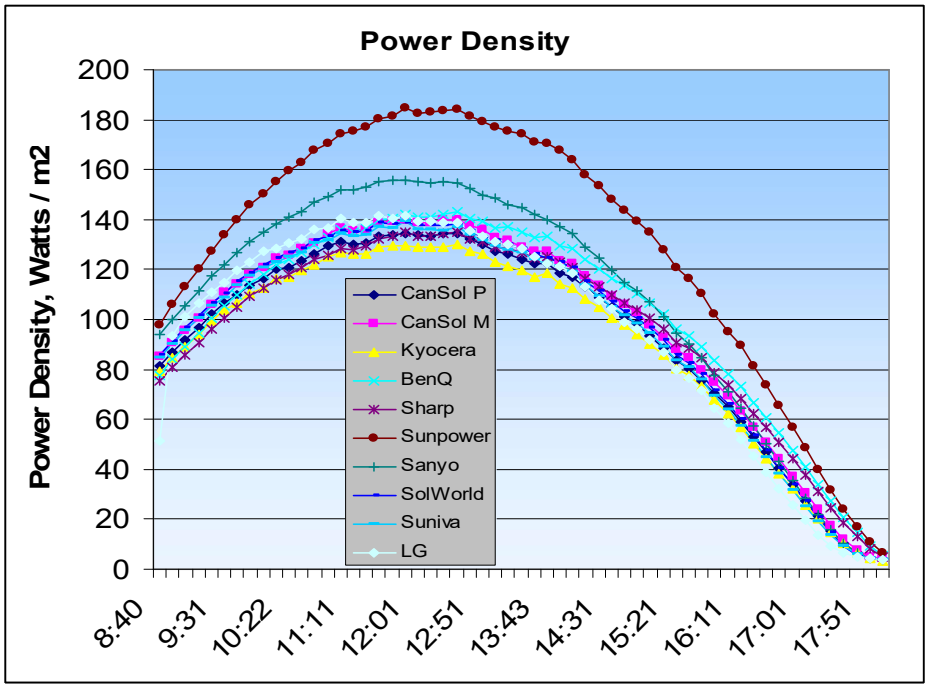

Figure 28. Power output density on Sept. 26, 2014

Table 18. Panel power and energy output comparison for Sept 26, 2014.

Panel	Watt-Hrs/ m2	Pmax /m2 Cell	Pmax /m2 Mod	$ / Watt pk
1	892	149.9	134.5	1.10
2	932	159.1	140.0	1.24
3	860	145.9	129.7	1.41
4	966	160.0	142.2	1.22
5	913	152.3	135.0	1.23
6	1229	206.3	184.5	2.59
7	1022	176.6	155.7	1.63
8	920	163.3	138.8	1.27
9	904	156.4	137.1	1.40
10	908	162.9	141.5	1.42

A comparison between panels for a particular day is shown in Table 18, including the cost per peak watt taken by dividing the purchase price of the panel by its peak power output. Columns 3 and 4 divided by 1000 represent the approximate measured efficiencies of the cells in the panel and the panel itself. Column 2 represents the integrated energy output over the day in watt-hours.

Forensic Analysis, Individual Lots.

Each of the 18 separate lots was extensively analyzed by the forensic techniques outlined earlier in this report. The net result is that no one parameter (Rs, FF, Voc, passivation, lifetime, etc.) was dominant in all lots, but instead different parameters were important in some lots but not in others, and for some lots no parameter dominated at all; in these, a combination of influences determined device behavior. However, areas where improvement could be made were identifiable, and all of them would benefit from the enhancements outlined earlier. The 18 lots consisted of 5 monocrystalline cells and 13 multicrystalline. No HIT or IBC cells were available for analysis, but HIT and an IBC panels were included in the 10 rooftop mounts described in the last quarterly report.

Detailed measurements of each of the 18 lots are described next.

.2 AllPowers Solar.

20 Multicrystalline Cells.

Comments: Shunt Resistance is Poor, Series Resistance is excellent. Both Voc and FF are high (> 624 mV and 0.79) except for 4 very poor "outlier" cells, 20% of the batch. Even within the non-outliers, there is a wide variation in J0 and n. The averages are:

<RSH> = 10.94 ohms, ⑨ = 10.9
<RS> = 0.431 ohm-cm^2, ⑨ = 0.083
<J0> = 4.3 E-11 amps/cm^2, ⑨ = 3.5 E-11
< n > = 1.162, ⑨ = .041
< Jsc> = 32.98 mA/cm^2, ⑨ = 0.437
<Voc> = 624.4 mV, ⑨ = 3.79
<FF> = 0.792, ⑨ = .0102
<Effic> = 16.31 %, ⑨ = 0.37

Efficiency and Parameter Correlations:

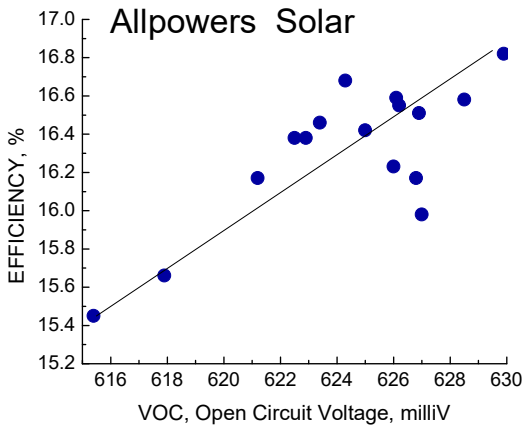

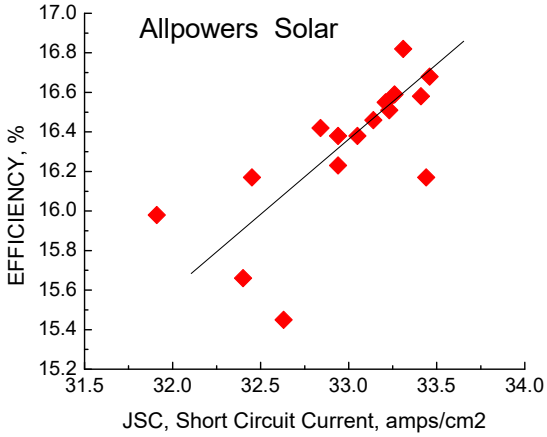

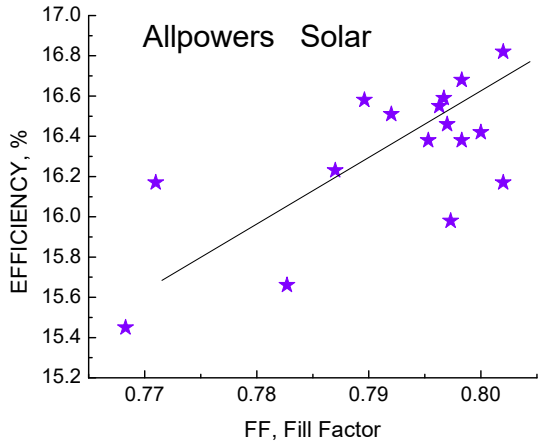

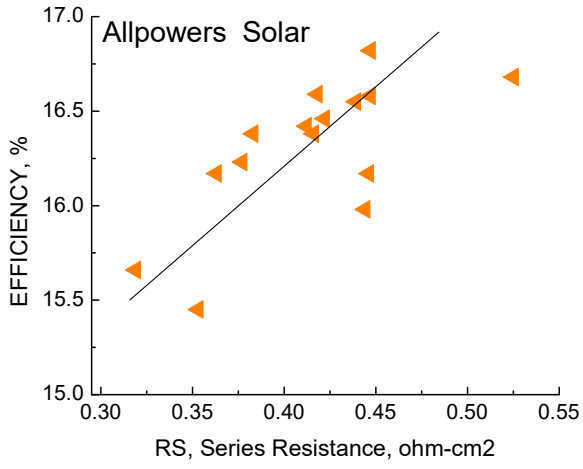

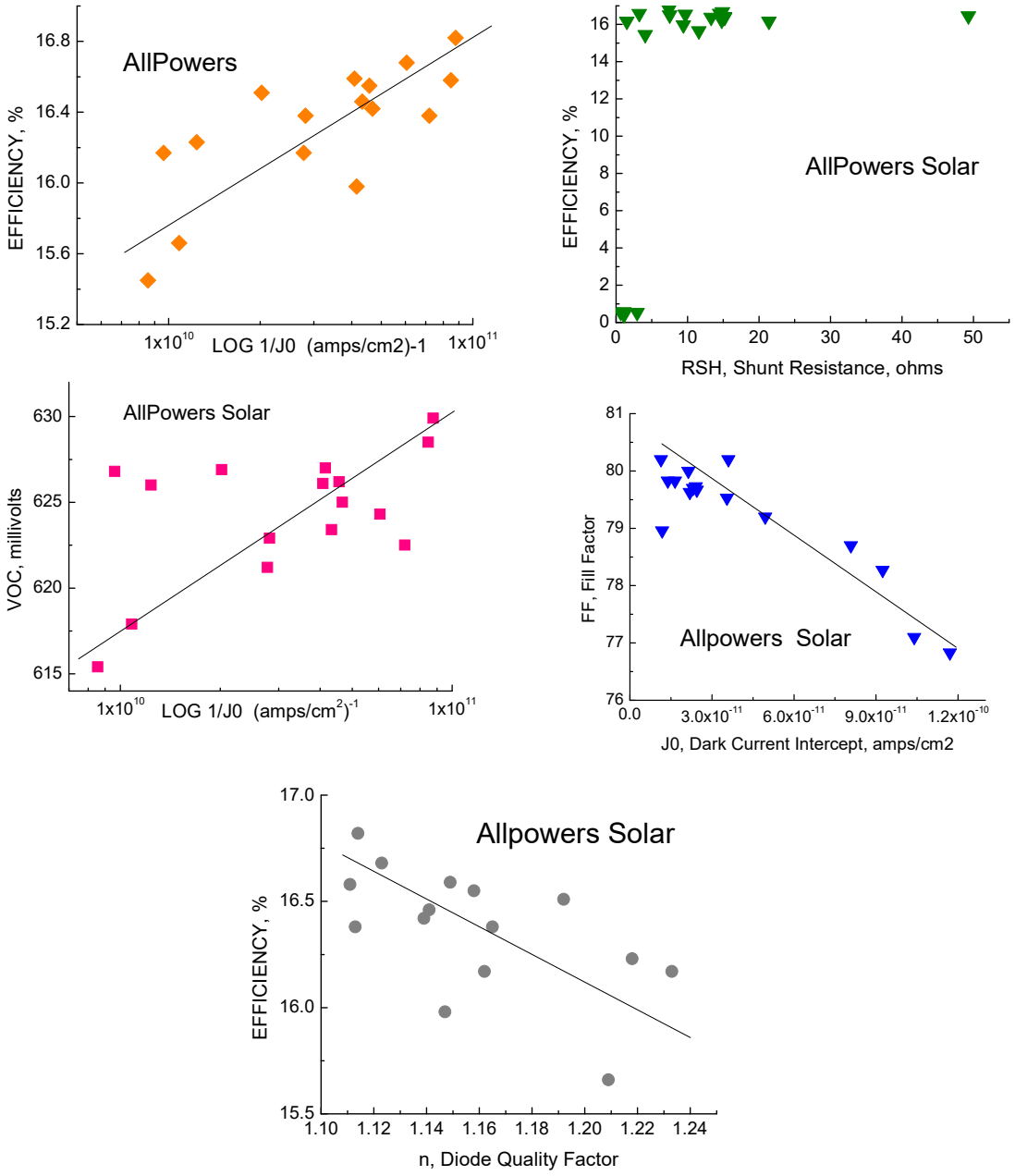

Figure 29. Correlations for AllPowers Solar.

There are relatively moderate dependencies of efficiency with Voc, Jsc, FF, series resistance and J0 as seen in Figure 29, and low dependence on diode quality, while FF in turn depends significantly on J0. Surprisingly, there is no dependence on RSH (except for the extreme outlier cases) even though the RSH is poor compared to most cell lots.

Figure 30 shows the forensic parameters for the 20 cells. The uniformity is relatively good except for the 4 “outlier” cells as mentioned before. The Rs, J0, and n are all better than for most multicrystalline cells.

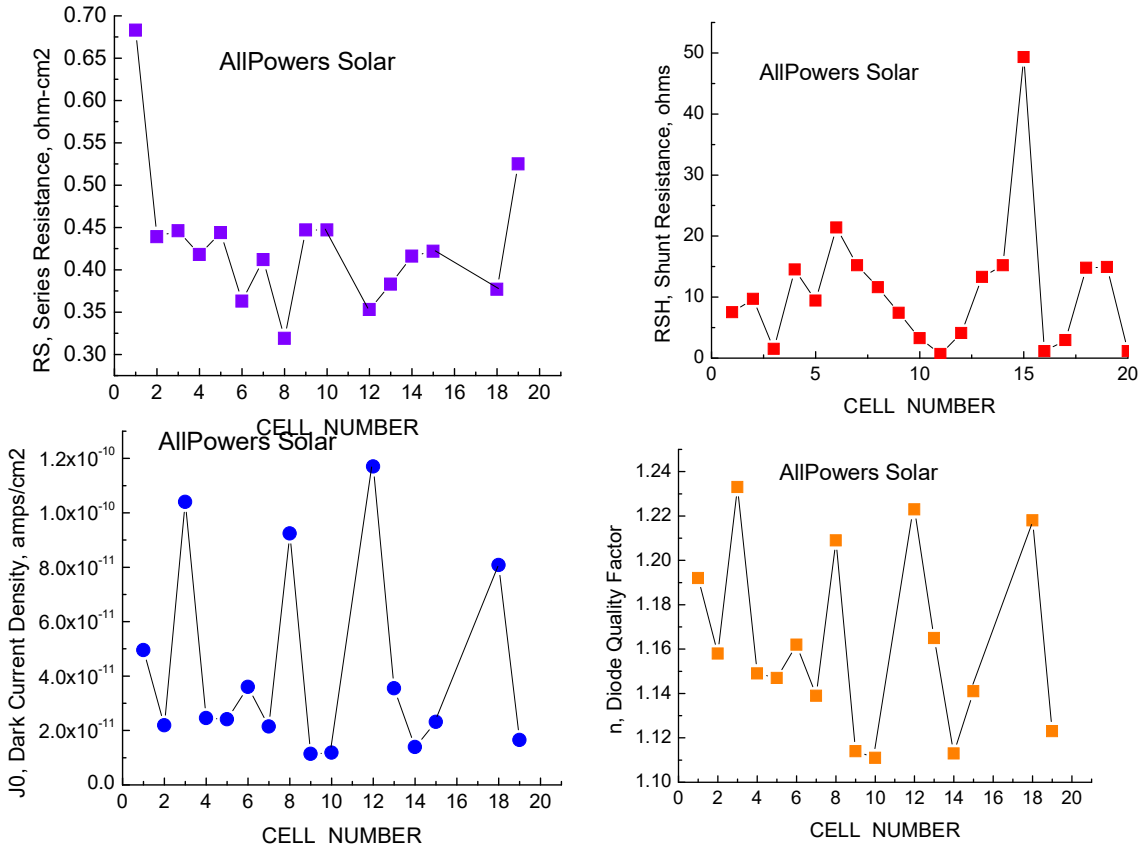

Figure 30. Forensic parameters for AllPowers cells

LBIC Maps.

The maps shown here in Figures 31 and 32 compare LBIC results for a "good" cell and a particularly bad one. At long wavelengths, the grain boundaries and dislocation networks with their reduced photocurrents are clearly seen, but even more striking are the extremely poor currents for the bad device where the photoresponse is 100x lower than normal. This indicates either a catastrophic processing error or very poor starting material quality control by the manufacturer.

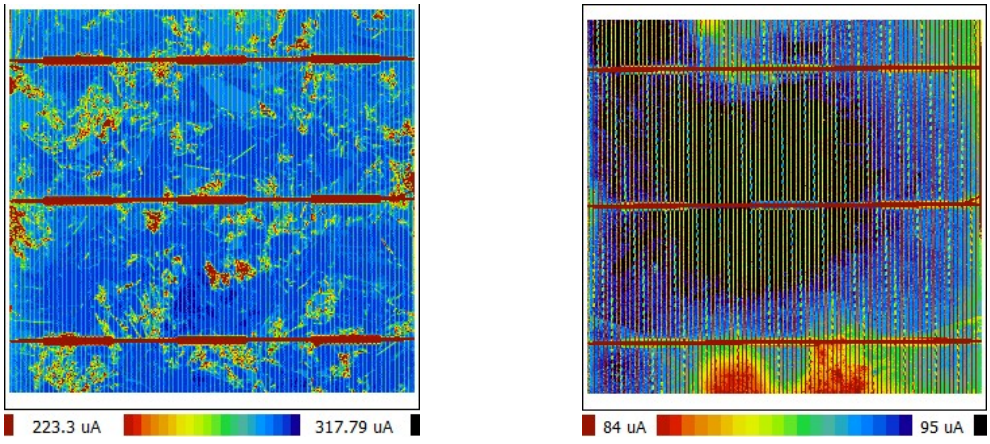

Figure 31. LBIC maps at 981 nm (left) and 404 nm (right) laser excitation. 16.2% cell.

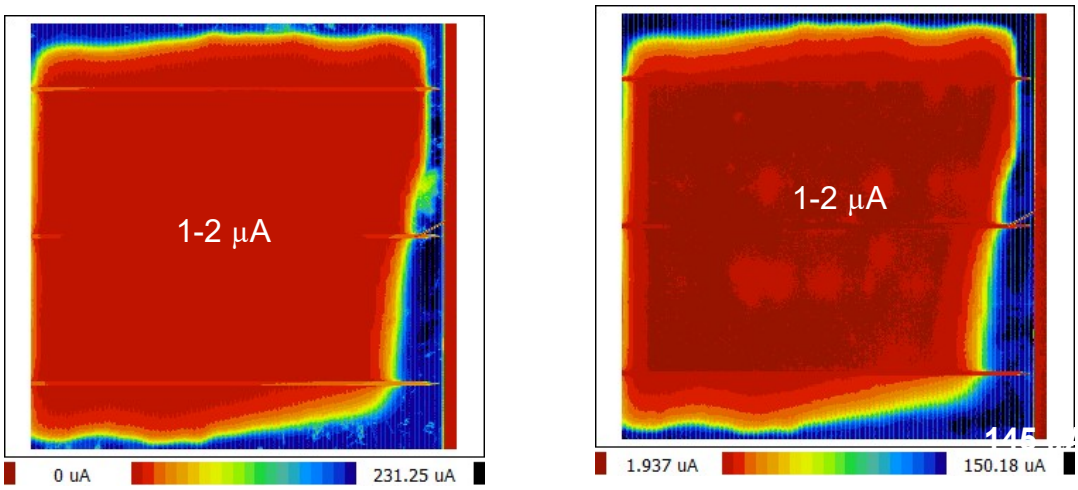

Figure 32. LBIC maps for 0.42% cell showing extreme non-uniformity: 981 nm (left), 404 nm (right).

Quantum Efficiency

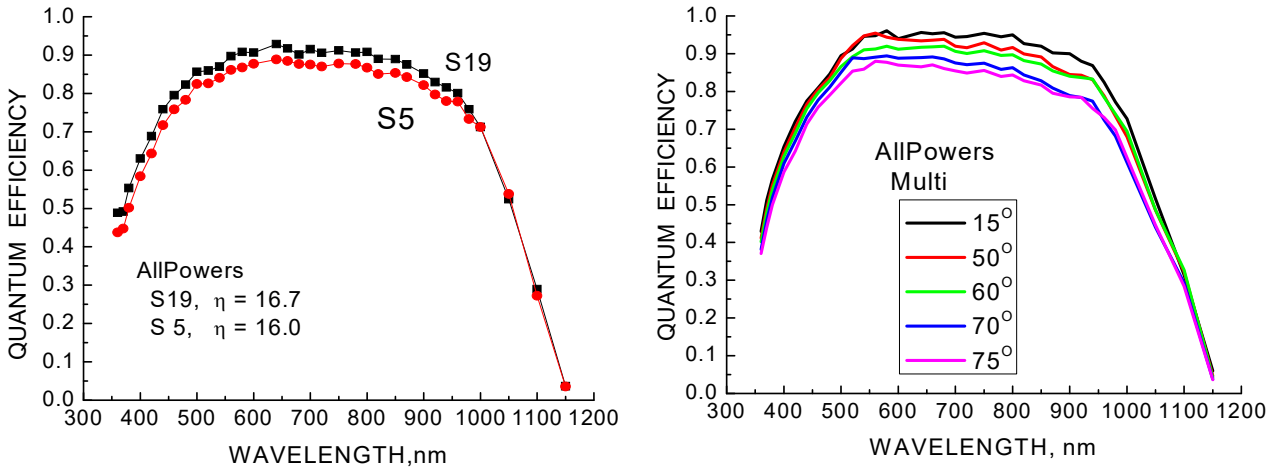

Figure 33. Spectral response for typical cells from the AllPowers lot; left, normal incidence; right: variable angle incidence.

Figures 33 and 34 shows the spectral responses for two cells from the AllPowers lot. A comparison with other multicrystalline turn-key lots shows that these cells have both better base lifetime (better long wavelength response) and better passivation and emitter properties (improved short wave response) than most multicrystalline lots, and the efficiencies are correspondingly higher. The photocurrents are 33.5 mA/cm2 for the better device (S19) and 31.9 mA/cm2 for the lower efficiency device (S5), consistent with the quantum efficiency being lower for the lower cell over the entire visible range.

Figure 36 also shows the QE as a function of incident angle for cell S19. The biggest effect of angle is in the visible and near IR range, with less effect at short wavelengths as observed with other multicrystalline lots.

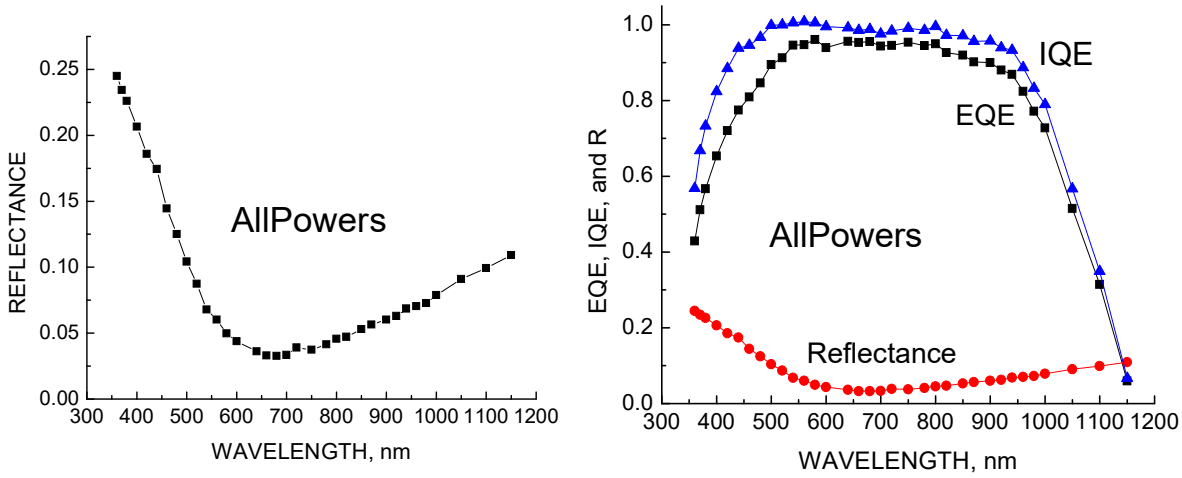

Figure 34. Reflectance (left) and IQE-EQE comparison (right)

Figure 34 shows the reflectance and the IQE-EQE comparison. The short wave response as evidenced by the IQE is indicative of the excellent passivation. The wavelength for minimum reflectance is at 650 nm; both the device performance and Isc would be slightly improved by shifting it closer to the solar maximum at 580-600 nm.

7.3 Big Sun Solar

11 Multicrystalline Cells.

Comments: Shunt Resistance is good, series Resistance is good. Voc is low (615 mV) but FF is a high (0.787). The lot is more uniform than most, with efficiencies ranging from 15.55 to 15.84 with low standard deviation. The averages are:

<RSH> = 295 ohms, ⑨ = 154
<RS> = 0.618 ohm-cm^2, ⑨ = 0.06
<J0> = 2.7 E-11 amps/cm^2, ⑨ = 2.0 E-11
< n > = 1.126, ⑨ = .033
< Jsc> = 32.41 mA/cm^2, ⑨ = 0.115
<Voc> = 615.2 mV, ⑨ = 1.2
<FF> = 0.787 ⑨ = .007
<Effic> = 15.69 %, ⑨ = 0.109

Efficiency and Parameter Correlations:

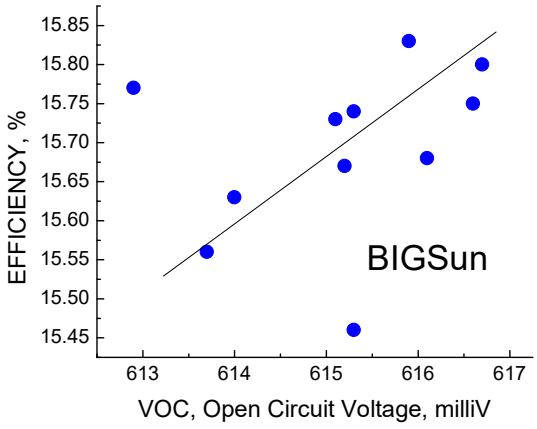

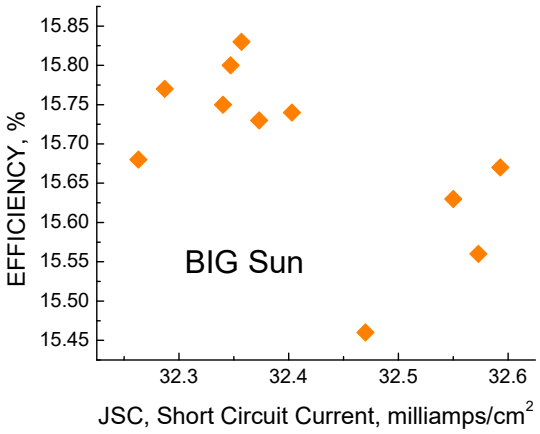

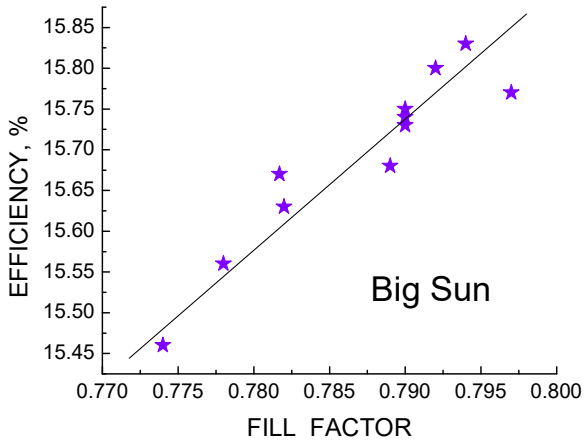

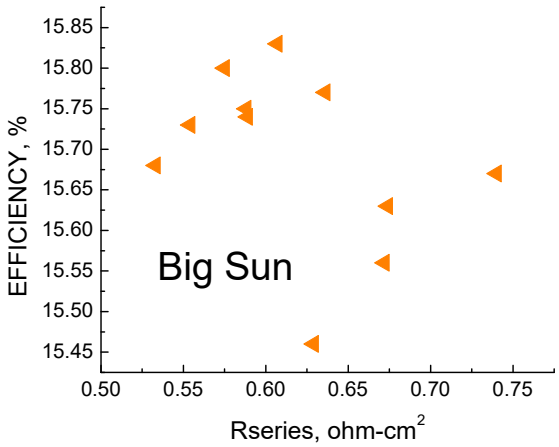

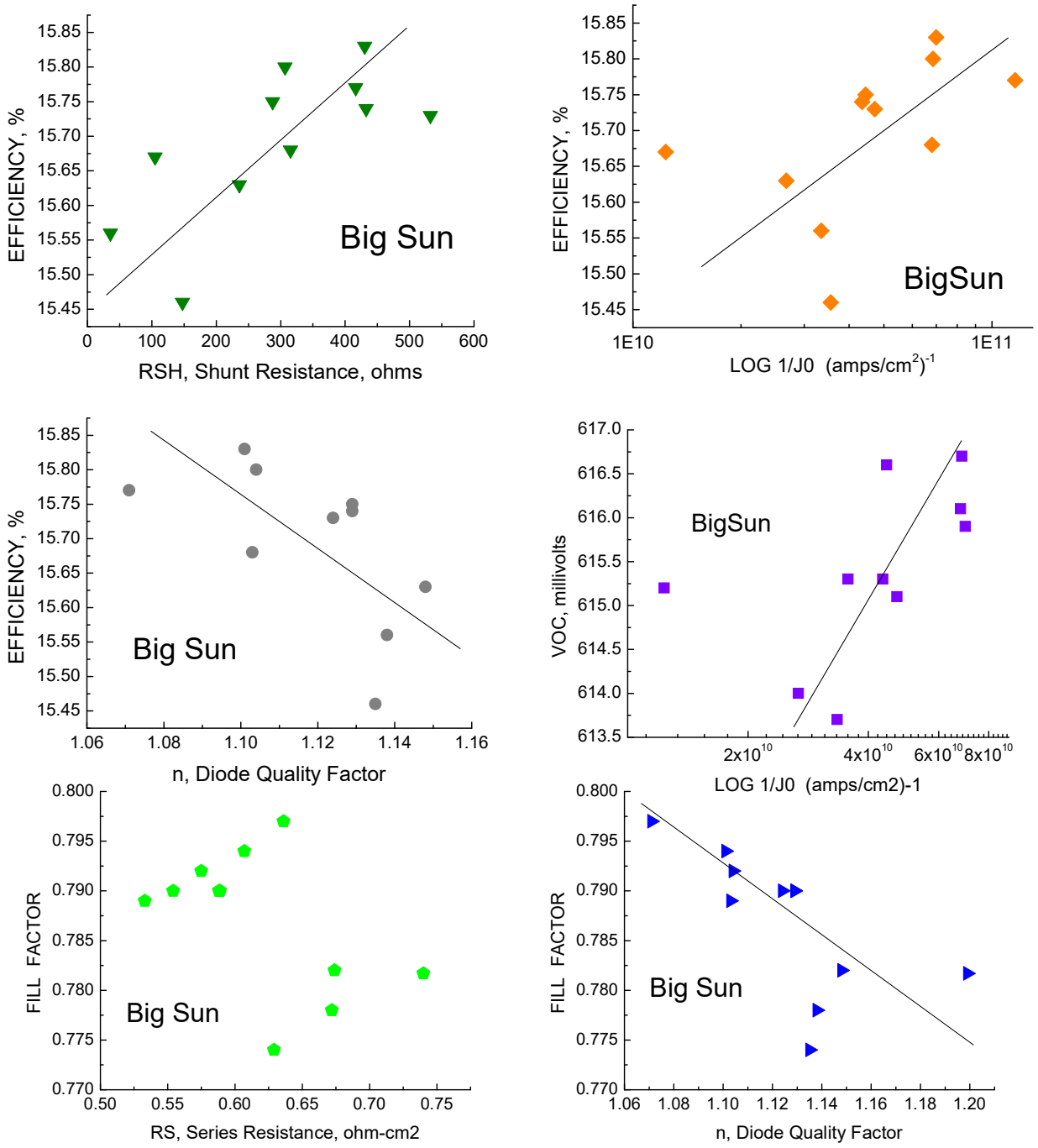

Figure 35. Correlations for Big Sun Solar cells.

The correlations between various parameters are shown in Figure 35. There are high correlations between efficiency and FF, but only a moderate relationship between efficiency and J0 and RSH, and with Voc and diode quality factor n. There are also moderate correlations between Voc and J0 and FF with n and Rs. There is no correlation between efficiency and both short circuit current and series resistance Rs. The graph of FF versus Rs almost suggests a bimodal behavior: two groups of cells exist with

correlations within each group, as if the cell lot were made up of units from multiple batches, but the number of cells is too small to make any definitive conclusions.

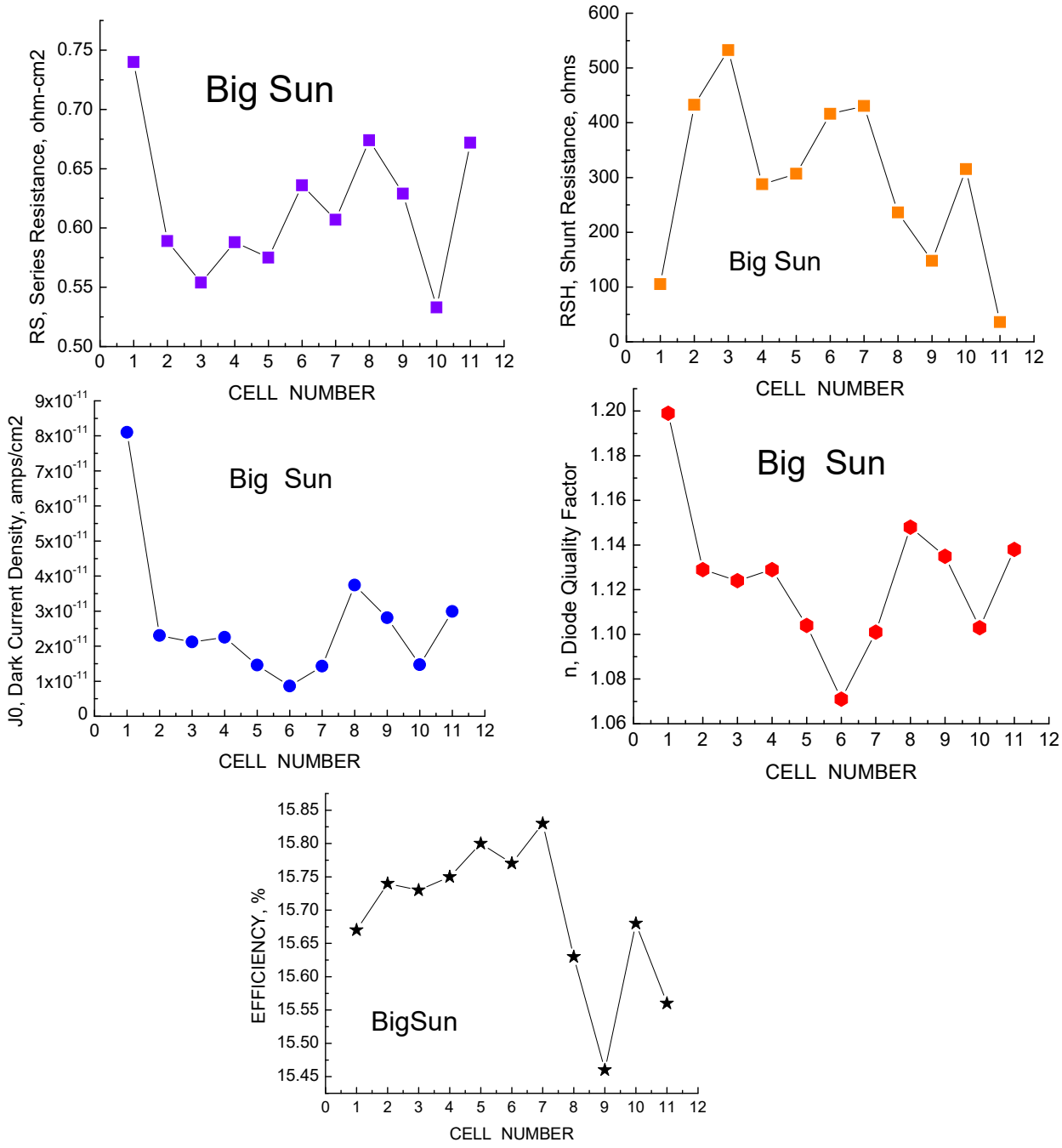

Figure 36. Forensic parameters for Big Sun solar cells.

Figure 36 shows the forensic device parameters for the Big Sun cells. The properties are relatively uniform except for the first device. The charts illustrate the correspondence between J0 and n very well; they are both high or both low and move in tandem so that the Voc, given by

$$Voc = n\frac{kT}{q}\ln(\frac{Jsc}{J0}+1)$$

remains relatively constant in spite of considerable swings in both parameters.

LBIC Maps.

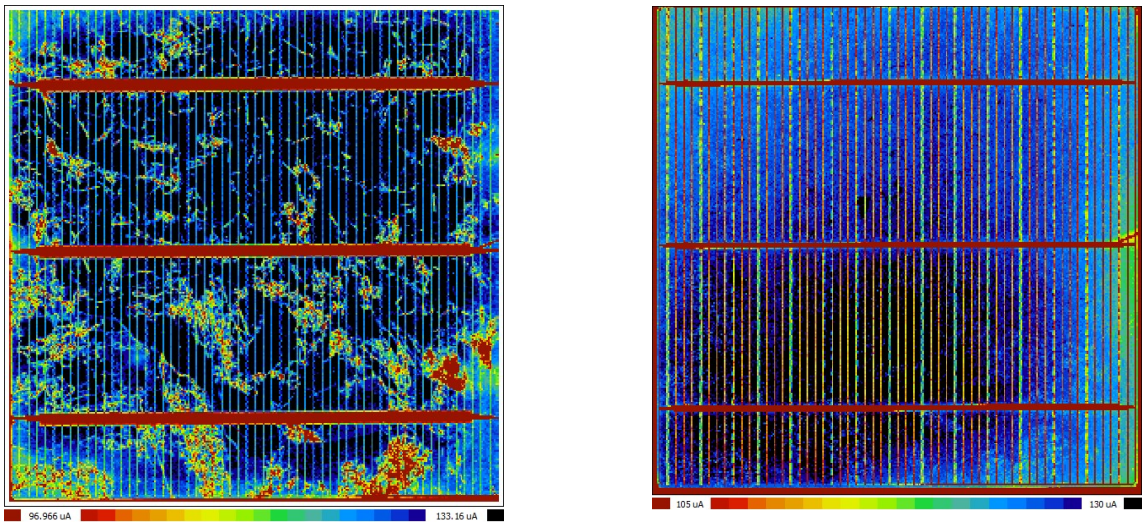

Figure 37. LBIC maps a typical Big Sun solar cell , 15.7% efficient. Left - 981 nm laser excitation; right - 404 nm laser.

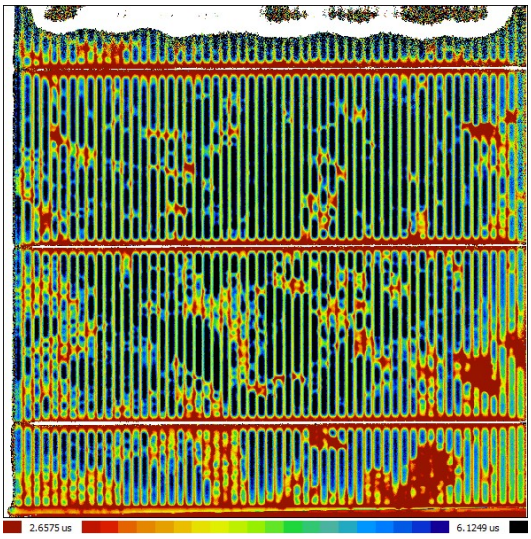

Figure 38. Lifetime map of the same cell showing correspondence between dislocation areas, LBIC at long wavelength, and lifetime.

Photoresponse measurements for a typical Big Sun cell are shown in Figures 37 and 38. As with previous multicrystalline cells, there is a high correspondence between high dislocation areas (red) and poor LBIC and lifetime. There are no “bad” cells in this lot to compare the typical cell against.

Quantum Efficiency

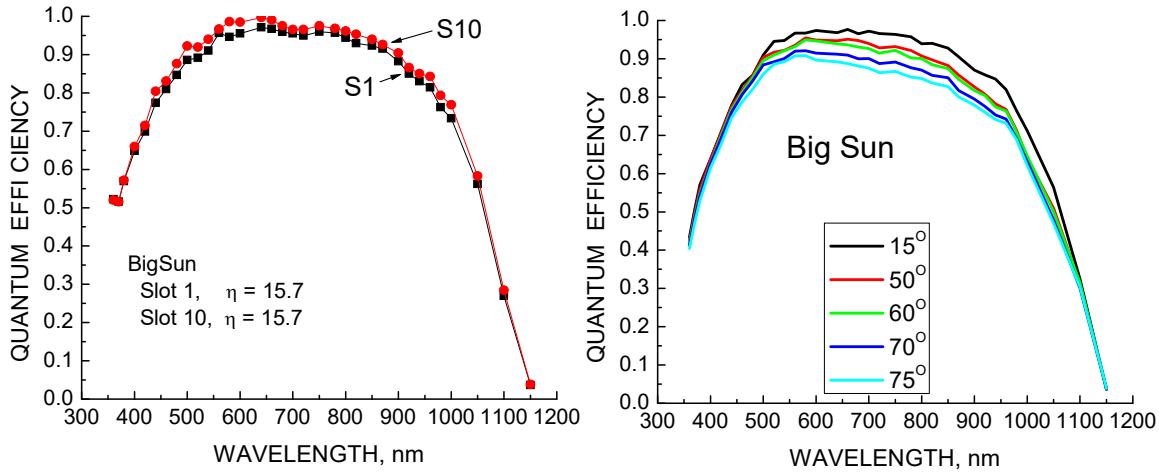

Figure 39. Spectral responses for multicrystalline cells from Big Sun Solar; normal incidence (left) and as a function of angle (right, cell S10).

Spectral responses for two typical cells from the BigSun turn-key lot are shown in Figure 39. The response versus angle shows the expected large effect in the visible region but the responses merge for short wavelengths as seen in most multicrystalline cells.
Figure 40 shows the reflectance and IQE – EQE comparison. The long wavelength response, particularly between 800 nm and 1000 nm wavelengths, indicate a relatively good lifetime in the base and the relatively sharp decreasing response for the IQE at short wavelengths indicates good surface passivation. The reflectance is relatively high and degrades the EQE at short wavelengths. The reflectance minimum at 680 nm wavelength is also too long and the device performance would be improved if the ARC coating were a bit thinner.

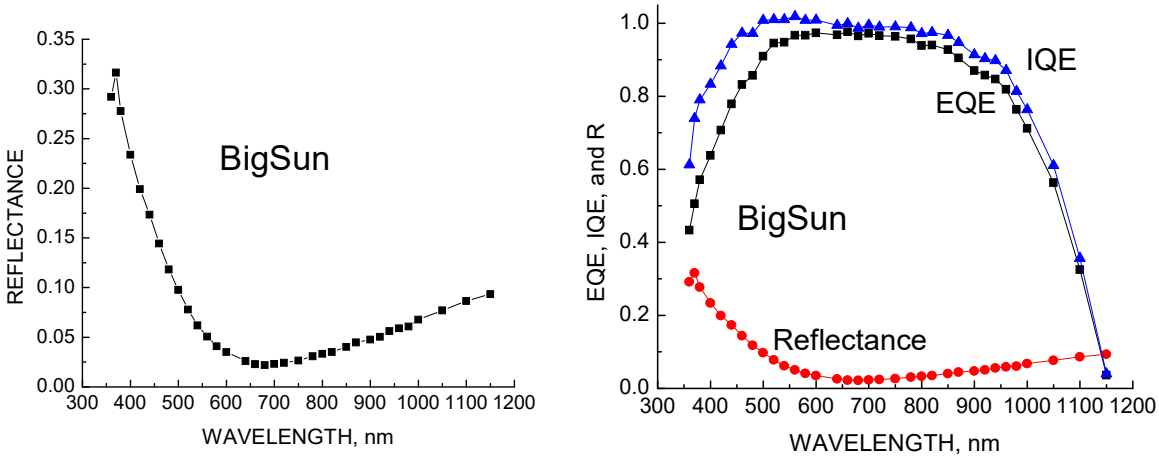

Figure 40
. Reflectance (left) and EQE – IQE comparison (right).

7.4 GinTech

10 Multicrystalline Cells.

Comments: Shunt Resistance is good, series Resistance is good. FF is high (0.78) but Voc is a bit low (616 mV). The variation among the 10 cells is fairly low as evidenced by the standard deviations. The average efficiency is only moderate but all the cells are similar. Figure 44 shows the correlations. The averages are:

<RSH> = 389ohms, ⑨ = 223
<RS> = 0.514 ohm-cm^2, ⑨ = 0.054
<J0> = 2.4 E-11 amps/cm^2, ⑨ = 1.2 E-11
< n > = 1.123, ⑨ = .023
< Jsc> = 32.764 mA/cm^2, ⑨ = 0.089
<Voc> = 615.9 mV, ⑨ = 1.30
<FF> = 0.784, ⑨ = .003
<Effic> = 15.82 %, ⑨ = 0.055

Efficiency and Parameter Correlations:

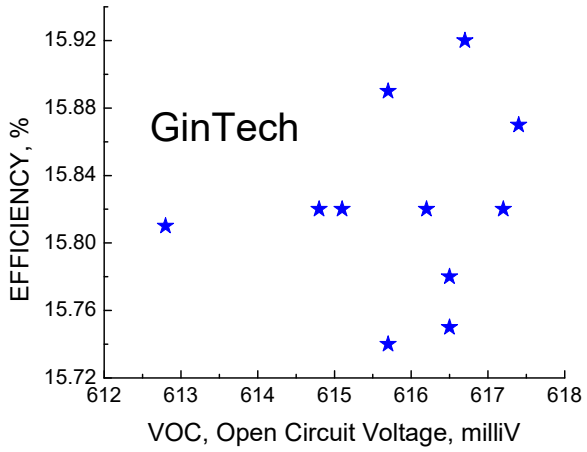

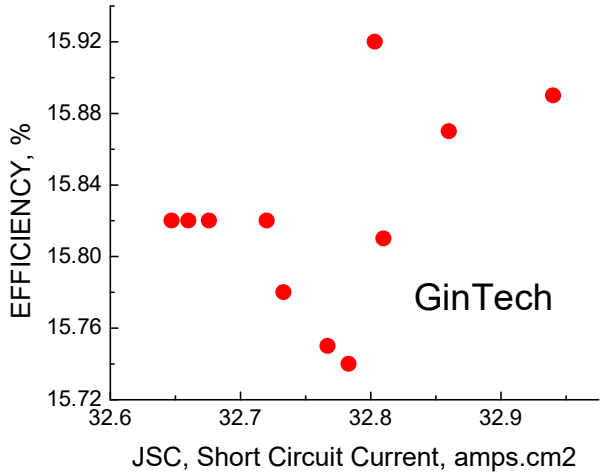

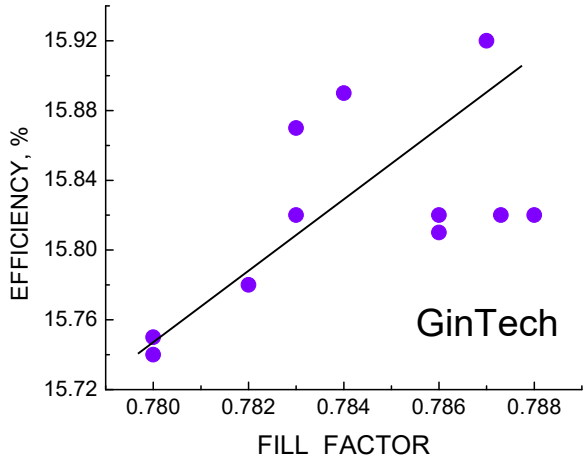

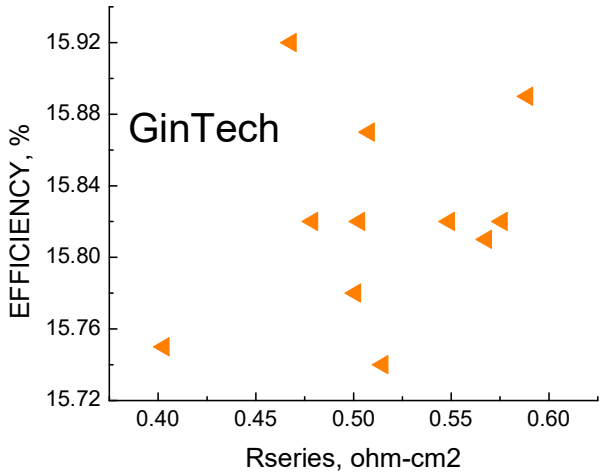

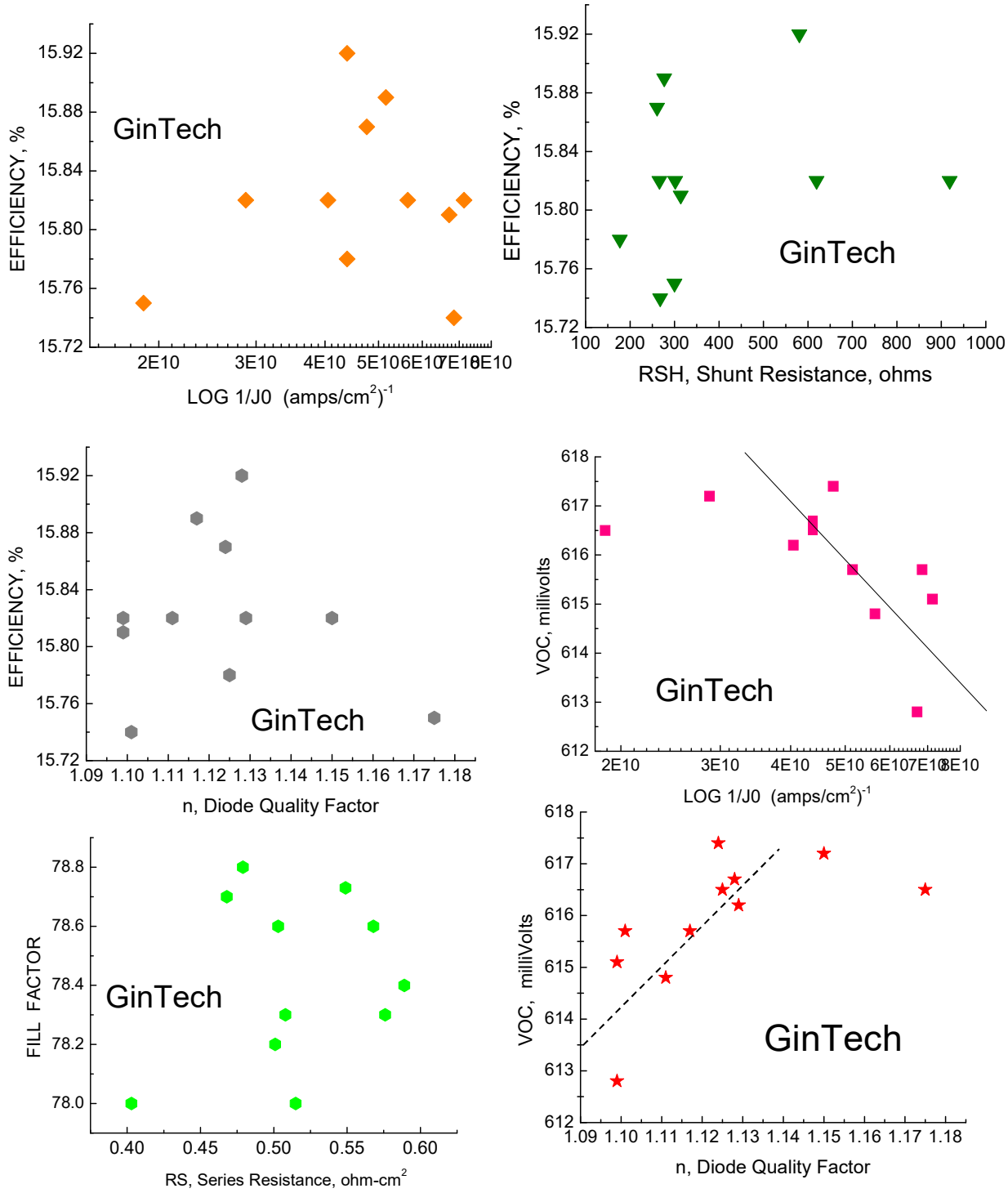

Figure 41. Correlations for GinTech cells.

Gintech is one of the lots that has almost no correlation of efficiency with any major device parameter, including Voc, Jsc, and FF. The only slight correlation of efficiency is with the FF. (There may be a hint of correlation of Voc with diode quality factor n, as shown by the dotted line above.) A surprising result is the anti-correlation, where Voc decreases with 1/J0 instead of increasing in accordance with Voc = (nkT/q) ln(Jsc*1/J0). There is even some indication of efficiency appearing to increase with increasing Rs. These are likely to be artifacts of dominance by some other parameter or combinations of parameters.

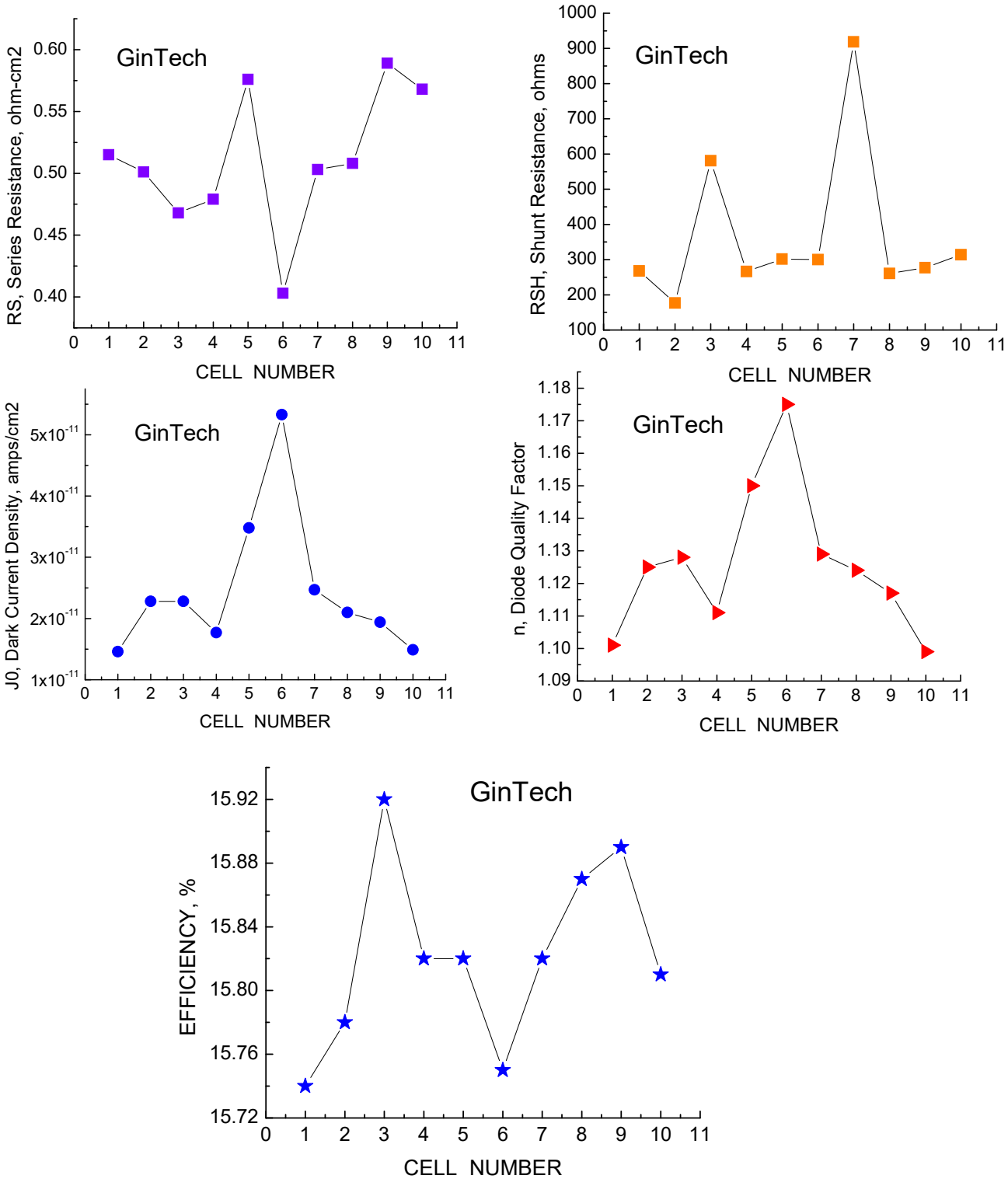

Figure 42. Forensic parameters for GinTech cells.

Figure 42 shows the array of forensic parameters for this lot. The range of efficiencies is low compared to other multicrystalline lots.

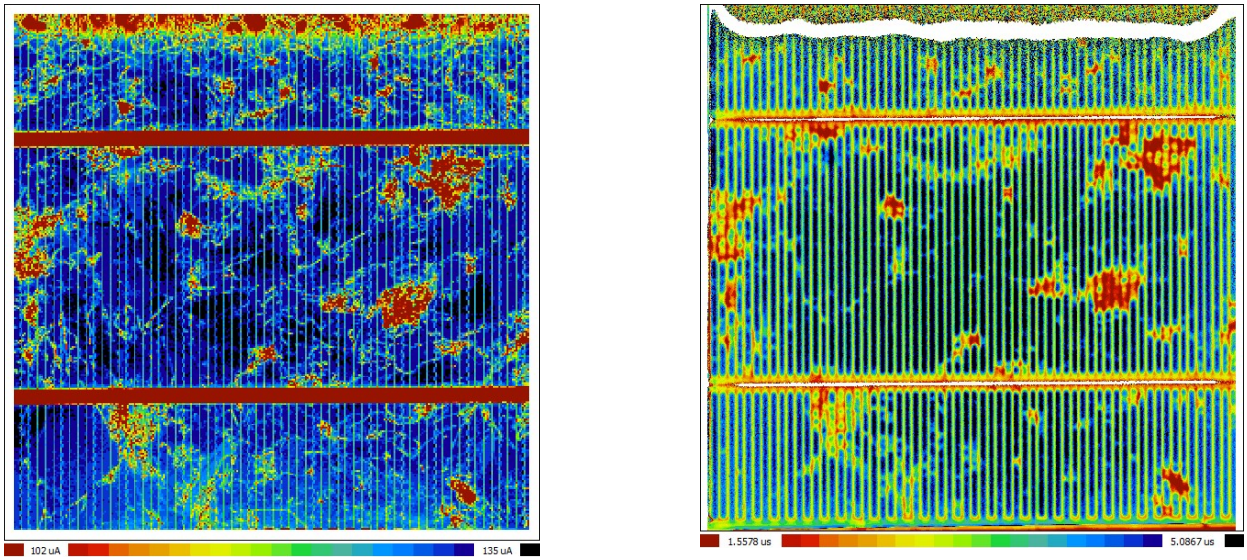

Figure 43. LBIC map at 981 nm excitation (left) and lifetime map (right), cell #9.

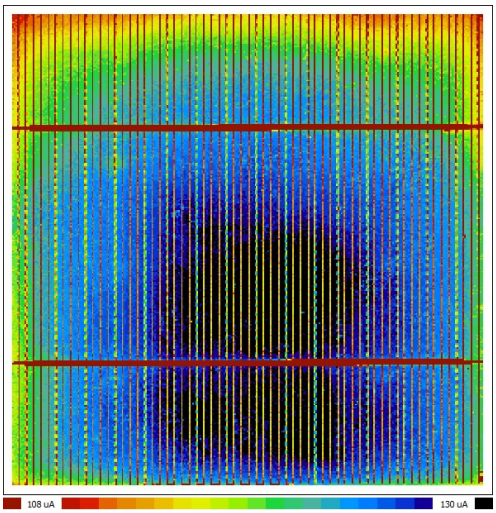

Figure 44. LBIC map at 404 nm excitation

Figures 43 and 44 show the LBIC and lifetime maps for the highest efficiency device, with 15.9% efficiency. The close correspondence between lifetime and dislocations with reduced photocurrent are evident in the LBIC map and lifetime maps in Fig 46. The LBIC map at short wavelength shows a small non-uniformity around the upper edge.

Quantum Efficiency.

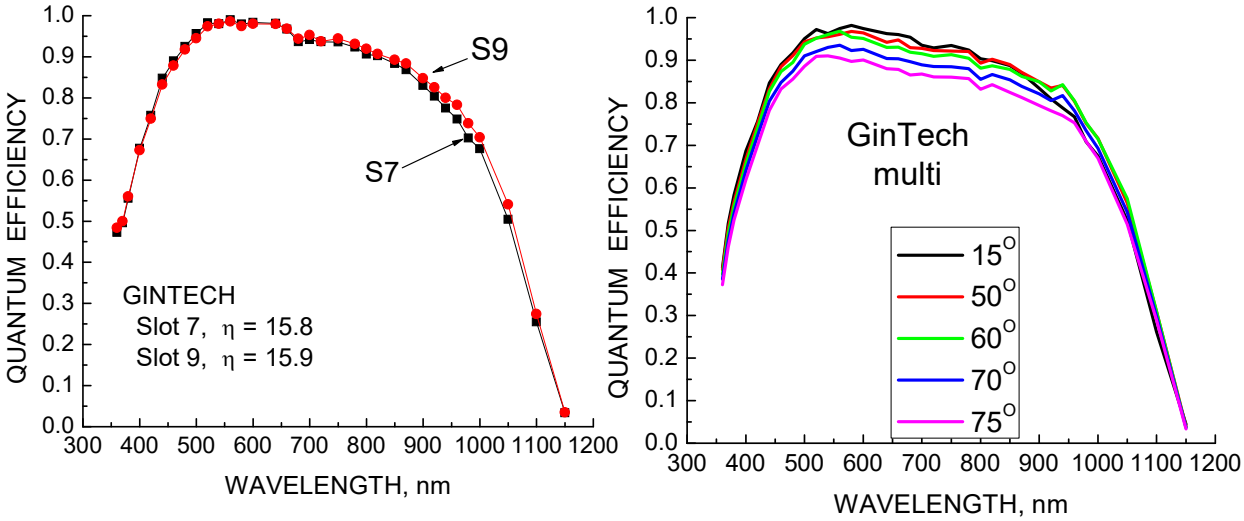

Figure 45. Spectral responses for the GinTech multicrystalline lot at normal incidence (left) and as a function of incident angle (right).

The spectral responses at normal incidence and versus incident angle are shown in Figure 45. The response versus angle shows the usual reduced values in the visible range and the responses merging at short wavelengths., which seems to be the norm for multicrystalline cells. Figure 46 shows the reflectance and IQE – EQE comparison. The slowly increasing quantum efficiency over the whole visible and near-IR range indicates poor base lifetime, and a diffusion length less than the wafer thickness. The reflectance minimum is at the perfect wavelength to match the solar maximum but the poor IQE at long wavelengths limits the IQE and Isc, likely due to poor quality starting material.

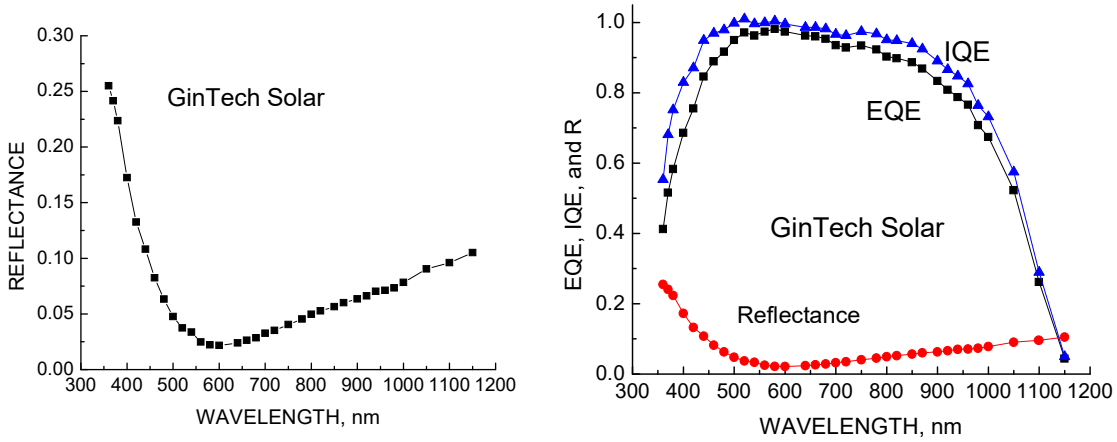

Figure 46. Reflectance (left) and IQE – EQE comparison (right).

7.5 Kyocera

31 Multicrystalline Cells.

Comments: Shunt Resistance is good, Series Resistance is excellent. FF is relatively poor in spite of good Rs and Rsh. The likely cause are the high values of J0 and n. Voc and Jsc are both very low and consequently so is the efficiency. The averages are:

<RSH> = 210 ohms, ⑨ = 131
<RS> = 0.209 ohm-cm^2, ⑨ = 0.174
<J0> = 8.4 E-9 amps/cm^2, ⑨ = 4.4 E-9
< n > = 1.536, ⑨ = .095
< Jsc> = 30.170 mA/cm^2, ⑨ = 0.912
<Voc> = 602.1 mV, ⑨ = 3.5
<FF> = 0.757 ⑨ = .004
<Effic> = 13.75 %, ⑨ = 0.45

Efficiency and Parameter Correlations:

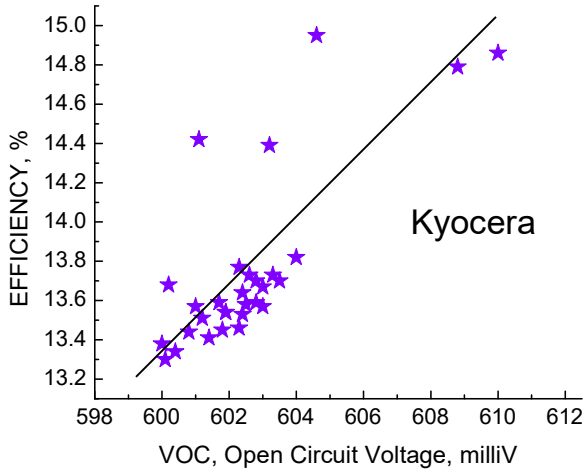

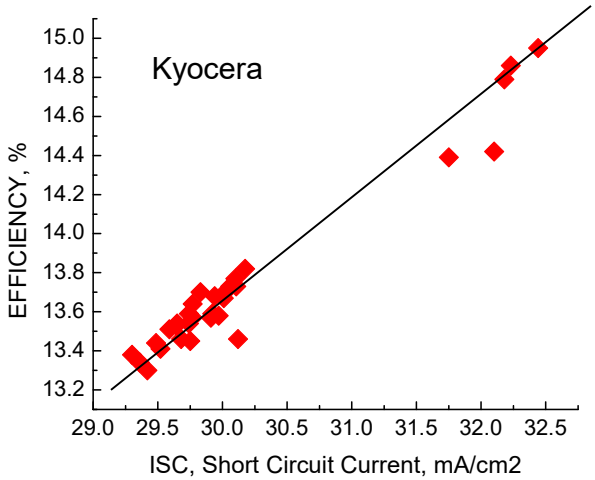

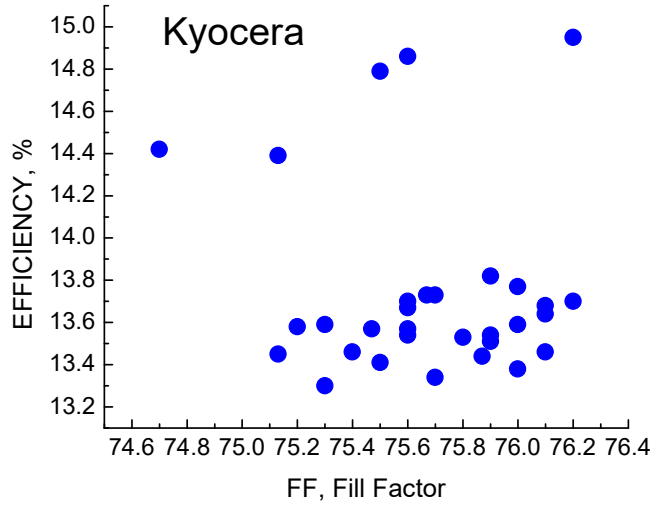

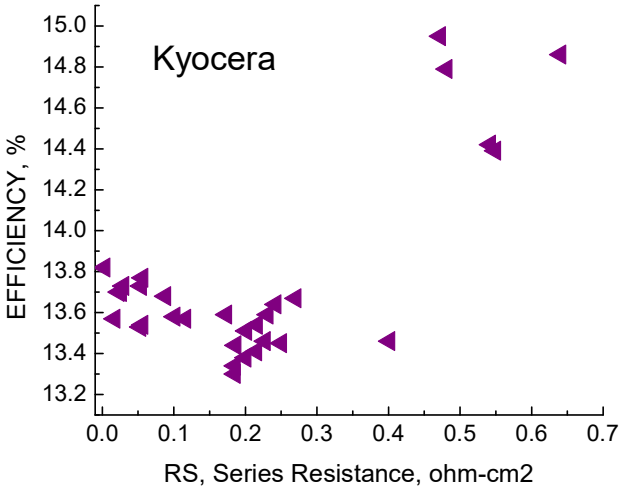

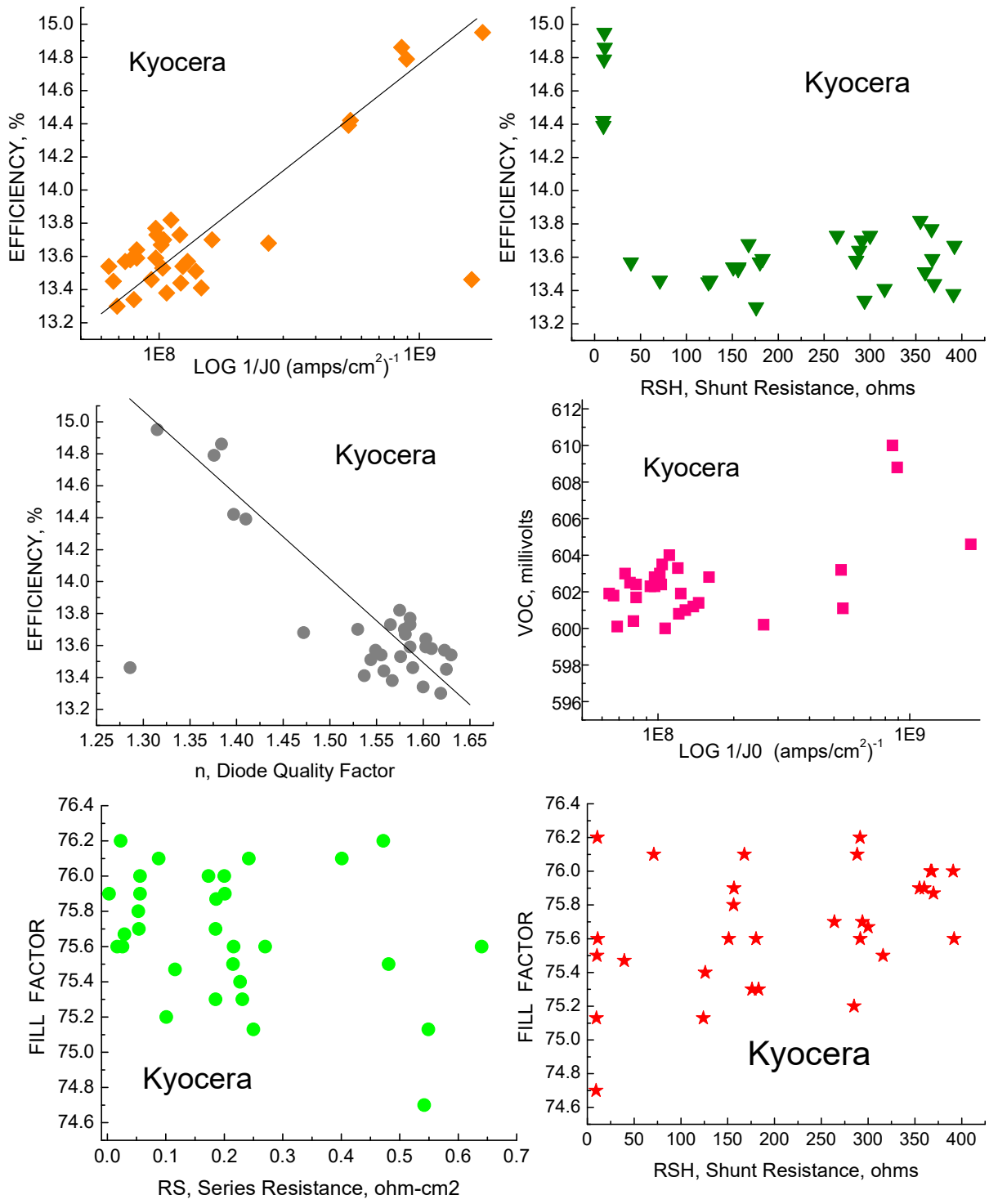

Figure 47. Correlations for Kyocera cells.

There are several correlations with this lot, as shown in Figure 50. Efficiency correlates well with Voc, Jsc, n, and log 1/J0, but not with FF or Rs. As in a few other lots, there seem to be two sets of cells with slightly differing properties, as seen for the efficiency – Isc, 1/J0, and n correlations.

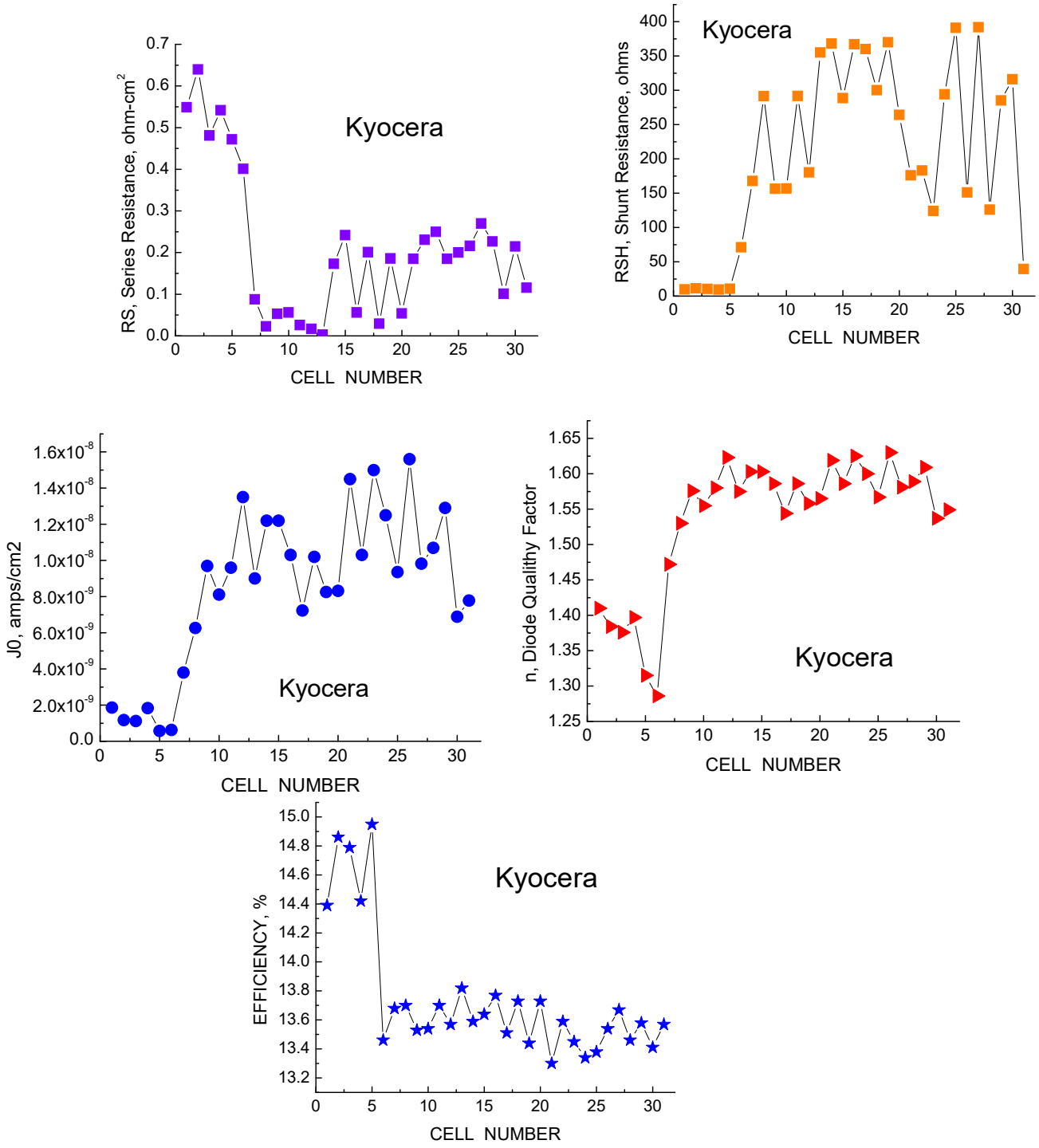

Figure 48. Forensic parameters for the Kyocera cells.

Figure 48 shows the device parameters for the 31 cells. This lot has dark currents 2 orders of magnitude higher than the others with a consequent lower Voc and efficiency. From the forensic plots above, it appears that the lot has two distinctive sections as already mentioned – the first 6 cells behave very differently from the remainder as if the vendor delivered cells from multiple lots without informing the buyer. This would cause

difficulty in combining these cells into a panel. The Semilab plots further confirm that there are two distinct sets of cells in the lot.

LBIC Maps.

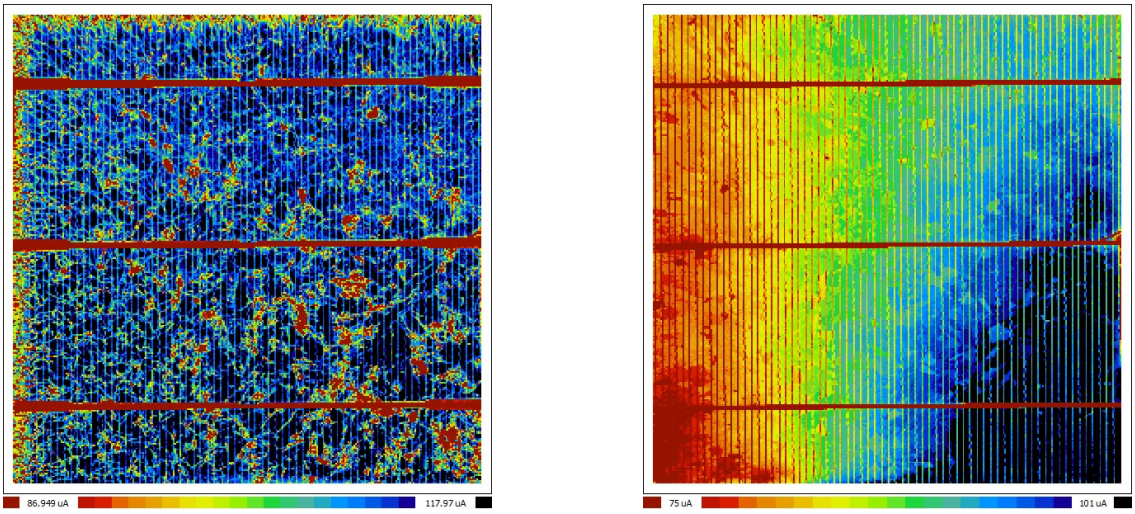

Figure 49 LBIC map at 981 nm (left) and 404 nm for Kyocera cell #5, 15% efficient.

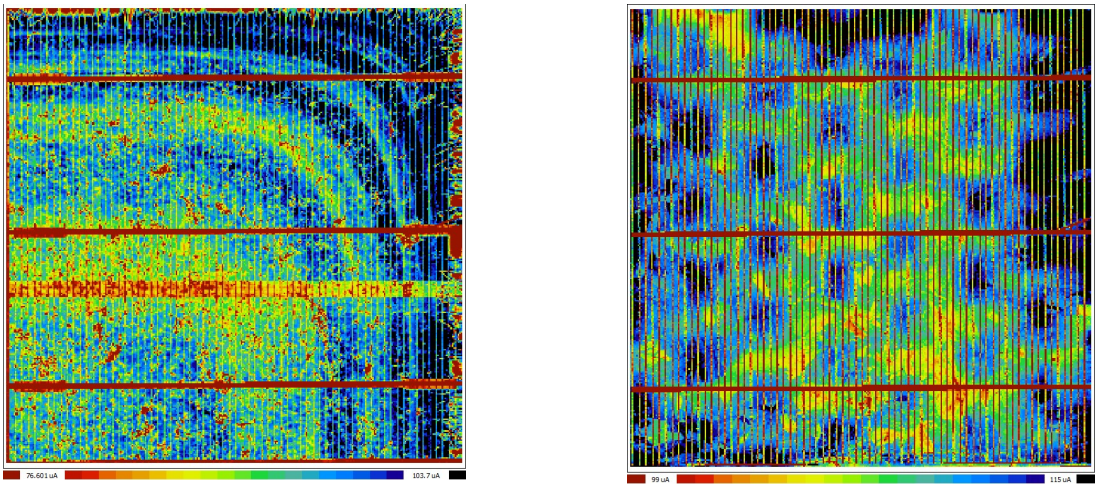

Figure 50. LBIC map at 981(left) and 404 nm (right) for cell #25, 13.4% efficient.

The upper maps in Fig.49 are typical of the 1st batch of 6 cells while the maps of Figure 50 are typical of the poor performing devices. It appears from Fig. 50 that both the base and the emitter suffer from unusual defect patterns resulting in reduced lifetime and photocurrent.

Quantum Efficiency

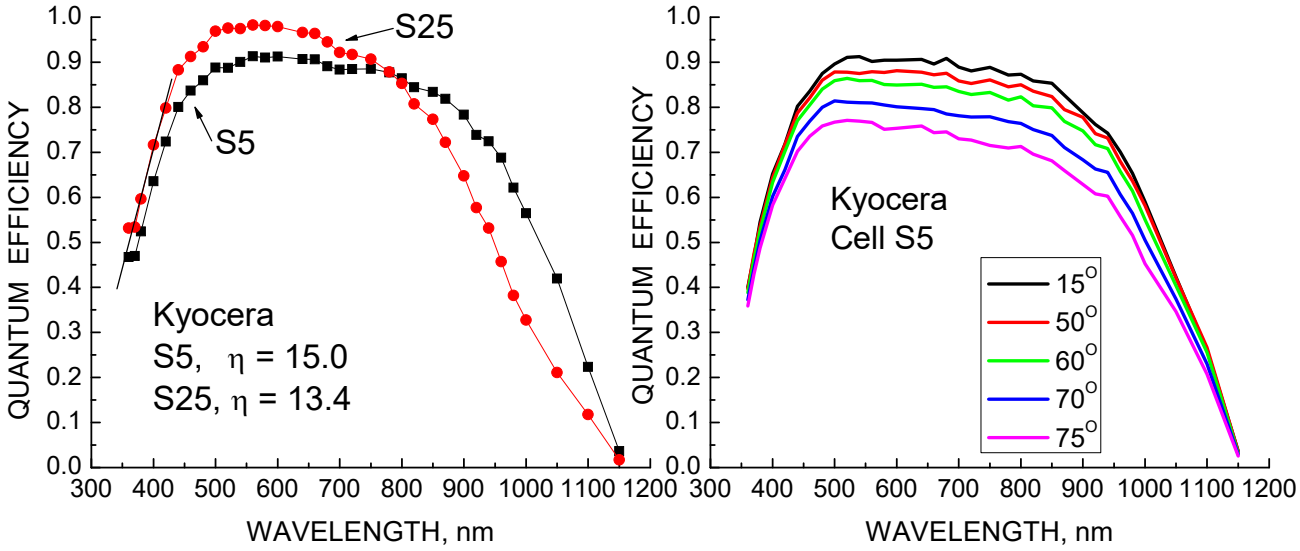

Figure 51. Spectral responses of devices from the Kyocera multicrystalline lot: normal incidence (left) and versus incident angle (right).

The spectral responses of two cells from the Kyocera lot are shown in Figure 51. Cell S5 is from the "1st batch" (see Fig. 51) of higher efficiency cells and S25 is from the 2nd batch. Figure 52 shows the reflectance and EQE – IQE comparison for the better cell, #5. The very gradual slope at long wavelengths would ordinarily imply very poor base lifetime, but much of that gradual slope can be attributed to the extremely non-optimum reflectance with the minimum blue-shifted to 450 nm. Interestingly, the passivation (short wave response) is actually a bit better for these cells than for other multicrystalline lots even though the efficiencies are much lower than normal. The effect of incident angle is also larger for the Kyocera cells than other multicrystalline lots. This appears to be related to the surface

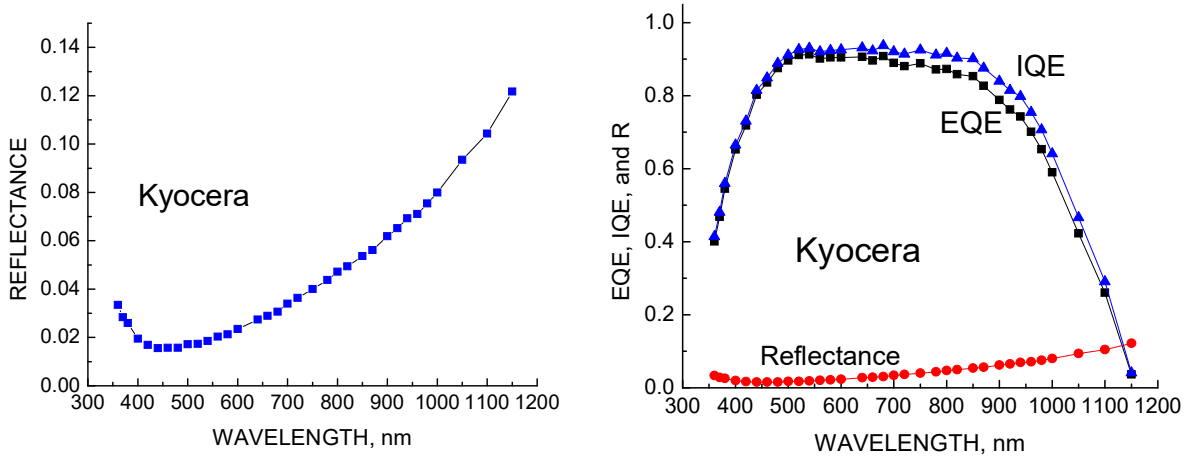

Figure 52 Reflectance (left) and EQE – IQE comparison (right) for cell S5.

appearance - while either mono or multi solar cells are blue because of the nitride AR coating added to the textured surface, the Kyocera cells have no noticeable color at all. It is possible these cells do not have an AR coat, though this would be very surprising and the only reason for it would be to lower the cost at the expense of performance, and the reflectance minimum does suggest that there is a coating present. However, a bare textured surface would also be consistent with the larger effect of incident angle shown in Figure 52.

7.6 ML Solar

20 Multicrystalline Cells.

Comments: Shunt Resistance is good, Series Resistance is good. Voc is poor (~ 607 mV) but FF is good (0.789). There is considerable variation, with efficiencies ranging from 14.5 to 16.3 and fairly high standard deviations. The averages are:

<RSH> = 373 ohms, ⑨ = 503
<RS> = 0.588 ohm-cm^2, ⑨ = 0.053
<J0> = 6.6 E-11 amps/cm^2, ⑨ = 4.4 E-11
< n > = 1.162, ⑨ = .033
< Jsc> = 32.124 mA/cm^2, ⑨ = 0.58
<Voc> = 606.9 mV, ⑨ = 9.8
<FF> = 0..789, ⑨ = .0093
<Effic> = 15.38 %, ⑨ = 0.474

Efficiency and Parameter Correlations:

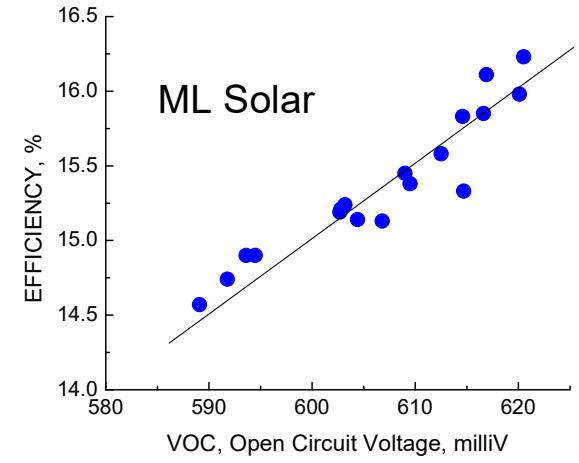

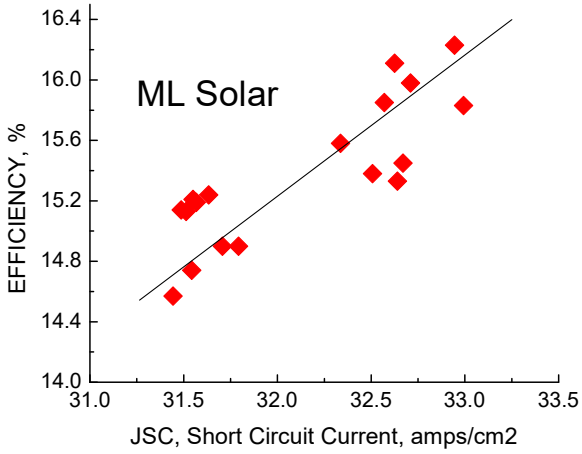

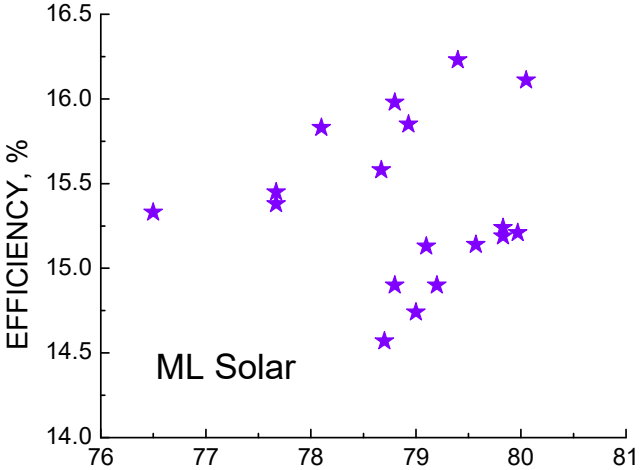

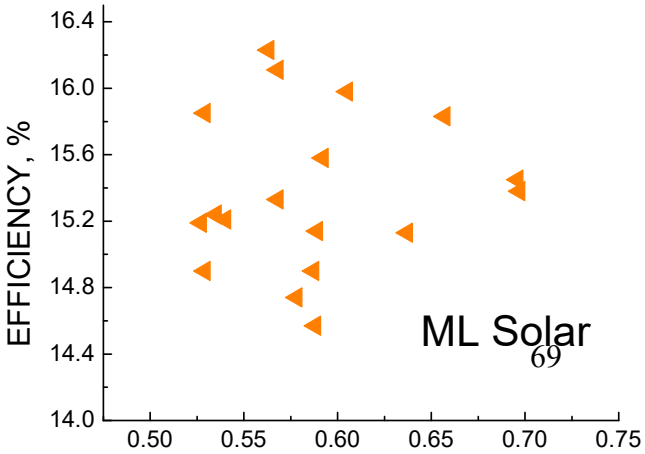

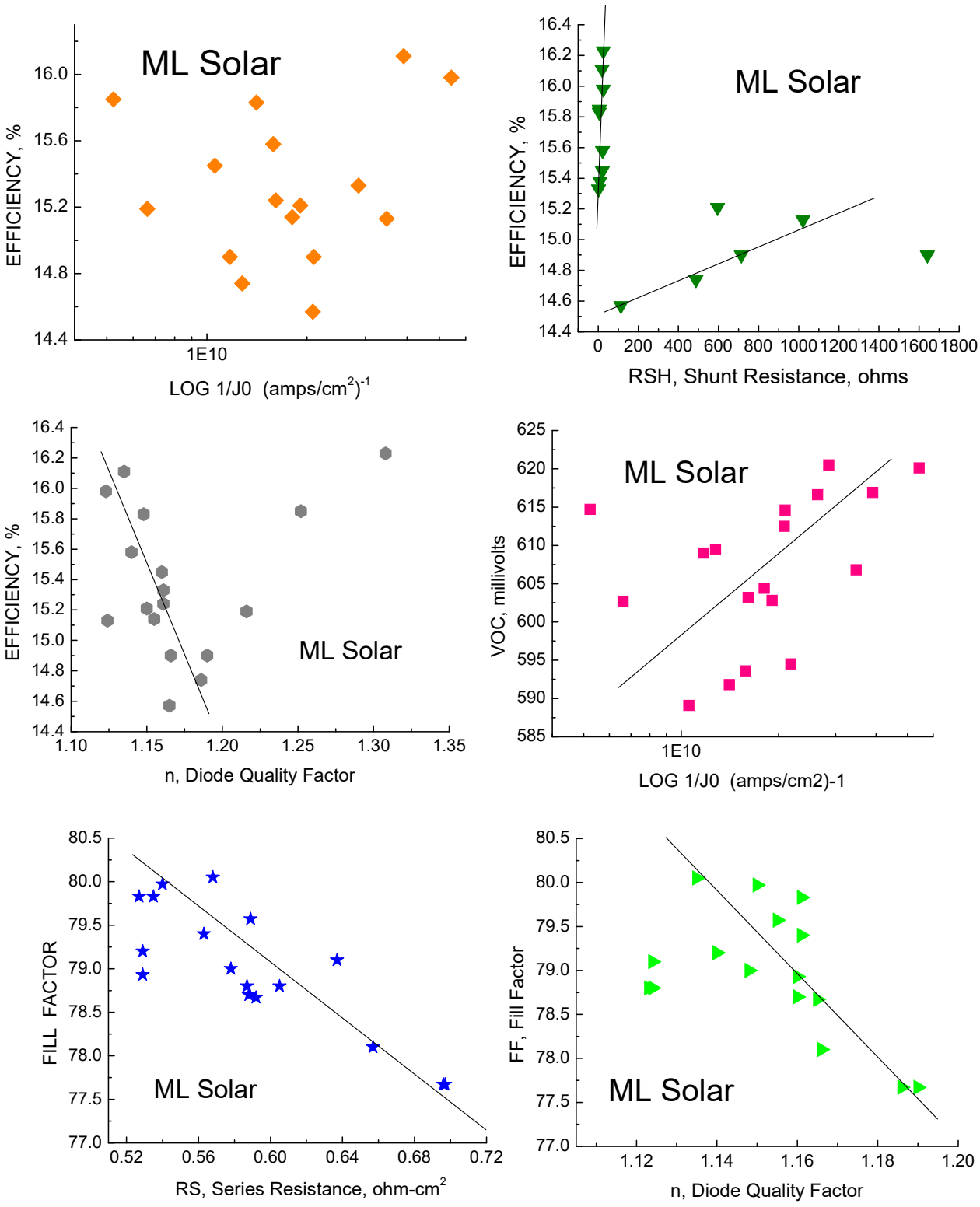

Figure 53a. Correlations for ML Solar cells.

These cells have higher correlations as shown in Figure 53a than most of the other lots. There are high correlations between efficiency and Voc and Jsc, and between FF and Rs.. There are also fairly strong correlations between efficiency and n, as well as between Voc and1/J0 and between FF and n. There are no correlations between efficiency and FF or Rs, unlike most other lots. For the shunt resistance there are two distinct populations, one with very low values of Rsh and one with much higher values, and both populations have reasonable correlations. The 20 cell lot has two "outlier" cells with very different properties than the rest; those two outliers have been excluded from the averages and standard deviations given above and from the chart in Fig. 53b

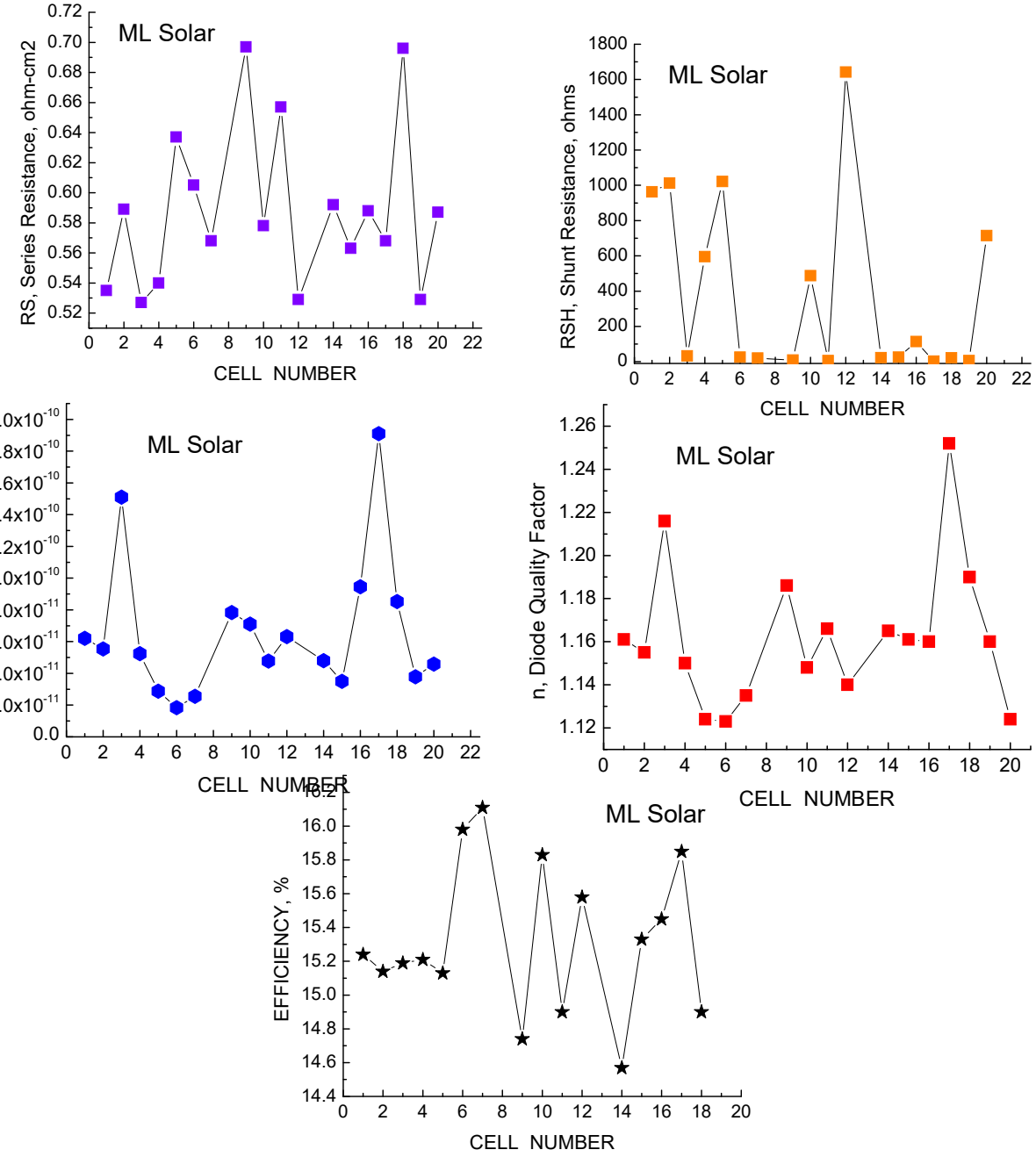

Figure 53b. Forensic parameters for ML Solar cells.

LBIC Maps

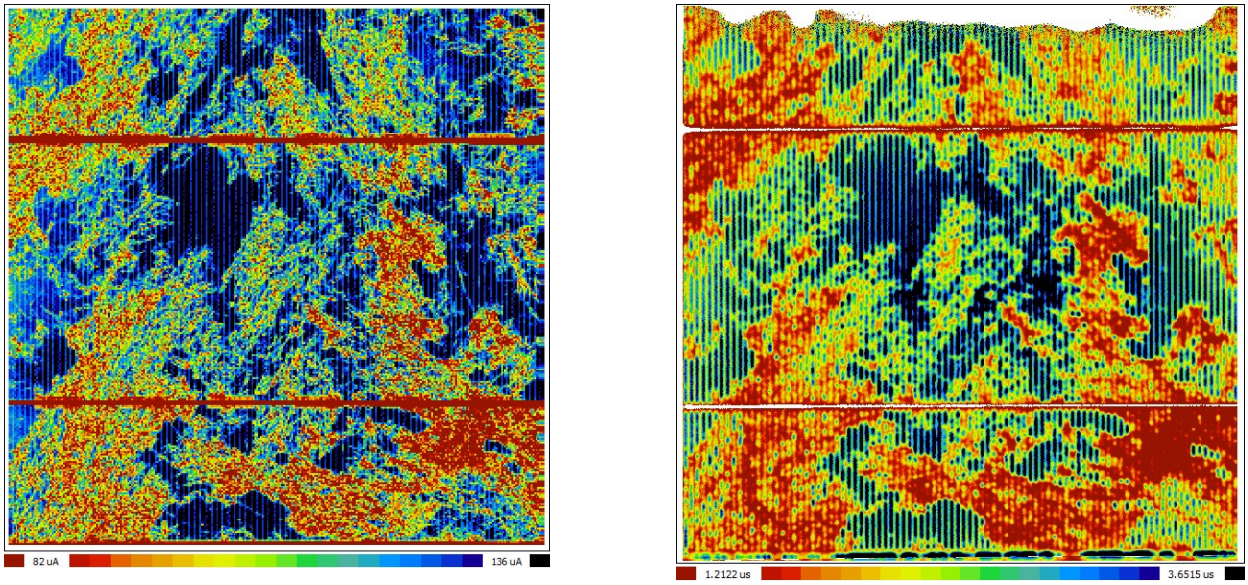

Figure 54. LBIC map at 981 nm (left) and lifetime map (right) for ML Solar cell #12.

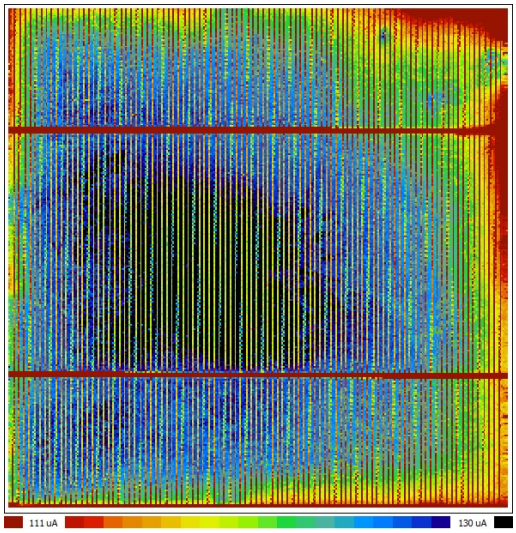

Figure 55. LBIC map for the same cell at 404 nm.

LBIC and lifetime maps are shown in Figures 54 and 55. This lot has a particularly high dislocation density and dislocation distribution compared to others and this is the likely cause of the lower efficiency for these cells and possibly the cause of the poor shunt resistance for many of the devices from this lot. Therefore, the starting material quality is a likely cause of the efficiency limitation for these

Quantum Efficiency

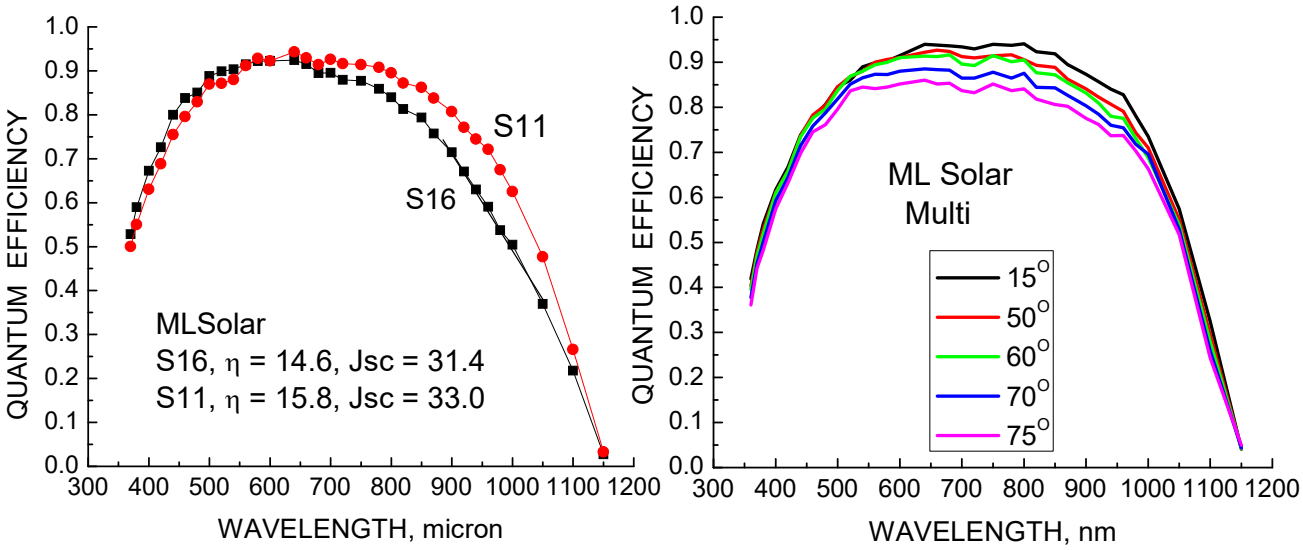

Figure 57 Spectral responses for multicrystalline lot ML Solar; normal incidence (left) and versus angle of incidence (right).

The spectral responses of two cells with low and higher efficiency are shown in Figure 57 (left). Both cells show the gradual rise with diminishing wavelength indicative of poor base lifetime, and mediocre passivation as evidenced by the gradually decreasing short wave response. The responses decrease with incident angle in the visible but are almost coincident at short wavelengths (Figure 57 (right)). Figure 58 shows the reflectance and IQE – EQE comparison for cell # 11. The reflectance minimum at 680 nm should be closer to 580 – 600 nm to match the solar maximum.

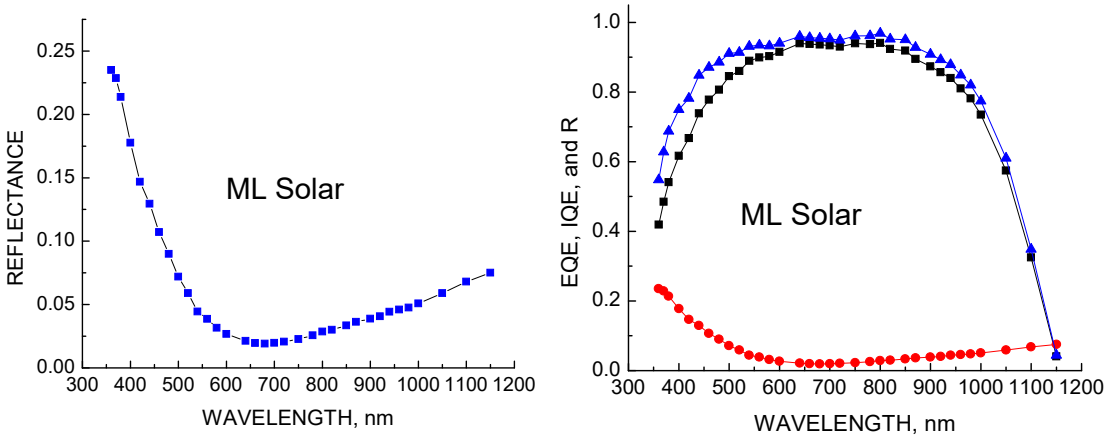

Figure 58 Reflectance (left) and IQE – EQE comparison (right) for cell #11.

7.7 TG Solar

10 Multicrystalline Cells.

Comments: Shunt Resistance is good, series Resistance is good. Voc is good (~ 620 mV) but FF is a bit low (0.769). There is considerable variation, with efficiencies ranging from 14.3 to 16.2 and fairly high standard deviations. The averages are:

<RSH> = 403 ohms, ⑨ = 240
<RS> = 0.510 ohm-cm^2, ⑨ = 0.136
<J0> = 9.1 E-11 amps/cm^2, ⑨ = 6.3 E-11
< n > = 1.201, ⑨ = .046
< Jsc> = 32.954 mA/cm^2, ⑨ = 0.351
<Voc> = 619.5 mV, ⑨ = 2.72
<FF> = 0.769, ⑨ = .026
<Effic> = 15.74 %, ⑨ = 0.345

Efficiency and Parameter Correlations:

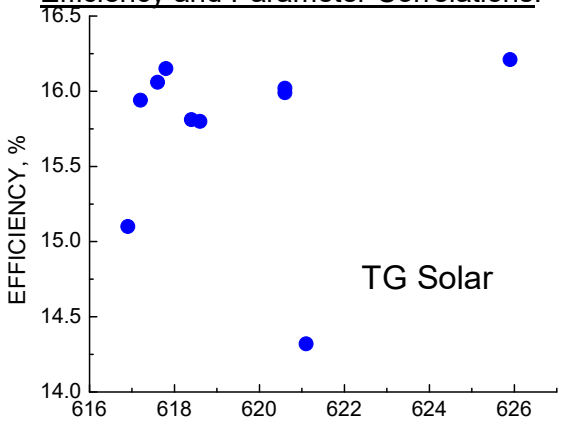

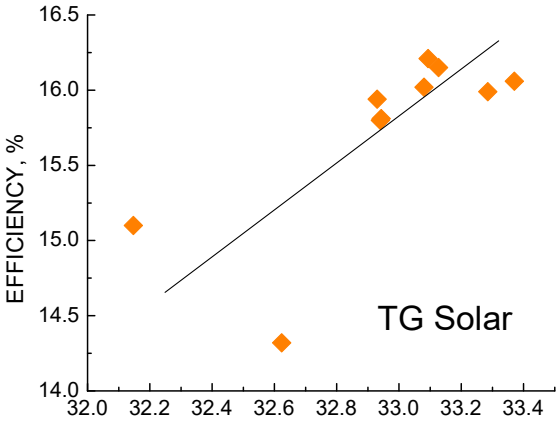

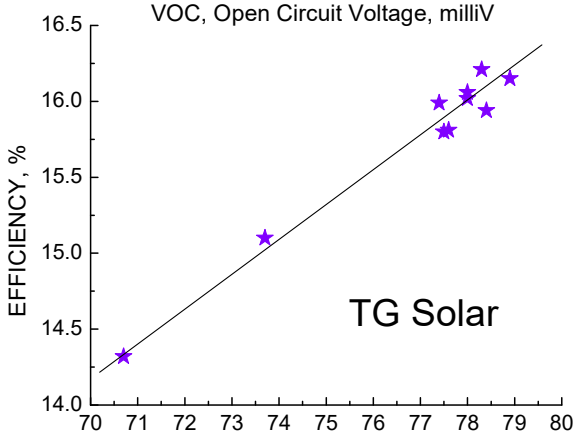

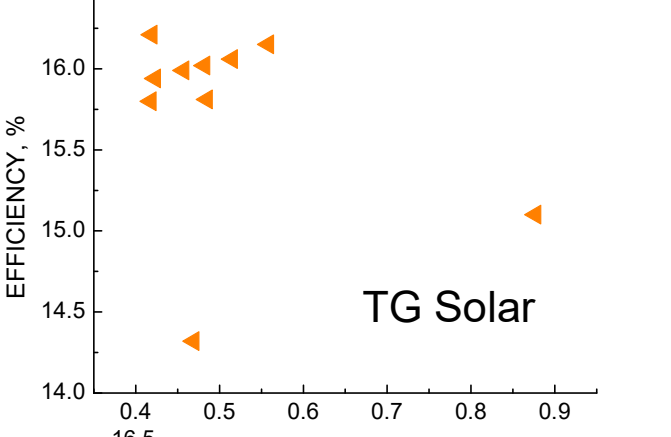

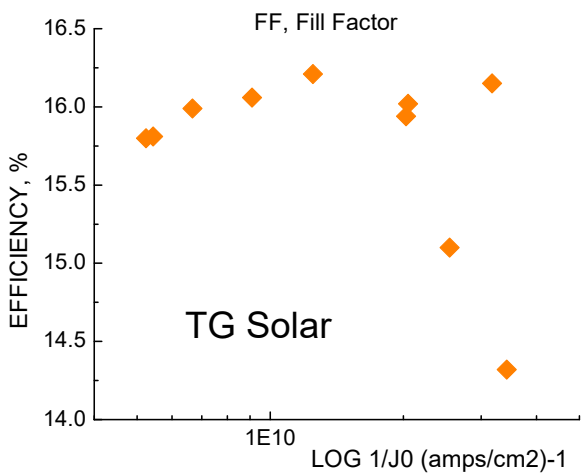

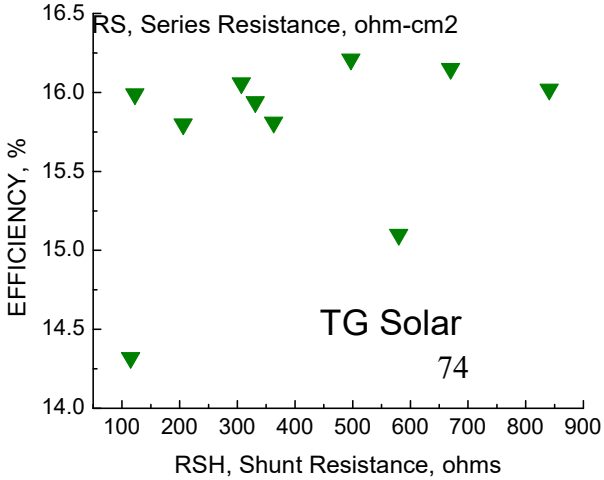

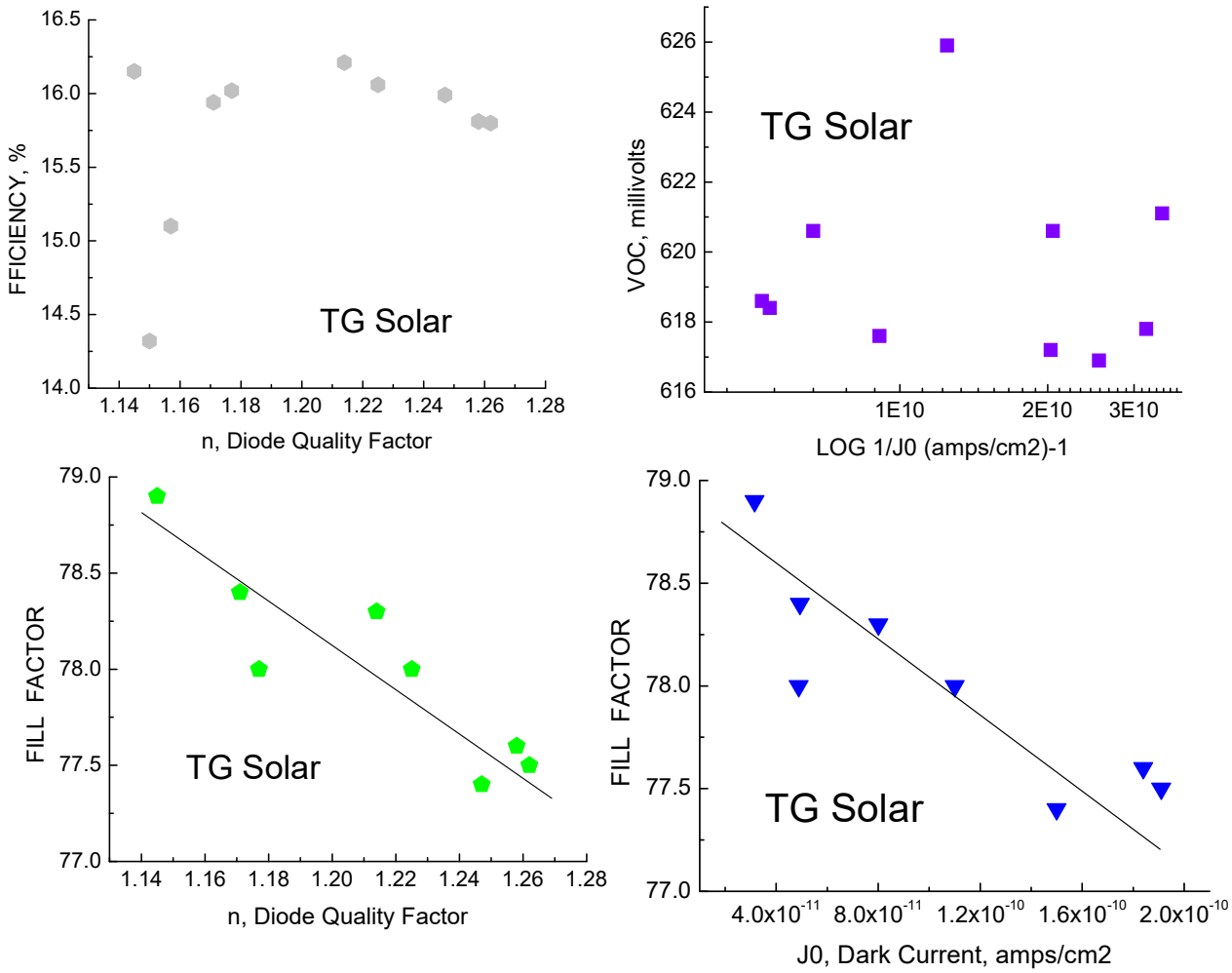

Figure 59. Correlations for TG Solar cells.

There is a high dependence of efficiency on FF and a low correlation with Jsc and J0, but there is no correlation of efficiency with Voc, Rs, Rsh, or diode quality n. There are two cells out of the 10 which don't fit any pattern, but if they are removed, then there is a high correlation of FF with J0 and n. As seen in other lots, there is no correlation of Voc with J0, which is unexpected since Voc is determined by J0:

$$Voc = n\frac{kT}{q}\ln(\frac{Jsc}{J0}+1)$$

The likely explanation is that the diode quality factor counteracts the effect of J0. These two terms, n and J0, are related to the lifetimes in the base and emitter and the presence of excess states inside the depletion region, an effect brought on by impurities in the starting material. The strongest correlation is of efficiency with FF, while FF in turn is dominated by n and J0 rather than a more expected series resistance. Figure 60 shows the variations of device forensic parameters for the 10 cells. Such large variations in J0 and n indicate significant ranges in material quality and/or processing.

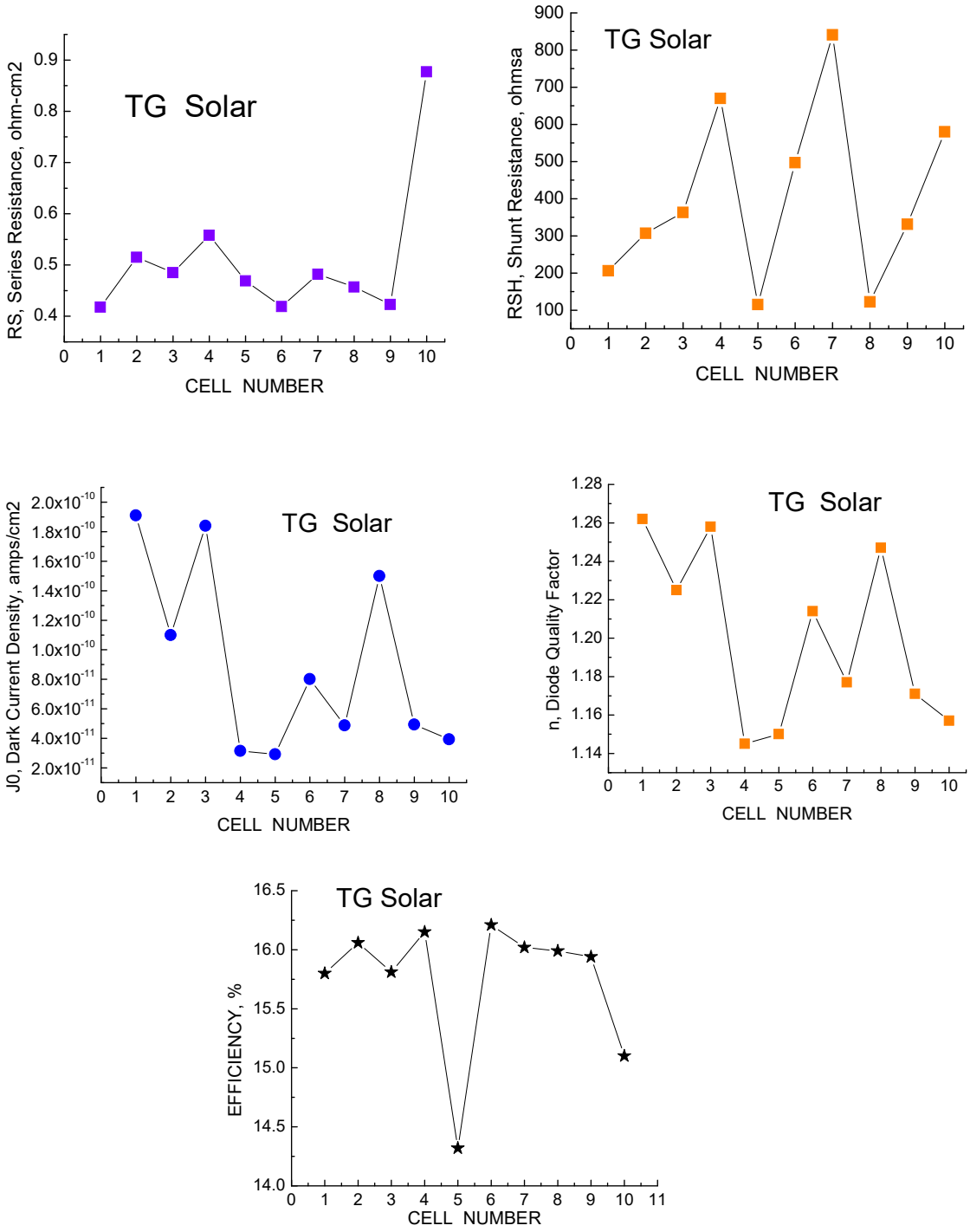

Figure 60. Forensic parameters for TG Solar cells

LBIC Maps.

Photoresponse measurements at long and short wavelengths are shown in Figure 61 and the corresponding lifetime map in Figure 62. Both the long wavelength LBIC and lifetime are indicative or processes only in the base. The high dislocation areas with their lower photocurrents are clearly seen. The long wavelength maps are independent of the emitter properties and upper surface passivation, while the short wavelength map on the right in Figure 61 is dependent *only* on the emitter and upper SRV and therefore the dislocation areas and grain boundaries effectively "disappear."

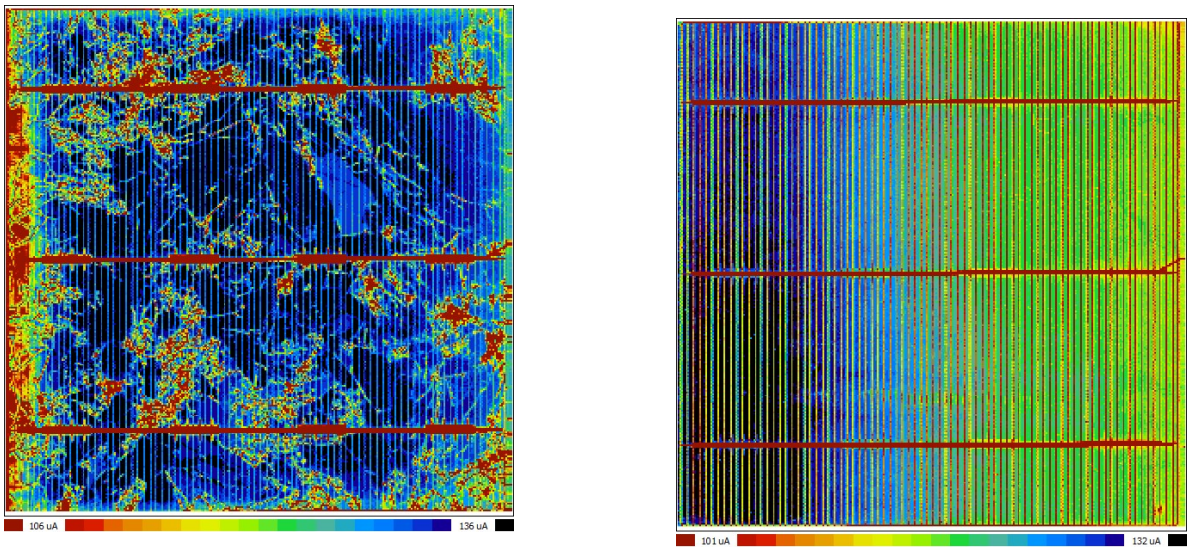

Figure 61. LBIC maps of a typical TG Solar device for 981 nm (left) and 404 nm (right) excitation.

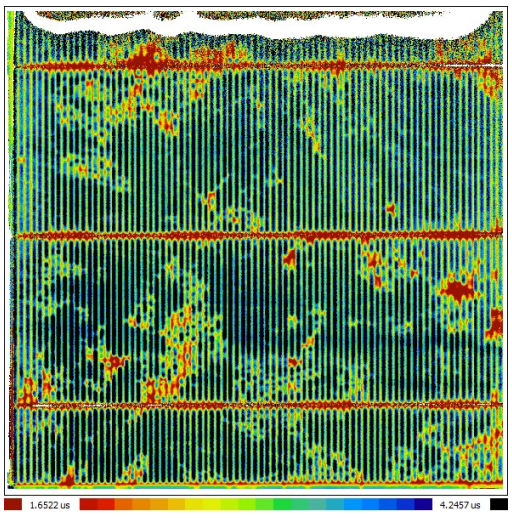

Figure 62. Lifetime map corresponding to the LBIC map in Fig. 64. (The white area near the top is an instrument artifact).

Quantum Efficiency.

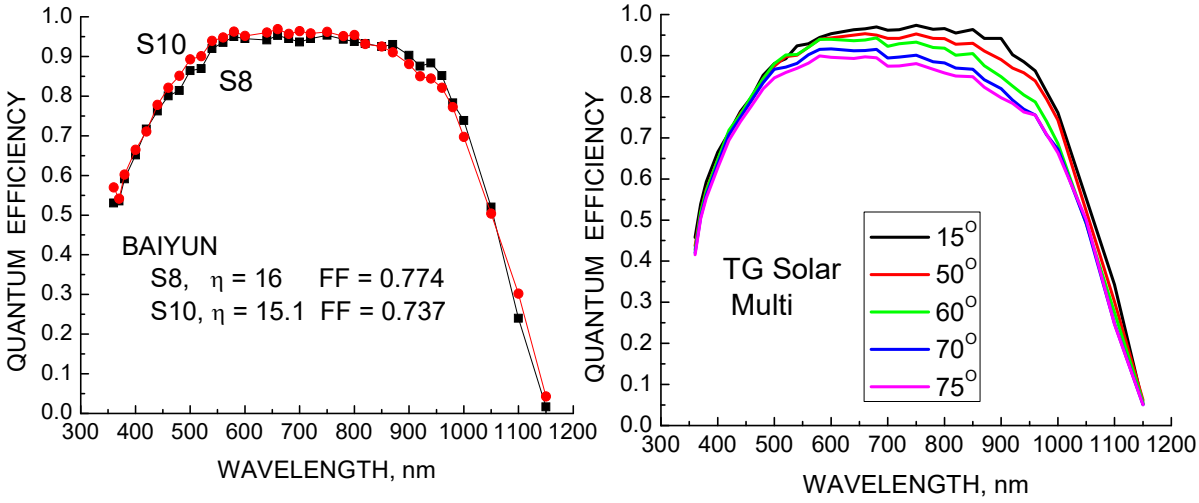

Figure 63. Spectral responses for TG Solar at normal incidence (left) and as a function of incident angle (right).

Figure 63 shows the spectral responses for two cells from this lot. The efficiencies of the two cells differ because of Fill Factor differences, but the spectral responses are nearly the same. The QE is affected by incidence angle mostly in the visible and near-IR, but the responses merge at short wavelengths as seen in most multicrystalline cells. Figure 64 shows that the reflectance is very non-optimum, with a minimum above 700 nm and steeply rising values for shorter wavelengths. The IQE is good for multicrystalline cells, implying good substrate lifetime and good passivation, but the reflectance degrades the Isc and the efficiency to some degree.

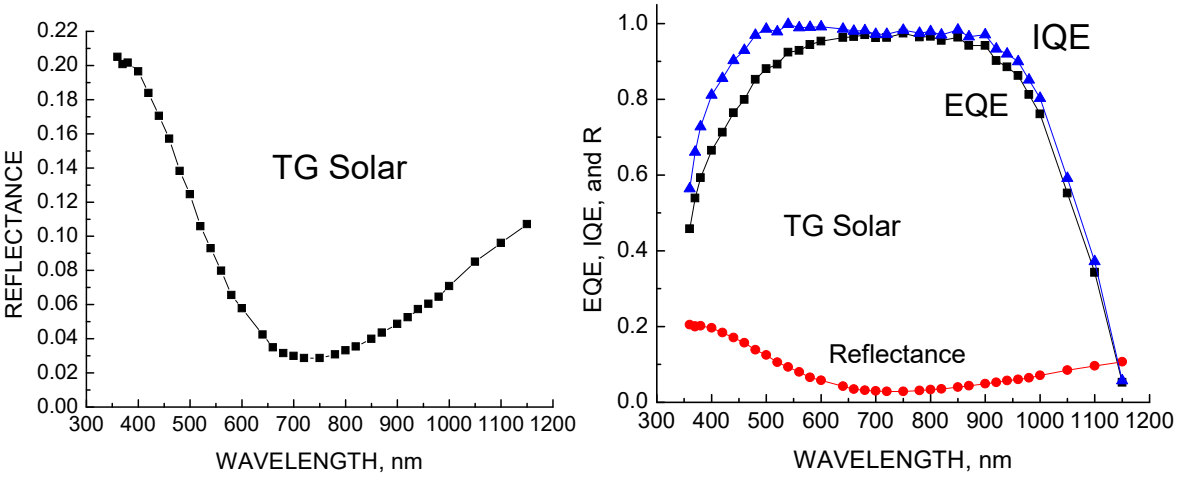

Figure 64. Reflectance (left) and IQE – EQE comparison (right) for cell #8.

7.8 YYOO Solar

10 Multicrystalline Cells.

Comments: Shunt Resistance is good, series Resistance is good. FF is moderate (0.77) but Voc is a bit low (608 mV). The lowest efficiency is 14.8 and the highest 15.3 so this lot is on the low end of the other multi lots, probably due to a high J0 and n. Though the # of cells is small, there is still a reasonable correlation of efficiency with Jsc and Voc, but not with FF or Rs. The averages are:

<RSH> = 331ohms, ⑨ = 209
<RS> = 0.531 ohm-cm^2, ⑨ = 0.046
<J0> = 3.7 E-10 amps/cm^2, ⑨ = 3.8 E-10
< n > = 1.266, ⑨ = .061
< Jsc> = 32.165 mA/cm^2, ⑨ = 0.171
<Voc> = 607.9 mV, ⑨ = 3.4
<FF> = 0.773, ⑨ = .005
<Effic> = 15.12 %, ⑨ = 0.19

Efficiency and Parameter Correlations:

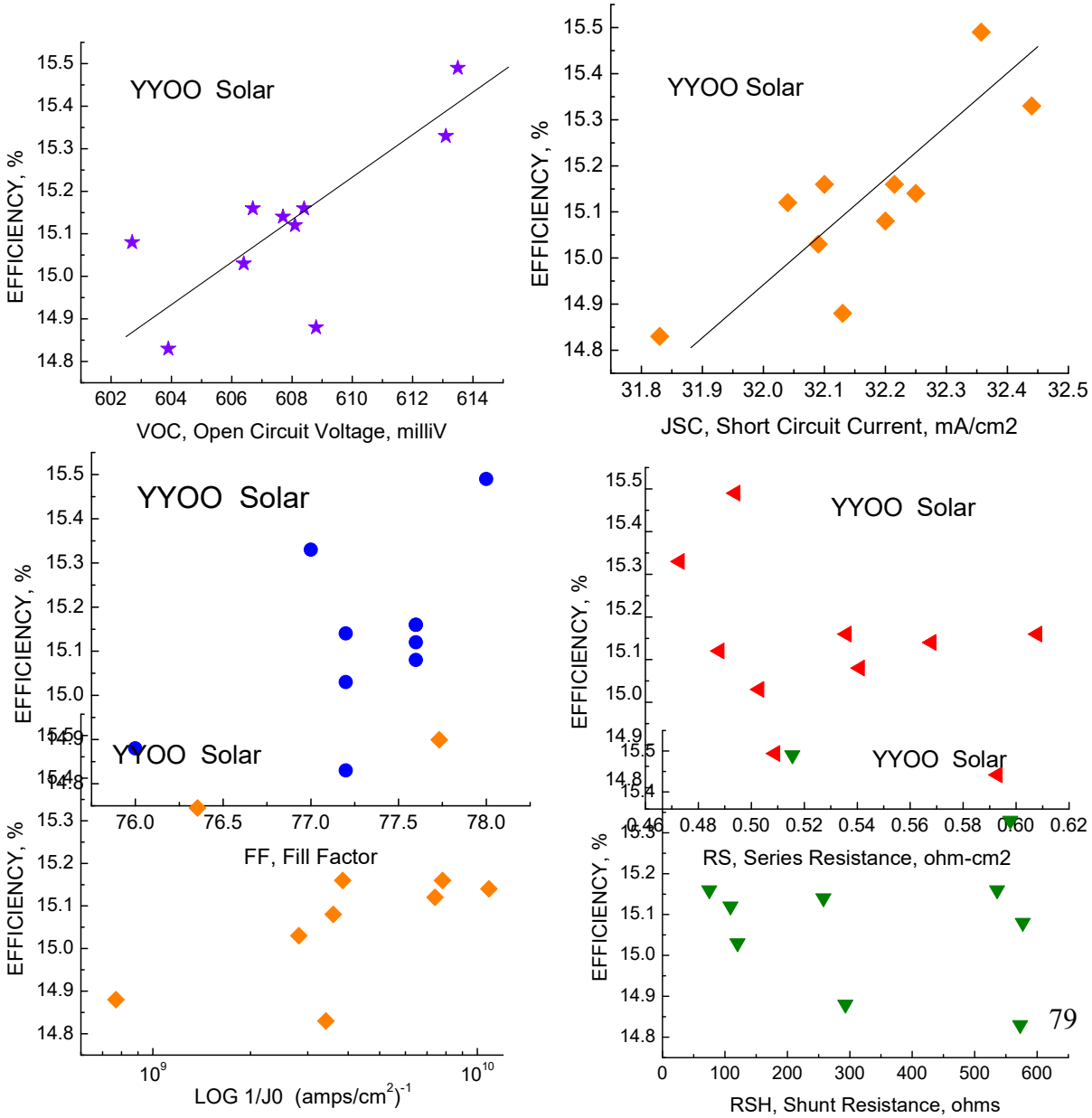

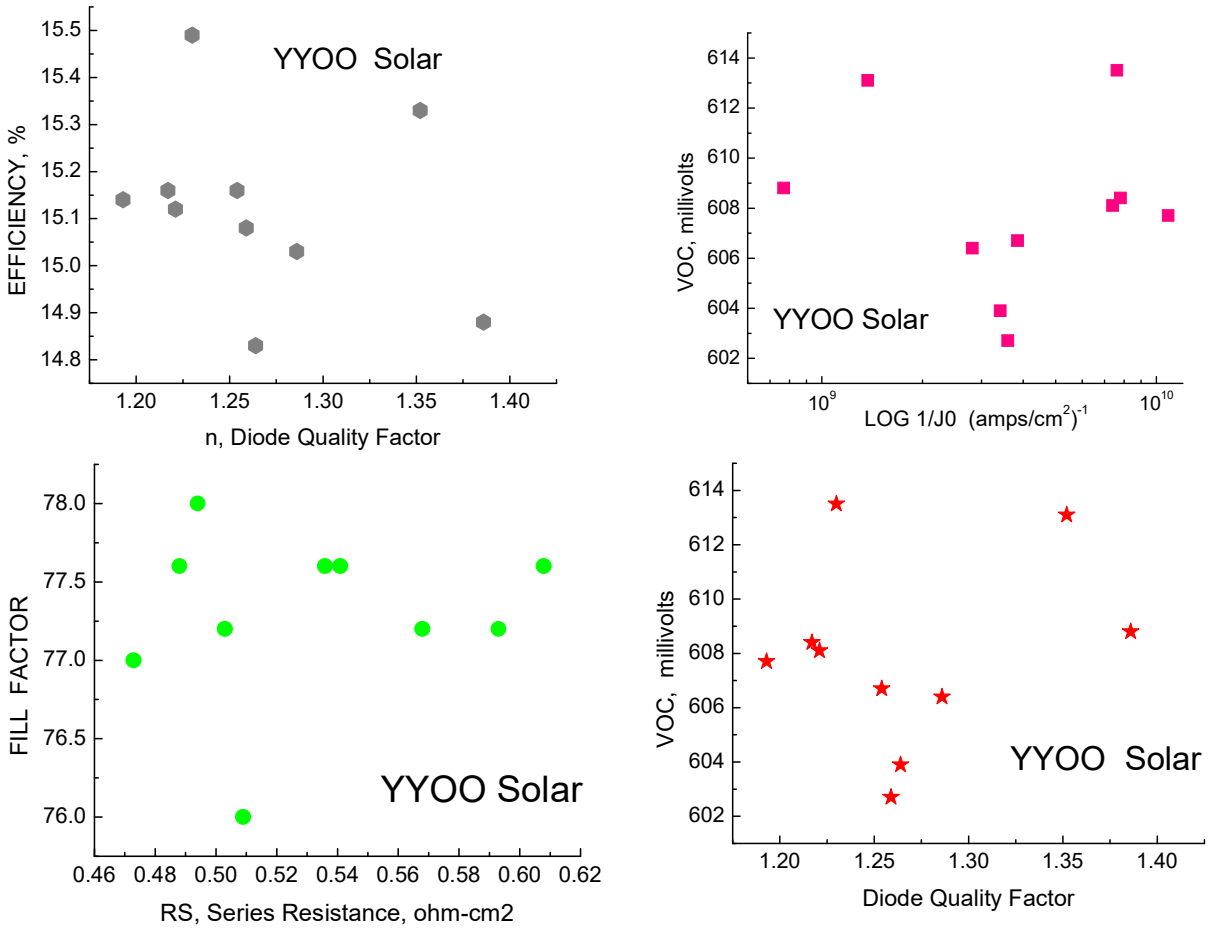

Figure 65. Correlations for YYOO Solar cells.

Correlations are shown in Figure 65. The statistical number of cells is small for YYOO and the 10 devices have a wide range of parameters. While nothing "stands out," there is a reasonable correlation of efficiency with Jsc and Voc, but not much else. All the major parameters: ~~, Jsc, Voc, and FF are relatively low.

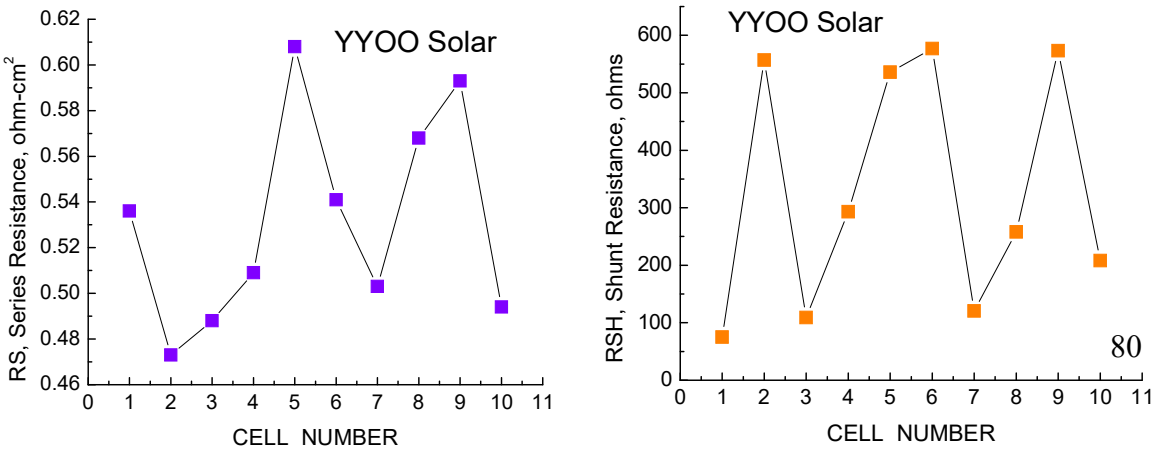

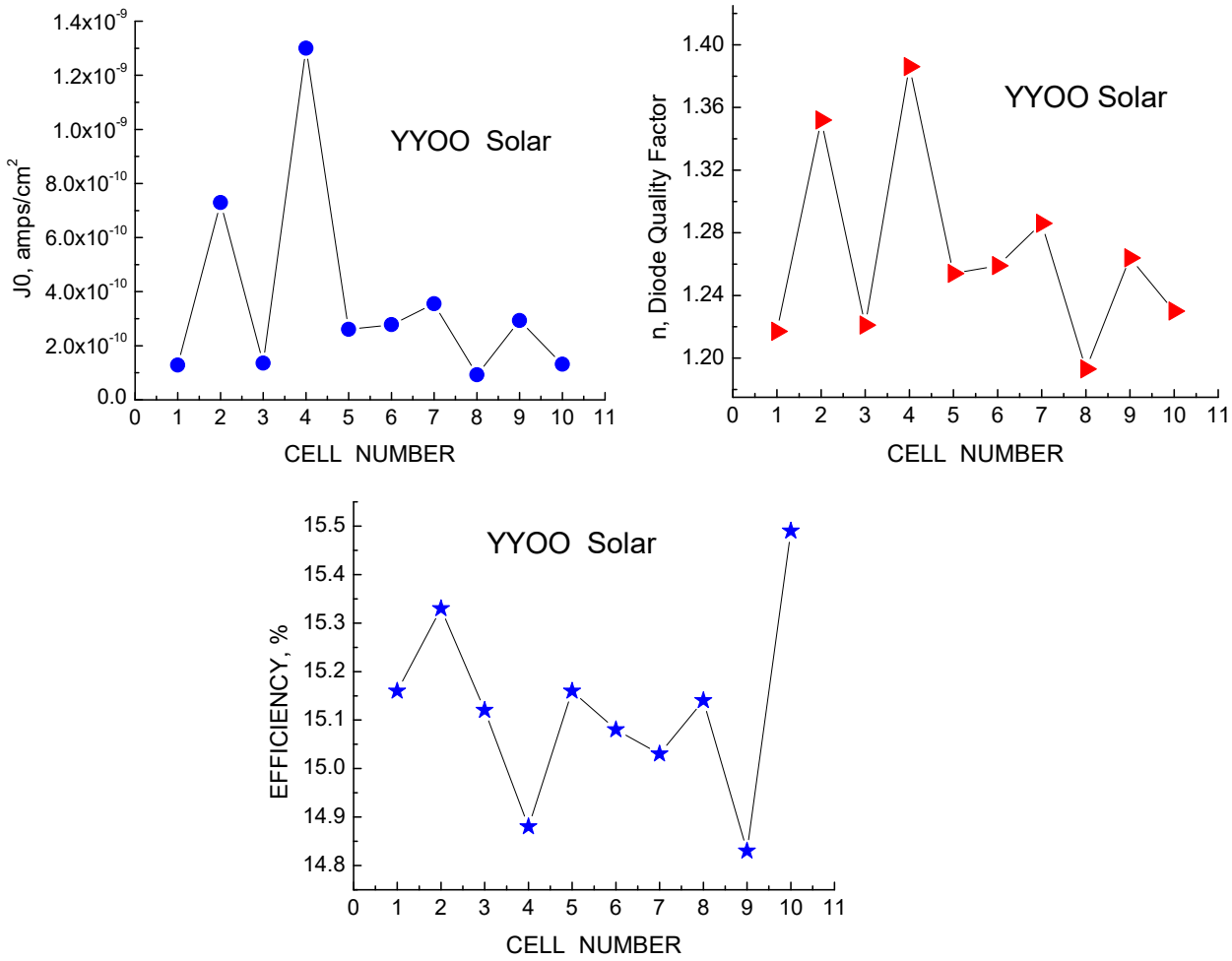

Figure 66. Forensic parameters for YYOO Solar.

The diode parameters J0 and n are high for this lot compared to others and Rs and Rsh show considerable variation; Rs variation could be either grid (process) variations or substrate resistivity differences. Rsh likely reflects a variability in substrate quality.

LBIC MAPS.

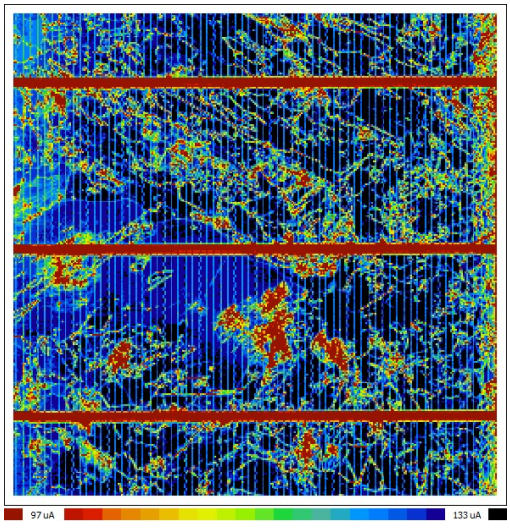

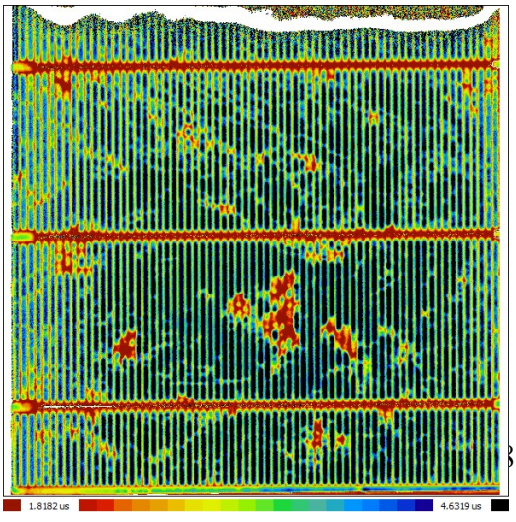

Figure 67. LBIC map at 891 nm excitation (left) and lifetime map (right), cell S2.

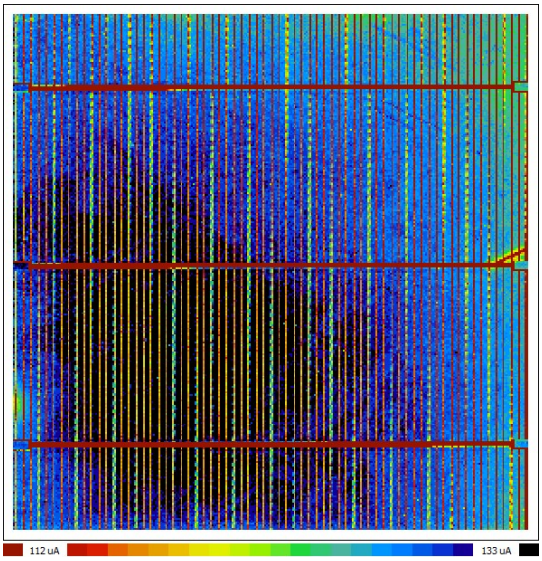

Figure 68. LBIC map for 404 nm excitation.

The LBIC map and lifetime map (Figure 67) are well correlated at long wavelengths, where the high dislocation lossy areas appear as red splotches against the blue background. The LBIC map in Figure 68 at short wavelength appears very uniform; the difference between black and blue areas is only 1 μA out of 125μA .

Quantum Efficiency

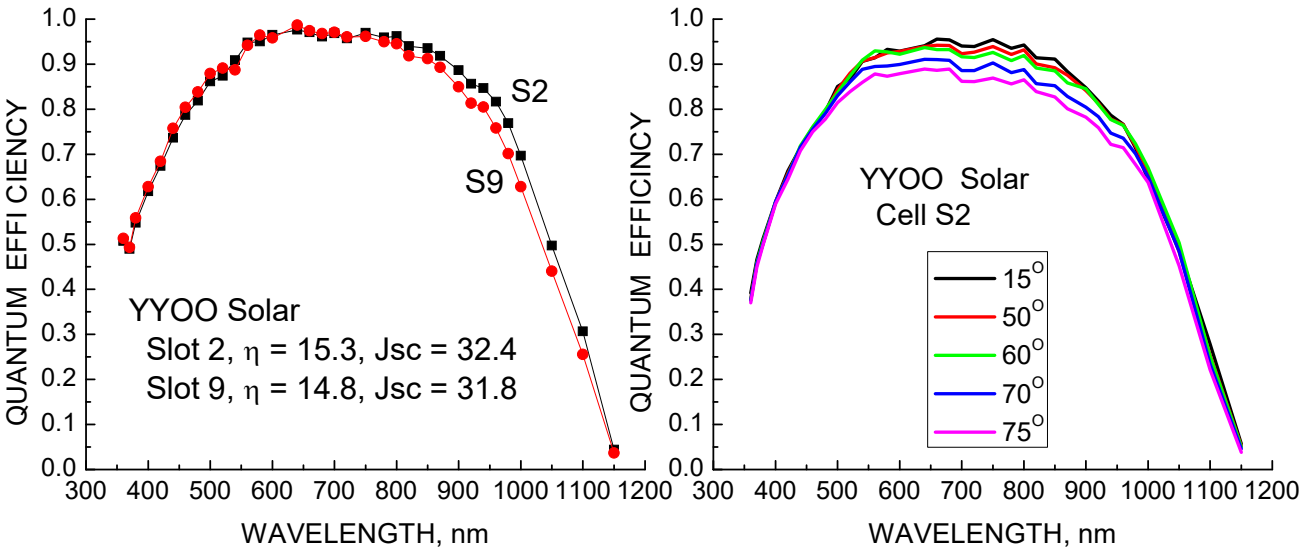

Figure 69. Spectral responses for multicrystalline lot YYOO Solar; normal incidence (left), versus angle of incidence (right)

Figure 69 shows the spectral responses for two cells from lot YYOO Solar. The response as a function of angle shows most of the effect in the visible range; the responses tend to merge at short and long wavelengths. Figure 70 shows the reflectance and the IQE/EQE comparison. The lifetimes are around 2 μsecs and result in the gradual slope of increasing response with decreasing wavelength in the IR. The passivation is poor, resulting in gradually diminishing response with decreasing wavelengths below 600 nm. The reflectance minimum is at 700 nm, too far into the IR. The ISC would have been higher if the minimum were closer to 580-600 nm to match the solar peak.

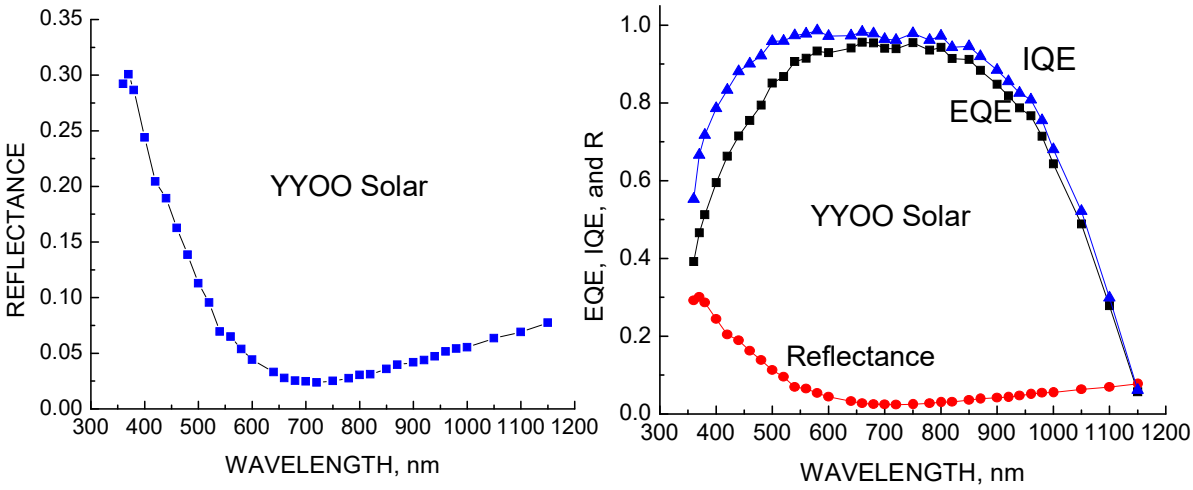

Figure 70. Reflectance (left) and IQE, EQE comparison (right).

7.9 LED Solar

20 Multicrystalline Cells.

Comments: Shunt Resistance is good, series Resistance is good. FF is high (0.79) and Voc is good (619 mV). The variation among the 10 cells is fairly low as evidenced by low standard deviations. The average efficiency is moderate with a range of 15.8 – 16.8% . The averages are:

<RSH> = 358ohms, ⑨ = 357
<RS> = 0.513 ohm-cm^2, ⑨ = 0.123
<J0> = 7.4 E-11 amps/cm^2, ⑨ = 8.4 E-11
< n > = 1.181, ⑨ = .45
< Jsc> = 32.83 mA/cm^2, ⑨ = 0.324
<Voc> = 619.3 mV, ⑨ = 4.7
<FF> = 0.790, ⑨ = .008
<Effic> = 16.09 %, ⑨ = 0.28

Efficiency and Parameter Correlations:

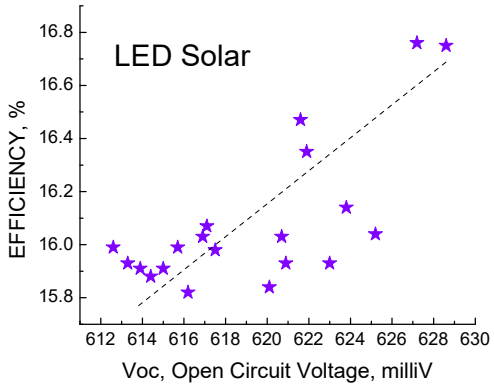

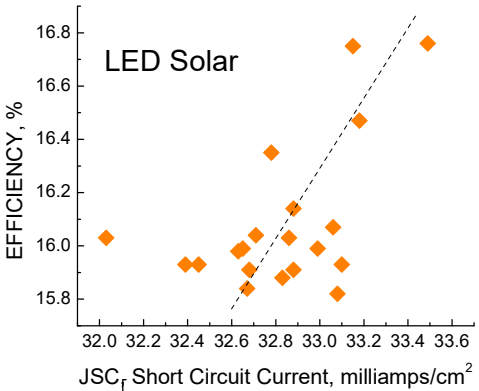

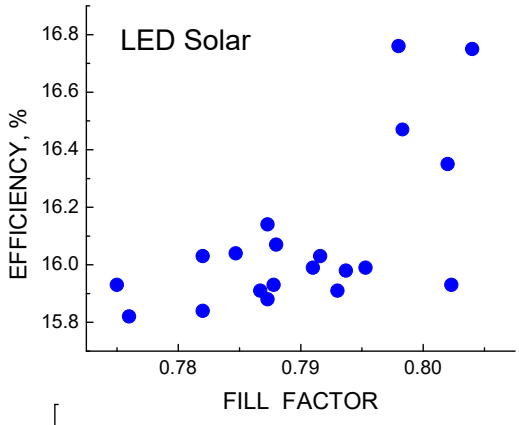

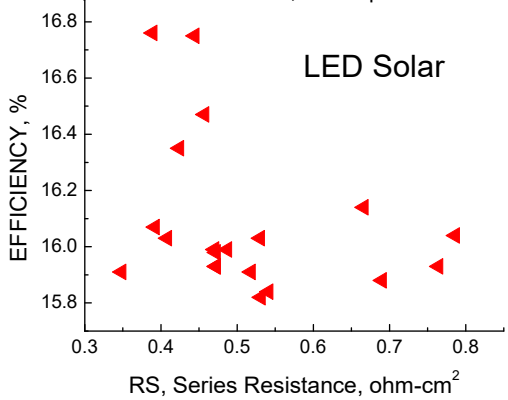

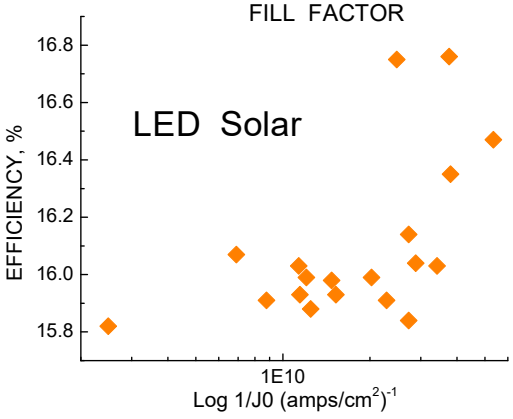

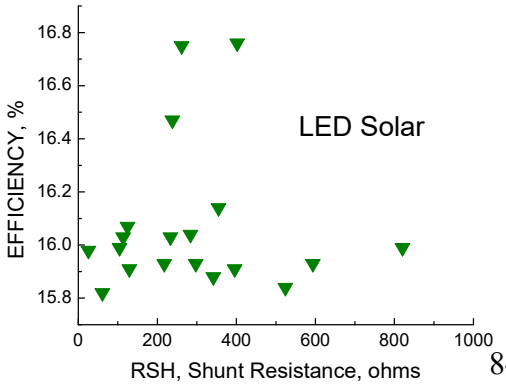

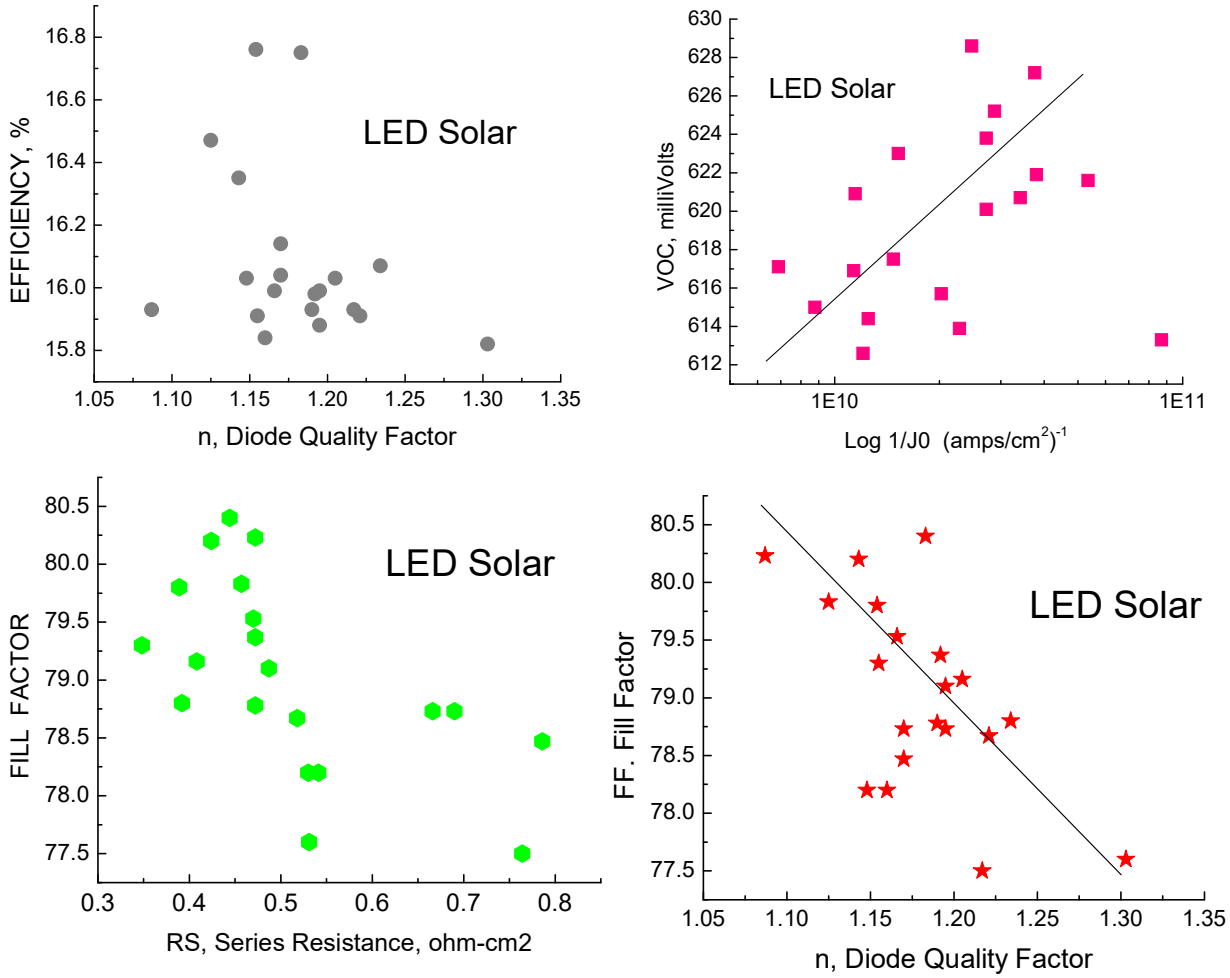

Figure 71. Correlations for LED Solar.

The lot from LED Solar consists of 20 multicrystaline cells. There are weak correlations between efficiency and Voc and Jsc, but no other parameter seems of importance (Figure 71). A weak dependence is observed between FF and diode quality factor, and between Voc and log 1/J0.

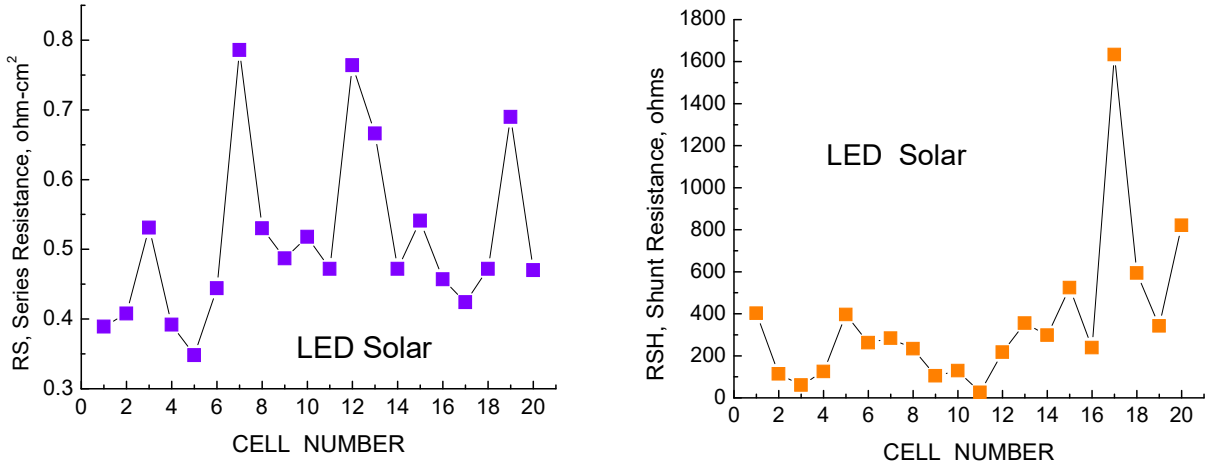

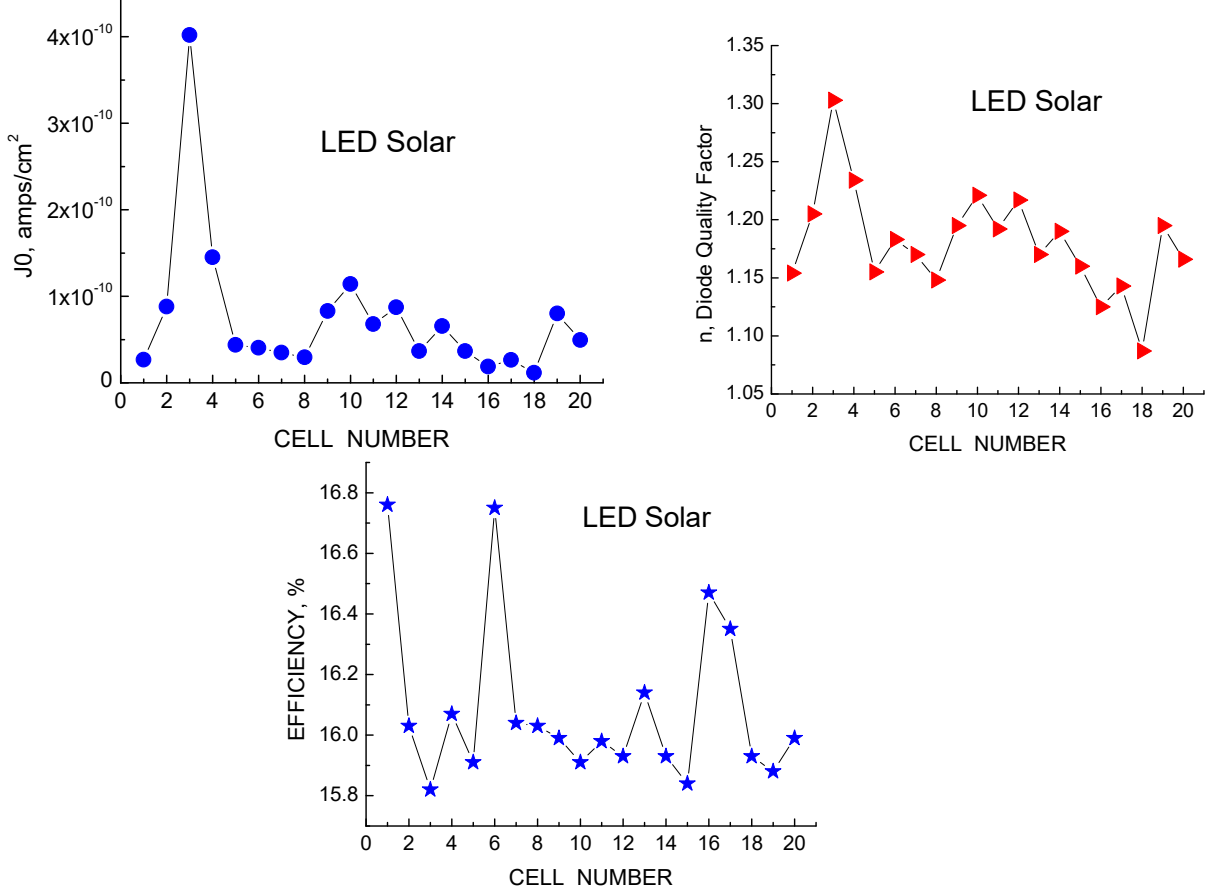

Figure 72. Forensic parameters for LED Solar.

Figure 72 shows the forensic parameters for this lot. The efficiency chart is the most interesting, showing what appears to be a bimodal distribution with a group of 16 cells clustered around 16% and some “high flyers” at 16.4 to 16.8 %, which are very good values for turn-key multi cells fabricated around 2013.

LBIC Maps.

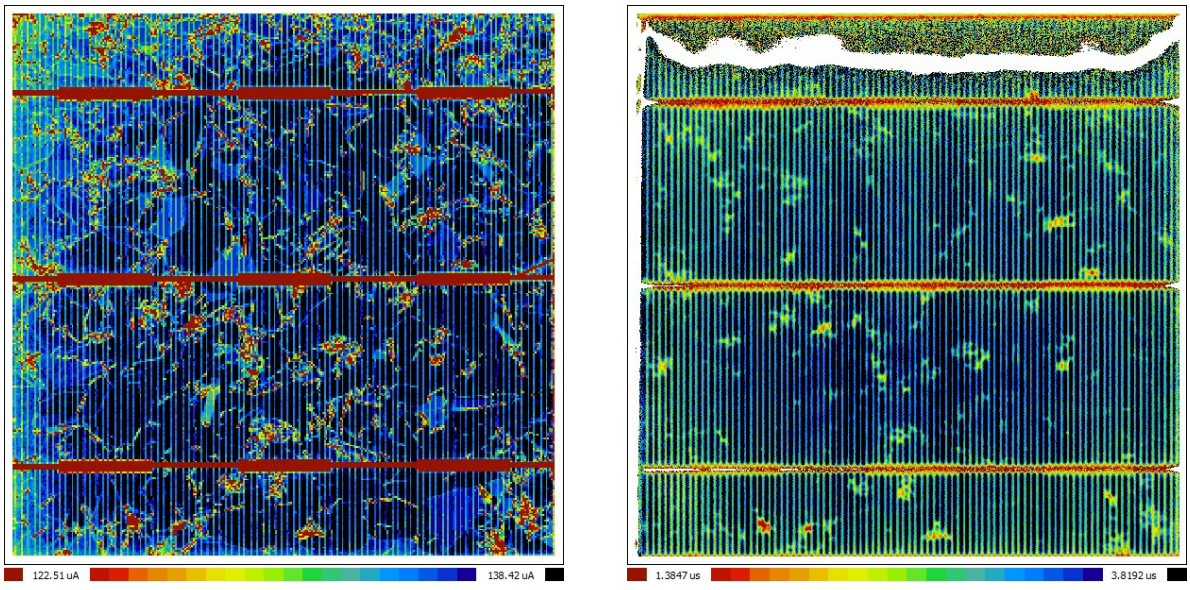

Figure 73. LBIC map at 981 nm (left) and lifetime map (right).

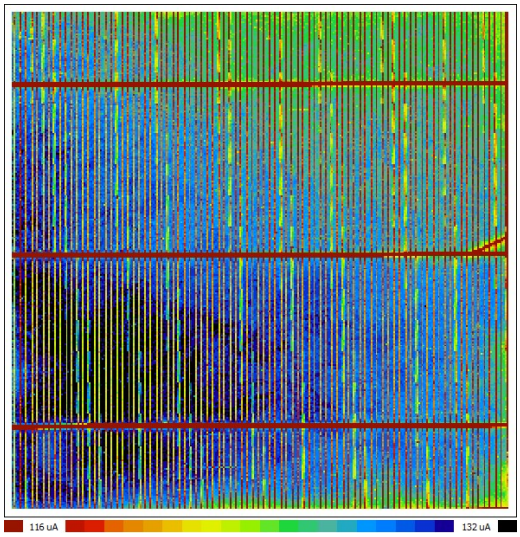

Figure 74. LBIC map at 404 nm excitation.

The LBIC and lifetime maps are shown in Figures 73 and 74, and while there is an apparent correspondence between dislocations and reduced photocurrent at long wavelengths, the correlation is significantly weaker than for other turn-key lots. Since the efficiency is also higher than for other multicrystalline lots in the study, the implication is that the starting material quality may be higher for these cells than others.

Quantum Efficiency.

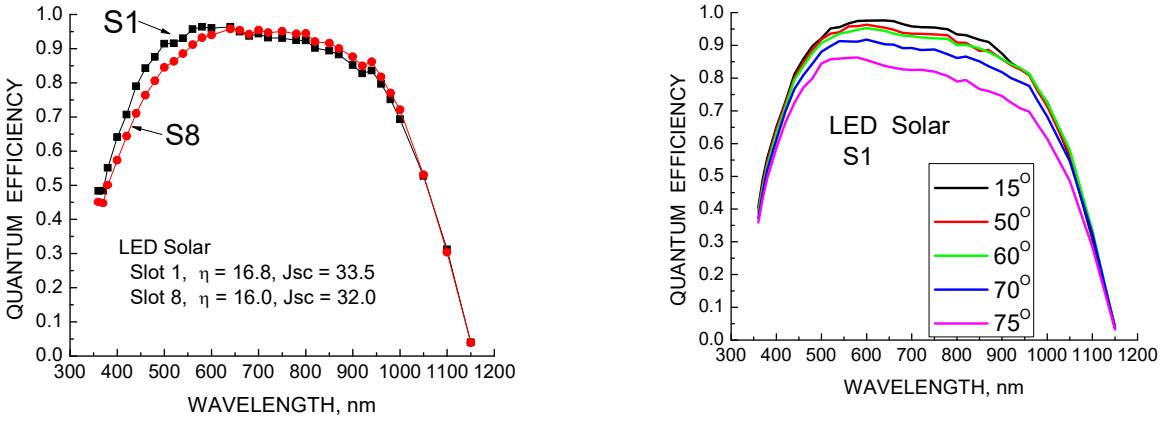

Figure 75. Spectral responses for multicrystalline lot LED Solar; normal incidence (left), versus angle of incidence (right).

Figure 75 shows the spectral responses for two cells from LED Solar. The lifetime is about the same for both cells but the passivation is better in the higher efficiency cell S1 than the other, S8. The responses versus angle of incidence are most affected in the visible and near-IR range, but they tend to merge at short wavelengths, which is seen in all multicrystalline cells. Figure 76 shows the reflectance and IQE – EQE for cell S1. The IQE confirms that both the lifetime and passivation are both very good, better than for most multicrystalline lots. The reflectance minimum is also close to the ideal wavelength value.

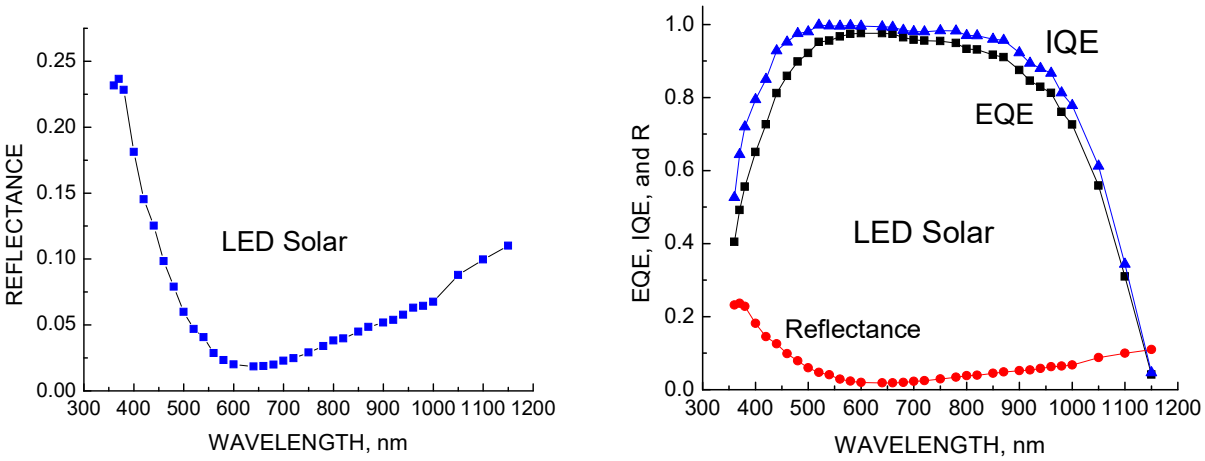

Figure 76. Reflectance (left) and IQE – EQE comparison (right) for cell #S1.

7.10 PVL 451

30 6-inch Multicrystalline Cells.

Comments: Shunt resistance is very good and series resistance is low. J0 and n are good for multicrystalline cells and Voc is relatively good. The net efficiency is about 15.8%, low for today's multi cells. The averages are:

<RSH> = 730 ohms, ⑨ = 434
<RS> = 0.444 ohm-cm^2, ⑨ = 0.044
<J0> = 2.3 E-11 amps/cm^2, ⑨ = 2.5 E-11
< n > = 1.124, ⑨ = .033
< Jsc> = 32.342 mA/cm^2, ⑨ = 0.114
<Voc> = 617.4 mV, ⑨ = 3.5
<FF> = 0.771, ⑨ = .005
<Effic> = 15.79 %, ⑨ = 0.08

Efficiency and Parameter Correlations:

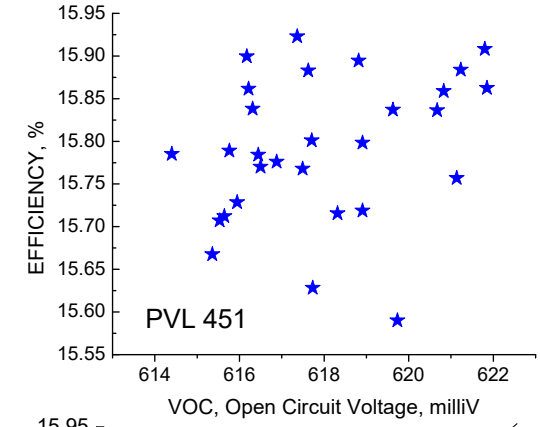

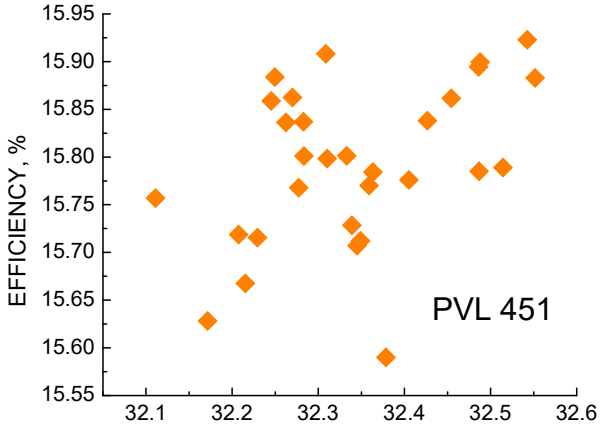

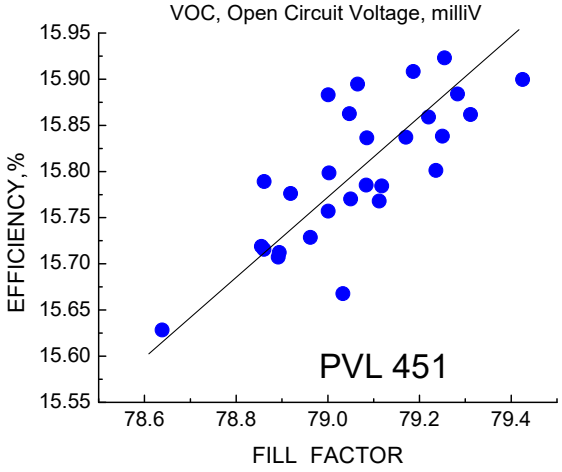

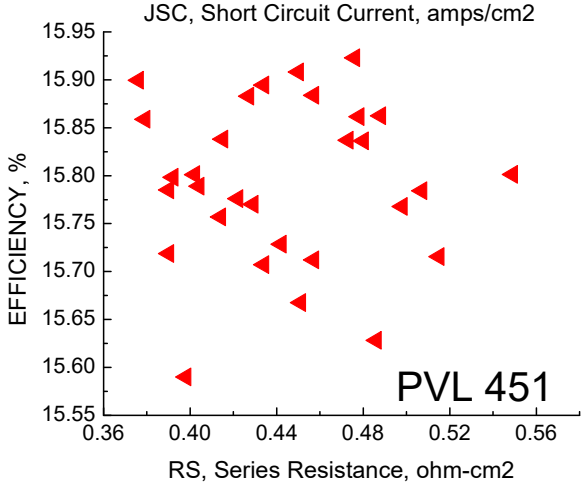

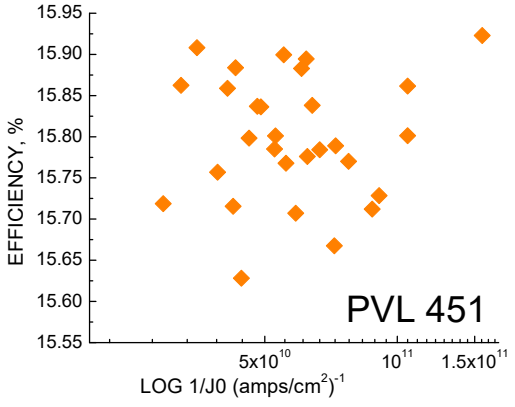

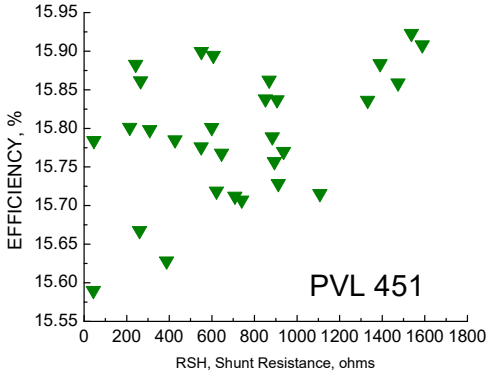

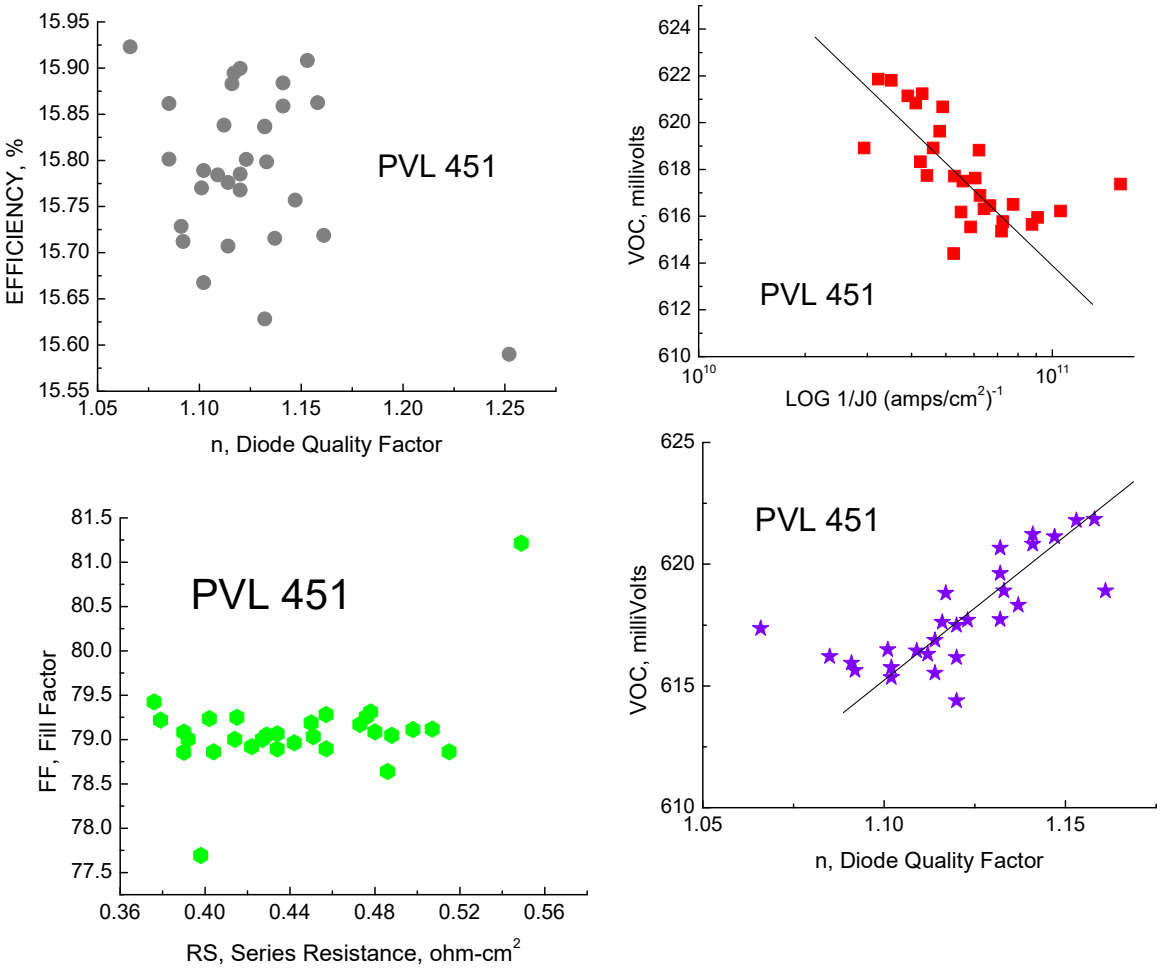

Figure 77. Correlations for Linuo multicrystalline lot 451.

Figure 77 shows the correlations for this multicrystalline lot. There is no relation between efficiency and Voc or Jsc, but a correlation is evident between efficiency and fill factor. There are reasonably good correlations between Voc and both J0 and n. As seen before, even though there is a relation between efficiency and fill factor, the fill factor itself doesn't appear to depend on any of the other device parameters: Rs, Rsh, J0, or n.

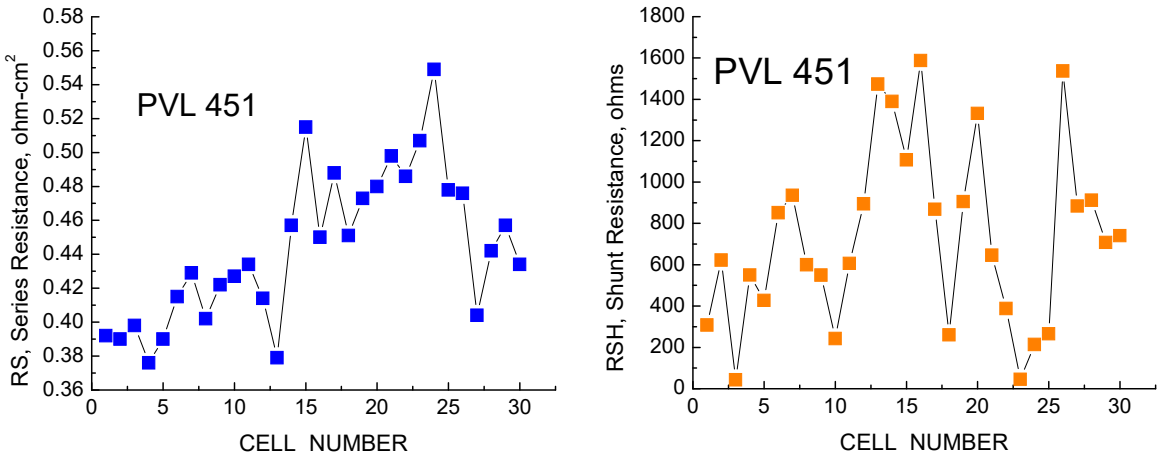

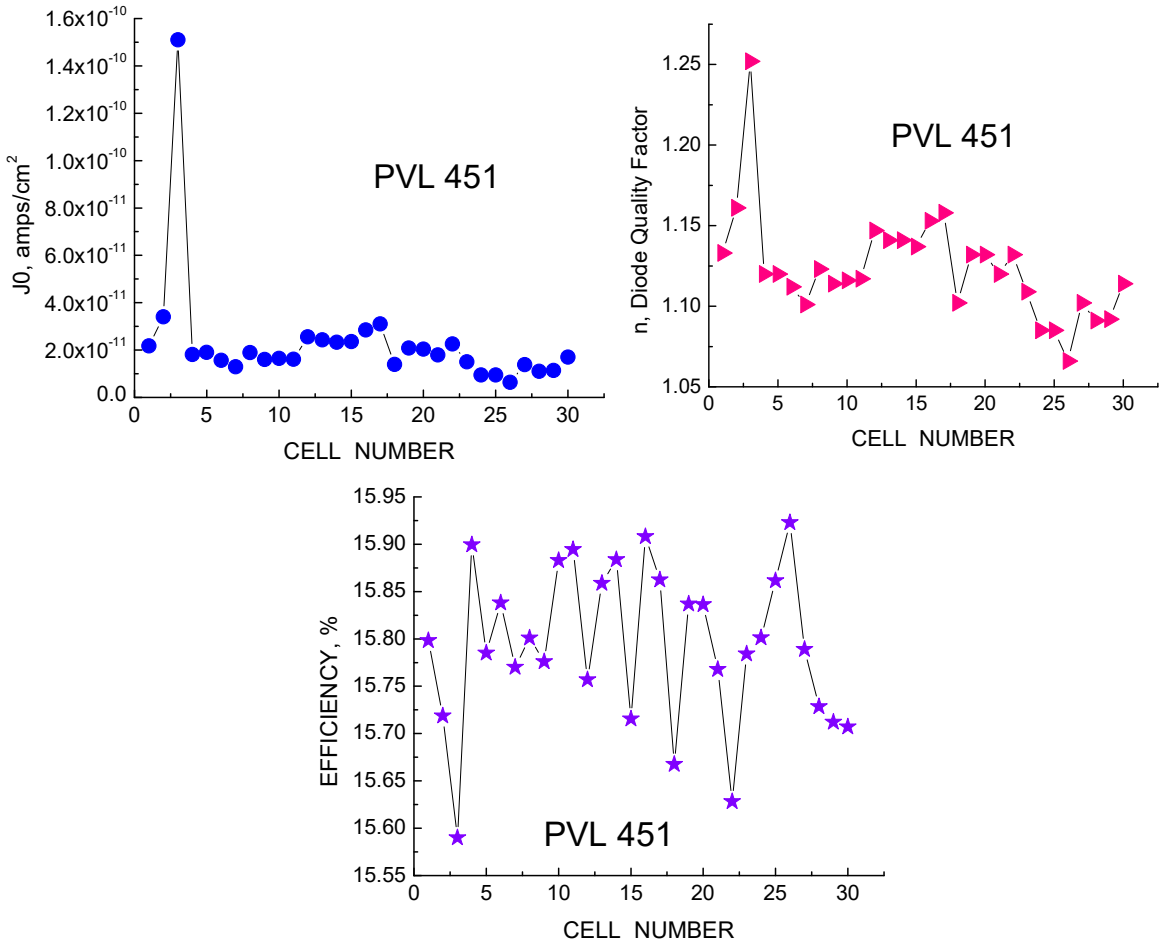

Figure 78. Forensic parameters for multicrystalline lot Linuo PVL 451.

Figure 78 shows the forensic device parameters for this turn-key lot. The device with high J0, high n, and lower efficiency stands out, exhibiting how these parameters are often closely related. There also appears to be a systematic increase in Rs as the cell number increases, as if the cells were processed in order and had a processing issue either with the emitter diffusion, grid contact, or base resistivity.

LBIC and Lifetime Maps

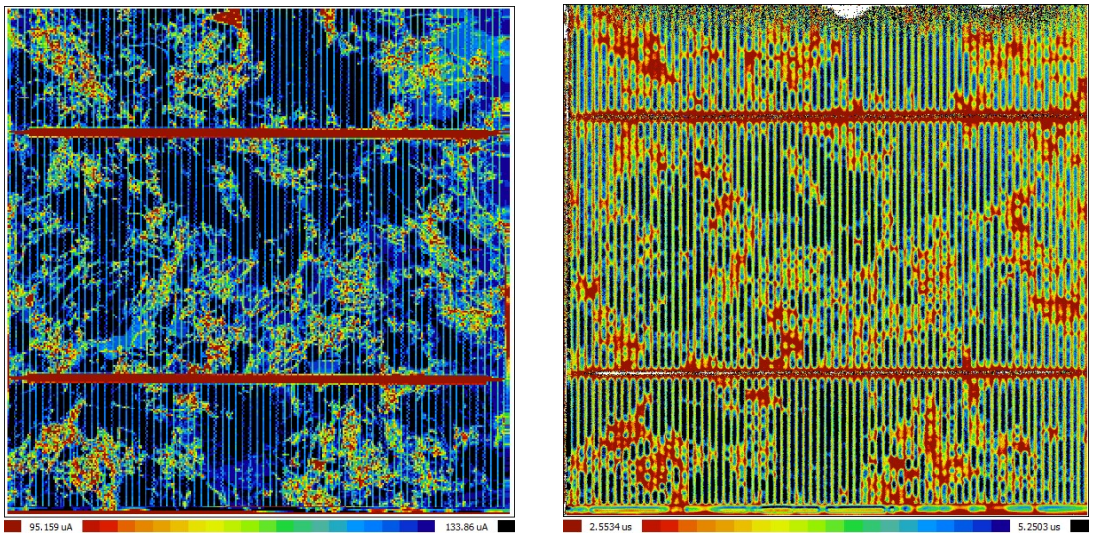

Figure 79. LBIC map at long wavelength (left) and lifetime map (right) for PVL 451 cell 25, 15.9% efficient.

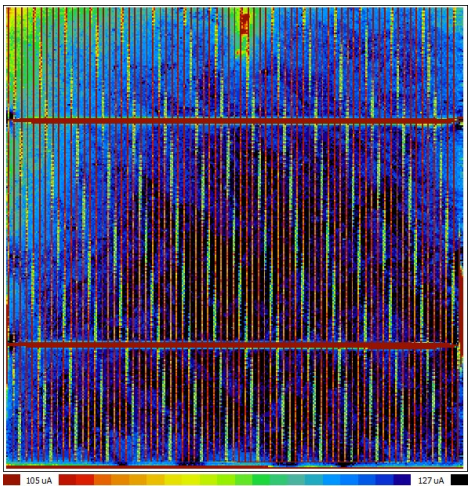

Figure 80. LBIC map for short wavelength excitation, PVL 451, cell 25.

Figures 79 and 80show the LBIC maps at long and short wavelength and the lifetime map in the finished device. The long wavelength response, indicative of collection from the base, shows the usual relation between dislocations (red areas), lifetime, and photoresponse. The short wavelength response is highly uniform, consistent with this being one of the better efficiency multicrystalline devices.

Quantum Efficiencies

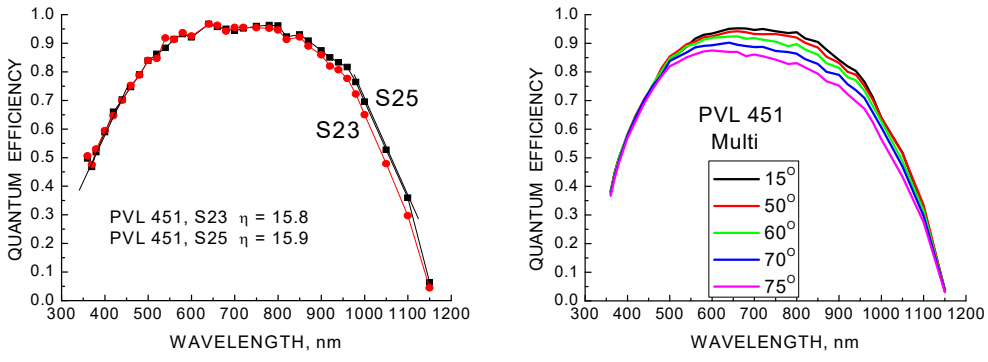

Figure 81. Spectral response for PVL451, cells 23 and 25 (left). Response versus incident angle (right) for cell #25.

Figure 81 shows the quantum efficiencies versus wavelength and the spectral response versus incident angle. The cells all received the standard acid surface texturing and Si_xN_y antireflective coating. Fig. 81 shows why the short circuit current and efficiency are low, due to poor responses at both long and short wavelengths. The gradual slope at long wavelengths is indicative of low substrate lifetime with a possible second contribution from a poor BSF. The short wavelength response is even worse, indicating poor passivation and a high loss in the emitter collection. The response as a function of incident angle shows the loss due to higher reflection at visible wavelengths but the responses merge at shorter wavelengths as usually observed for all multicrystalline material. The merging response is apparently the result of the scalloped surface texturing combined with the AR coat, an effect not seen in monocrystalline cells. Figure 84 shows the reflectance and EQE-IQE. The reflectance minimum is located at 720 nm, much higher than the 580-600 nm ideal for the solar maximum, probably because the SiNx AR coating is too thick.

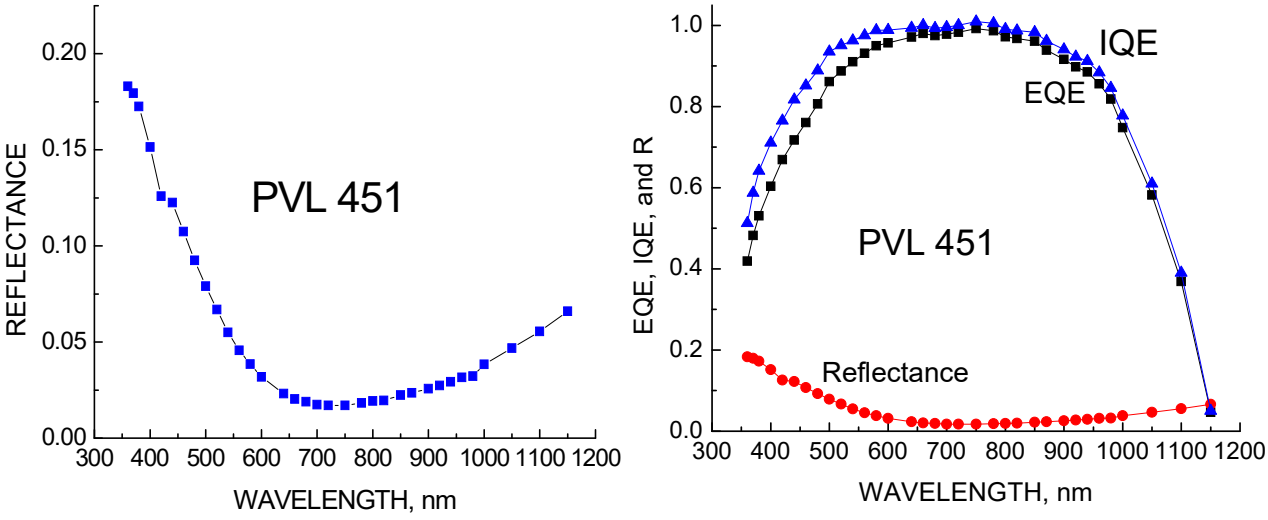

Figure 82. Reflectance (left) and IQE – EQE comparison (right) for cell #25.

7.11 PVL 161

30 6-inch Multicrystalline Cells.

Comments: Shunt resistance is very good and series resistance is low. J0 and n are good for multicrystalline cells but Voc is only moderate. The net efficiency is about 15.55%, low for today's multi cells. The averages are:

<RSH> = 708ohms, ⑨ = 501
<RS> = 0.434 ohm-cm^2, ⑨ = 0.093
<J0> = 3.7 E-11 amps/cm^2, ⑨ = 5.3 E-11
< n > = 1.130, ⑨ = .049
< Jsc> = 32.211 mA/cm^2, ⑨ = 0.153
<Voc> = 614.1 mV, ⑨ = 2.2
<FF> = 0.786, ⑨ = .007
<Effic> = 15.55 %, ⑨ = 0.13

Efficiency and Parameter Correlations:

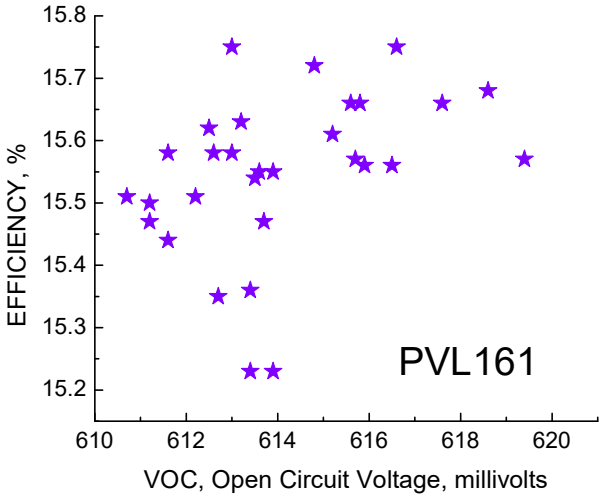

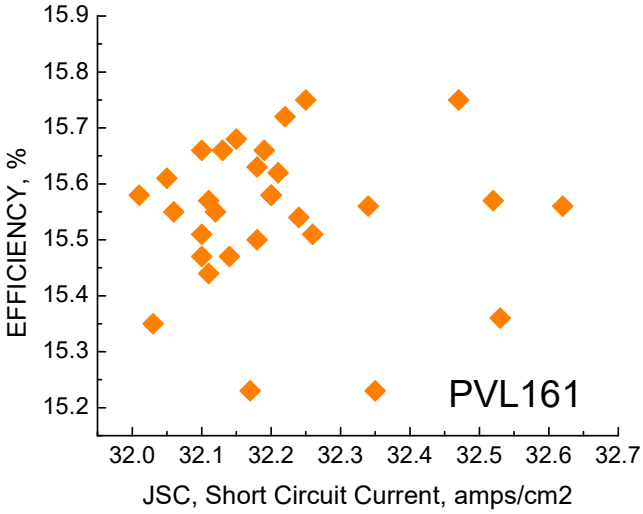

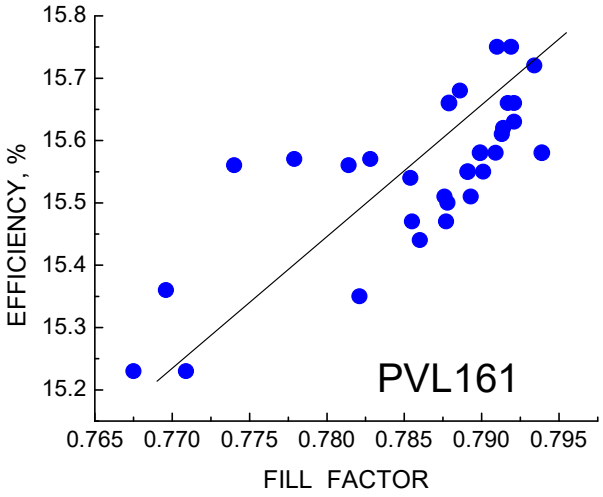

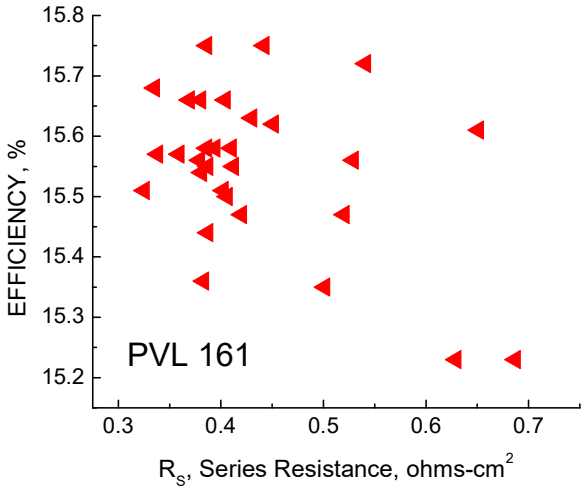

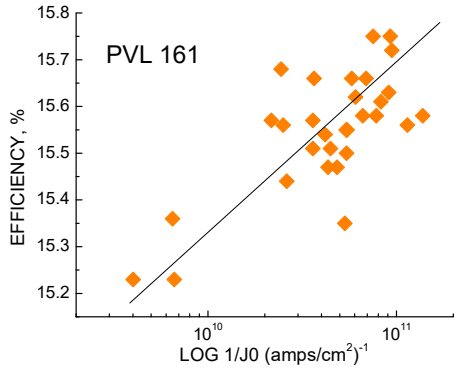

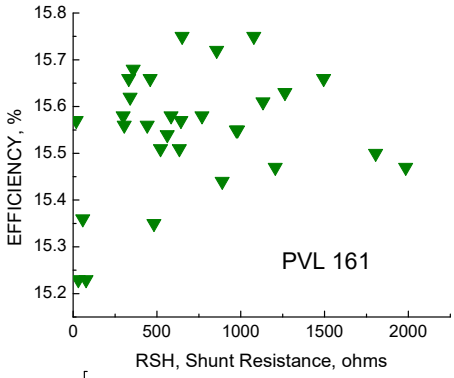

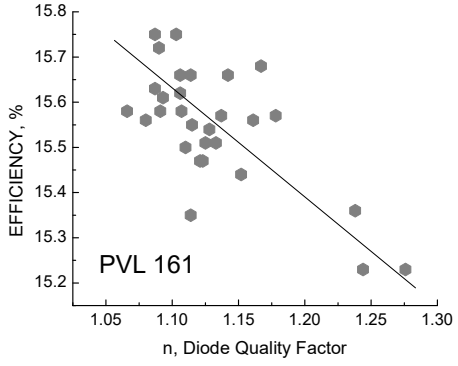

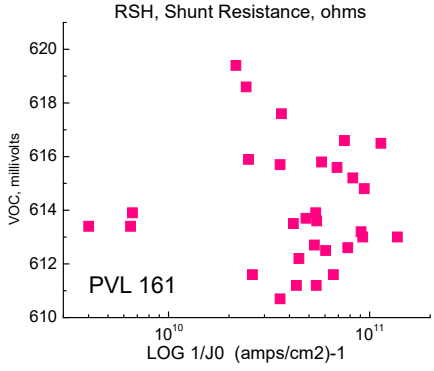

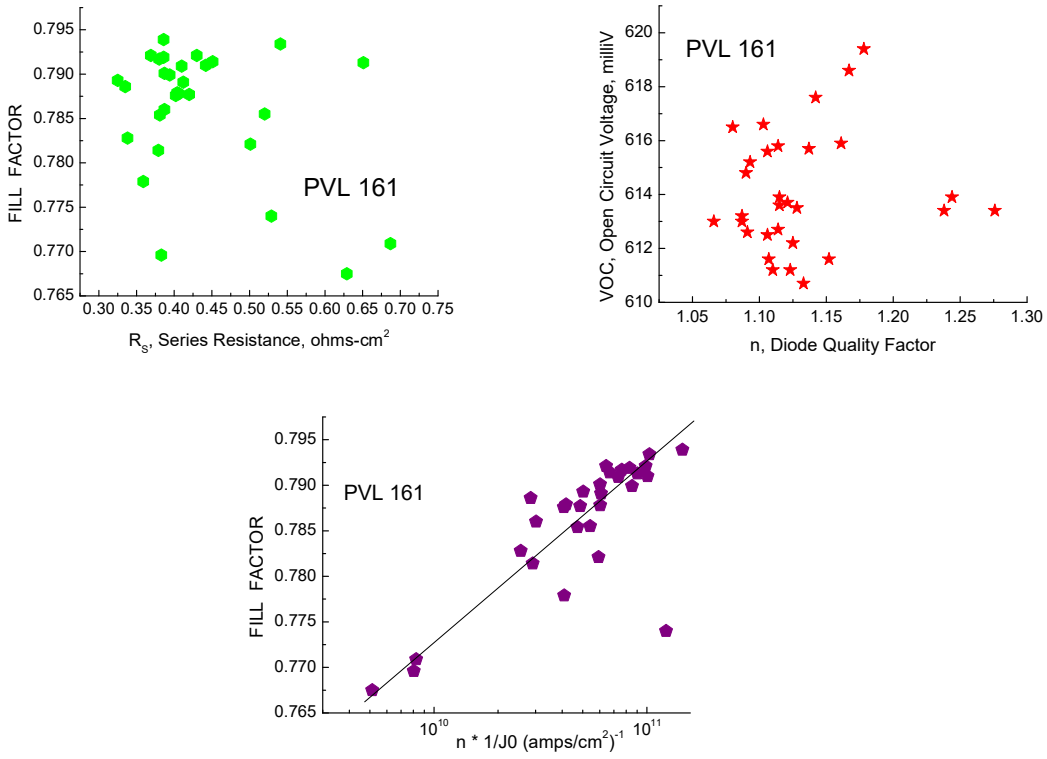

Figure 83. Correlations for PVL 161, 6-inch multicrystalline lot.

Figure 83 shows the correlations for multicrystalline lot PVL 161. The strongest correlations are between efficiency and FF, J0, and n, with only a hint of dependence on Voc or Jsc. The FF in turn is correlated with the product of diode quality factor and 1/J0, n*1/J0 in the

last chart of Figure 83. As with most other lots, there is little or no dependence on series or shunt resistance.

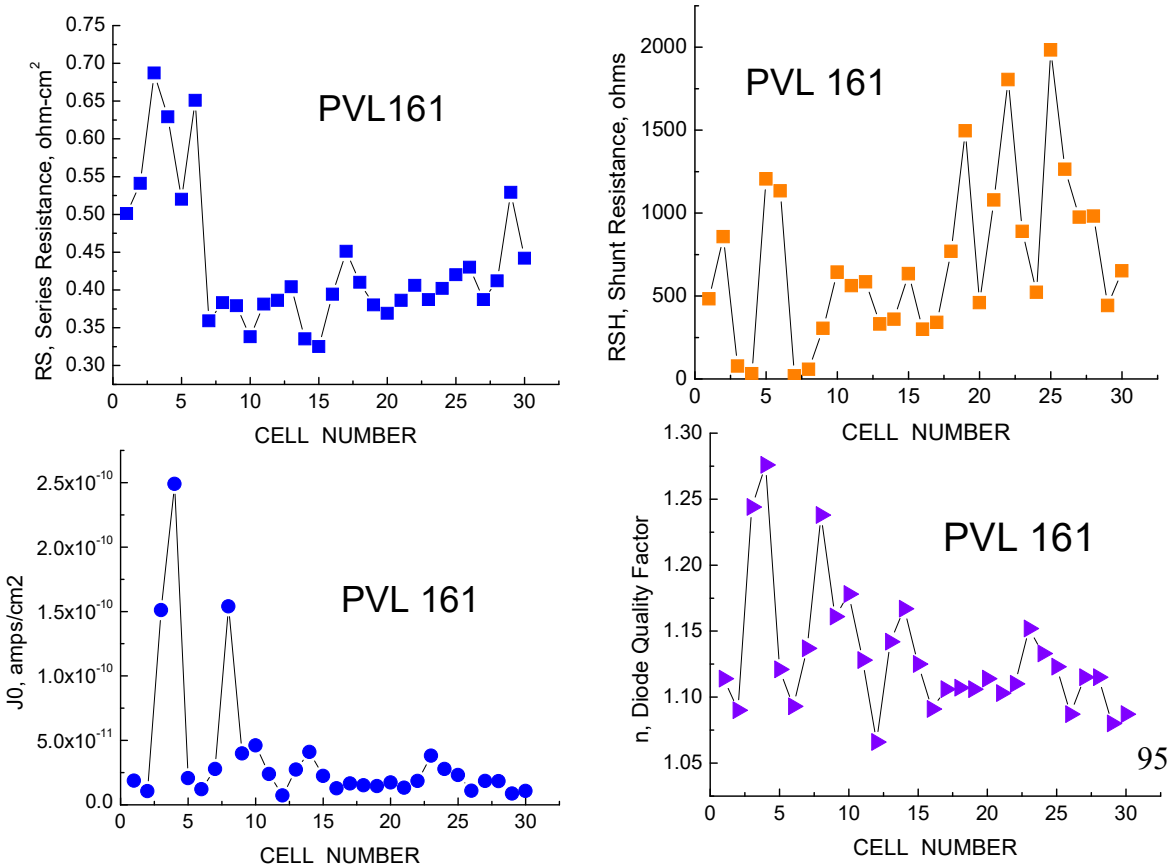

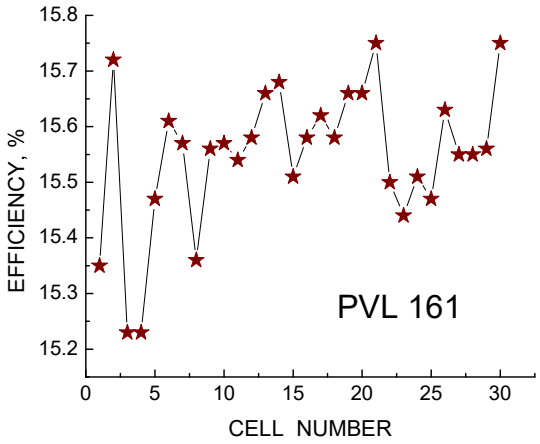

Figure 84. Forensic parameters for Linuo multicrystalline lot PVL 161.

Figure 84 shows the forensic device parameters by cell number for this lot. The series and shunt resistances show considerable variation, at least for the first few cells, as do J0 and n. The efficiencies are low for modern multicrystalline cells. The lot was not gettered and received the standard $POCL_3$ diffusion and alloyed Al back.

LBIC Maps.

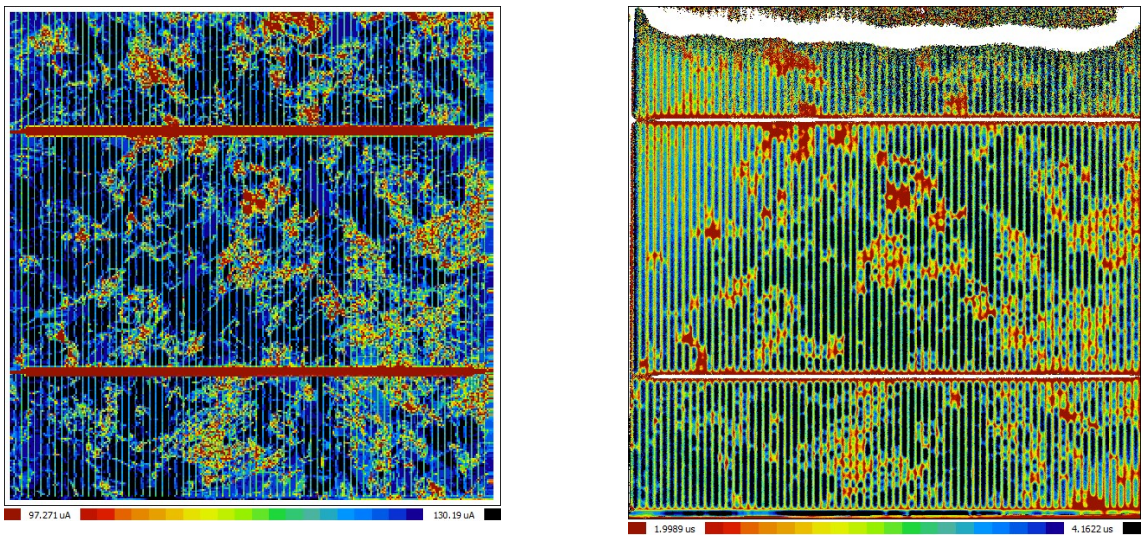

Figure 85. LBIC map at long wavelength (left) and lifetime map (right), PVL161 Box 2, cell 23.

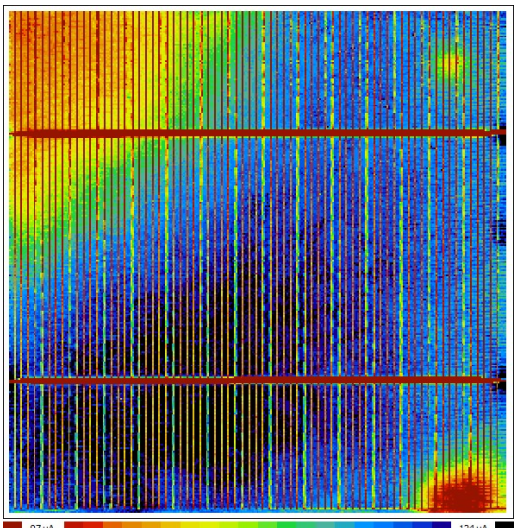

Figure 86. LBIC map at short wavelength, 15.5% efficient cell.

Figures 85 and 86 show the LBIC and lifetime maps for a typical cell from this multicrystalline lot. The correlation between high dislocation areas (red), reduced lifetime, and reduced LBIC are apparent in Figure 85. The LBIC map at short wavelengths shown in Fig. 88 indicates non-uniformities at the upper and lower corners which lower the short circuit current to a small degree.

Quantum Efficiencies

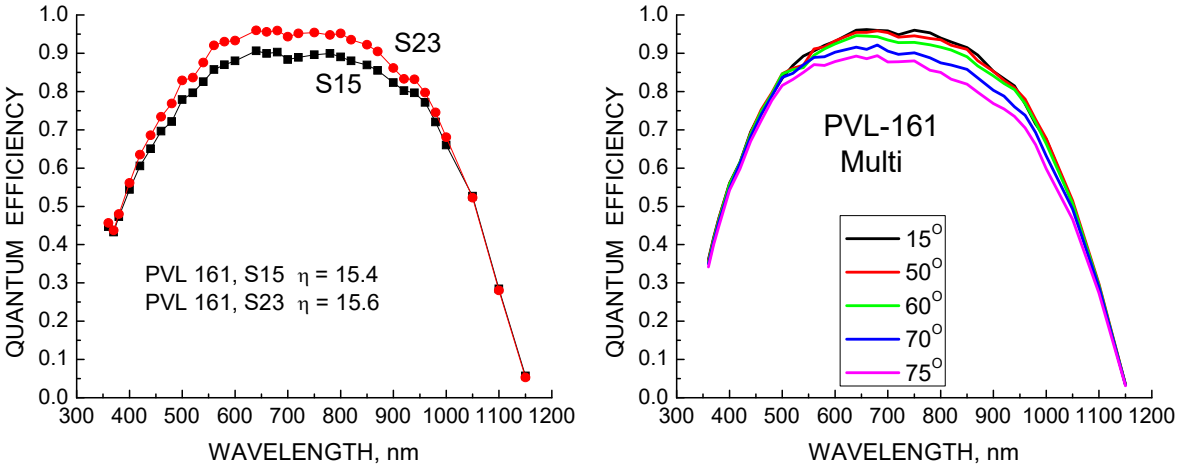

Figure 87. Spectral response (left)for 2 cells from lot PVL161 (Box 1, cells 15, 23) and spectral response versus incident angle (right) for cell S23.

Figure 87 shows the quantum efficiencies versus wavelength for two cells from PVL161 and Figure 88 shows the reflectance and IQE for cell #23. The cells all received the standard acid surface texturing and Si_xN_y antireflective coating. The gradual slope at long wavelengths is indicative of low substrate lifetime with a possible second contribution from a poor BSF. The short wavelength response indicates poor passivation and a high loss in the emitter collection. The reflectance minimum is located around 720 nm, much higher than the solar maximum at 580-600 nm.

The response as a function of incident angle shows the loss due to higher reflection at visible wavelengths but the responses merge at shorter wavelengths as usually observed for all cells made from multicrystalline material, apparently the result of the scalloped surface texturing combined with the AR coat. This merging is not seen with mono cells.

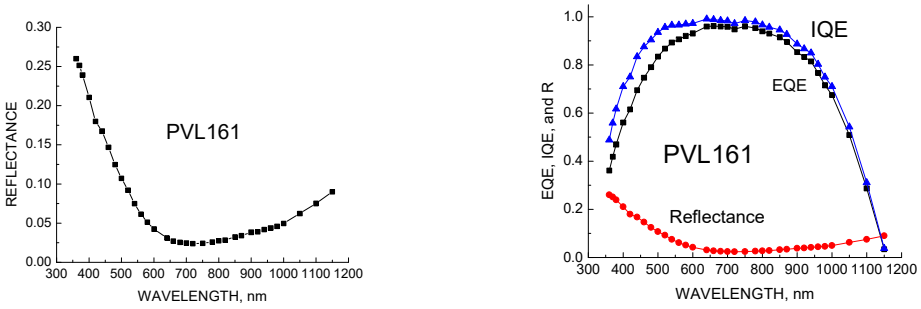

Figure 88. Reflectance (left) and IQE – EQE comparison (right) for cell #23.

7.12 Brick Casting Cells

39 6-inch Multicrystalline Cells.

Comments: Shunt Resistance is good, series Resistance is good. FF is variable and Voc covers a wide range. The correlations between efficiency and Jsc and Voc are very high. The Voc is a bit low even for multicrystalline cells. The averages are:

<RSH> = 222ohms, ⑨ = 111
<RS> = 0.598 ohm-cm^2, ⑨ = 0.090
<J0> = 6.5 E-11 amps/cm^2, ⑨ = 6.5 E-11
< n > = 1.167, ⑨ = .041
< Jsc> = 32.838 mA/cm^2, ⑨ = 0.435
<Voc> = 610.9 mV, ⑨ = 5.1
<FF> = 0.772, ⑨ = .007
<Effic> = 15.49 %, ⑨ = 0.36

Efficiency and Parameter Correlations:

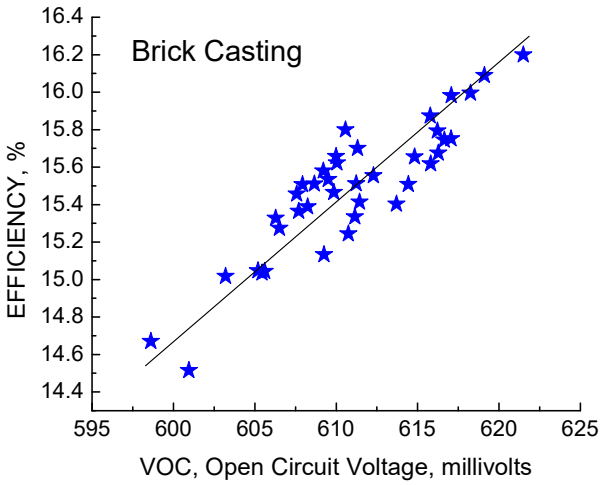

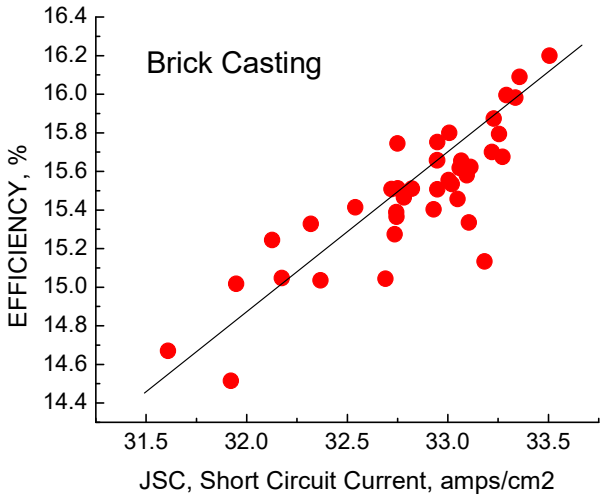

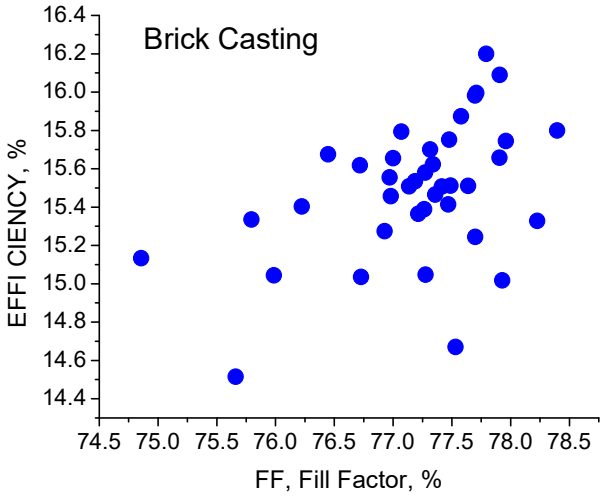

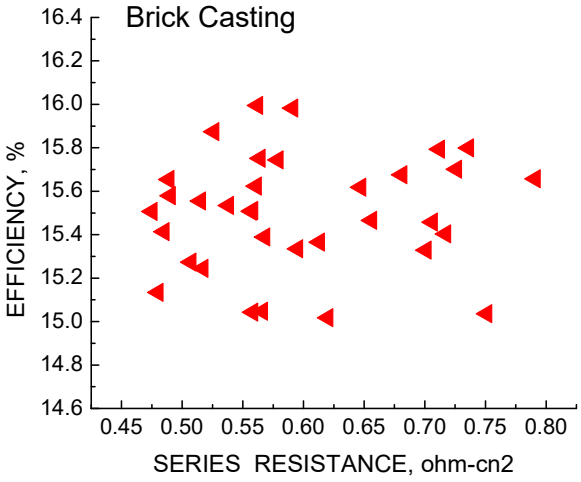

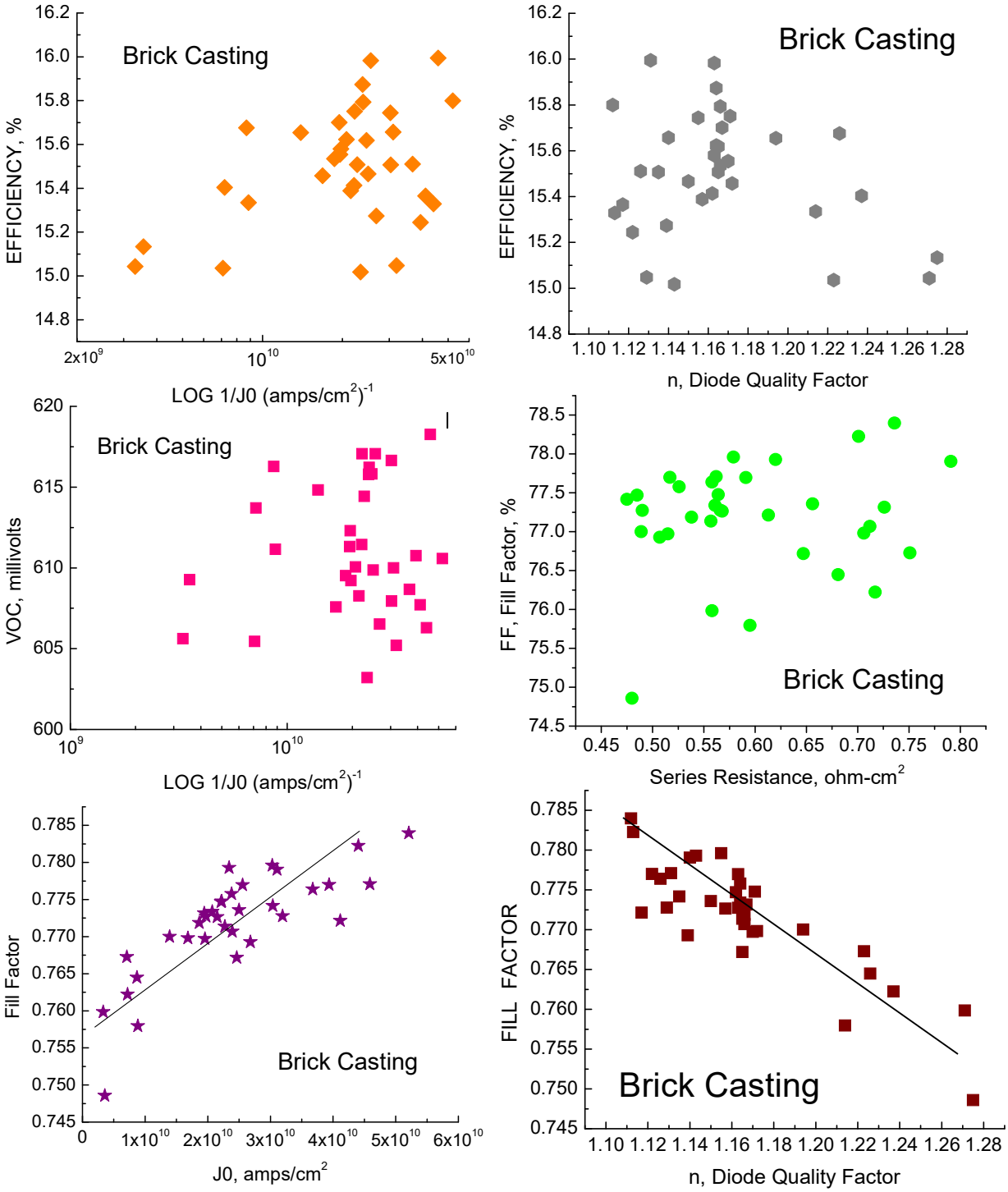

Figure 89. Correlation for multicrystalline cells from several bricks from the same casting.

The 39 cells in this lot come from several “bricks” cut from a single multicrystalline casting. The correlations between efficiency and both Voc and Jsc are very high, as are the correlations between FF and both J0 and n. There is no relation between series resistance and either efficiency or FF, a surprising result also observed for many other cell lots.

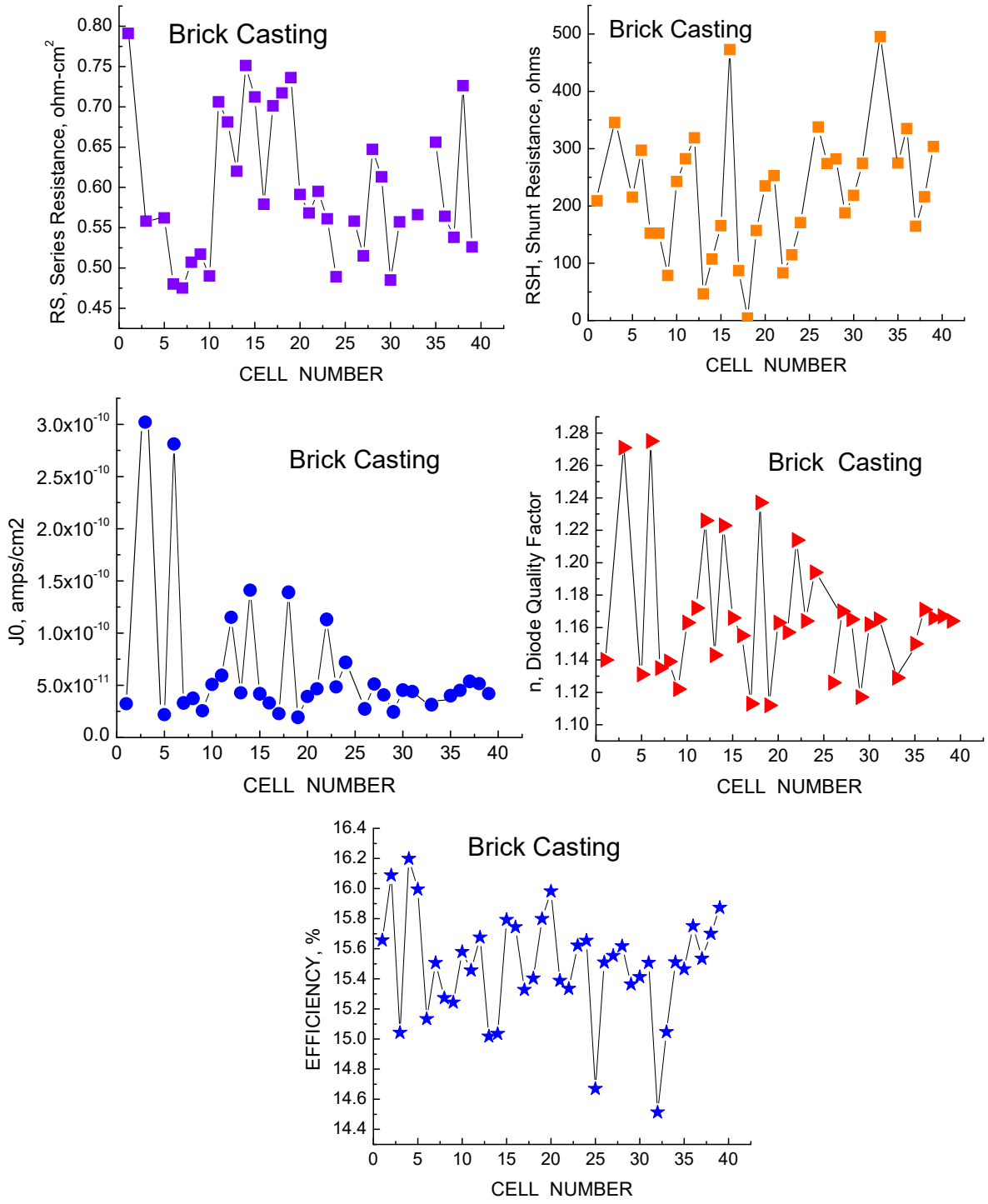

Figure 90. Forensic parameters for the bricks from the multicrystalline casting.

Figure 90 shows the various device parameters for this lot for the 39 cells. There is considerable variation, particularly in Rs , Rsh, and efficiency. This could be due to cells taken from multiple bricks from the casting. Each casting is cut into 25 bricks and wafers are sliced from each one. Bricks closer to the edges of the ceramic container tend to have more contamination than bricks from the middle.

LBIC Maps.

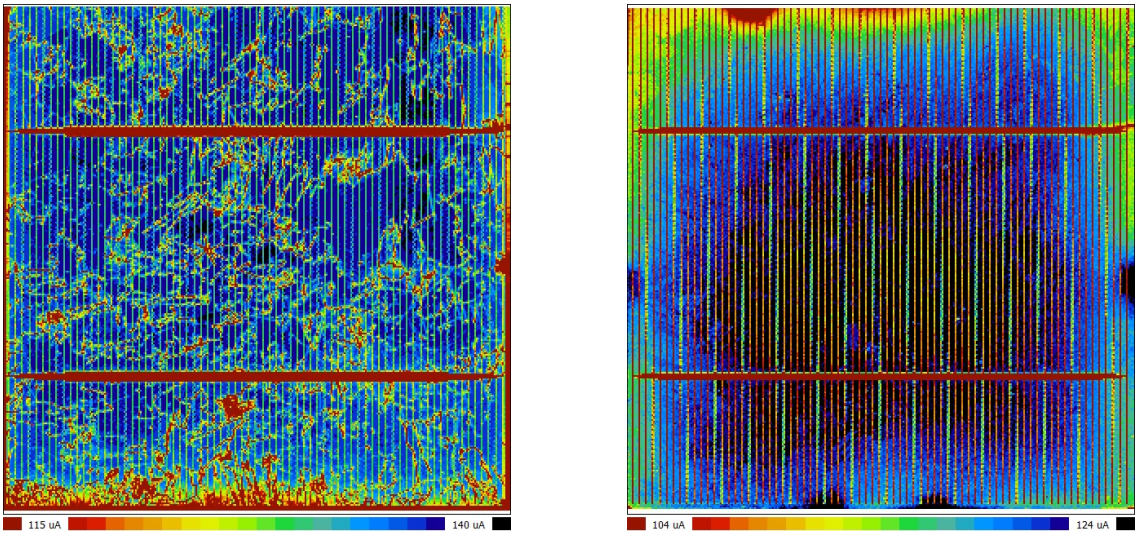

Figure 91 LBIC maps at 981 nm (left) and 404 nm (right) excitation for brick-casting cell #9, 16.0 % efficient cell.

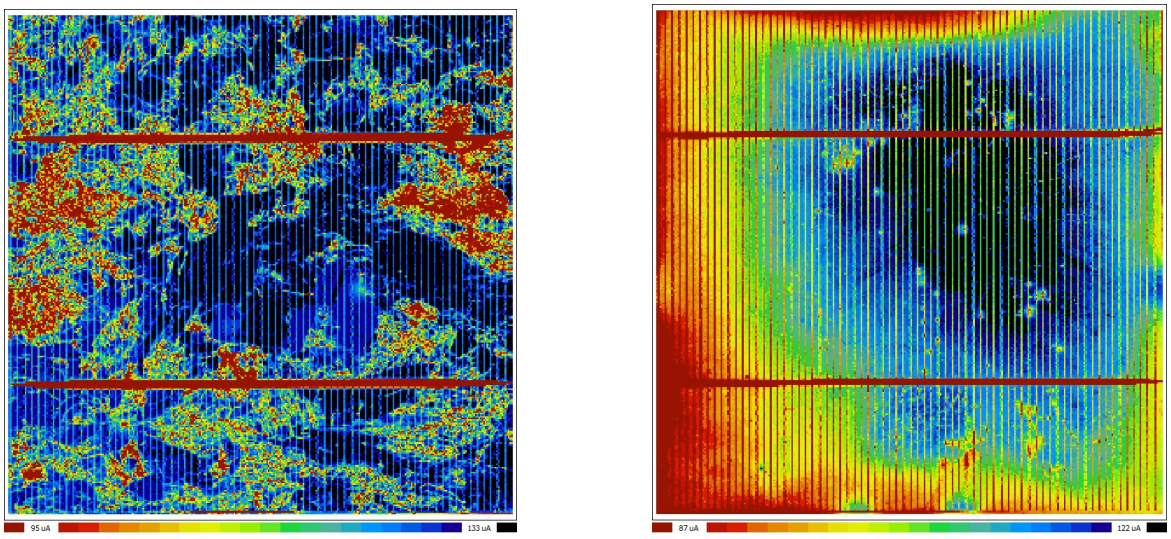

Figure 92. . LBIC maps at 981 nm (left) and 404 nm (right) excitation for brick-casting cell # B2S1, 15.0% efficient cell.

Figures 91 and 92 are a good comparison of high efficiency and low efficiency cells from the casting lot. The long wavelength map shows much higher dislocation areas for the lower efficient device, indicating lower quality starting material, while the short wavelength maps indicate much more emitter non-uniformity in the poor cell indicative of substrate quality, diffusion process problems, passivation issues, or all three.

Trap Densities in Starting Material.

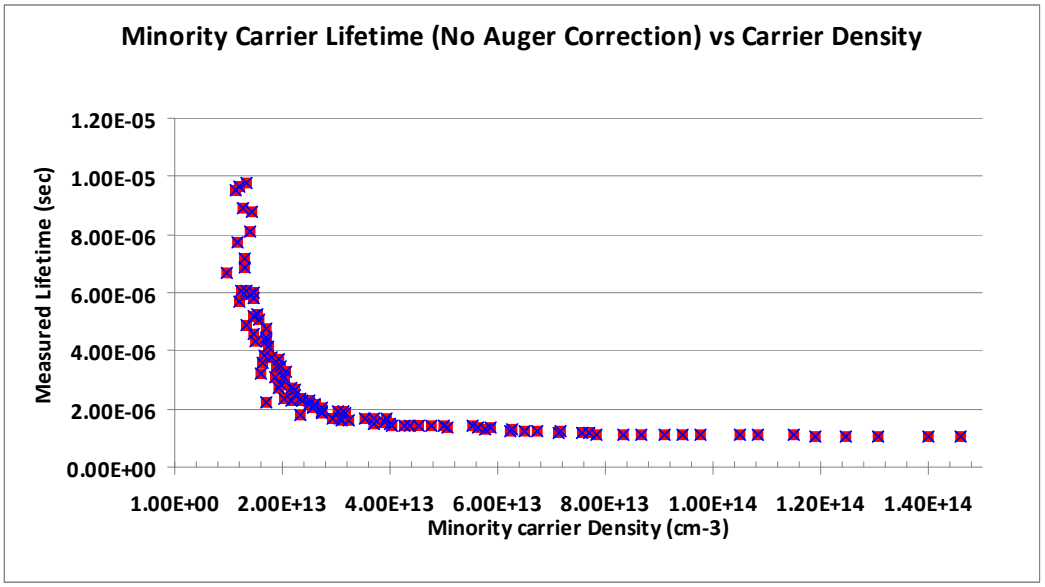

Figure 93. Lifetime versus carrier concentration for casting cell #9. The indicated trap density is $4x10^{13}$ cm^{-3}.

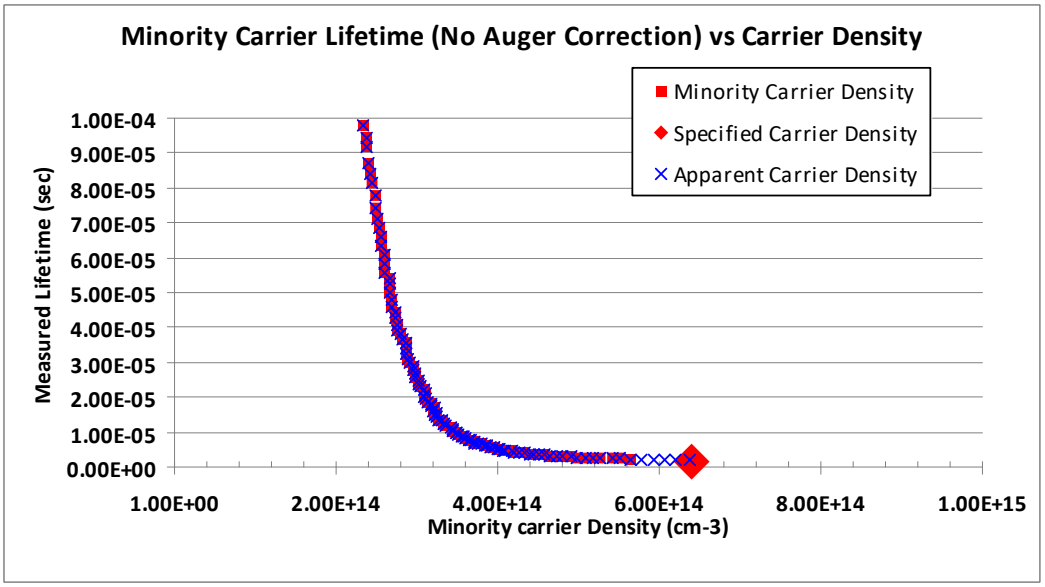

Figure 94 Lifetime versus carrier concentration for casting cell B2S1. The indicated trap density is $6x10^{14}$ cm^{-3}.

Figures 93 and 94 show the Sinton lifetime measurements which are also used to obtain the wafer resistivity and trap density. The 15% cell has a 10x higher trap density than the 16% device, suggesting that such measurements could be used to separate out starting material of less quality. Table 19 shows the resistivities, lifetimes, and trap densities for

24 starting wafers from six bricks of the casting ingot illustrating the fairly wide range of parameters for solar cell starting material.

Table 19. Resistivities, lifetimes, and trap densities for starting wafers from the cast ingot.

SAMPLE	Resistivity	Lifetime	Trap Density (E14)
Brick 1, A, #4	1.69	1.53	1.70
Brick 1, B, #4	1.80	1.36	1.25
Brick 1, C, #4	2.11	1.40	1.32
Brick 1, D, #4	2.12	1.38	1.36
Brick 2, A, #4	1.91	1.22	0.82
Brick 2, B, #4	2.10	1.26	0.82
Brick 2, C, #4	1.75	1.17	1.09
Brick 2, D, #4	2.08	0.98	0.60
Brick 3, A, #4	1.85	1.08	0.60
Brick 3, B, #4	2.01	1.20	0.94
Brick 3, C, #2	2.14	1.30	1.24
Brick 3, C, #4	1.65	1.57	3.79
Brick 3, D, #4	1.63	1.48	2.20
Brick 4, A, #4	1.6	1.28	2.53
Brick 4, B, #4	1.6	0.99	0.48
Brick 4, C, #4	1.9	1.09	0.71
Brick 4, D, #4	2.2	1.02	0.70
Brick 5, A, #4	1.50	1.53	2.82
Brick 5, B, #4	1.60	1.74	1.86
Brick 5, C, #4	1.90	1.22	1.12
Brick 5, D, #4	2.02	1.33	1.32
Brick 6, A, #4	1.8	1.11	1.03
Brick 6, B, #4	2.10	1.14	1.06
Brick 6, C, #4	1.61	1.44	2.16
Brick 6, D, #4	1.98	1.11	0.83

Quantum Efficiency

The spectral responses of a typical cell from this brick / casting lot are shown in Figures 95 and 96. These cells had mediocre efficiency, not bad and not good. The IQE curve suggests that the lifetime is poor, 1-2 microseconds, but the main problem is the short wave response, implying poor passivation, even after accounting for the high reflectance. The QE as a function of incidence angle shows the response merging at both long and short wavelengths and varying as expected in the visible region, typical of multicrystalline cells.

The reflectance minimum is located at 700 nm, significantly higher than the 580-600 nm solar maximum, probably because the SiN_x AR coating is too thick.

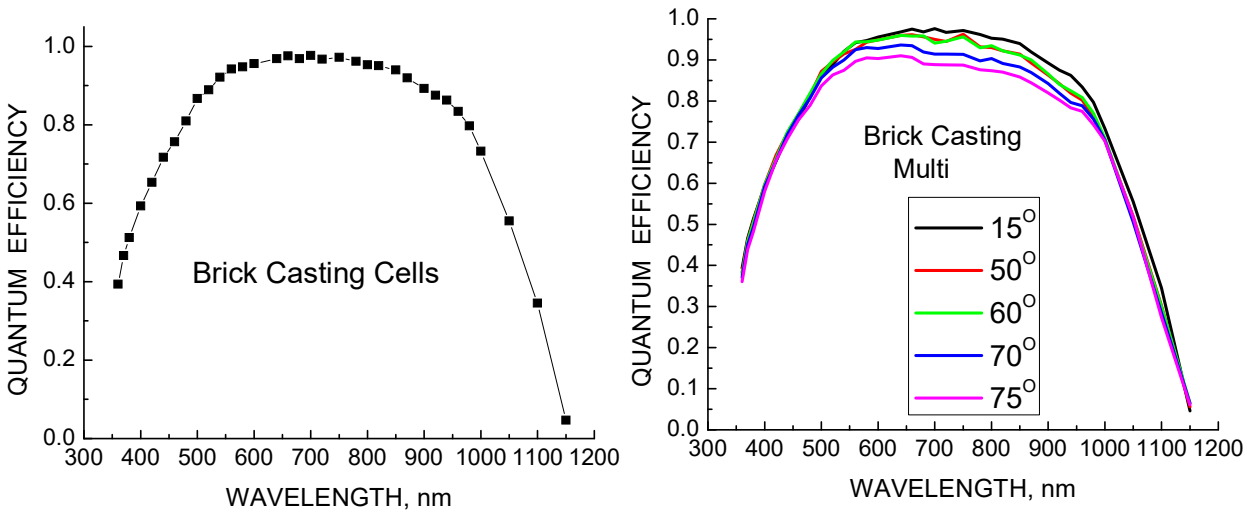

Figure 95 Spectral responses of brick-casting multicrystalline cells; normal incidence (left), versus angle of incidence (right).

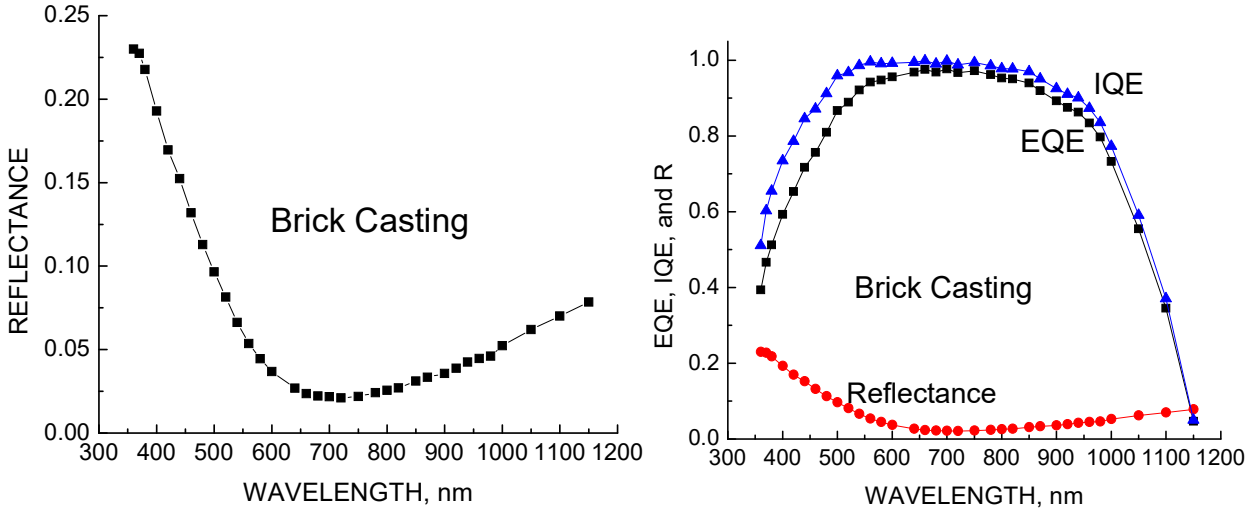

Figure 96. Reflectance (left) and EQE – IQE comparison (right) for cell S9.

7.13 Linuo NNML

15 6-inch Multicrystalline Cells.

Comments: Shunt resistance is relatively good and series resistance is moderate. J0 and n are good for multicrystalline cells but Voc is lower than other multi lots. The net efficiency is slightly above 15%, low for modern multi cells. Several cells were included in this turn-key process run that had either very poor lifetime or wafer resistivities out of spec. These are excluded from the average data. The averages are:

<RSH> = 146 ohms, ⑨ = 57
<RS> = 0.619 ohm-cm^2, ⑨ = 0.022
<J0> = 4.1 E-11 amps/cm^2, ⑨ = 2.1 E-11
< n > = 1.153, ⑨ = .028
< Jsc> = 35.59 mA/cm^2, ⑨ = 0.469
<Voc> = 613.5 mV, ⑨ = 1.1
<FF> = 0.769, ⑨ = .007
<Effic> = 15.38 %, ⑨ = 0.21

Efficiency and Parameter Correlations:

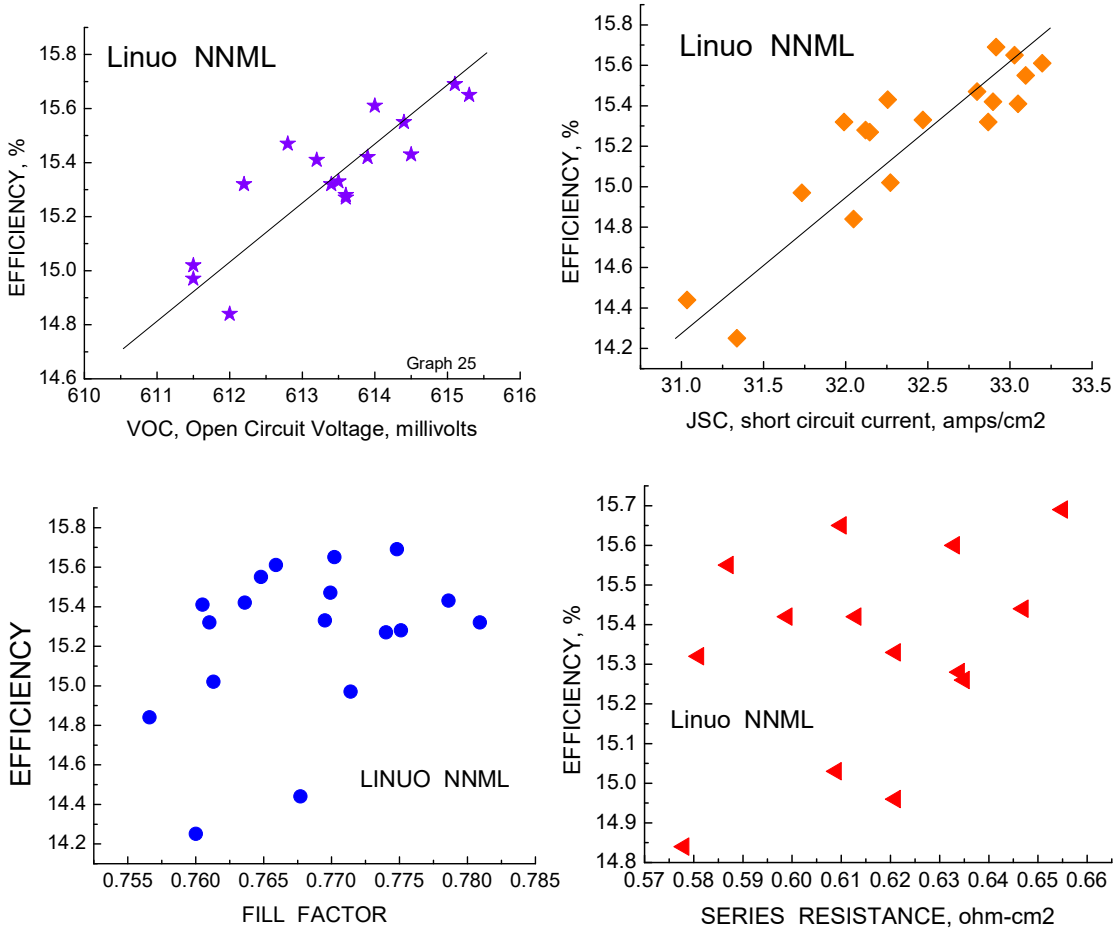

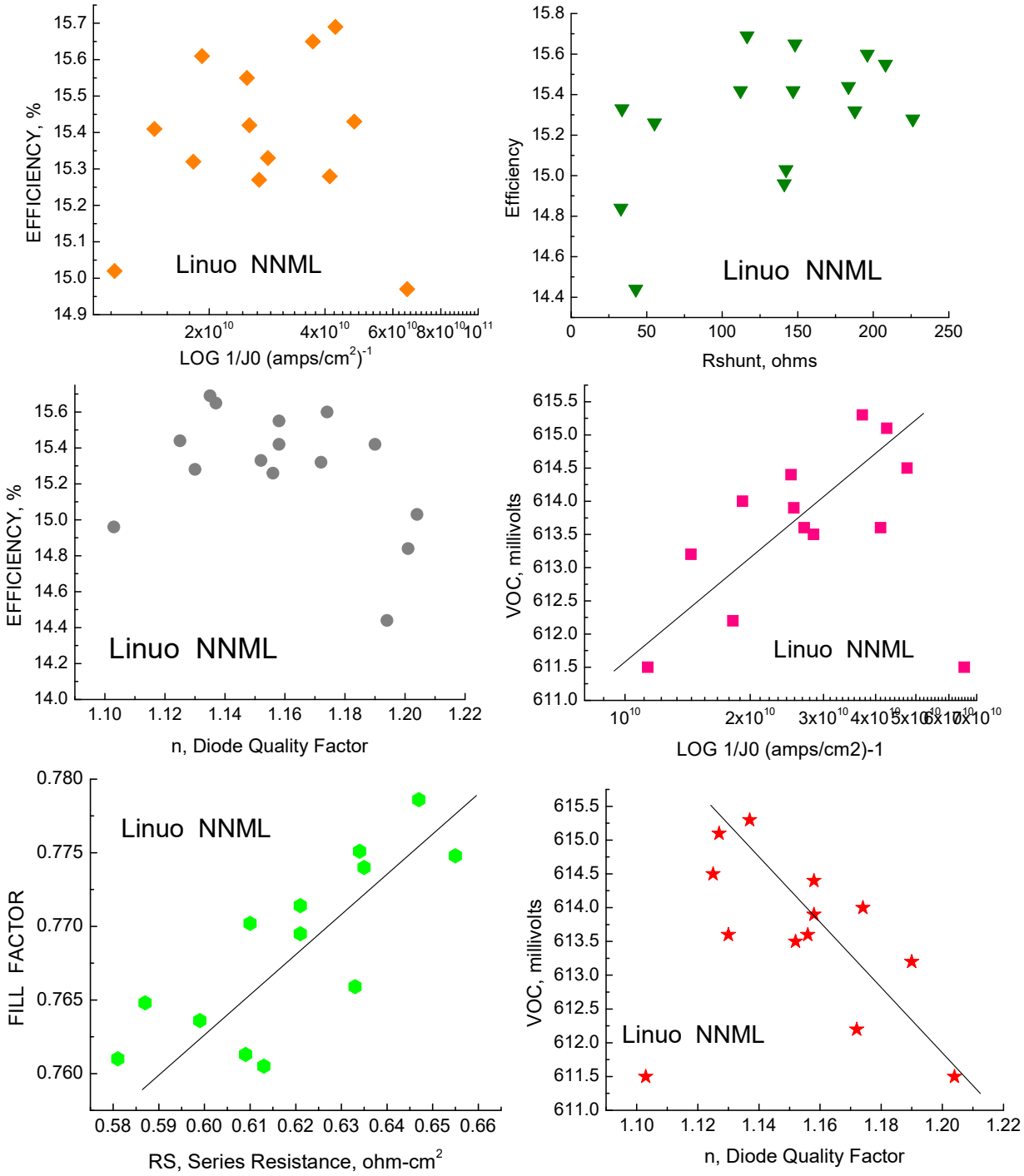

Figure 97. Correlations for Linuo multicrystalline cells from NNML.

Figure 97 shows the correlations between various parameters for this Linuo multicrystalline lot. There are strong correlations between efficiency and Jsc and Voc, but not FF or Rs. There are weaker correlations between Voc and 1/J0 and n, and between FF and series resistance. The Voc's are somewhat low, surprising since but both 1/J0 and n are relatively good.

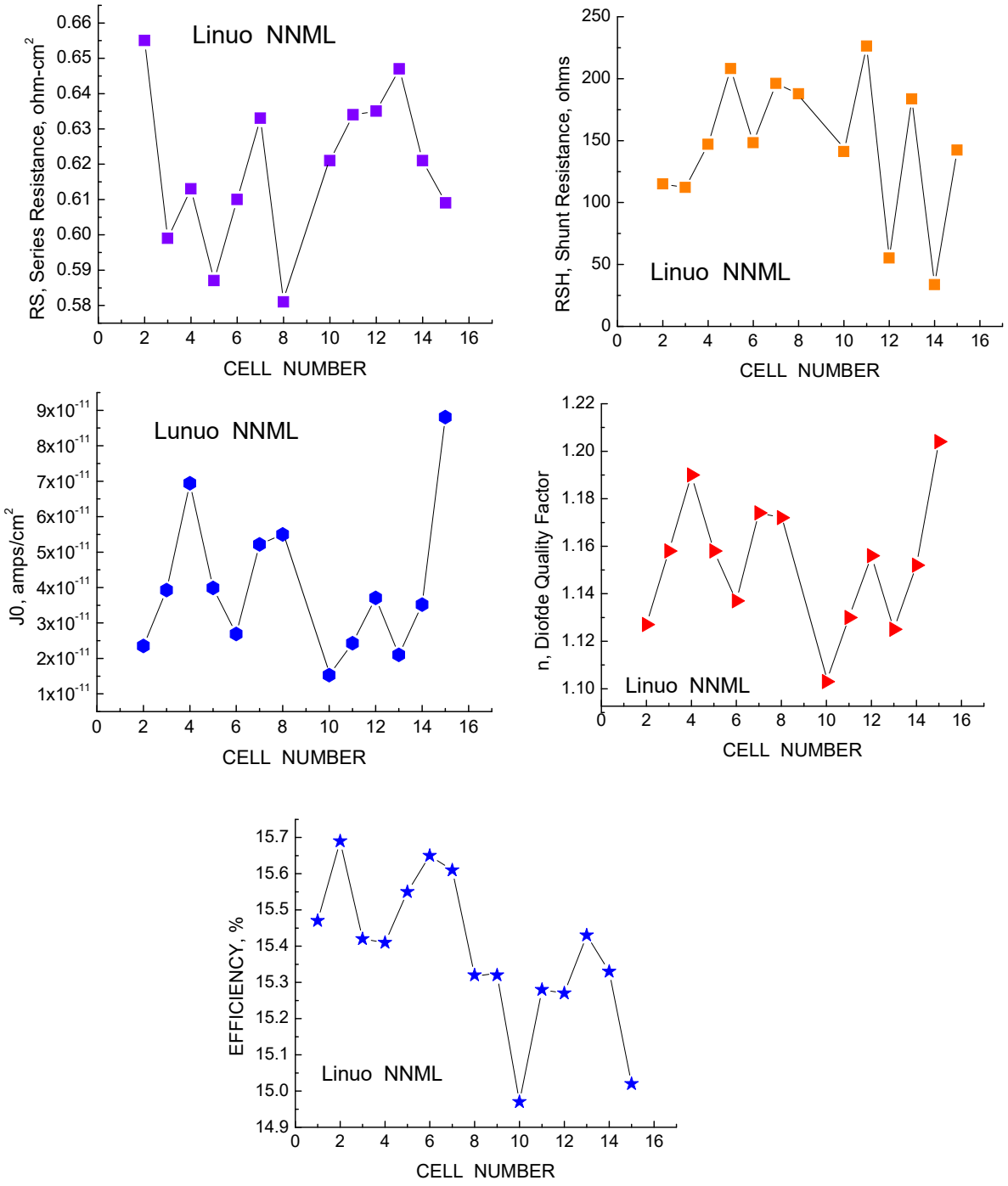

Figure 98. Forensic parameters for Linuo multicrystalline lot NNML.

Figure 98 shows the key device parameters for this Linuo multicrystalline lot. All forensic parameters are relatively good but the efficiency is on the low end of multcrystalline lots in general. Low Jsc contributes to below average performance, but both FF and Voc are a bit low as well.

LBIC Maps.

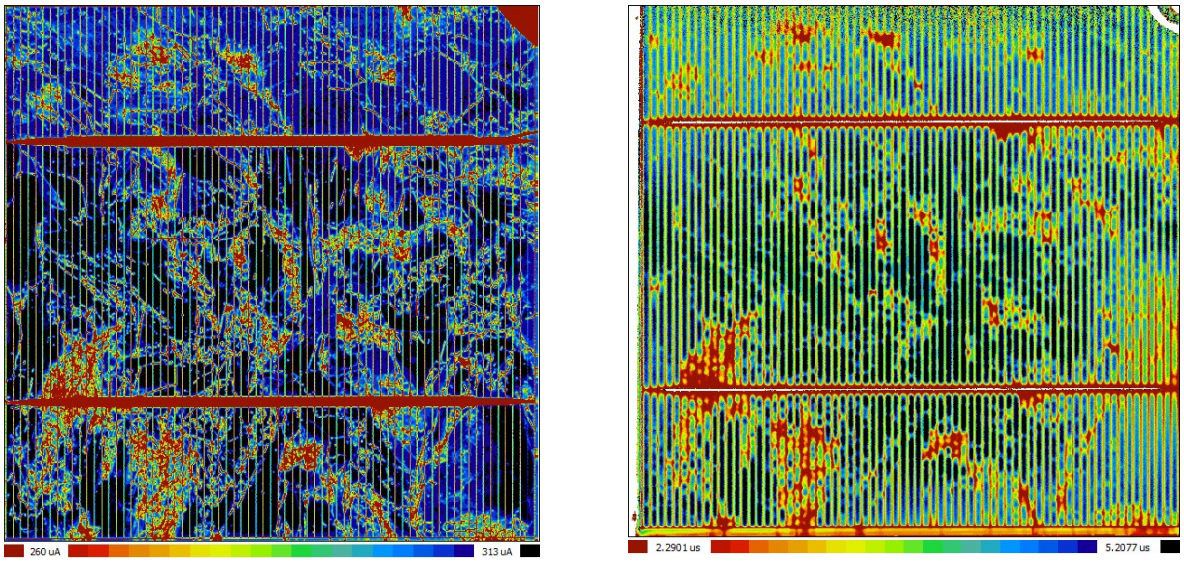

Figure 99. LBIC map at 950 nm (left) and lifetime map (right) of NNML #3, 15.7 % efficiency.

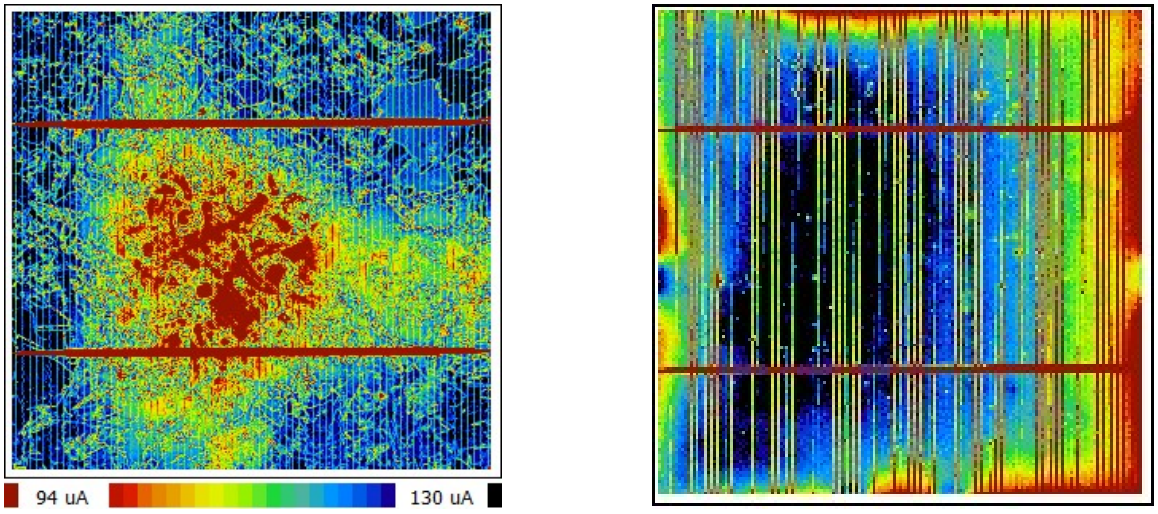

Figure 100. LBIC map at 981 nm (left) and 404 nm (right) for NNML cell #15, 14.4%.

Figure 99 shows an LBIC map at long wavelength and a lifetime map for one of the best cells, illustrating the close correspondence between high dislocation areas (red) and lower lifetime. Figure 100 illustrates a severe dislocation problem in the base of a worse cell resulting in poor photocollection (LBIC map, left) and an additional process problem resulting in poor photocurrent around the emitter perimeter (right), though poor substrate quality could be the cause of both problems.

Starting Wafer Lifetime Measurements.

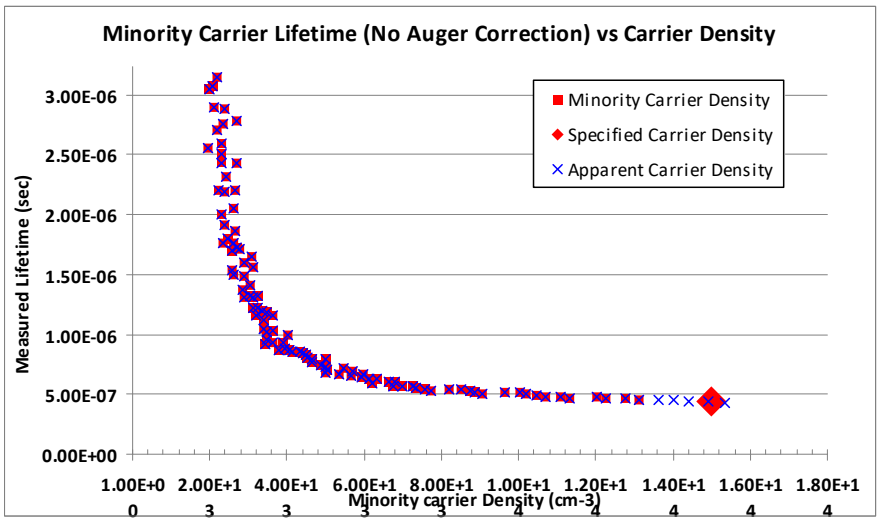

Figure 101. Sinton lifetime plot for a poor efficiency device NNML2-17 (14.3%). Trap density $7x10^{13}$ cm^{-3}; lifetime 0.44 microseconds.

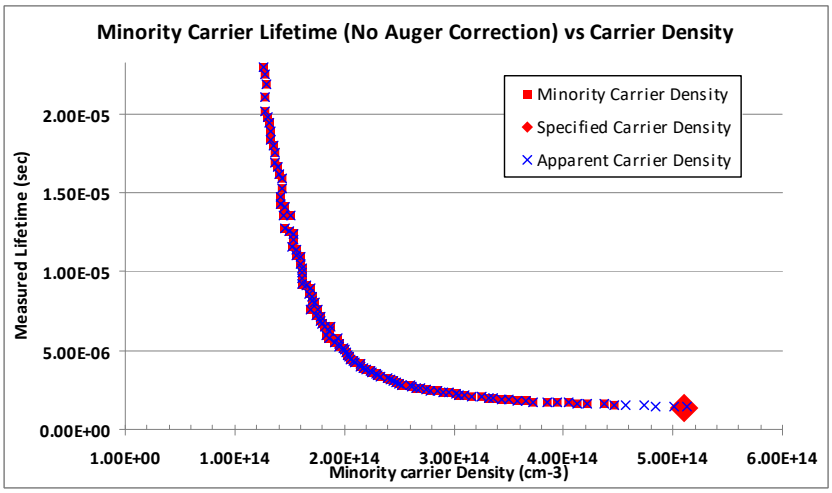

Figure 102 Sinton lifetime plot for a higher efficiency device NNML2-3 (15.7%). Trap density $3.8x10^{14}$ cm^{-3}; lifetime 1.43 microseconds.

Figures 101 and 102 show lifetime measurements as a function of photocarrier density, and Table 20 lists data for the entire NNML turnkey lot. What is apparent is that there is no relationship of starting wafer trap density and eventual efficiency and only a weak relation between lifetime and efficiency in the poorest lifetime samples. It is likely that the high doping density (>10^{16} cm^{-3}) simply masks the effects of traps which have 100x lower concentration. At the same time, the lifetime in these raw wafers (measured after saw damage etch but no other passivation) is not indicative of the lifetime in processed and passivated wafers, and the lifetimes measured in the raw wafers are likely governed by surface recombination, masking the bulk lifetime. In support of this hypothesis, the lifetime measured by Semilab Photoconductivity Decay *in finished cells* is generally 4-5x higher than the raw wafer measurements. The implication is that specifications can be set for raw wafers

(after saw damage etch) below which starting wafers are rejected but for measured lifetimes higher than the specification, there is no significant correlation between lifetime or trap densities and finished cell performance. Indeed, specifications for resistivity and lifetime for raw wafers are the only rejection criteria used in the solar cell industry today, other than gross physical defects such as chips or cracks.

Table 20. Correlations between starting material lifetime, trap densities and finished cell performance.

SAMPLE	Resistivity	Lifetime	Trap Density (E14)	Cell Efficiency)
NNML2-1	1.61	1.13	1.94	15.47
NNML2-3	1.66	1.25	2.36	15.69
NNML2-5	1.61	1.25	2.46	15.42
NNML2-7	1.62	1.37	2.37	15.42
NNML2-9	1.63	1.32	2.88	15.55
NNML2-11	1.59	1.32	2.66	15.65
NNML2-13	1.60	1.30	2.52	15.6
NNML2-15	1.78	0.64	0.90	15.32
NNML2-17	1.66	0.43	0.73	14.26
NONML-1	1.63	1.10	1.34	15.33
NONML-3	1.63	1.61	1.66	14.96
NONML-5	1.65	1.12	1.56	15.28
NONML-7	1.66	1.18	1.99	15.26
NONML-9	1.65	1.17	1.88	15.44
NONML-11	1.64	1.25	2.03	15.33
NONML-13	1.61	1.27	2.32	15.03
NONML-15	1.44	0.57	1.30	14.44
NONML-17	1.49	0.67	1.44	14.84

Quantum Efficiencies.

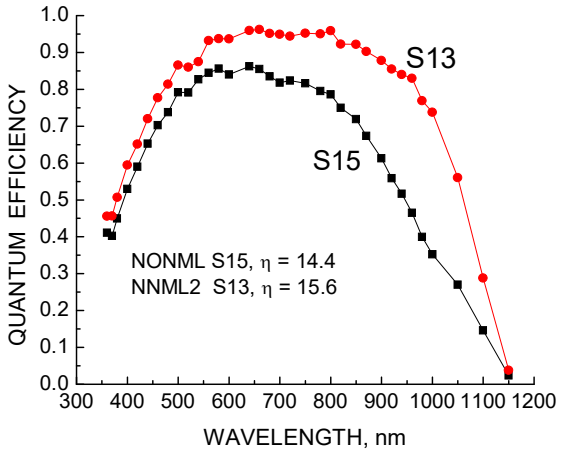

Figure 103 Spectral responses of two cells from multicrystalline lot NNML.

Figure 103 shows the spectral responses for two cells from this lot. S13 is typical of 15.5-15.6% efficient cells from this lot with a Jsc of 33.2 milliA/cm^2, while cell S15 is 14.4% efficient due to a 31.0 mA/cm2 photocurrent and a 7 millivolt lower Voc. The quantum efficiency comparison shows that S15 has a much lower lifetime in the base, about ¼ that of cell 13, while both have similar passivations (short wave response). The LBIC map in Figure 100 showed that the poor cell has a large area in the middle of the base with very poor collection and very likely a high density of defects as well. The wafer quality is so poor that even the short wavelength LBIC shows evidence of significant non-uniformity. This lot therefore gives strong evidence of the importance of starting wafer quality, which can be determined by photoluminescence in several forms (defect band, band to band, lifetime map).

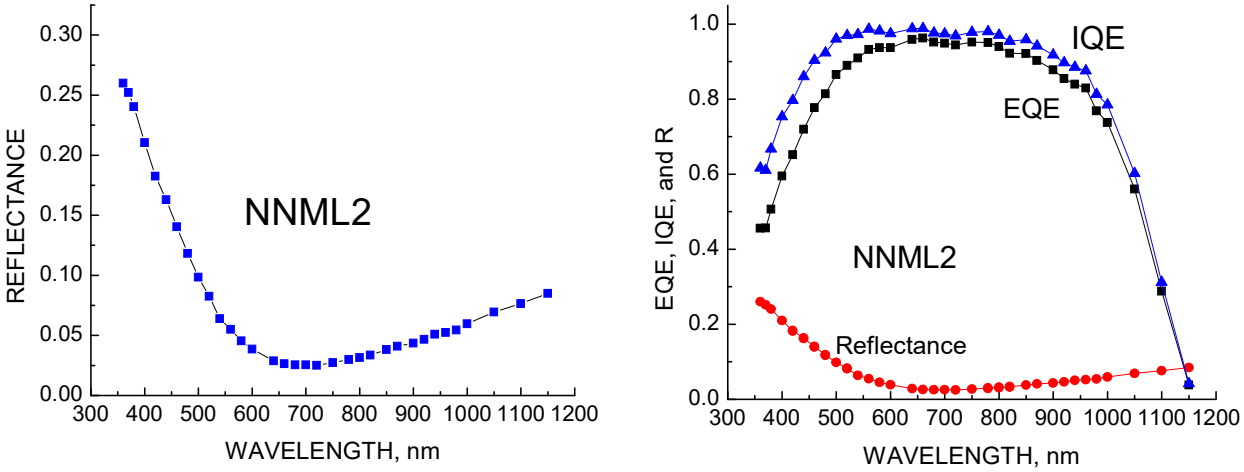

Figure 104. Reflectance (left) and IQE-EQE comparison (right) for cell #13.

Figure 104 shows the reflectance and IQE of cell #13 as well as the EQE. The reflectance minimum at 680 nm is too high and the Isc would be improved if the AR coating were a bit thinner. The IQE still confirms the conclusion that the starting lifetime and passivation are both less than optimum and the starting material is likely lower quality than desired.

7.14 Linuo GTML

15 6-inch Multicrystalline Cells.

Comments: Shunt resistance is relatively good and series resistance is moderate. J0 and n are good for multicrystalline cells but Voc is lower than other multi runs. The net efficiency is slightly above 15%, low for modern multi cells. These cells received raw wafer gettering before fabrication, which improved the lifetimes and the efficiency distribution but the average efficiency wasn't much affected. The averages are:

<RSH> = 237ohms, ⑨ = 100
<RS> = 0.640 ohm-cm^2, ⑨ = 0.083
<J0> = 4.0 E-11 amps/cm^2, ⑨ = 1.6 E-11
< n > = 1.153, ⑨ = .023
< Jsc> = 32.534 mA/cm^2, ⑨ = 0.263
<Voc> = 613.4 mV, ⑨ = 1.4
<FF> = 0.772, ⑨ = .004
<Effic> = 15.4 %, ⑨ = 0.15

Efficiency and Parameter Correlations:

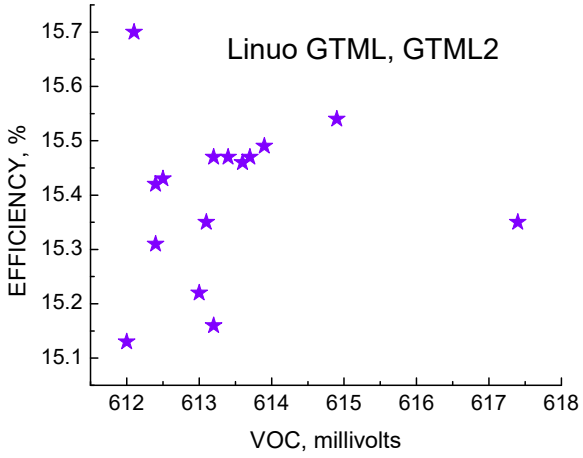

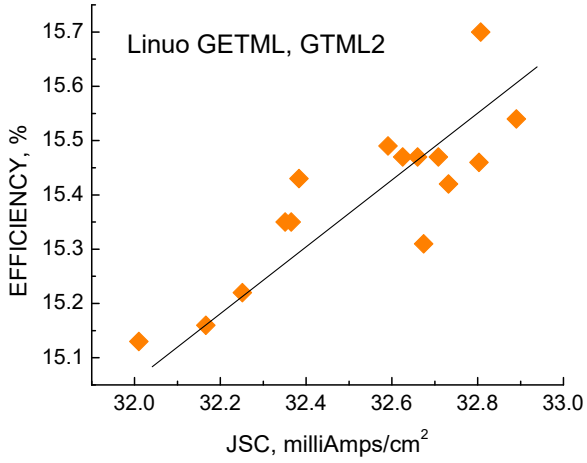

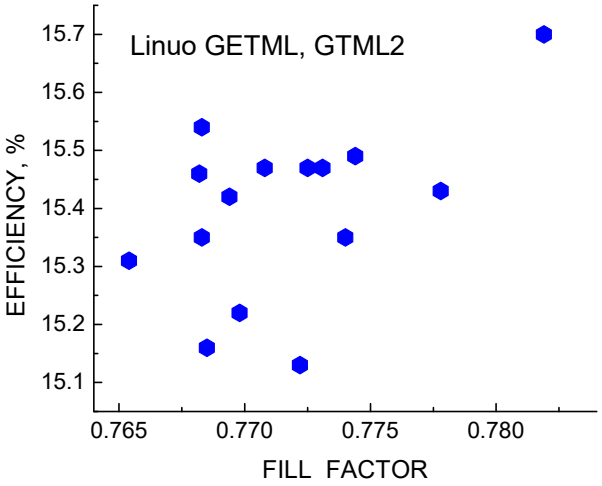

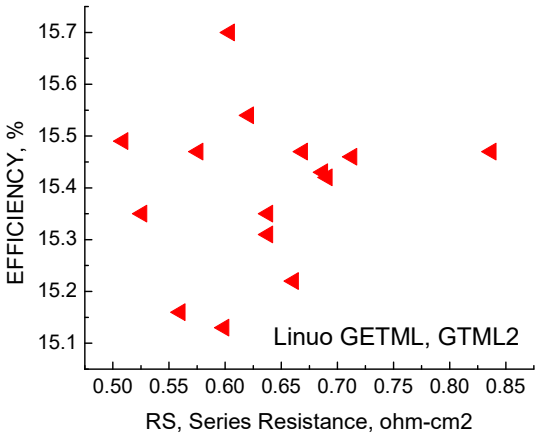

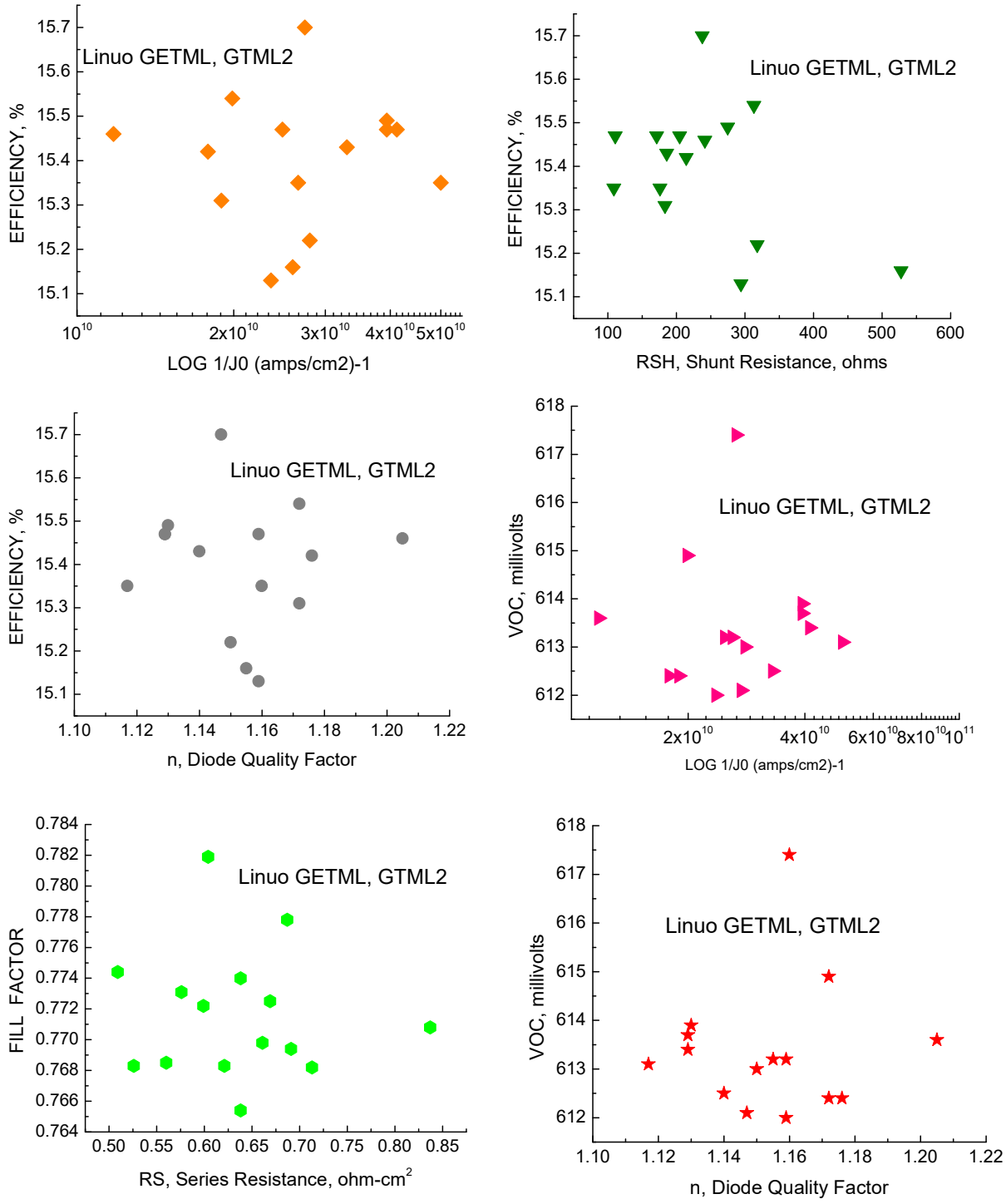

Figure 105. Correlations for Linuo gettered lot GETML, GTML2.

Figure 105 shows the correlations for this lot. The only significant relationship appears to be between efficiency and Jsc. All other parameters seem more random, with just a small hint (perhaps) between efficiency and Voc.

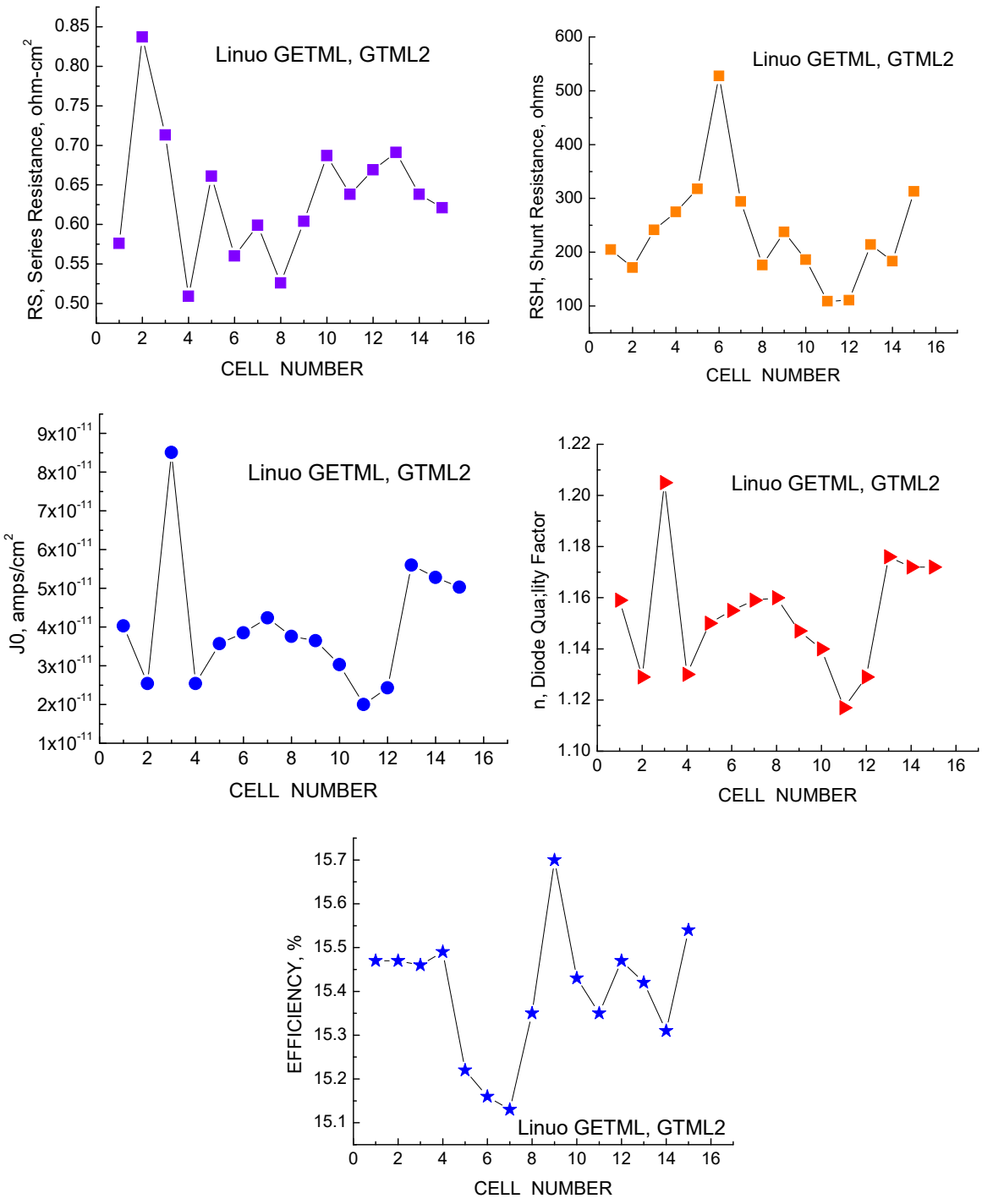

Figure 106 Forensic parameters for Linuo GETML,GTML2 gettered lot.

Figure 106 shows the forensic device parameters for this Linuo lot. The efficiency, series resistance, and shunt resistance all show significant variation.

LBIC Maps.

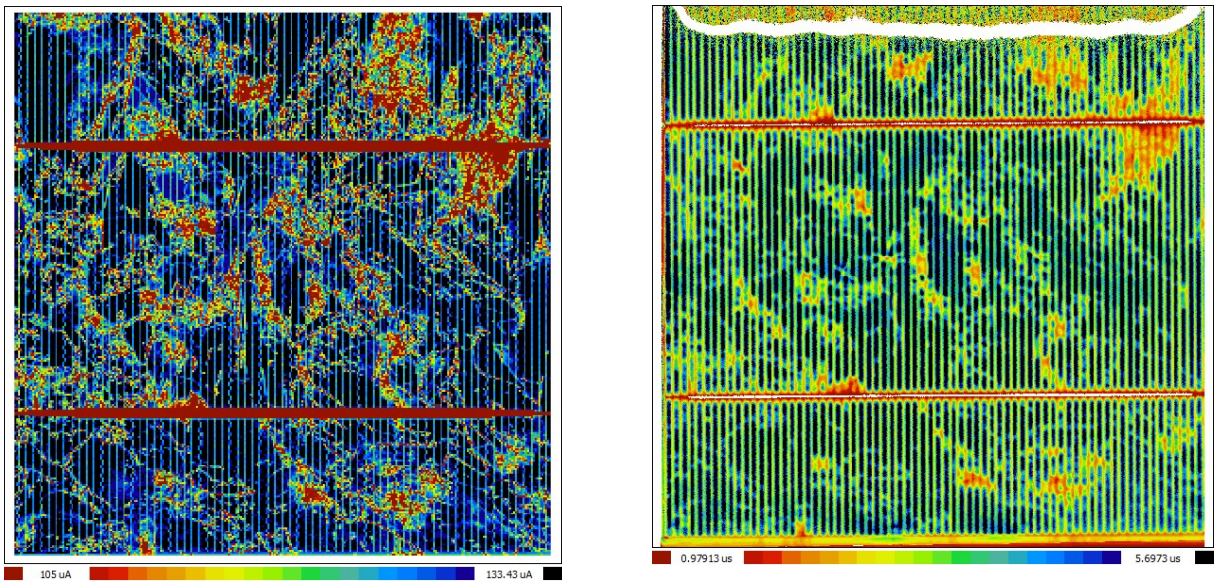

Figure 107. LBIC map at 981 nm (left) and lifetime map (right) for Linuo GTML2, #3.

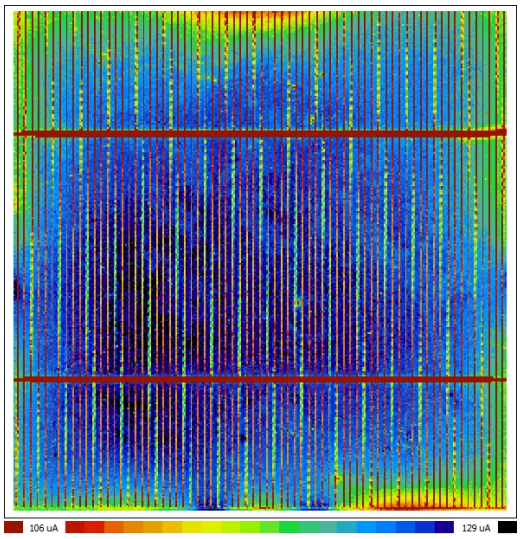

Figure 108. LBIC map for GTML2 #3 at 404 nm excitation.

Figures 107 and 108 show the LBIC maps and lifetime map for a 15.46% efficient cell from this lot. A close correspondence is observed between high dislocation areas, lower photoresponse, and lower lifetime. The emitter LBIC at short wavelength is more uniform and doesn't show edge problems. All the cells from this lot showed the same characteristics, indicating that the gettering has improved the uniformity.

Lifetime and Trap Densities.

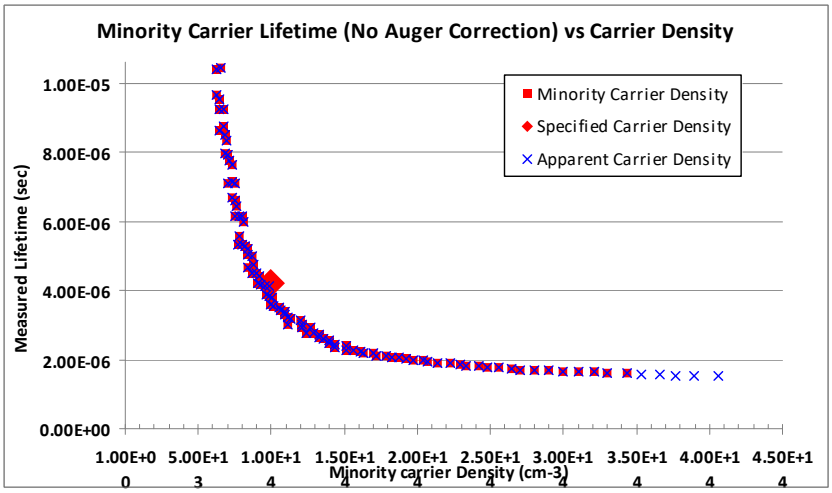

Figure 109. Lifetime versus carrier concentration for Linuo GETML #1.

Table 21. Resistivity, lifetime, trap density, and efficiency for Linuo GETML, GTML2.

SAMPLE	Resistivity	Lifetime	Trap Density (E14)	Cell Efficiency)
GETML-1	1.38	1.15	1.46	15.71
GETML-3	1.59	1.93	1.62	15.42
GETML-5	1.61	1.26	1.72	15.35
GETML-7	1.59	1.19	1.51	15.48
GETML-9	1.60	1.15	1.64	15.44
GETML-11	1.62	1.28	2.35	15.31
GETML-13	1.61	1.11	1.54	15.53
GETML-15	1.66	0.58	0.90	15.46
GTML2-1	1.62	1.20	2.0	15.47
GTML2-3	1.63	1.62	2.02	15.47
GTML2-5	1.64	1.60	1.71	15.46
GTML2-7	1.63	1.13	1.42	15.49
GTML2-9	1.64	1.19	1.56	15.22
GTML2-11	1.65	1.56	1.84	15.16
GTML2-13	1.68	1.15	1.76	15.12
GTML2-15	1.68	1.27	2.48	15.35

Figure 109 shows a lifetime vs photocarrier density plot and Table 21 shows starting wafer parameters for wafers from the Linuo GETML, GTML2 lot. These parameters are measured on the raw wafers before gettering and therefore are approximately the same as for the non-gettered lot NONML,NNML2. As before, there is no noticeable correlation between finished device properties and lifetimes or trap densities on the starting wafers,

masked by surface recombination which dominates the effective lifetime measurement and the high doping level which counteracts the trapping effects.

Quantum Efficiencies.

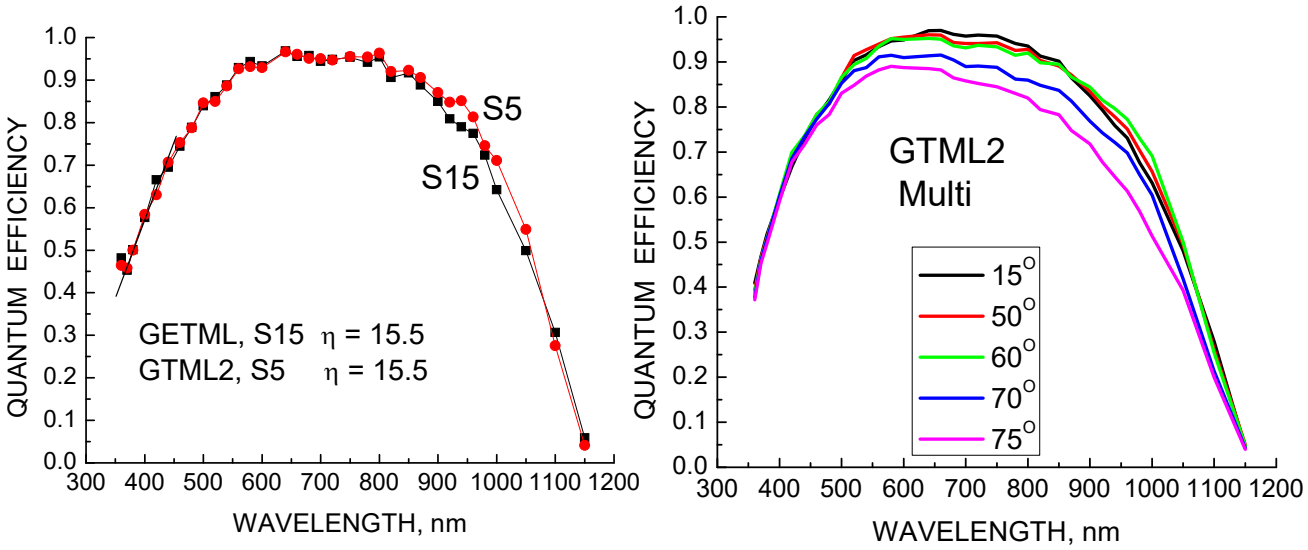

Figure 110 Spectral response at 10 degrees incidence (left) and as a function of incident angle (right).

Figures 110 and 111 show the quantum efficiencies versus wavelength for GETML and GTML2. These cells received gettering at 900^{O}C for an hour prior to processing. The cells all received the standard acid surface texturing and Si_xN_y antireflective coating. The gradual slope at long wavelengths is indicative of low substrate lifetime even though the gettering improved the lifetime by 30%. (If the diffusion length is longer than the wafer thickness even without gettering, the effect of gettering on the lifetime won't be indicated in the spectral response). The short wavelength response indicates poor passivation and a high loss in the emitter collection.

The response as a function of incident angle shows the loss due to higher reflection at visible wavelengths but the responses merge at shorter wavelengths as usually observed for all cells made from multicrystalline material. The merging response is apparently the result of the scalloped surface texturing combined with the AR coat, an effect not seen in monocrystalline cells. This lot shows slightly more variation with incident angle at long wavelengths than most other multicrystalline lots.

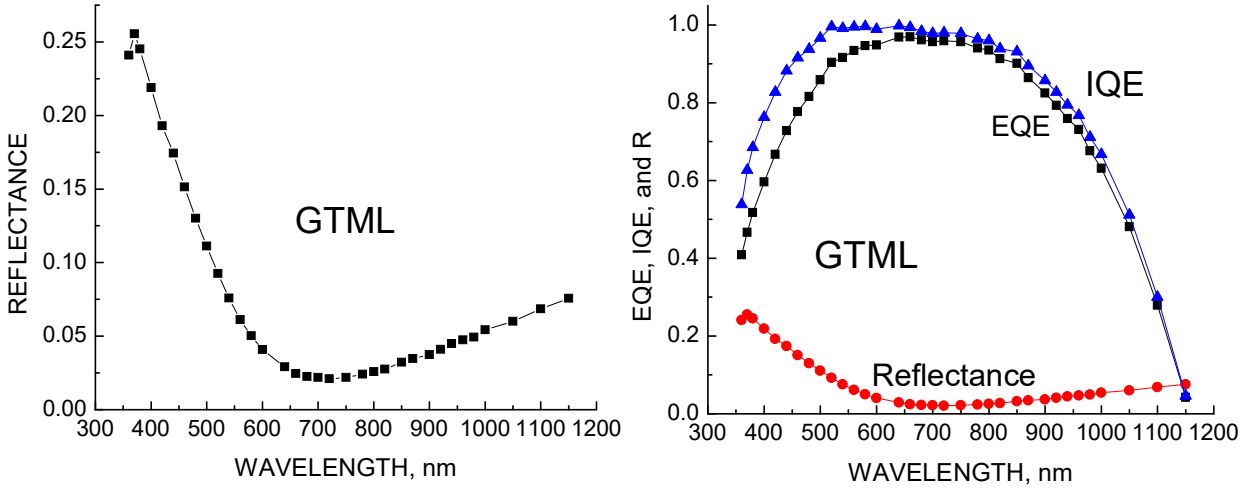

Figure 111. Reflectance (left) and IQE – EQE comparison (right).

The reflectance minimum at 700 nm is too high and should be closer to 600 nm to better match the solar maximum. The cause is likely to be a SiN_x ARC which is too thick, and both the EQE and Isc are degraded in consequence. The poor long wave response is indicative of poor base lifetime and poor quality starting material, which the gettering was unable to improve enough to enhance the IQE.

7.15 TG Solar

10 6-inch Monocrystalline Cells.

Comments: Shunt Resistance very low, yet high enough to not limit the efficiency. J0 and n are good (low) and Voc is high, with the result that the efficiency is well above 17%. One cell among the 10 is an outlier and a second one slightly worse than the rest, otherwise the lot uniformity is high. The averages are:

<RSH> = 8.3ohms, ⑨ = 4.5
<RS> = 0.535 ohm-cm^2, ⑨ = 0.027
<J0> = 4.7 E-12 amps/cm^2, ⑨ = 1.2 E-12
< n > = 1.073, ⑨ = .025
< Jsc> = 35.40 mA/cm^2, ⑨ = 0.150
<Voc> = 638.8 mV, ⑨ = 1.5
<FF> = 0.785, ⑨ = .005
<Effic> = 17.74 %, ⑨ = 0.15

Efficiency and Parameter Correlations:

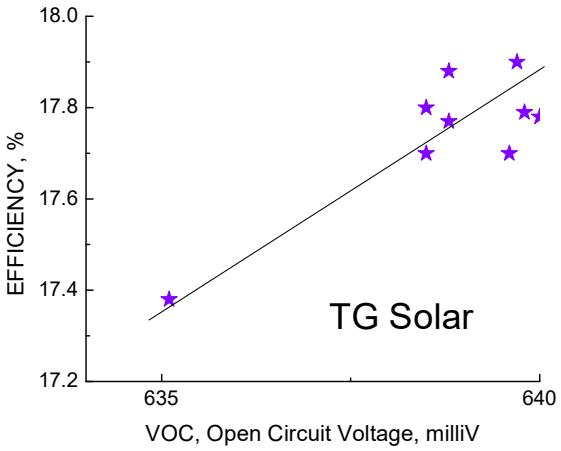

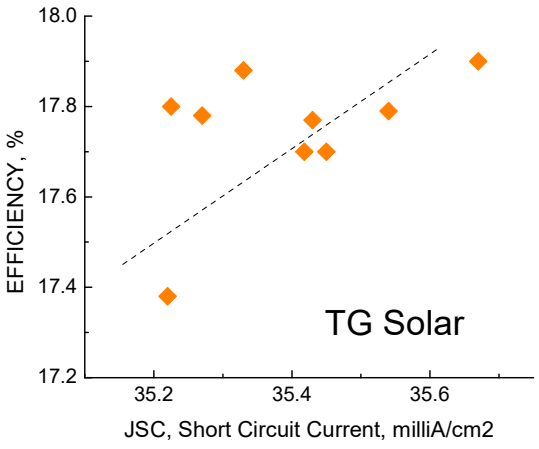

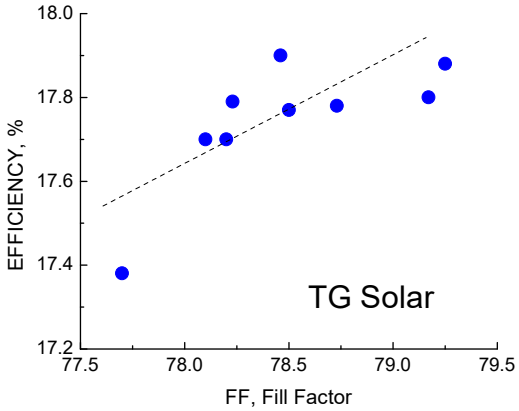

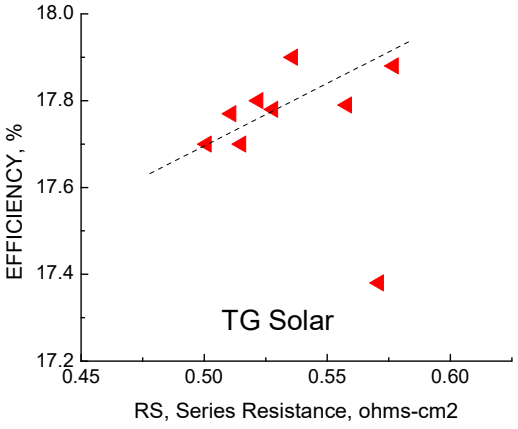

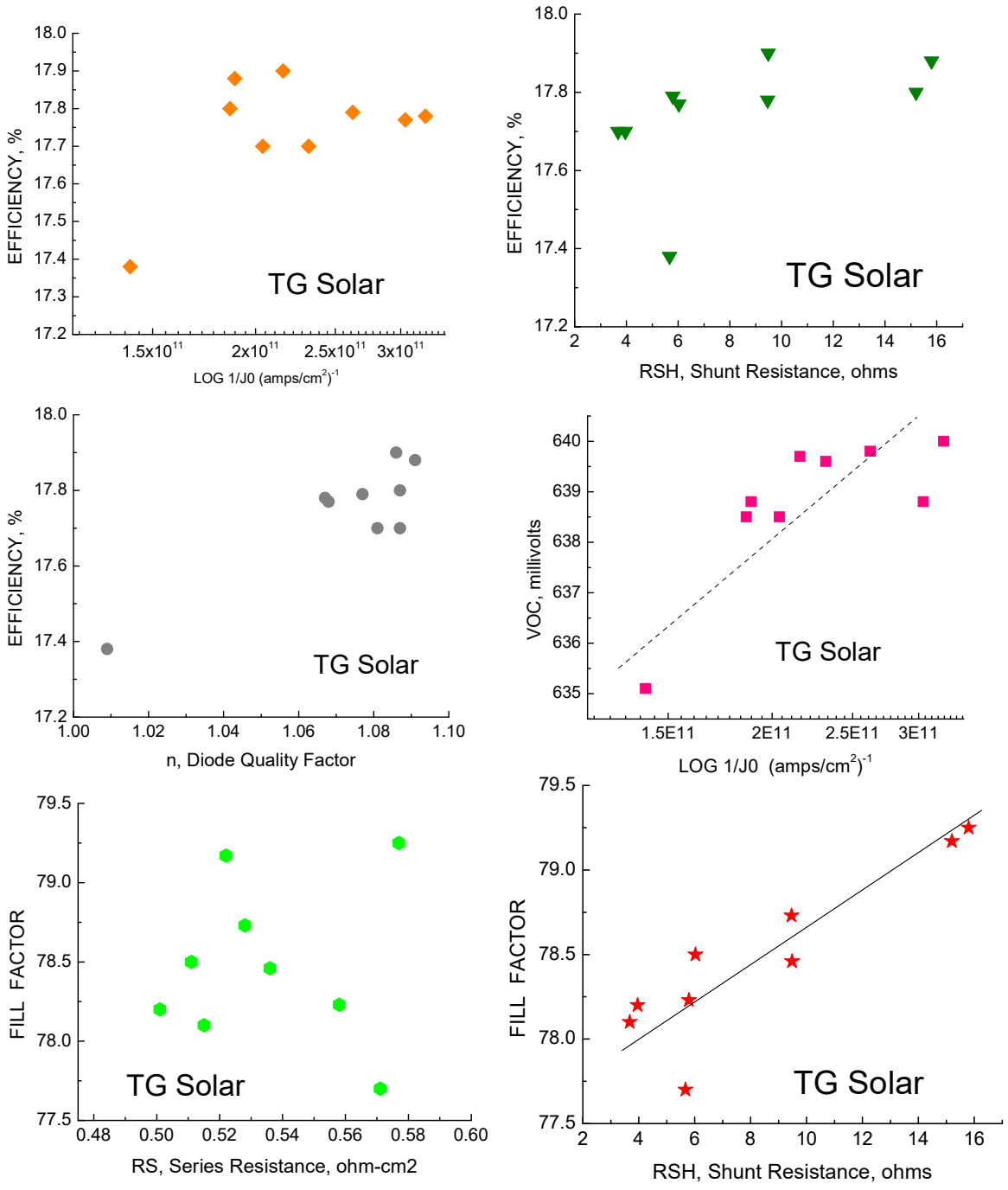

Figure 112. Correlations for TG Solar 6-inch mono cells (without 1 outlier).

Figure 112 show the correlations for TG solar mono cells. These are unusual in that they are 6-inch square rather than the usual 5 inch. They are also high efficiency. There are weak correlations of efficiency with Jsc, Voc, FF, Rs, and perhaps n. (The use of dotted lines is to denote that the correlations are speculative, based on only 9 cells). There are also reasonable correlations of Voc with log 1/J0 and FF with Rsh. It is surprising that these cells have the highest efficiency while having the lowest shunt resistance of all the lots.

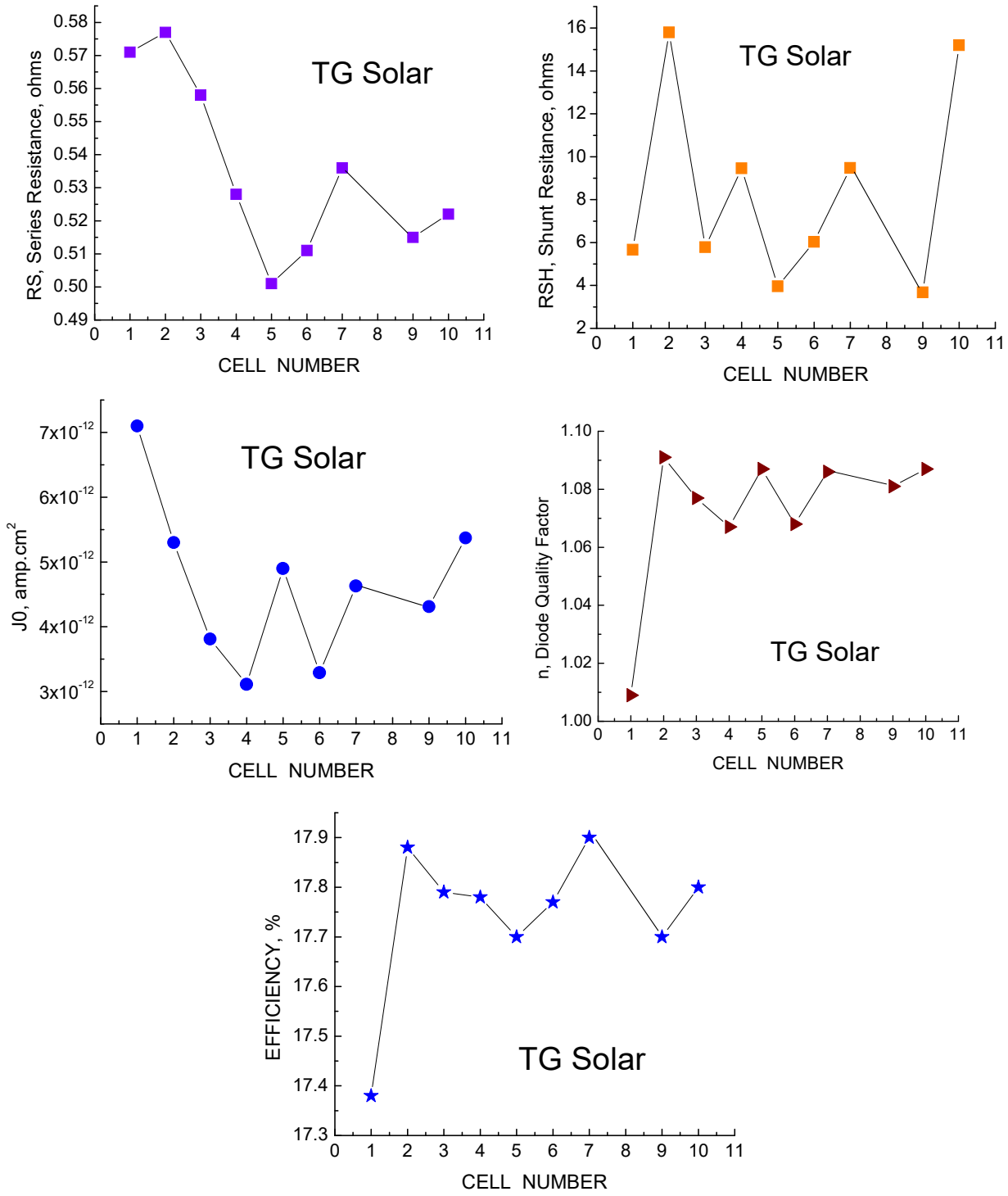

Figure 113. Forensic parameters for TG Solar multicrystalline cells.

Figure 113 shows the forensic parameters for these 10 cells. The uniformity is good except for the 1st device. The dark current J0 in particular is more uniform than other mono lots.

LBIC Maps.

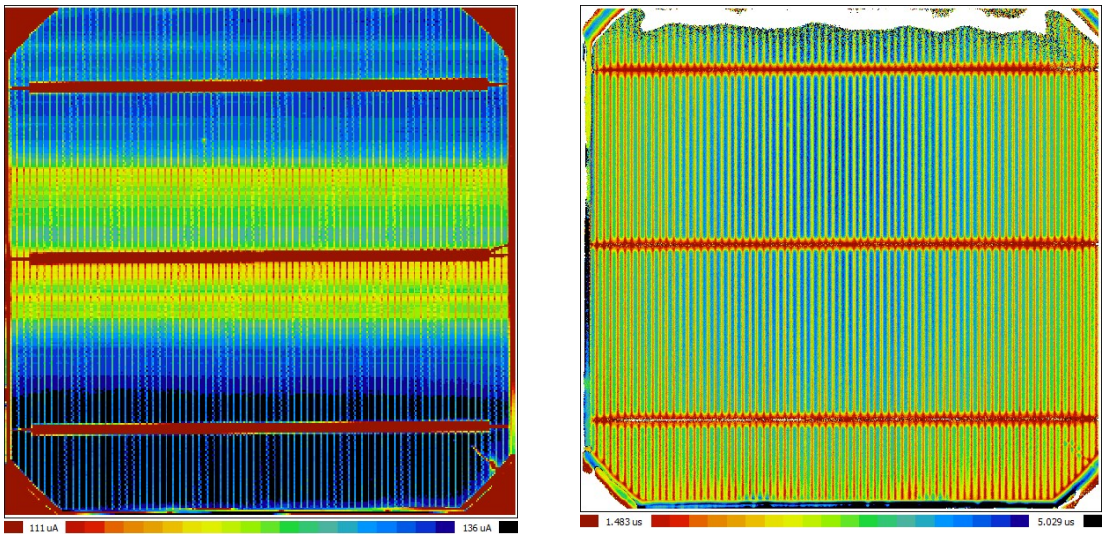

Figure 114. LBIC map at 981 nm (left) and lifetime map (right) for TG Solar cell # 7.

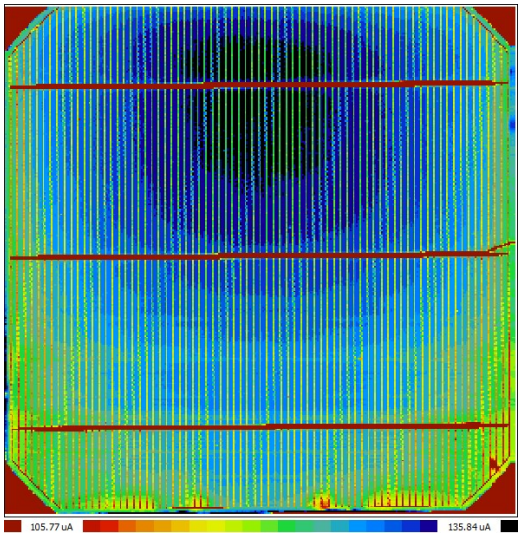

Figure 115. LBIC map for 404 nm excitation, TG Solar cell #7.

Figures 114 and 115 show the LBIC and lifetime maps for a representative cell from the TG Solar mono lot. The cell efficiency was actually 17.9% in spite of the mid-wafer band of lower photocurrents apparent at the long wavelength in Figure 116. The lifetime map (Figure 114, right side) is very uniform for this mono lot, as is the LBIC map at short wavelength shown in Figure 115.

Quantum Efficiency.

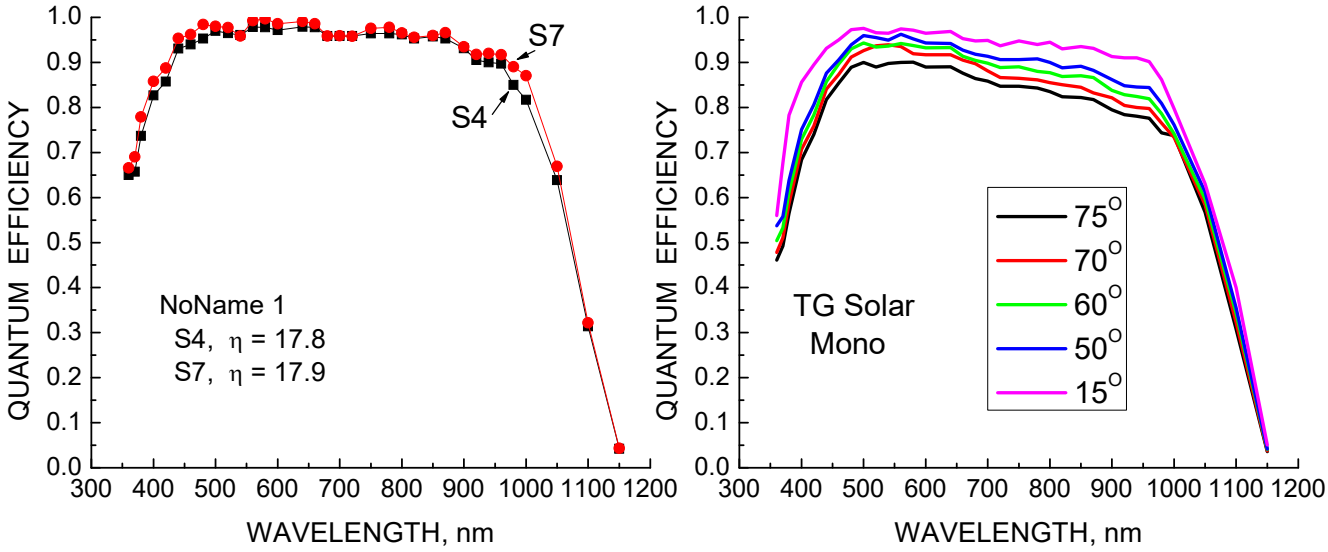

Figure 116. Spectral responses for cells from mono lot TG Solar; normal incidence (left), versus angle of incidence (left).

The spectral responses (Figure 116) for this high efficiency monocrystalline lot show high substrate lifetime (sharp long wavelength response) and excellent passivation (short wavelength response). The response as a function of angle shows the expected decline in the visible as well as at short wavelengths similar to other mono lots. The reflectance is so low that the EQE and IQE (Figure 117) are nearly indistinguishable. The high, "square" spectral response is responsible for the high values of Isc and efficiency, and the good base lifetime and surface passivation contribute to the high Voc value also.

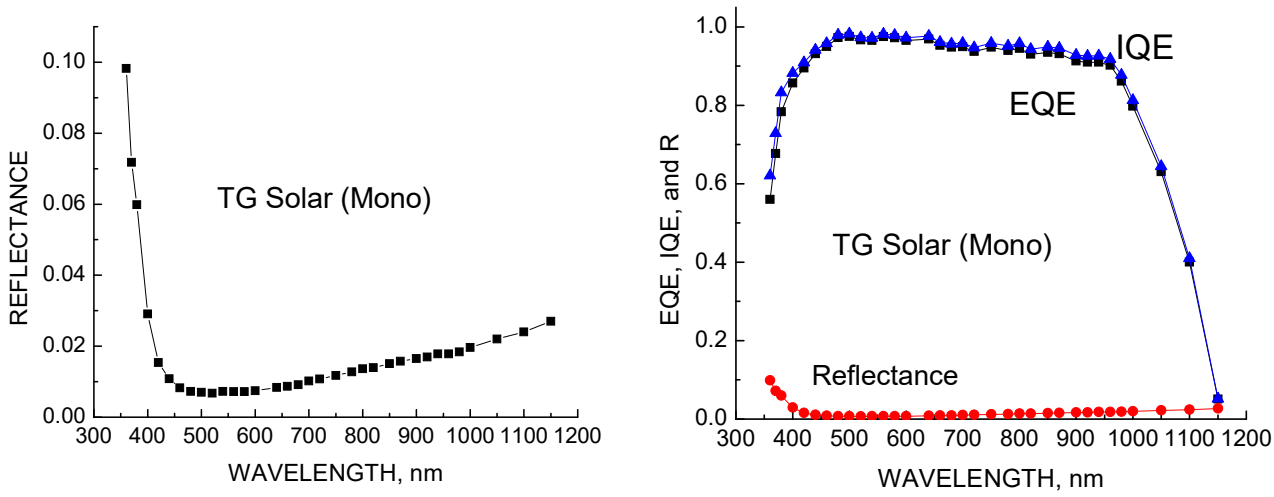

Figure 117. Reflectance (left) and EQE – IQE comparison (right) for cell #7.

7.16 Green Energy

20 5-inch Monocrystalline Cells.

Comments: Shunt Resistance is good, series Resistance is high but expected for the smaller 5 inch monos compared to the 6 inch multis. The Voc is a bit low (619mV) for monocrystalline cells. The J0 and n are unusually high for either mono or multi cells, and likely reduce the efficiency. The Jsc is also low for mono cells .The averages are:

<RSH> = 221ohms, ⑨ = 85
<RS> = 0.741 ohm-cm^2, ⑨ = 0.035
<J0> = 7.1 E-9 amps/cm^2, ⑨ = 6.7 E-9
< n > = 1.536, ⑨ = .105
< Jsc> = 32.71 mA/cm^2, ⑨ = 0.328
<Voc> = 618.7mV, ⑨ = 6.3
<FF> = 0.771, ⑨ = .003
<Effic> = 15.6 %, ⑨ = 0.56

Efficiency and Parameter Correlations:

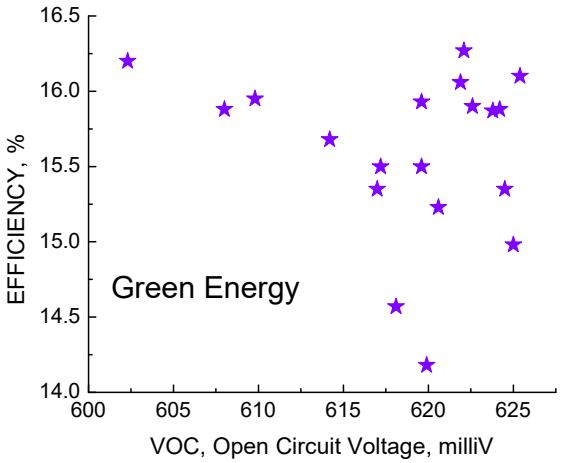

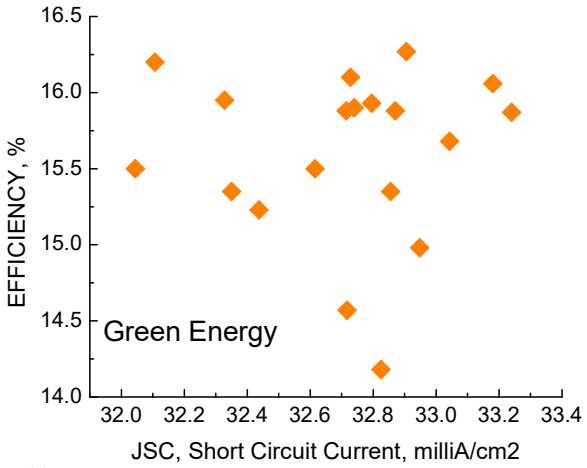

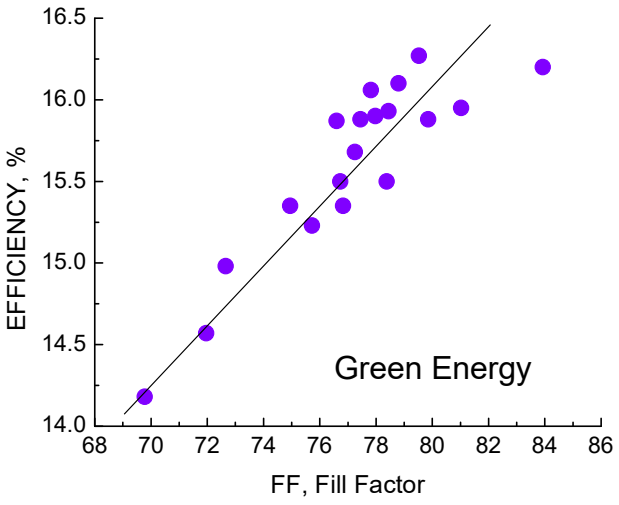

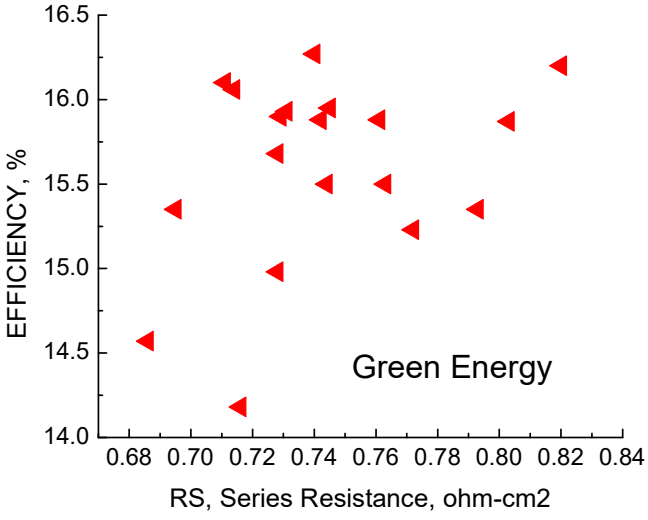

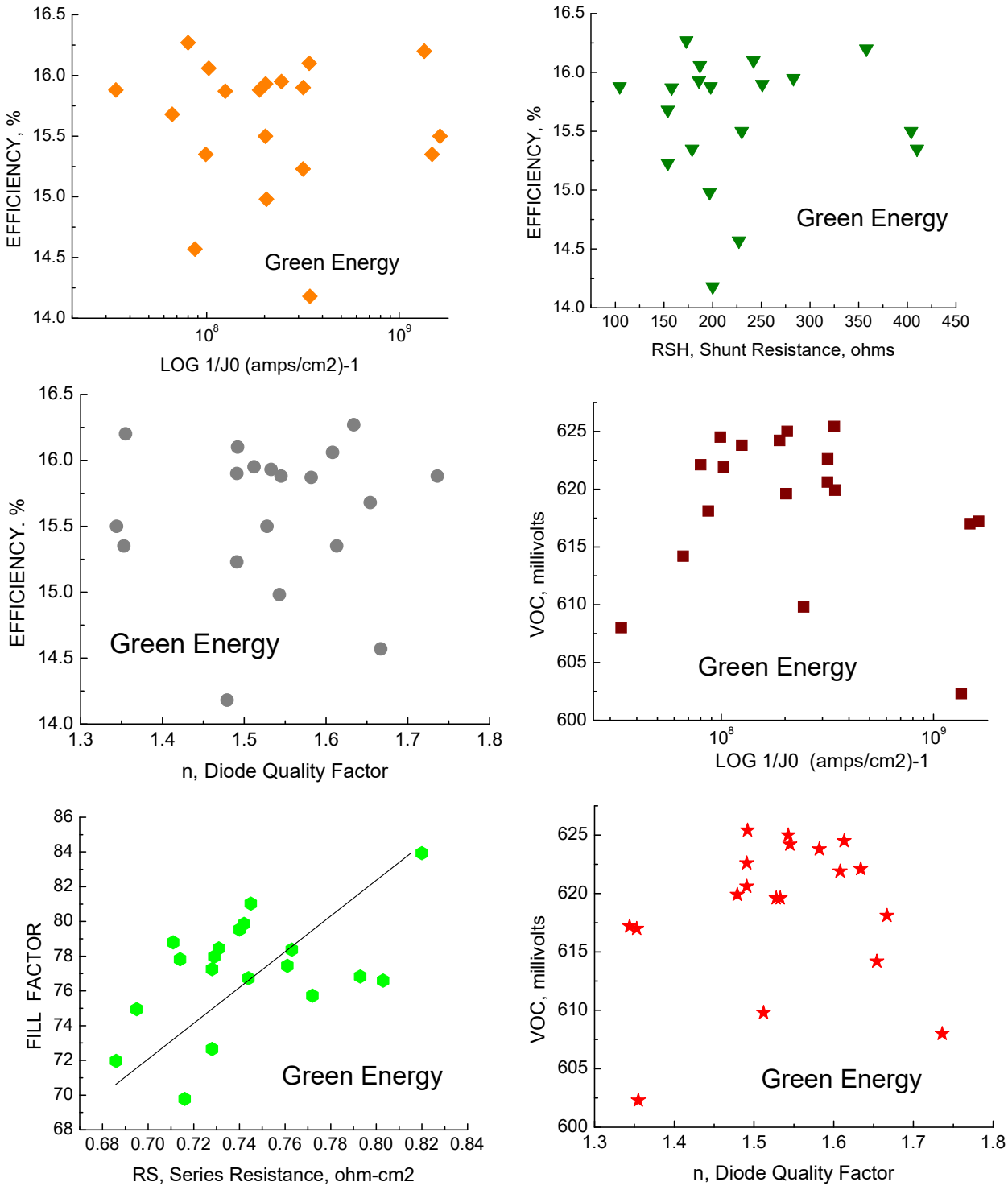

Figure 118. Correlations for Green Energy cells.

The only strong correlation for Green Energy cells is the efficiency-FF relation as shown above in Figure 118. There is no relation between efficiency and Voc or Jsc and only a slight possible correlation between FF and series resistance. The efficiency is unexpectedly low for mono cells and the J0 and n are both high, likely contributing to the poor efficiencies.

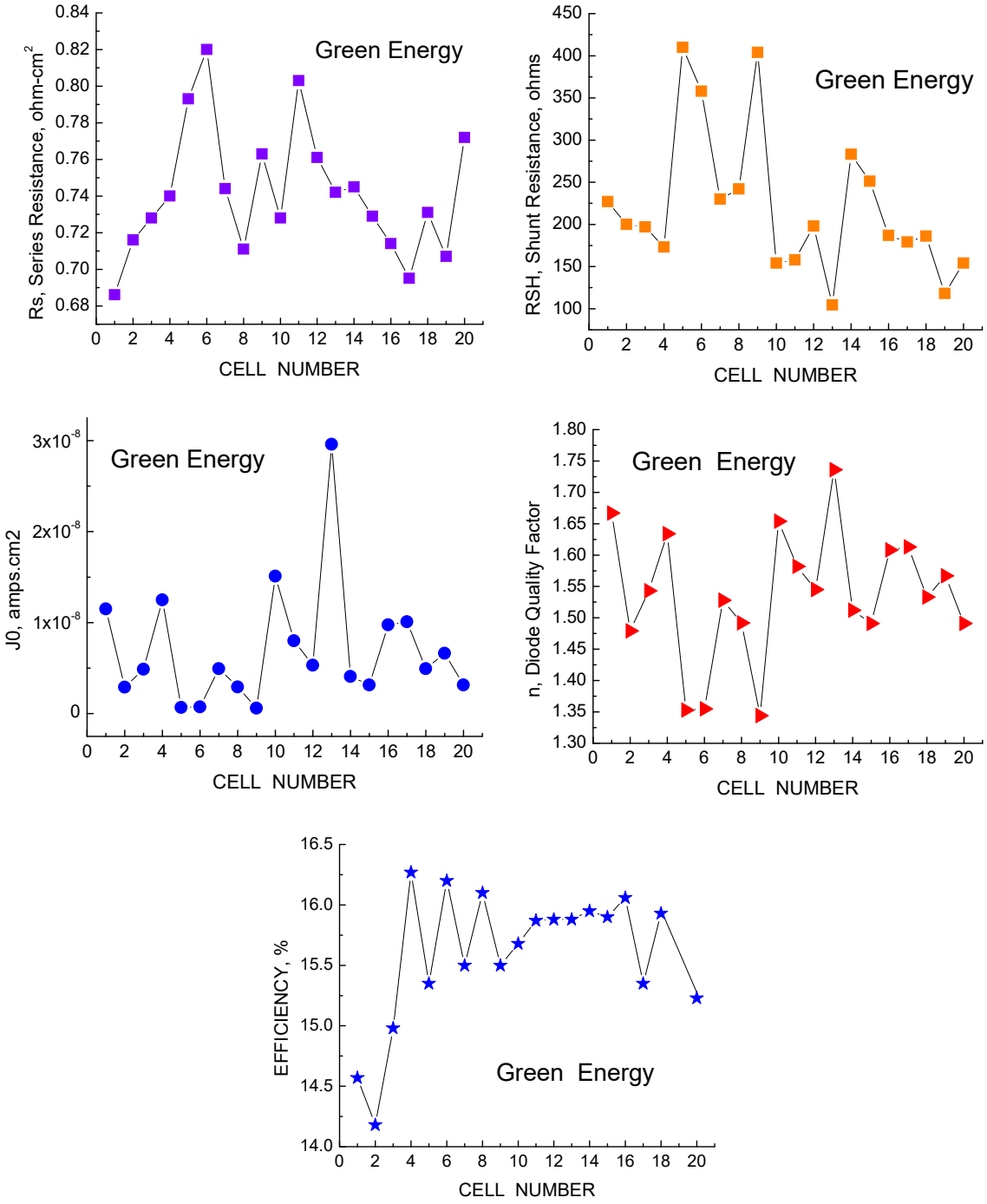

Figure 119. Forensic parameters for Green Energy mono cells.

Device parameters for the Green Energy lot are shown in Figure 119, which as already mentioned displays the undesirable high values of J0 and n and relatively mediocre efficiencies. This lot also had a wide distribution, with cells ranging from 14.2% to 16.3%. Cell #4 in the following LBIC maps is the highest efficiency device.

LBIC Maps.

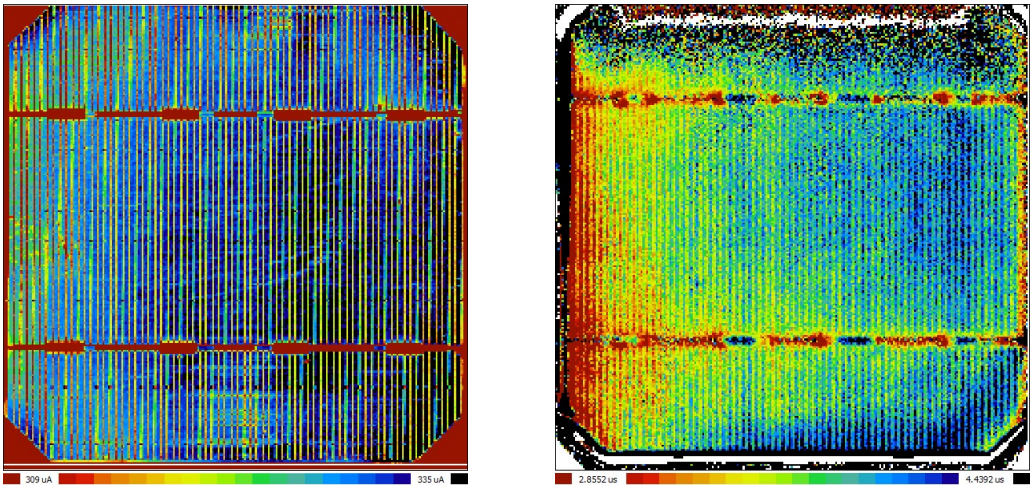

Figure 120. LBIC map at 981 nm (left) and lifetime map (right) of Green Energy cell # 4.

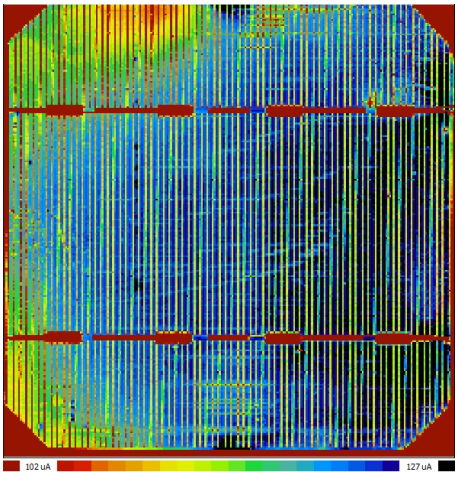

Figure 121. LBIC map for 404 nm excitation of Green Energy cell #4.

LBIC and lifetime for one of the Green Energy mono cells are shown in Figures 120 and 121. This was the highest efficiency cell and shows a high degree of uniformity at both long and short wavelength excitation. No particular problems are evident from the LBIC maps. This cell efficiency is 16.3% limited by a lower than expected short circuit current.

Quantum Efficiency

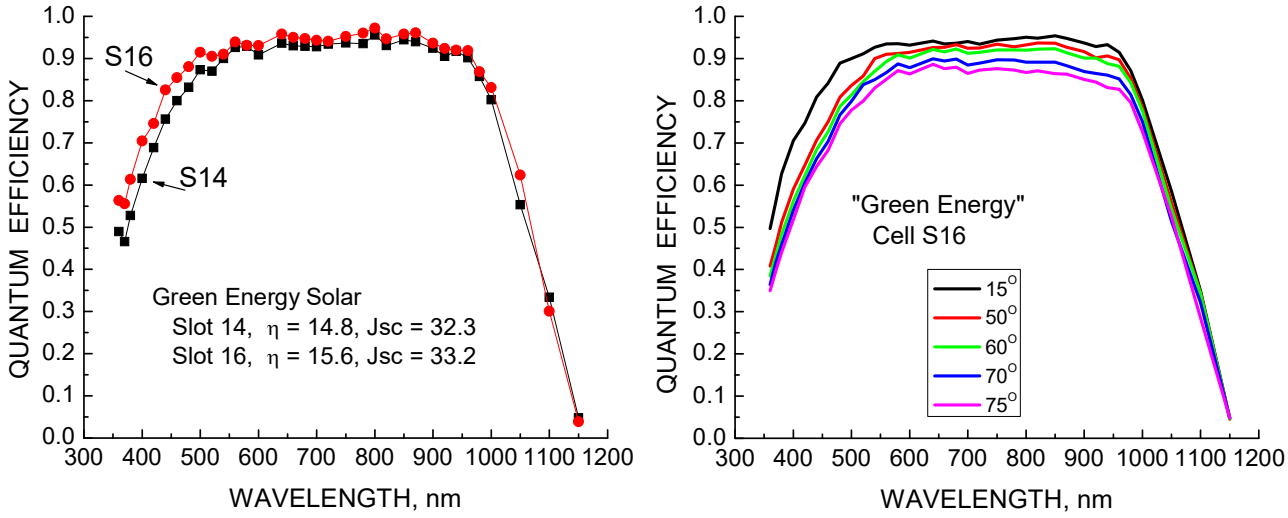

Figure 122 Spectral responses for Green Energy Solar mono cells; normal incidence (left), versus angle of incidence (right).

Figure 122 compares the EQE for two cells with slightly different efficiencies and Isc's and shows the effect of incidence angle. Like other mono cells, the quantum efficiency is more affected by incident angle at short wavelengths than at long wavelengths. The IQE of Figure 123 illustrates one reason why the efficiency and Isc are lower for these mono cells. The lifetime in the base is good as evidenced by the long wavelength response, but the short wave response deteriorates with decreasing wavelength, probably due to sub-optimal passivation, which can lower both Voc and Isc. On the other hand, the reflectance is remarkably low, making the EQE and IQE nearly indistinguishable.

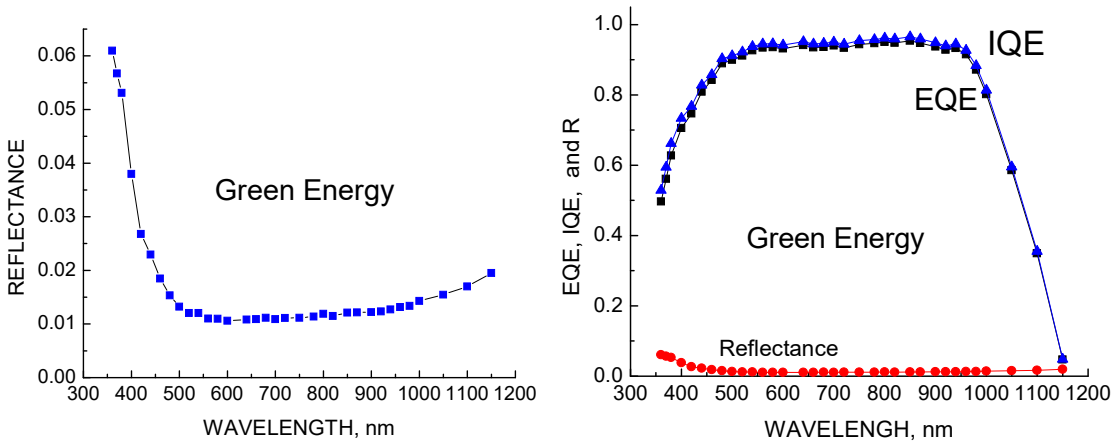

Figure 123. Reflectance (left) and EQE – IQE comparison (right) for cell #16.

7.17 TOP Solar

17 5-inch Monocrystalline Cells.

Comments: Shunt Resistances are very high, most in the thousand+ range. The series resistance is also high but does not have a strong effect on the efficiency. Jsc, Voc, and efficiency are all good, and the only factor which significantly impacts the efficiency is the fill factor. Voc would have been higher if J0 and n were lower. The averages are:

<RSH> = 2565 ohms, ⑨ = 2260
<RS> = 0.872 ohm-cm^2, ⑨ = 0.081
<J0> = 1.4 E-9 amps/cm^2, ⑨ = 2.1 E-9
< n > = 1.328, ⑨ = .138
< Jsc> = 35.549 mA/cm^2, ⑨ = 0.357
<Voc> = 623.8 mV, ⑨ = 3.5
<FF> = 0.781, ⑨ = .003
<Effic> = 16.34 %, ⑨ = 0.64

Efficiency and Parameter Correlations:

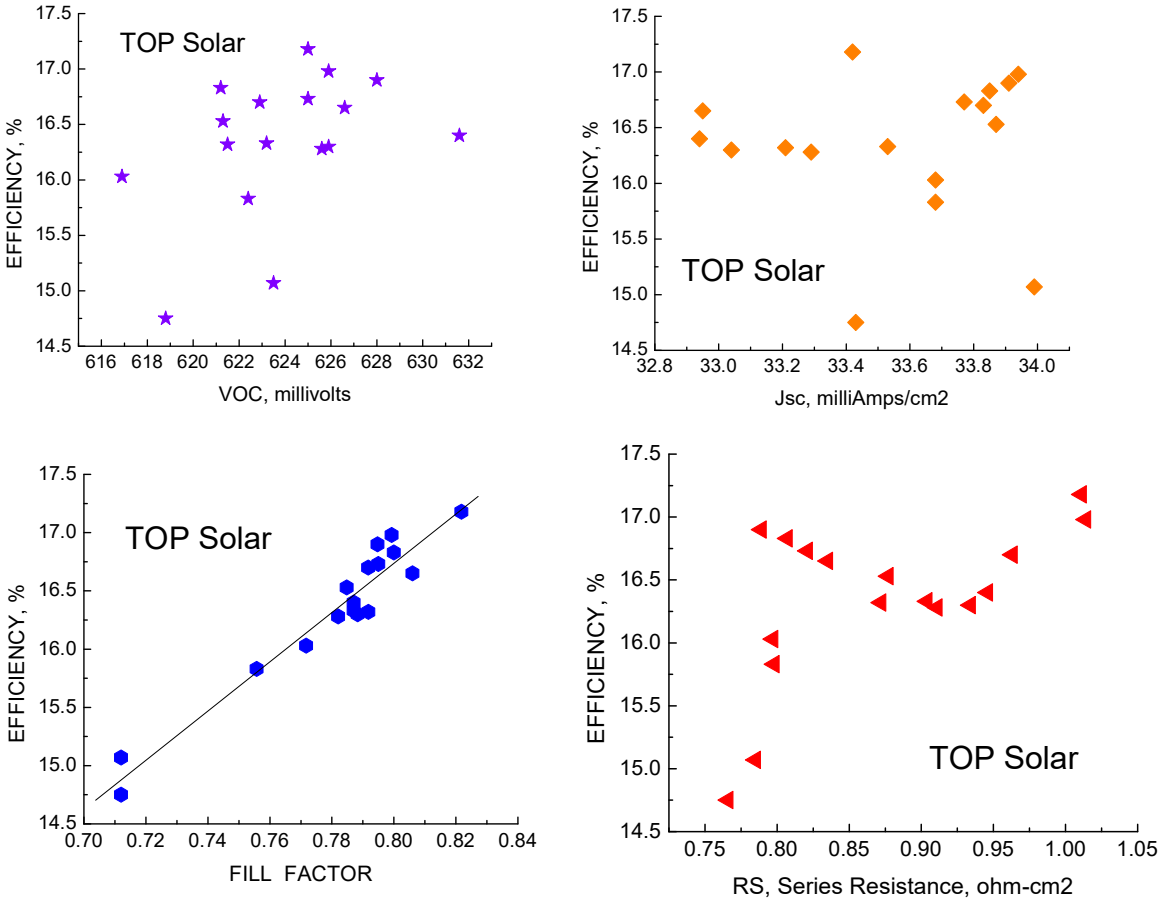

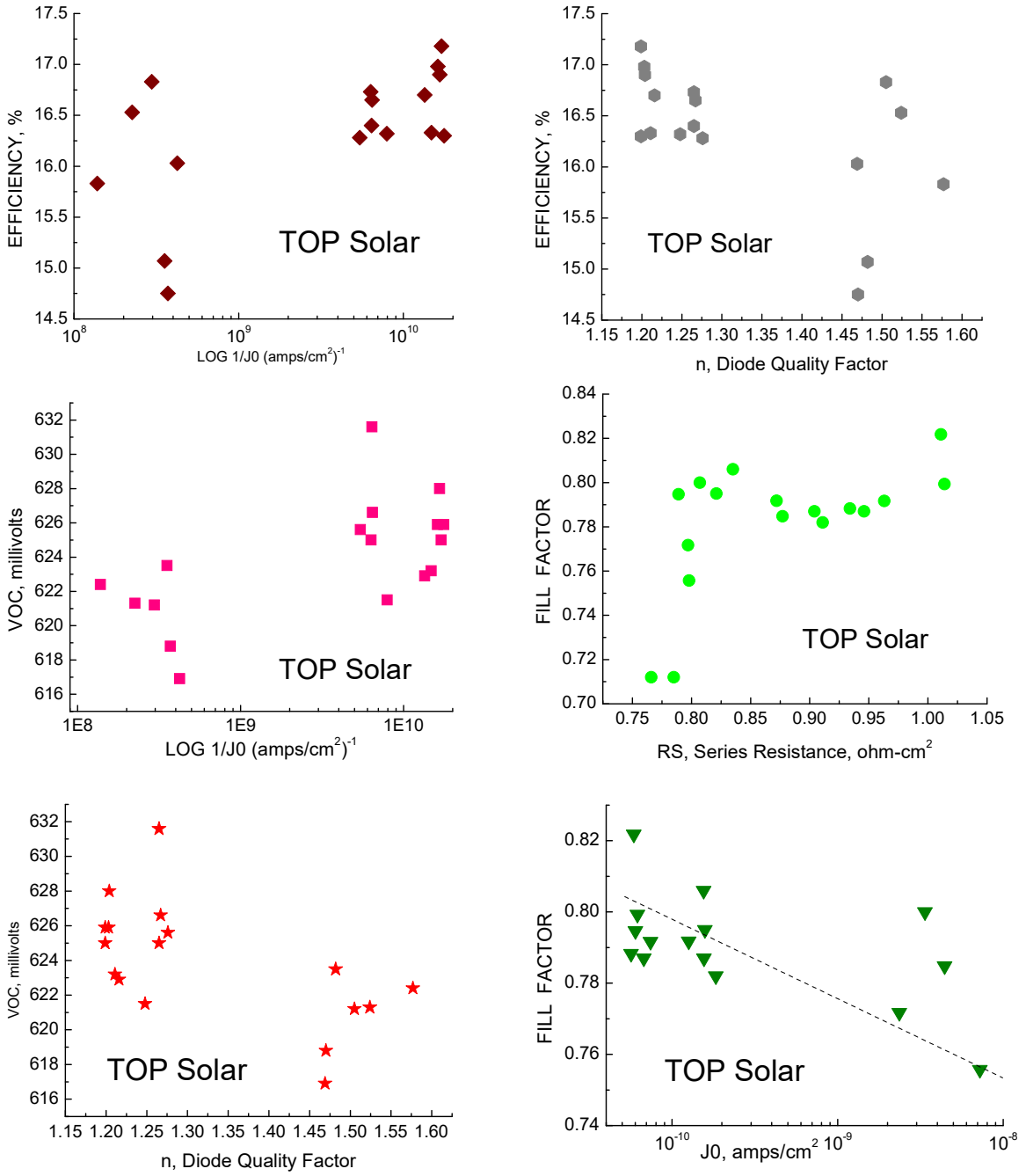

Figure 124. Correlations for TOP Solar5-inch monocrystalline cells.

Figure 124 shows the correlations for TOP Solar mono cells. (These devices were very difficult to measure; almost all the devices exhibited high shunt leakage unless manipulated multiple times on the measuring chuck, as if the top electrodes were nearly shorted to the base.) A high correlation is seen between efficiency and FF, but not for any of the other device parameters. Many of the charts above show two groups separated by a gap, again suggesting they may come from multiple batches.

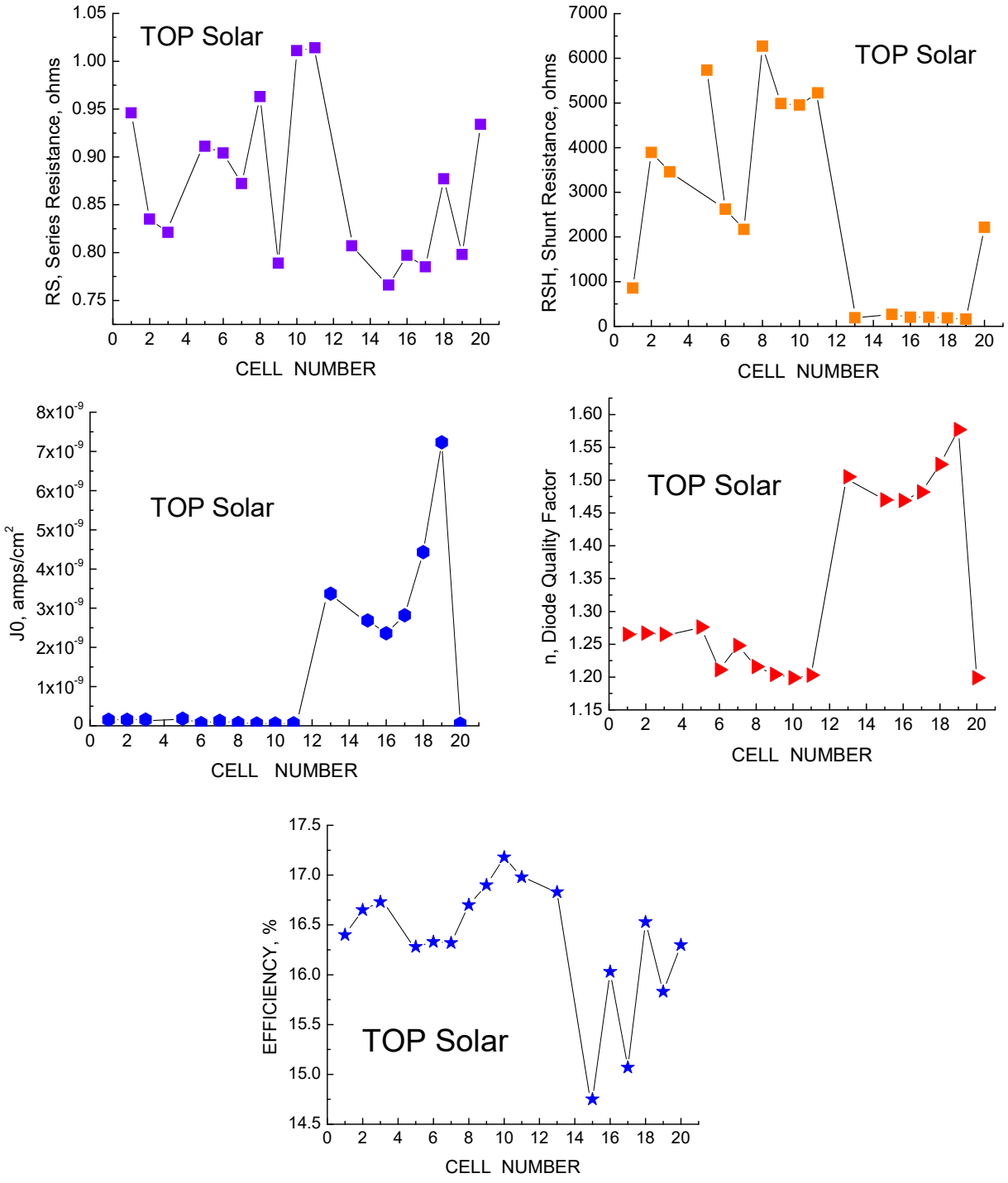

Figure 125. Forensic parameters for TOP Solar mono cells.

Most of the charts in Figure 125 exhibit the two different regions. The J0 and Rsh plots are especially striking as one group exhibits values several hundred times that of the other group, furthering the evidence that the cells come from multiple batches although sold as one lot. These cells exhibited a strong tendency to short circuit. It was necessary to mount the cells multiple times in different configurations to find a mounting that didn't result in a high shunt leakage. Efficiencies were good once non-shunting placement was found.

LBIC Maps.

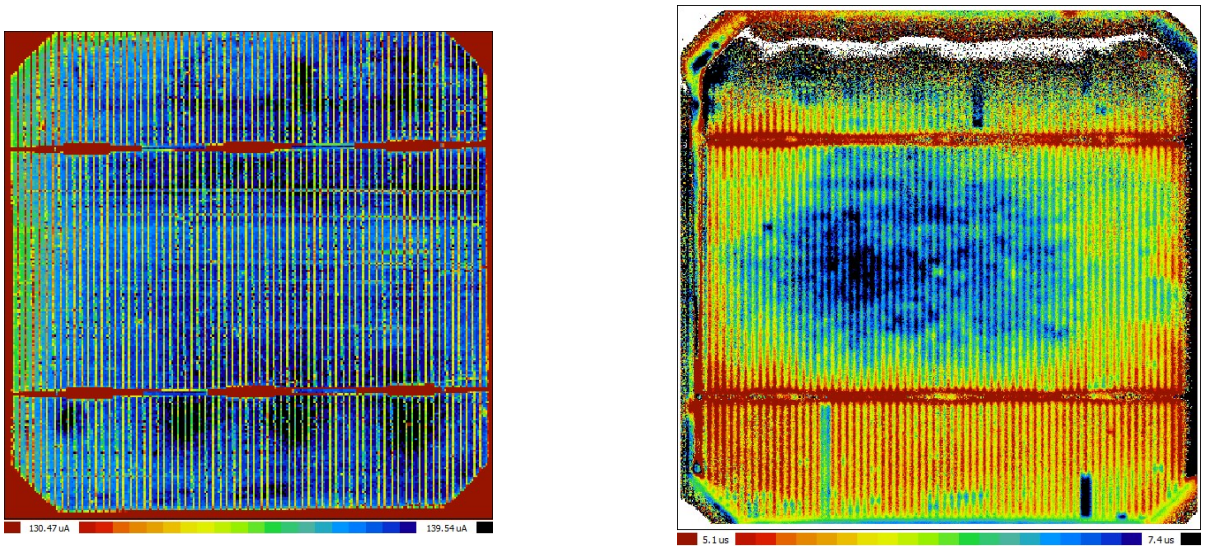

Figure 126. LBIC map for 981 nm excitation (left) and lifetime map (right), Top Solar cell #3 16.7% efficiency.

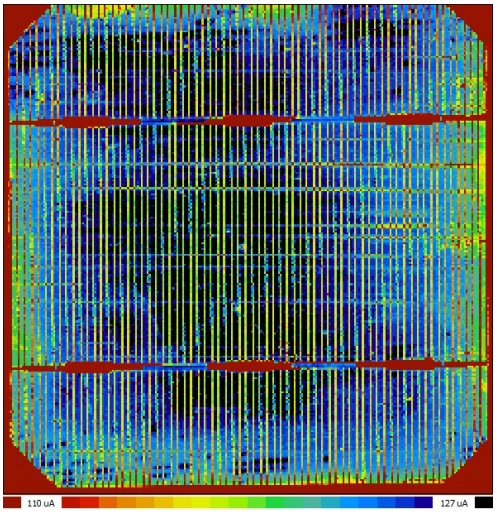

Figure 127. LBIC map at 404 nm excitation for Top Solar cell #3.

LBIC maps for Top Solar cells in the 1st group with low J0 and high Rsh show high uniformity as seen in the LBIC maps above (Figures 126, 127). High lifetimes in the finished cells were observed (5-8 microseconds), which can be compared to lifetimes for multicrystalline cells (1.5-3 microseconds).

Quantum Efficiency

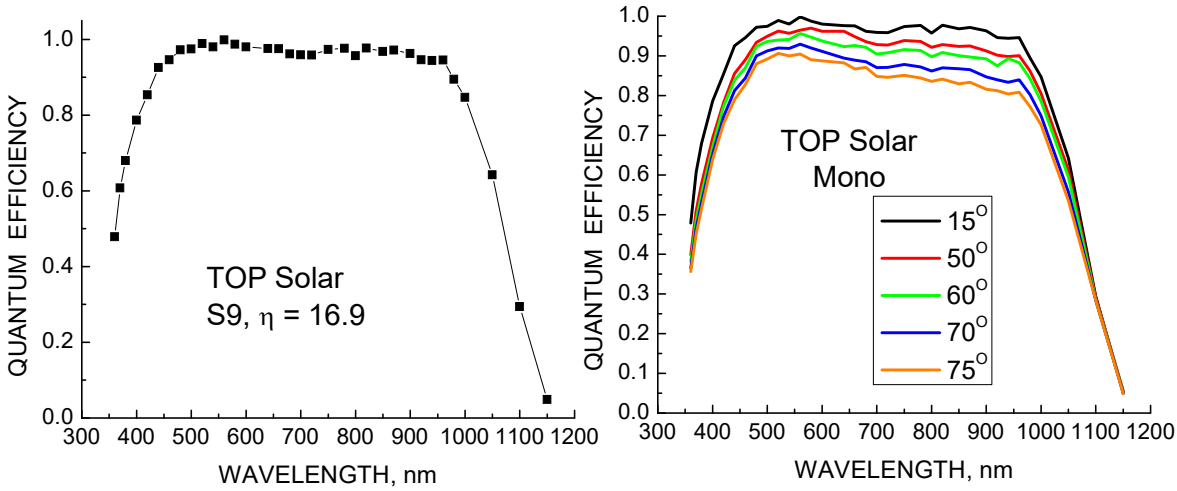

Figure 128. Spectral responses for TOP Solar mono cells; normal incidence (left), versus incident angle (right).

Figures 128 and 129 show the spectral responses for a typical cell from the TOP Solar monocrystalline lot. The fast rise at long wavelength, the flat response over almost all the visible, and the sharp decline at short wavelengths all indicate good base lifetime and good passivation, with a diffusion length exceeding the junction depth (emitter thickness) and low surface recombination velocity. The response versus incidence angle shows the decline in the visible range but also the drop at short wavelengths, due probably to the pyramidal textured surface. Integrating the spectral response over the whole spectral range shows that mono cells decrease more than multicrystalline devices, though the mono short circuit currents start out higher. The reflectance is remarkably low at normal incidence, making the IQE and EQE almost indistinguishable.

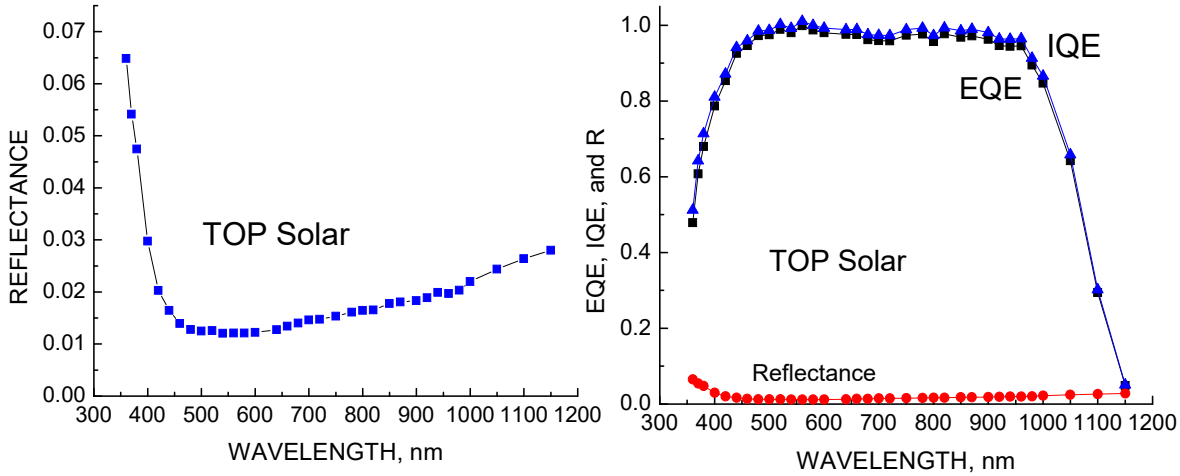

Figure 129. Reflectance (left) and IQE – EQE comparison (right) .

7.18 Linuo 201

25 5-inch Monocrystalline Cells.

Comments: This is a monocrystalline lot with extensive measurements on finished cells and starting wafers. Jsc, FF, and efficiency are all good but Voc is somewhat low for mono cells. Efficiencies are state-of-the-art for turn-key cells fabricated in 2011. The averages are:

< Jsc> = 36.12 mA/cm^2, ⑨ = 0.166
<Voc> = 622.6 mV, ⑨ = 2.1
<FF> = 0.791, ⑨ = .003
<Effic> = 17.84 %, ⑨ = 0.10

Efficiency and Parameter Correlations:

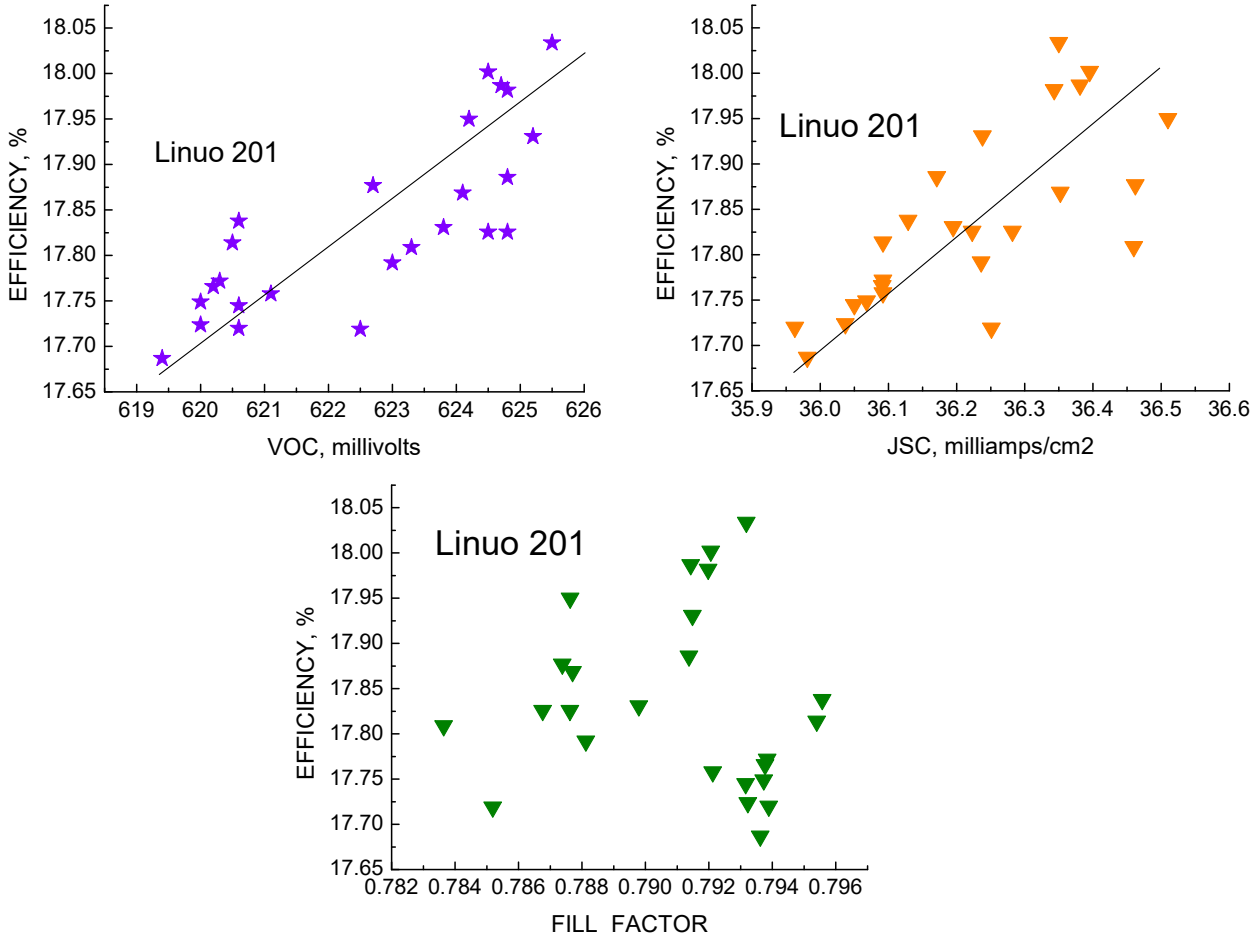

Figure 130. Correlations between major solar cell parameters, mono lot 201.

Figure 130 shows the correlations between major cell parameters. There are moderate correlations between efficiency and Voc and Jsc, but no correlation between efficiency and FF. There are no apparent “outliers” in the 25 cell lot; all cells behaved much the same.

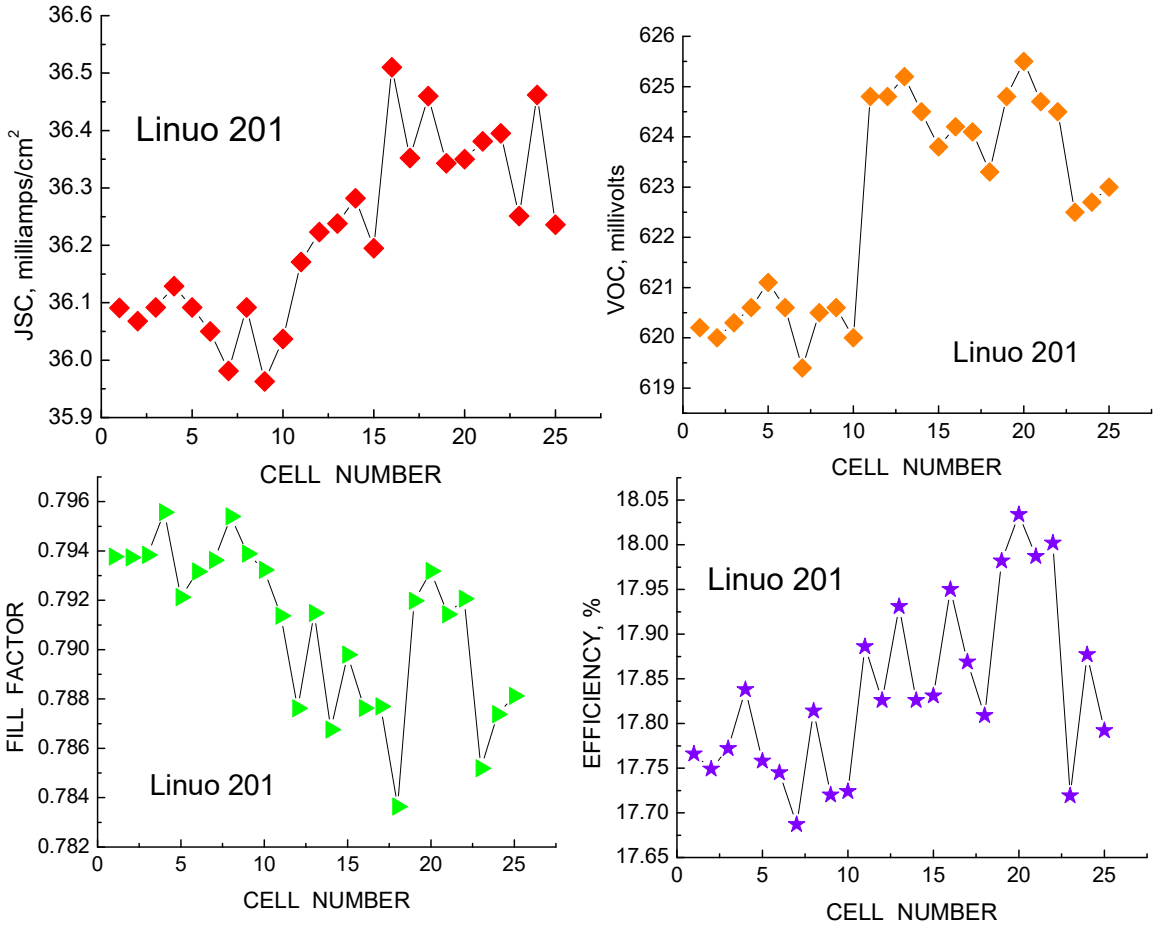

Figure 131. Device parameters versus cell number.

Figure 131 shows the major parameters for all the cells in the lot. There appears to be two groups of cells with the 1st 10 differing slightly from the remainder, but the difference is small. The efficiencies for the 25 cells are relatively uniform, lying between 17.7 and 18%.

"Starting" Wafer Maps

Linuo 201 is one of the lots for which measurements could be made on wafers before the start of processing. The goal was to identify measurement techniques that can correlate with finished cells and possibly separate out starting wafers that would result in poor cells. The techniques available were lifetime maps by photoconductivity decay and "Sinton" lifetime decay under high light intensity and Eddy Current detection. Figure 132 shows a typical Sinton (Eddy Current decay) measurement and a typical lifetime map on a raw starting wafer. The measurement also yields the wafer resistivity.

As with the Linuo 111 lot, the measurements were made on the raw wafers "as received" and therefore contain saw damage at each surface from the wafering process. This damage extends about 15 microns below each surface. The measured lifetimes in the raw wafers are very low, but this is likely due to surface recombination losses exacerbated by the saw damage. It can be concluded that raw wafer lifetime measurements for "as-received" wafers will normally be in the 1-1.5 μsec range due to the surface losses, and do not correlate with finished cell properties.

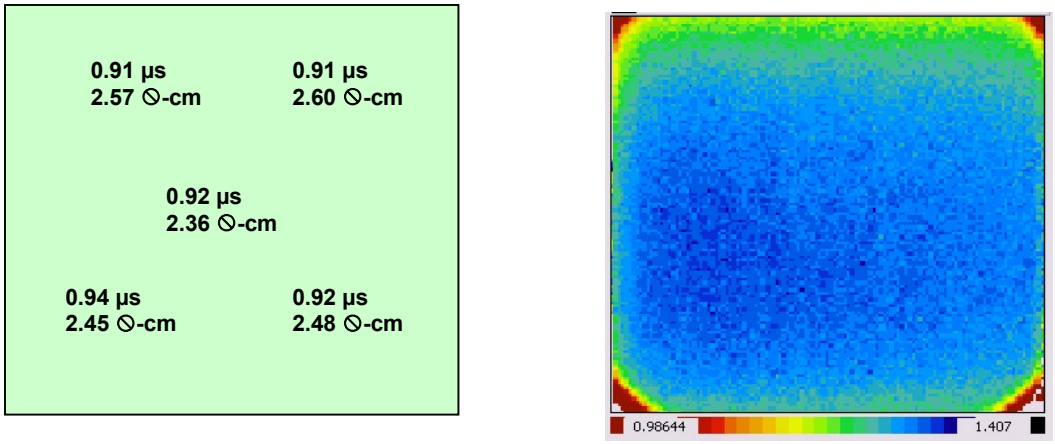

Figure 132. Lifetime and resistivity (left) and lifetime map (right) of Linuo lot 201, wafer S10, after saw damage etch but without surface passivation.

Figure 133 shows a comparison Sinton Eddy Current (EdC) lifetime measurements of the same wafer in the raw state and after etch and passivation. The average lifetime after passivation is 182 µsecs, while the raw wafer average is 0.9 µsecs, showing that the wafer is high quality even with the poor raw wafer measurement.

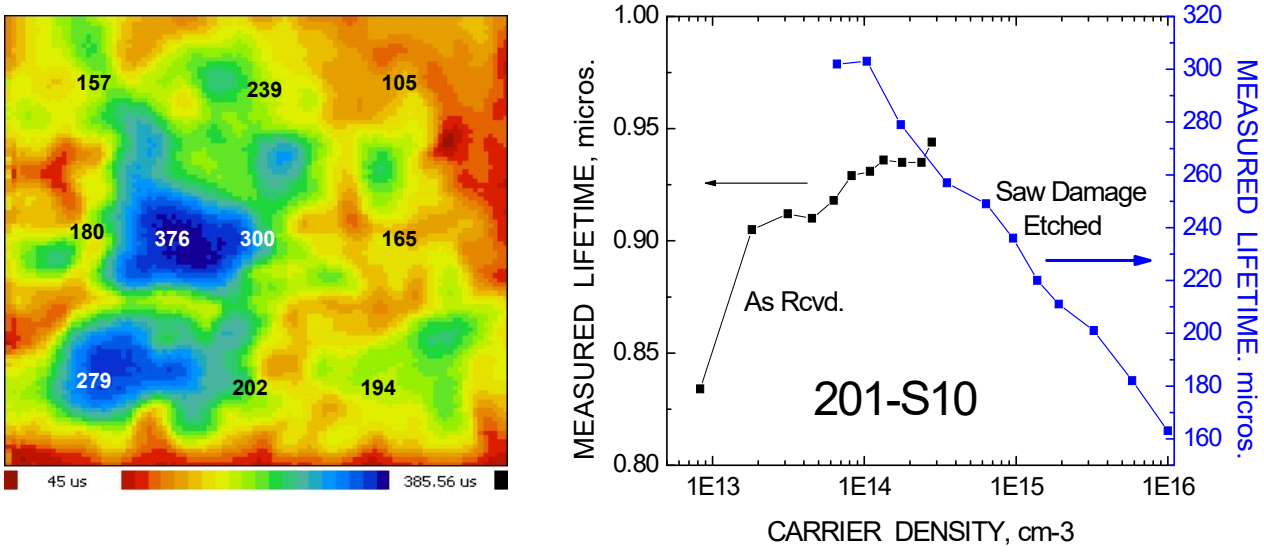

Figure 133. Lifetime measurements on wafer S10 after saw damage and iodine passivation (left) and a comparison of lifetimes in the raw wafer and after treatment (right).

As with the similar mono lot (Linuo 111), it can be concluded that, except in severe cases where measured raw wafer lifetimes are unusually low (< 0.5 µsec), the raw wafer lifetime is likely dominated by surface recombination on both sides due to the lack of passivation and not a useful measure of starting wafer quality (unless, to reiterate, the lifetime is unusually bad). With passivation, however, the "true" value of the wafer lifetime can be obtained and would be a very good quality control "figure of merit." This could be done on one or two wafers from an incoming lot and could reduce the binning distribution, resulting in greater yield and profit, while adding a bit to the process cost and impacting throughput in a minimal way. The resistivity obtained with

the measurement is also a useful parameter, not affected by surface losses, and can be used to discriminate between wafers which lie inside or outside of established specifications.

LBIC and Lifetime Maps.

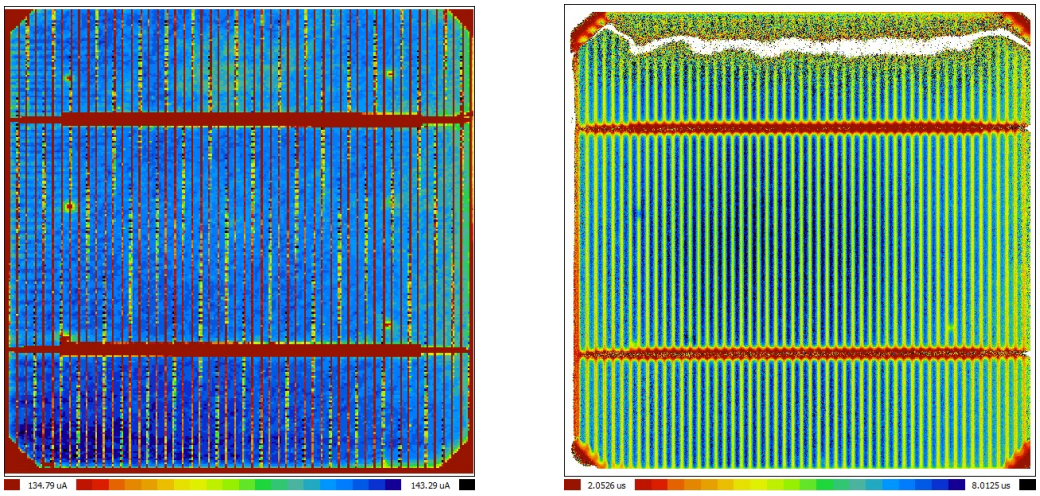

Figure 134. LBIC map at long wavelength (left) and lifetime map (right) for Linuo 201, wafer S21.

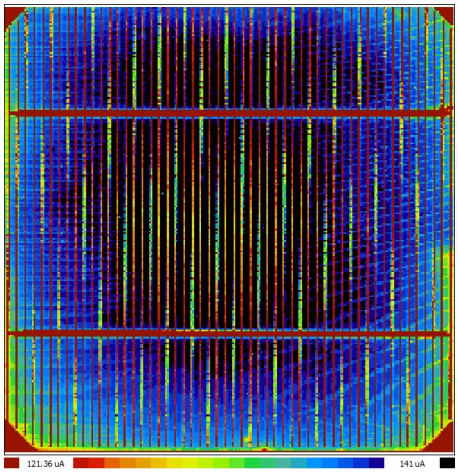

Figure 135. LBIC map for short wavelength (404 nm) excitation, Linuo 201 S21.

Figures 134 and 135 show the LBIC and lifetime maps for a finished solar cell, illustrating a very high degree of uniformity. A high degree of uniformity was suggested by the raw wafer map in Figure 131 as well. The lifetimes in Figure 133 of 7-8 μsecs as measured in a finished cell are much lower than the values for the etched and passivated starting material shown in Figure 132 because of the emitter grid and base Al contacts, the high surface recombination, and the high emitter doping level, all of which obscure the true base lifetime. (Even though the cell shown in Figure 134 is passivated, the SRV is higher due to the high emitter doping level compared to the low doped surface of Figure 132.)

Quantum Efficiency

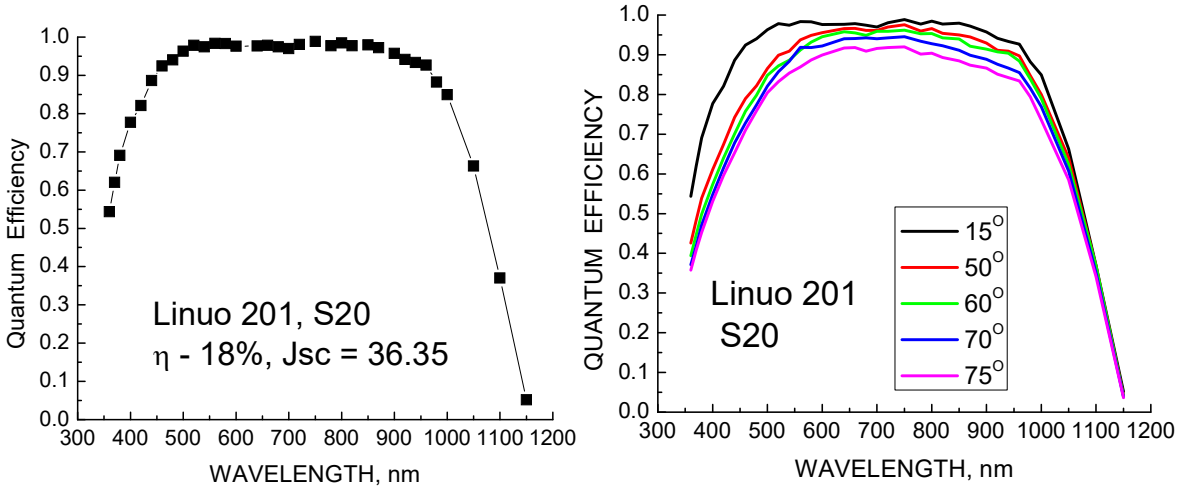

Figure 136. Spectral response at normal incidence (left), versus angle of incidence (right).

Figure 136 shows the spectral responses for a typical cell from the the Linuo 201 monocrystalline lot. The fast rise at long wavelength, the flat response over almost all the visible, and the sharp decline at short wavelengths all indicate good base lifetime and excellent passivation, with a diffusion length exceeding the junction depth (emitter thickness) and low surface recombination velocity. The response versus angle shows the drop in the visible range but also the drop at short wavelengths, due probably to the pyramidal textured surface. The integrated spectral response for mono cells decreases more than for multicrystalline devices, though the mono short circuit currents start out higher. The impact of the decrease with incidence angle is that the cells of this type will lose more in Jsc and efficiency as the sun traverses the sky than will multicrystalline cells that exhibit less effect of angle.

Figure 137 shows the reflectance and EQE/IQE comparison for these mono cells. The very low reflectance over most of the range is typical of well-textured and coated mono cells, making the EQE and IQE almost indistinguishable. The reflectance minimum is around 570-620 nm, ideal for matching to the solar spectral peak. The whole IQE/EQE spectrum demonstrates excellent lifetimes and passivation in the finished cells.

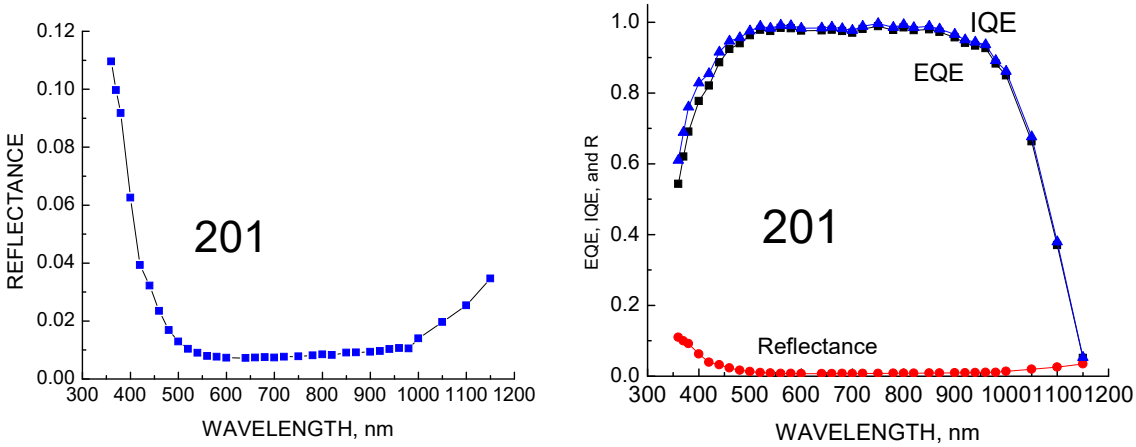

Figure 137. Reflectance (left) and IQE/EQE comparison (right).

7.19 Linuo 111

72 5-inch Monocrystalline Cells.

Comments: This is a large monocrystalline lot with extensive measurements on finished cells and starting wafers. Jsc, FF, and efficiency are all good, though Voc is somewhat low for mono cells. Efficiencies are state-of-the-art for turn-key cells fabricated in 2011. The averages are:

< Jsc> = 36.22 mA/cm^2, ⑨ = 0.244
<Voc> = 625.9 mV, ⑨ = 1.1
<FF> = 0.788, ⑨ = .006
<Effic> = 17.87 %, ⑨ = 0.14

Efficiency and Parameter Correlations:

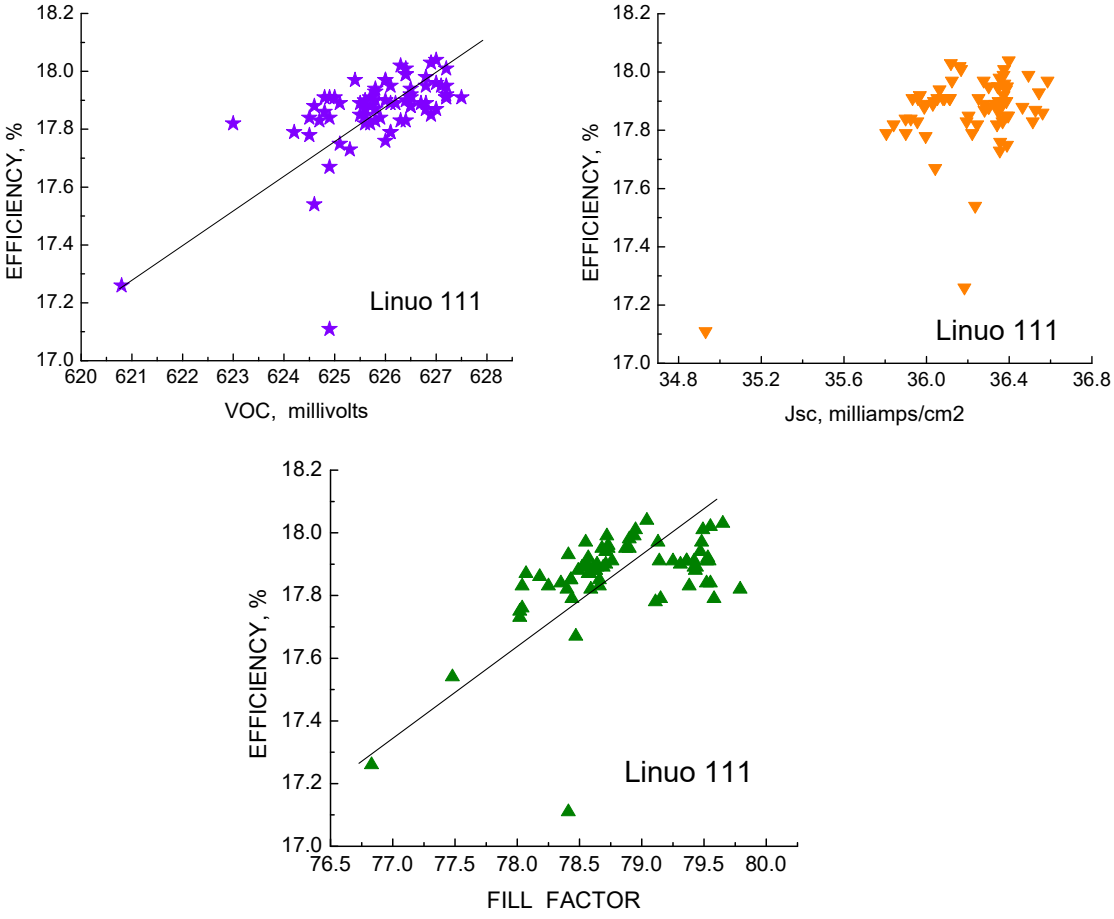

Figure 138. Correlations between major solar cell parameters.

Figure 138 shows the correlations between major cell parameters. There are moderate correlations between efficiency and V_{OC} and FF, but a weaker one between efficiency and J_{SC}. A few "outliers" are apparent.

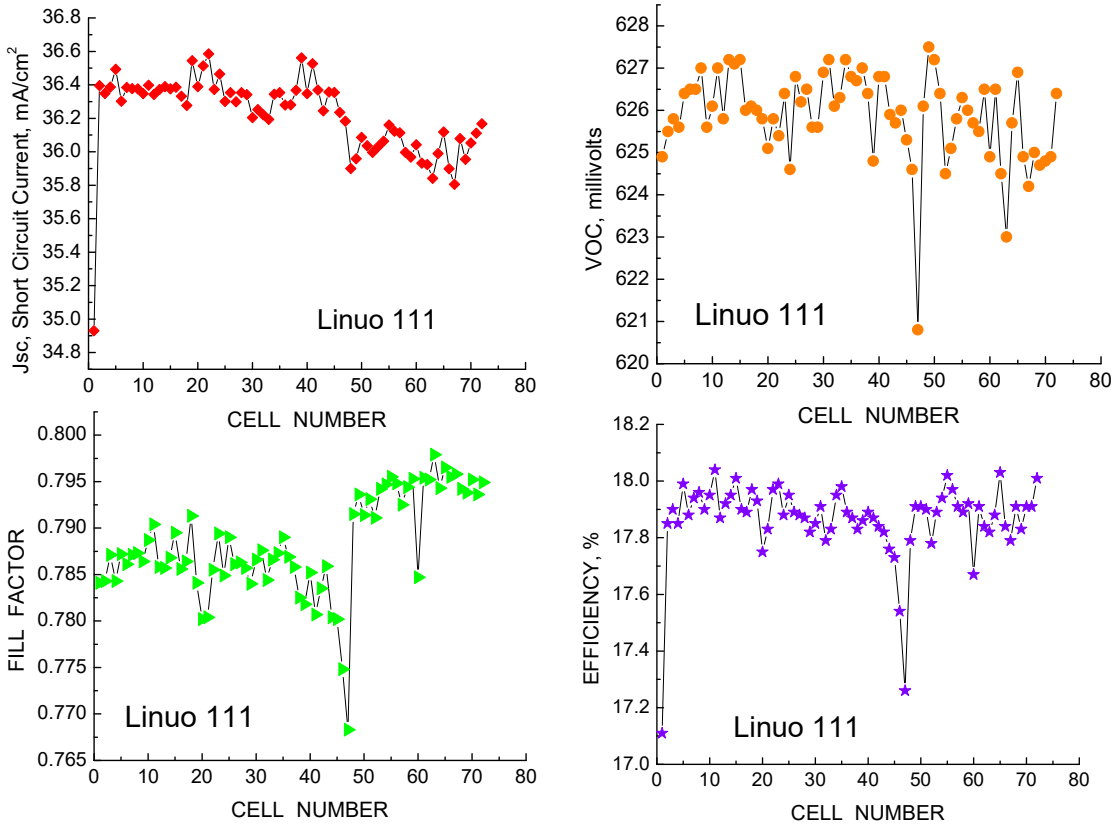

Figure 139. Device parameters versus cell number – 72 cells in all.

Figure 139 shows the major parameters for all the cells in the lot. There is a high degree of uniformity for Jsc and Voc with the exception of several "outliers" though even the outliers are relatively good. The efficiencies are impressively uniform except for these outliers.

"Starting" Wafer Maps

Linuo 111 is one of the lots for which measurements could be made on wafers before the start of processing. The goal was to identify measurement techniques that can correlate with finished cells and possibly separate out starting wafers that would result in poor cells. The techniques available were lifetime maps by photoconductivity decay and "Sinton" lifetime decay under high light intensity and Eddy Current (EdC) detection. Figure 140 shows a typical EdC lifetime measurement and a typical lifetime map on a raw starting wafer. The EdC measurement also yields the wafer resistivity.

The measurements were made on the raw wafers "as received" and therefore contain saw damage at each surface from the wafering process. This damage extends about 15 microns below each surface. The measured lifetimes in the raw wafers are very low, but this is likely due to surface recombination losses exacerbated by the saw damage. It can be concluded that raw wafer lifetime measurements will normally be in the 1-1.5 μsec range due to the surface losses, and do not correlate with finished cell properties. Only if raw wafer lifetime measurements were much below these values could any conclusions be made about wafer quality and poor lifetime wafers discarded before beginning expensive processing.

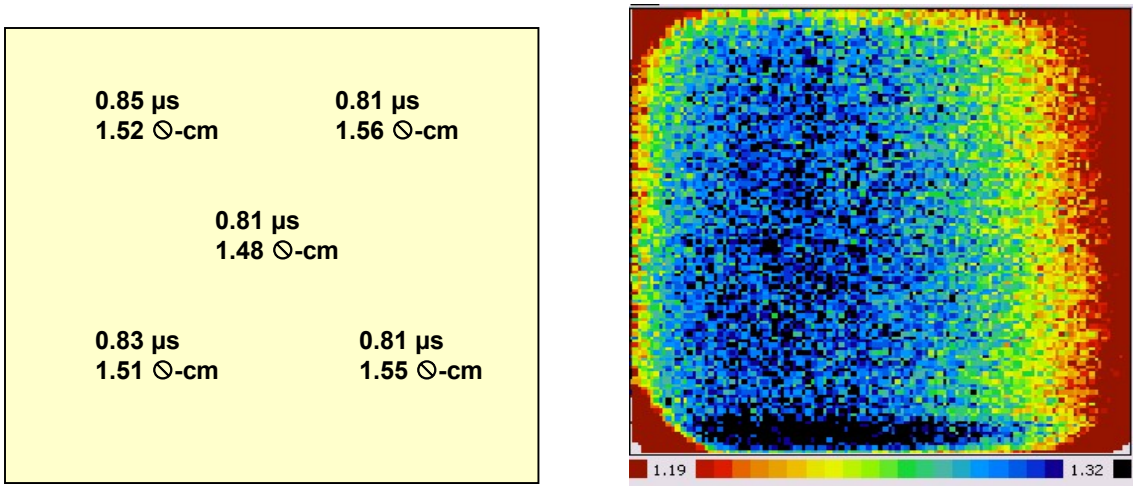

Figure 140. Sinton lifetime and resistivity (left) and lifetime map (right) of Linuo lot 111, wafer S15, after saw damage etch but without surface passivation.

However, if the saw damage is removed and the lifetime measurements are made with passivated surfaces, as by iodine-methanol solution, the true lifetime in the bulk of the starting wafers can be revealed. Figure 141 shows a comparison of Sinton lifetime measurements of the wafer in the raw state and after etch and passivation. The average lifetime after passivation is 107 µsecs , while the raw wafer average is 0.8 µsecs, showing that the wafer is high quality even though the raw wafer measurement was very low. As shown with the Linuo 111 lot, wafer quality control by measuring one or two incoming raw wafers of a prospective wafer lot after passivation could bring benefits in later binning and yield.

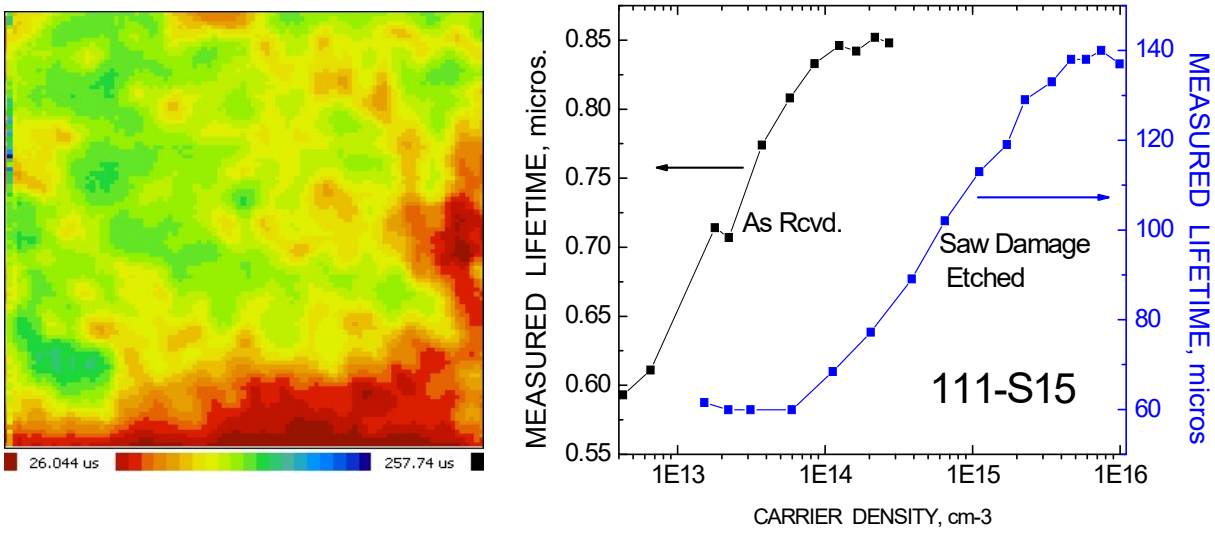

Figure 141. Lifetime measurements on wafer S15 after saw damage and iodine passivation (left) and a comparison of lifetimes in the raw wafer and after treatment (right).

LBIC and Lifetime Maps

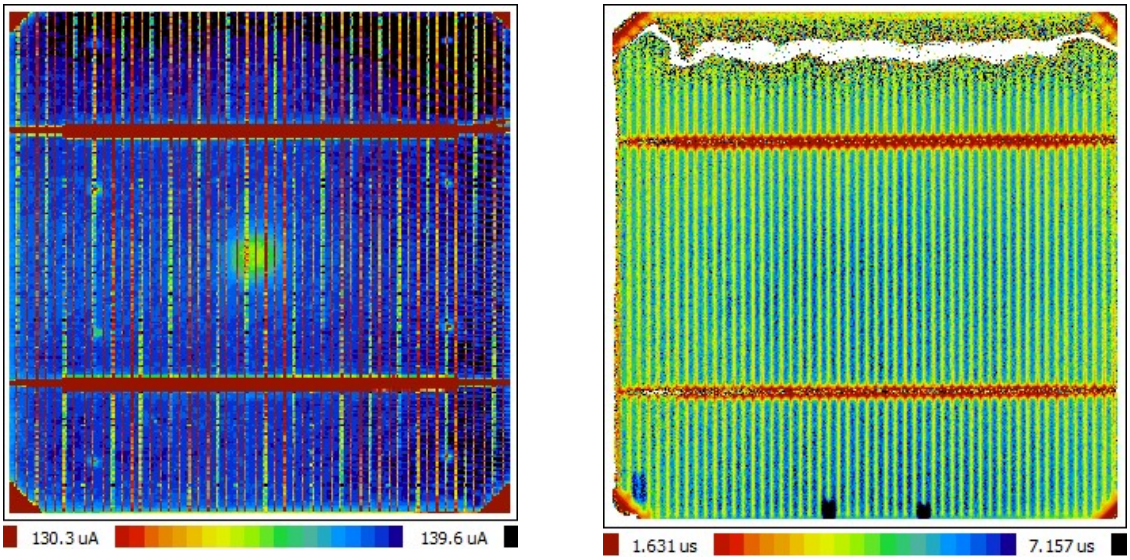

Figure 142. LBIC map at 981 nm (left) and lifetime map (right) for Linuo 111, cell S16.

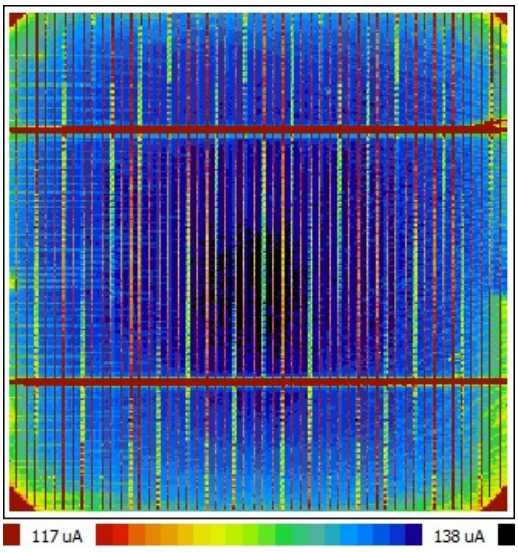

Figure 143. LBIC map at 04 nm wavelength for Linuo 111, cell S16.

Figure 142 shows the long wavelength LBIC and lifetime maps for finished cells from this lot, and Figure 143 shows the LBIC at short wavelength. The maps indicate a very high degree of uniformity. The indicated finished cell average lifetime of 4.8 μsecs in the base region is considerably higher than the raw wafer lifetime as shown in Figure 142, even after all the processing and with the front and back recombination losses and grid contacts. The true base lifetime in the finished cell, as suggested by Figure 143, is probably closer to 100 μsecs.

Quantum Efficiency.

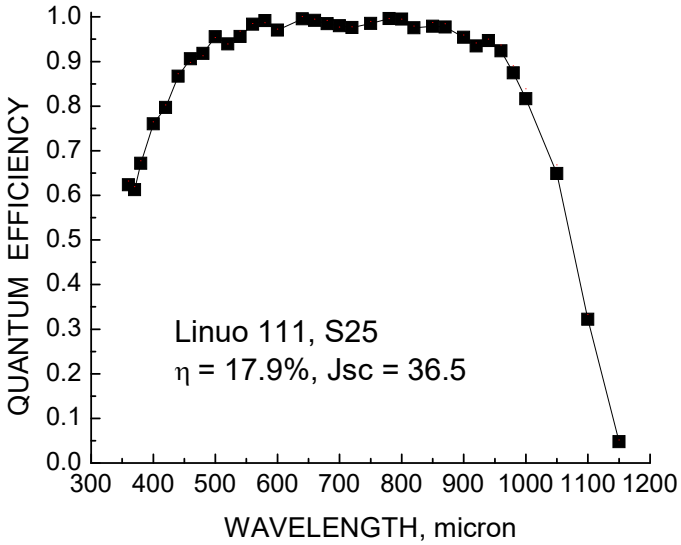

Figure 144. Spectral response of mono cell Linuo 111, S25.

Figure 144 shows the spectral response of a typical cell from this lot. The base lifetime is high as evidenced by the steep rise at long wavelengths. The curve is almost square but the gradual drop-off at short wavelengths implies that the surface passivation and/or reflectance are good but not quite as good as the previous mono lot: Linuo 201. Figure 145shows the reflectance and EQE/IQE comparison. The reflectance is very low over the entire IR to visible range and only begins to increase below 500 nm. The minimum is around 580-620 nm, ideal for the solar spectral peak. The IQE and EQE are nearly indistinguishable because of the low reflectance, typical for many mono cells.

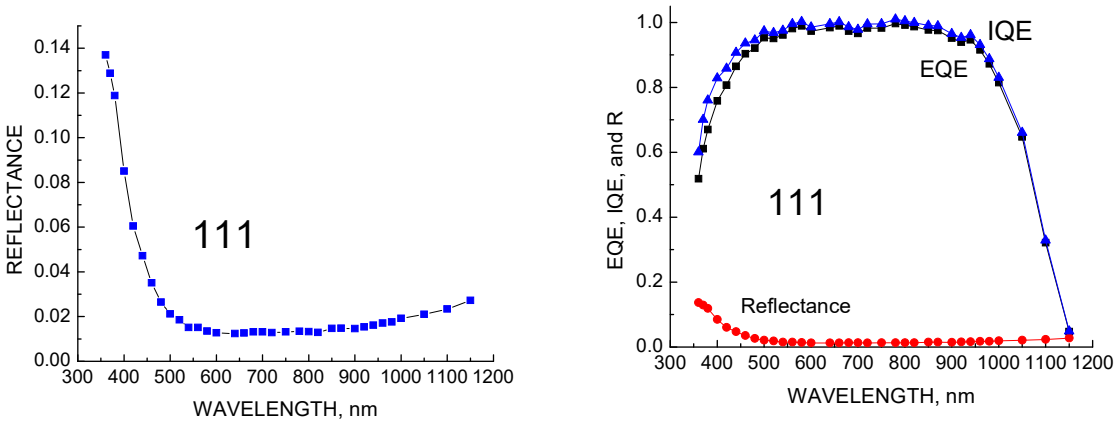

Figure 145. Reflectance (left) and IQE/EQE comparison (right).

7.20 Linuo NNMN

29 5-inch Monocrystalline Cells.

Comments: Shunt resistance is good but series resistance is a bit high. J0 and n are good (low) but Voc is only moderate (620 mV), surprising with the low values of J0 and n. Jsc is relatively high. The net efficiency is above 17%, but lower than expected probably due to the low values of Voc, FF, and higher Rs. Several cells were measured in this turn-key run that had either very poor lifetime or wafer resistivities out of spec. These are excluded from the average data. The averages are:

<RSH> = 146 ohms, ⑨ = 50
<RS> = 0.666 ohm-cm^2, ⑨ = 0.118
<J0> = 1.5 E-11 amps/cm^2, ⑨ = 1.0 E-11
< n > = 1.107, ⑨ = .030
< Jsc> = 35.85 mA/cm^2, ⑨ = 0.21
<Voc> = 620.4 mV, ⑨ = 2.6
<FF> = 0.770, ⑨ = .020
<Effic> = 17.12 %, ⑨ = 0.53

Efficiency and Parameter Correlations:

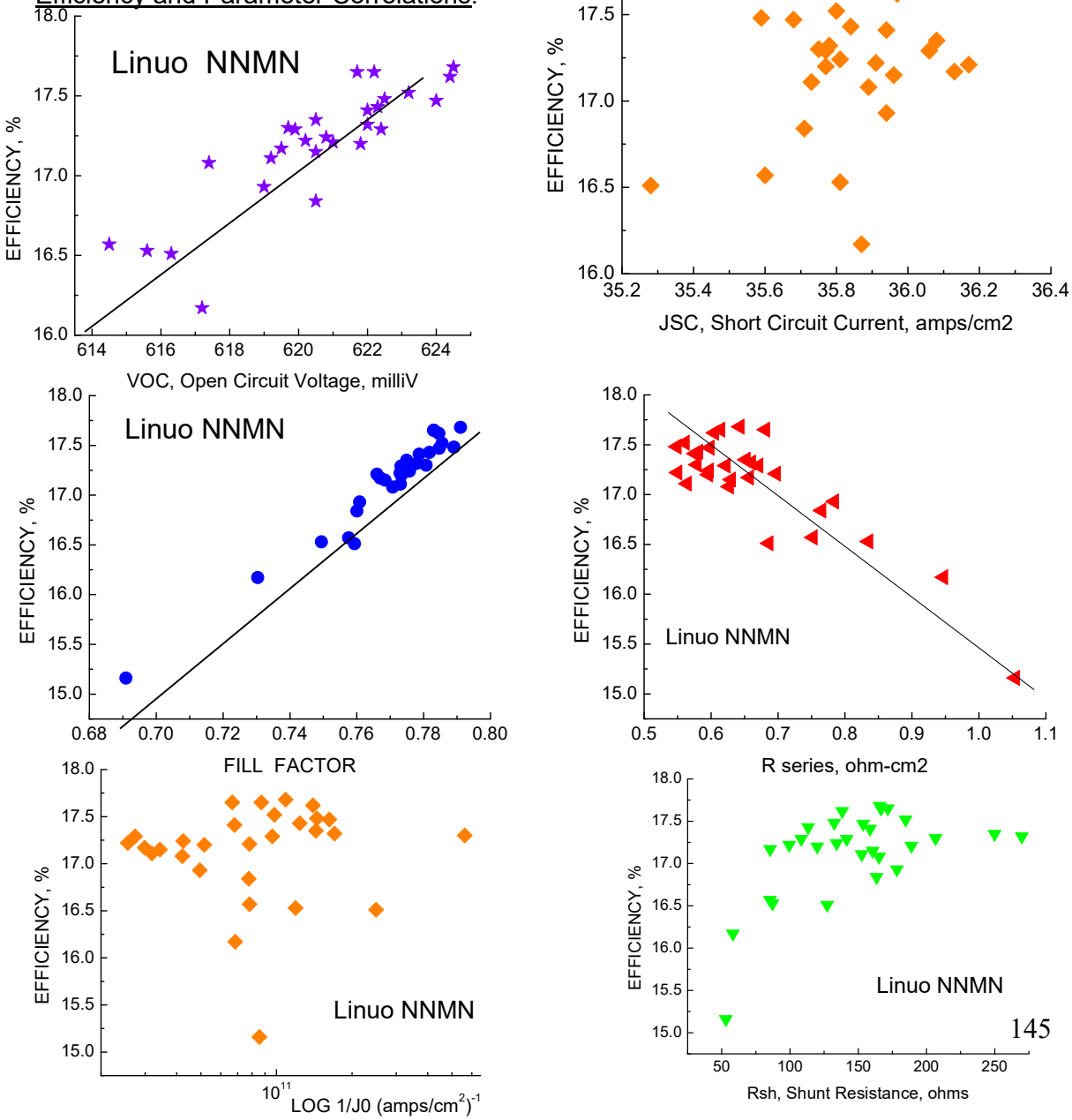

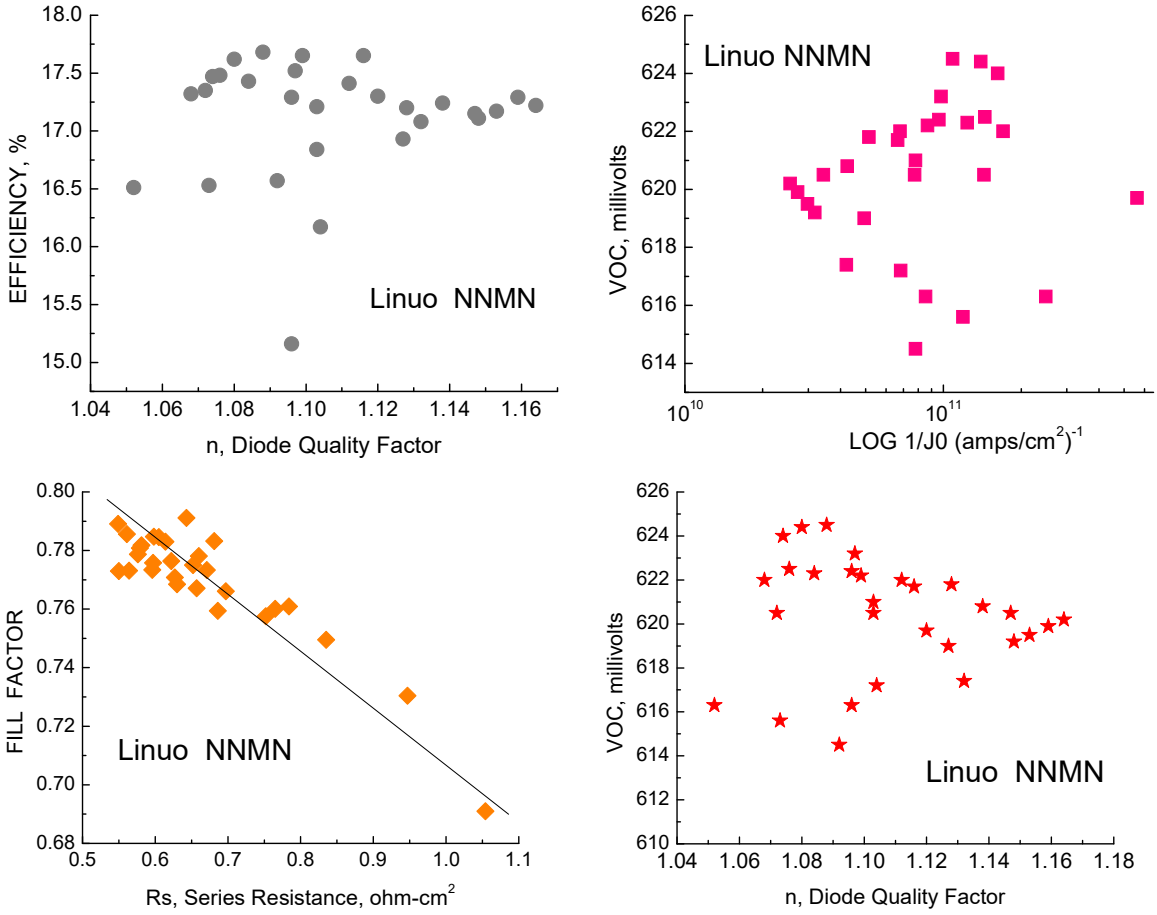

Figure 146. Correlations for Linuo lots NNMN.

Figure 146 shows strong correlation between efficiency and Voc, FF, and Rs but no dependence on Jsc , J0, or n. There is a hint of a weak dependence on Rsh, even though the values of Rsh are high. The FF has a strong correlation with series resistance but Voc has no relation to either log 1/J0 or n.

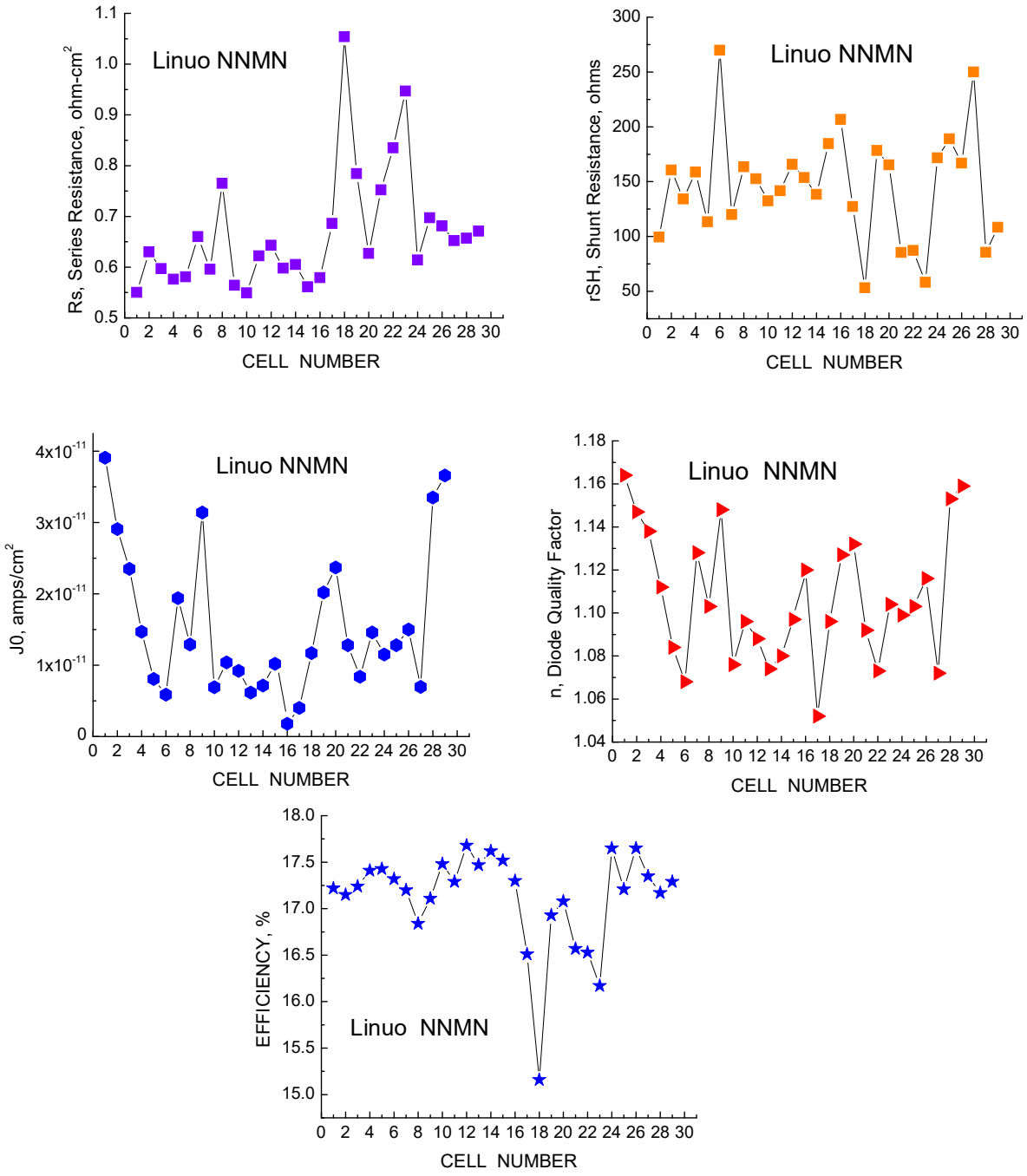

Figure 147. Forensic parameters for Linuo monocrystalline 5-inch cells.

Linuo monocrystalline cells are generally good, with state of the art efficiencies and good uniformity as shown in Figure 147. The dark currents J0 are low as are the diode quality factors n (low is good). The cell efficiencies averaged over 17% for this lot, not as high as the other two Linuo lots that were analyzed but higher than most multicrystalline lots in the year 2011 time-frame.

LBIC Maps.

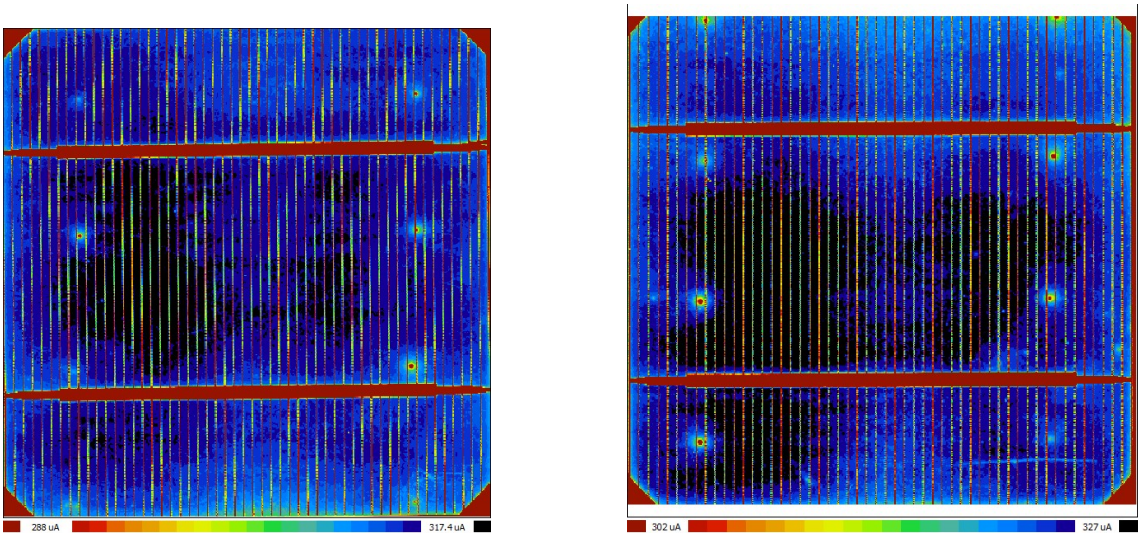

Figure 148. LBIC maps at 981 nm (left) and 404 nm (right) for Linuo NNMN cell 3-5, 17.3% efficient.

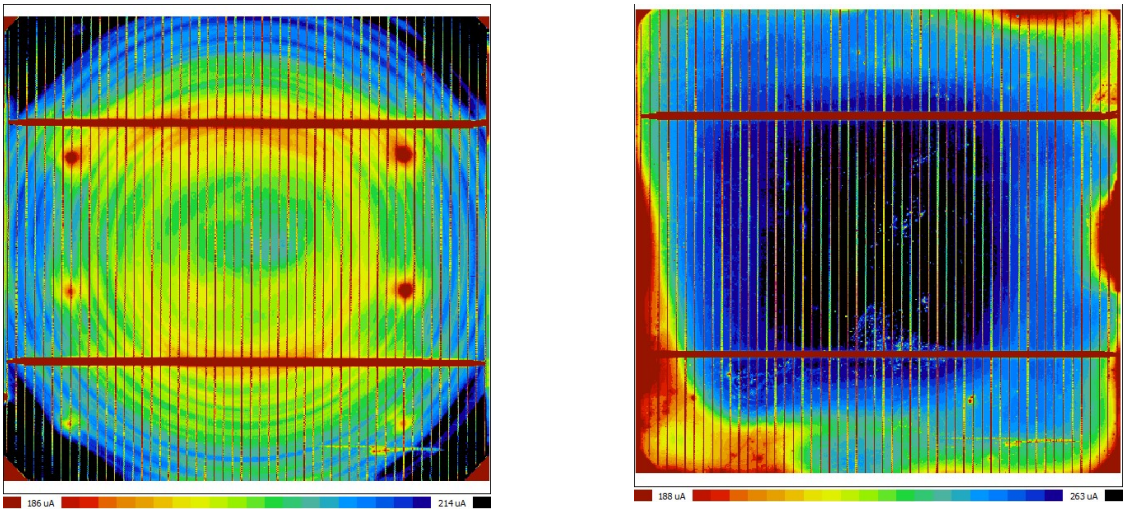

Figure 149 LBIC maps for 981 nm (left) and 404 nm (right) for Linuo NNMN cell 3-17, 13.1% (one of the outlier cells not included in Figure 148).

Figures 148 and 149 compare LBIC maps at long and short wavelengths for a typical good cell and a poor cell. The poor cell exhibits a circular LBIC pattern in the base (Fig. 150, left) indicative of defect precipitation and/or possibly oxygen precipitation, and exhibits significant emitter problems around the periphery (Fig. 149, right side). By comparison, the high efficiency cell shows a high degree of uniformity at both long and short wavelengths (Fig. 148).

Quantum Efficiency

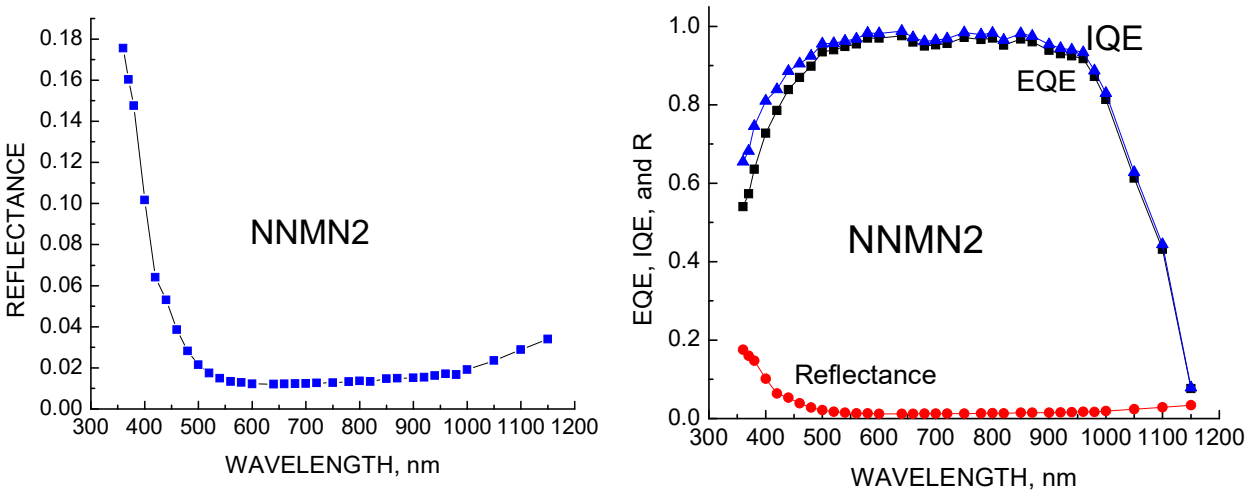

Figure 150. Reflectance (left) and EQE – IQE comparison (right) for cell # 11.

The reflectance and spectral responses (EQE and IQE) for typical cells from this lot are shown in Figure 150. The reflectance is low throughout the IR and visible regions but rises below 500 nm more than the other mono lots. The quantum efficiencies suggest relatively good substrate (base) lifetime but less than optimum passivation as evidenced by the gradual decline in IQE below 600 nm.

8.0 Conclusions

The purposes of this project were to explore the value of UMG material for Si solar cells, to assess processes such as gettering which could improve material quality and subsequent device performance, to suggest enhancements that could improve solar cell improvements, and to perform detailed forensic measurements on finished cells with the aim of identifying efficiency limiting factors and suggestions for improvement. Visits to multiple turn-key manufacturers were made as part of the project. As outlined in the quarterly reports as well as this final report, these goals have been met and many questions answered during the course of the project. Some highlights include:

- UMG material was shown to be viable for Si solar cell manufacture but the need for UMG disappeared with the decreased price of Si raw material. Efficiencies obtained with UMG were acceptable in the 2010 time-frame but not likely to reach the 17-18% of modern multicrystalline cells.
- Gettering was shown to improve the average lifetime in solar grade Si material by 2-10x with the poorest lifetime substrates improving the most. In multicrystalline material the highest dislocation density regions did not improve as much as the low DD regions. Gettering improved both the average efficiency and the efficiency distribution, but the extra cost and reduced throughput are significant drawbacks.
- Highly detailed forensic measurements on 18 commercial lots from 10 different manufacturers showed that there was no dominant efficiency-limiting factor common to all of them; instead, different factors dominated in different lots. Material quality did play a role in most, and all the lots would have benefited from more wafer metrology and quality control. Processing differences were indicated by the wide range of shunt and series resistances and by quantum efficiency and lifetime maps which indicated poor lifetime in the base region in some lots and poor emitter quality and/or passivation in others.
- True incoming raw wafer lifetime measurements would be a valuable quality control and could be done on a few representative wafers from a prospective lot by saw damage etch and chemical surface passivation. Without this treatment, band-to-band photoluminescence measurements like other lifetime-determined measurements are dominated by surface losses. However, defect band photoluminescence can be carried out after saw damage etch but without surface passivation and is highly correlated with device performance.
- Several enhancements to device performance have been described such as material quality control, back surface field formation such as local BSF, emitter design such as selective emitter to reduce the emitter doping level without Rs penalty, thinner grids also without Rs penalty but with reduced shadowing, better optical layer control to match the solar spectrum and reduce reflectance, processing steps such as laser doping and laser contact formation, and different processing and device design such as ion implantation to better control emitter and BSF profiles and structures such as HIT cells and IBC cells. In most cases, for the 18 forensic lots that were described, it was pointed out how these various enhancements would have improved the device performance.
- Thin film Si solar devices were explored by fabricating cells on 5,10, 20, and 40 micron thick films deposited on “low cost substrates,” in this case using P+ Si substrates to simulate UMG P+ low cost material. Thin film Si cells on glass, carbon, or plastic substrates are problematic due to lattice mismatch and contamination. Thin film Si on P+ (inactive) Si substrates is the optimum form of thin film Si device, providing perfect lattice match and preventing contamination. Devices nearly 13% efficient

were fabricated on 40 micron films and over 7.5% on 5 micron films. Methods to raise these efficiencies for these same thicknesses were described.

* "Real-world" solar panel measurements were made by installing 10 panels from 9 different manufacturers on the IBM building rooftop, with a goal of comparing the 10 panels over a period of time to account for temperature, angle of incidence, diffuse versus direct radiation, and average energy output over a day or other extended time sequence. Although these measurements were just begun when the project ended, interesting observations were already noted: the best panels in the morning were sometimes the worst in the afternoon; forensics on the panels showed that they differed considerably in series resistance; the solar cells comprising some panels were not optimized optically; power output available on a totally overcast day with no direct sunlight amounted to 15% of the power output on a bright, cloudless day; the HIT and IBC panels were considerably more efficient than the conventional mono or multicrystalline panels.

8.1 Follow-on

The techniques identified in this project would be beneficial to any solar cell manufacturer, and though proven for Si cells specifically, would be beneficial for other materials as well. The added process of metrology steps would likely raise costs a small degree, but would more than pay for themselves by higher average efficiencies, reduced binning, and improved yield. Incoming wafer quality control, for example, could be carried out on a few wafers out of a large batch and prevent costly processing on ultimately sub-par material. Design changes such as selective emitter and local BSF have significant benefits in device performance and can be done in a variety of ways while keeping diffusion as the main device process. Better attention to optical properties would be beneficial as well. The use of HIT, IBC, or EWT technologies, though adding cost, brings an immediate boost to performance and n-type substrates prevent light-induced decay which robs panel performance over time.

After fabrication and binning, laboratory analysis of cells in the better and worse categories by techniques like spectral response can identify problem areas and suggest means of process repair. DLIT and electroluminescence can identify both material problems and contact problems. Manufacturers would benefit by having a diagnostic laboratory equipped with a few of these capabilities in their arsenal.